HPV RESEARCH GROUP

INSTITUTE OF CANCER & GENETICS

SCHOOL OF MEDICINE

CARDIFF UNIVERSITY

Validation and Use of a Model System to Investigate Topical Treatment of Vulval Intraepithelial Neoplasia

By Tiffany Onions

2013

Thesis submitted in partial fulfilment of the requirements for the degree of Doctor of Philosophy

DECLARATION

This work has not previously been accepted in substance for any degree and is not concurrently submitted in candidature for any degree.

Signed …… (candidate) Date ……

STATEMENT 1

This thesis is being submitted in partial fulfillment of the requirements for the degree of

……

Signed …… (candidate) Date ……

STATEMENT 2

This thesis is the result of my own independent work/investigation, except where otherwise stated. Other sources are acknowledged by explicit references.

Signed …… (candidate) Date ……

STATEMENT 3

I hereby give consent for my thesis, if accepted, to be available for photocopying and for inter-library loan, and for the title and summary to be made available to outside organisations.

Signed …… (candidate) Date ……

Acknowledgements

It would not have been possible to write this thesis without the support of the inspiring people around me, to only some of whom it is possible to give particular mention here.

Above all, I dedicate this thesis to my parents, Julie and Gordon. I know how lucky I have been, and always will be, to have their endless love and encouragement; their belief in me kept me going!

I am also especially grateful to Mikey for his support and understanding. I could not have persevered without the reassurance he offered, and everyday his smile kept my spirits high!

I have developed friendships with many colleagues over the past few years, and I would like to thank every member of the HPV Research Group for their advice and kindness. I would particularly like to express thanks to Dr Dean Bryant for his help and patience.

I would like to extend further gratitude to my supervisors, Dr Ned Powell and Dr Amanda Tristram, for their invaluable assistance and guidance. I would also like to thank my personal tutor, Dr Mandy Tonks, for always making time for me.

Finally, I would like to thank the National Institute for Social Care and Health Research for providing funding to support this research project.

This thesis is also dedicated in loving memory of my gransha, Malcolm, who was an inspiration to everyone! He was more excited than I was when I embarked on this PhD, and would no doubt be puffed-up with pride at the submission of this thesis if he was here now.

Summary

The aims of this study were to develop novel in vitro models of Human Papillomavirus (HPV) - associated vulval and vaginal neoplasia and to use them to investigate the mechanism(s) of action of the nucleoside analogue, Cidofovir (CDV), for which a mechanism is unknown. Single cell clones were successfully isolated from heterogeneous vulval and vaginal parental populations. The clonal cell lines were characterised morphologically and in terms of cell proliferation; a range of growth rate and morphological variants were identified. Clonal lines were also characterised with respect to HPV integration state using Amplification of Papillomavirus Oncogene Transcripts (APOT) and Detection of Integrated Papillomavirus Sequences (DIPS). Cell lines were identified that represented naturally occurring episomal and integrated HPV infections. HPV gene expression analysis was also performed using quantitative real-time reverse transcription PCR (qRT-PCR) which displayed different expression profiles for each line. Patterns of HPV gene expression appeared to correlate with gene disruptions associated with integration. Characterised clonal lines were used to investigate the effects of CDV on cell viability, morphology and HPV gene expression. CDV (10 μM) reduced cell viability in all HPV-positive clonal lines and HPV negative HEK cells; viable cell counts showed that a more considerable response was detected in vulval lines compared to vaginal lines and that response in HEK lines was similar to vulval lines. Cell enlargement was observed in response to treatment in the clonal lines but not the HEK line. CDV treatment did not cause significant reduction in expression of HPV E6 or E7. mRNA sequencing confirmed HPV integration and gene expression profiles. Differentially Expressed Gene (DEG) analysis identified a large percentage of the top 20 most significant Gene Ontology (GO) categories to be involved in nucleotide synthesis and RNA polymerase activity. Gene Ontology Over Representation Analysis (GO-ORA) showed that 4 GO categories relating to cellular senescence were found in over 300 GO categories comprising the top 500 most significant gene transcripts.

Table of contents

Table of Figures

Table of Tables

1 Introduction

1.1 Human papillomavirus (HPV) and HPV associated cancer

Papillomaviruses (PVs) belong to the *Papillomaviridae* family and are small (52-55nm diameter) viruses that consist of a double stranded, circular, DNA genome of approximately 8kb. PVs are non-enveloped. They have an icosahedral capsid consisting of 72 capsomeres. The capsomeres include L1 and L2 proteins; L1 is the major protein forming ~80% of the capsid and functions to mediate viral infectivity (Joyce et al., 1999). PVs are a diverse group of viruses that infect a broad range of hosts including humans, other mammalian species, and birds. Over the past few decades, PVs have been linked to chronic infection of stratified squamous epithelia of the skin and mucosa, causing benign, pre-malignant, and malignant lesions (Munoz et al., 2006, Howley and Lowy, 2007). Each PV genus is classified according to the host species it infects and the resulting manifestation of disease. Nucleotide sequencing has provided a means of phylogenetically assessing PVs by comparing the nucleotide sequence of the L1 open reading frame (ORF), which is highly conserved in all PVs. Within a genus, DNA comprising the L1 ORF shares at least 60% homology with all members within the same genus. PV genera are divided by species, representing 60-70% L1 sequence identity to other PV of the same species; viral type (71-89% L1 identity); viral subtype (90-98% L1 identity) and variant (over 98% L1 identity). Phylogenetic classification presents 12 genera of PVs, 5 of which are human associated (human papillomaviruses (HPV)) and the remaining are entirely animal associated (de Villiers et al., 2004). The 5 genera of HPVs are represented by the letters of the Greek alphabet: α, β, γ, μ, and ν.

1.1.1 Structure and taxonomy

HPVs belonging to the α genus infect both cutaneous and mucosal epithelia, causing a variety of benign lesions such as cutaneous or mucosal warts, as well as pre-malignant lesions, and

cancer. HPV types belonging to the α genus, such as HPV2 and 57, infect cutaneous epithelia and cause common cutaneous warts. Mucosal α-HPV types, such as HPV 6, 11, 16 and 18, are the most clinically relevant infections and are associated with genital warts, respiratory papillomas, and anogenital pre-malignant lesions and cancers. HPVs of the β genus are implicated in infections specific to individuals with epidermodysplastic verruciformis and immunodeficiency diseases, and are commensals of the hair and skin in healthy individuals (Knipe and Howley, 2007). HPVs of γ, μ and ν genus, such as HPV1 and HPV 4, are associated with cutaneous warts.

1.1.2 Epidemiology

Epidemiology refers to the factors contributing to the cause, frequency, and distribution of disease in the human population. According to the Centers for Disease Control in the United States of America (CDC), HPV is the most common sexually transmitted infection (Centers for Disease Control, 2013) and by age 50, at least 80% of women will have acquired, and most likely subsequently cleared, a genital HPV infection.

Mucosal HPV types associated with cancer are categorised as high risk (HR); the most significant HR HPV types are 16, 18, 45 and 31. Low risk (LR) mucosal HPVs represent types that are not associated with cancer, such as types 6 and 11. In the human population, persistent infection with HR HPV infection is clinically significant because it contributes to the global cancer burden. Infection with HR HPV types 16 and 18 is the underlying cause of approximately 70% of cervical cancers (Muñoz et al., 2004, World Health Organisation (WHO), 2013). In an updated European meta-analysis of HPV type distribution in cervical intraepithelial neoplasia (CIN), HPV 16 and/or 18 was found in 52%, 61% and 76% of cytologically detected high-grade squamous intraepithelial lesions, histologically confirmed cervical intraepithelial neoplasia grade 2/3, and invasive cervical carcinoma, respectively (De Vuyst et al., 2009). World-wide studies over the last decade have also demonstrated the association between

persistent infection with HR HPVs and other genital cancers, for example, HR HPV DNA has been detected in cancers of the cervix, vulva and vagina in women, and in men HPV has been shown to cause cancers of the penis and oropharynx (Stanley, 2007, Giuliano et al., 2008), illustrated in Table 1.1. In both sexes HPV has been shown to infect the anal canal, perianal, and oropharyngeal regions, and over the past decade the increased incidence of certain head and neck cancers has been attributed to increased prevalence of HPV in the oral cavity (Marur and Forastiere, 2008). LR HPV types of the α genera, such as HPV 6 and 11, predominantly cause genital warts in both sexes and although they are not usually linked to cancer, they are associated with considerable psychosocial distress (Ireland et al., 2005) and contribute to the clinical burden of HPV related disease. Genital warts affect around 1% of the sexually active population (Brentjens et al., 2002).

1.1.2.1 *Risk factors*

Both sexes are able to carry, transmit, and become infected by HPV via sexual contact therefore the risk of infection is related to the sexual behaviour of an individual. Early age at start of sexual activity, sexual relations with a high risk individual, and a high number of sexual partners, contribute to the increasing likelihood of HPV infection and transmission (Pecorinio, 2008). Infection with HPV usually occurs within the first several years of sexual initiation. The age of highest sexual activity in the female population ranges from 18 to 25 years (late teens and young women). During this time the incidence of HPV infection without clinical concern (defined as HPV positive but without clinical symptoms) is highest. In a study involving meta-analysis of cervical HPV prevalence in 5 continents, the age distribution of cervical HPV infection showed a bimodal curve (Bruni et al., 2010); a first peak in prevalence at younger ages (late teens / early twenties) was common to all populations. A second smaller peak at approximately 40 years of age was also identified in some populations. This is thought to be related to circumstances such as divorce or menopause. Aside from the relationship between

Site	Attributable to HPV (%)	Developed countries			Developing countries		
		Total cancers	Attrib. to HPV	% all cancer	Total cancers	Attrib. to HPV	% all cancer
Cervix	100	83, 400	83, 400	1.7	409, 400	409, 400	7
Penis	40	5, 200	2, 100	0.0	21, 100	8, 400	0.1
Vulva,vagina	40	18, 300	7, 300	0.1	21, 700	8, 700	0.1
Anus	90	14, 500	13, 100	0.3	15, 900	14, 300	0.2
Mouth	3	91, 200	2, 700	0.1	183, 100	5, 500	0.1
Oropharynx*	12	24, 400	2, 900	0.1	27, 700	3, 300	0.1
All sites		5, 016, 000	111, 500	2.2	5, 827, 500	449, 600	7.7

1.1 Cancers attributable to HPV infection

The table shows the estimated cancer burden attributable to HPV infection (data relates to the year 2002). Certain anogenital and oropharyngeal cancers are thought to have increased in incidence since 2002 due to the increased prevalence of HR HPV in the population (especially oropharyngeal cancers). Adapted from (Stanley, 2007).

age and sexual behaviour, age is also a contributing risk factor because age is related to cellular changes in the transformation zone which increase the risk of infection (Burd, 2003). The transformation zone of the cervix is a region where one type of epithelia replaces another (metaplasia) and is the site from which most cervical cancers originate (Jordan and Singer, 1976).

The prevalence of neoplastic lesions differs in different regions of the genital tract. The incidence of cervical intraepithelial neoplasia (CIN) is much higher than incidence of vulval or vaginal intraepithelial neoplasia (VIN and VaIN). This may be because HPV does not infect all regions of the female genital tract at the same frequency.

1.1.2.2 *Persistent infection with HR HPV*

In most cases HR HPV cause transient infections which clear spontaneously (Evander et al., 1995). In a relatively small percentage of individuals with HR HPV infection (~10%), transient infection is not cleared and HPV chronically persists (Holowaty et al., 1999, Ostor, 1993). Persistent infection with HR HPV can cause development of histological changes within infected epithelia; this is usually attributable to the 4 most significant HR HPV types, 16, 18, 45, and 31, and highly associated with the risk of developing neoplasia and progression to cancer (Howley and Lowy, 2007). HPV 16 is currently the most prevalent type and is frequently associated with anogenital neoplasias and cancers. During persistent infection, the immune status of the host, co-infection with other sexually transmitted microorganisms, long term use of oral contraceptives, diet, and tobacco use are also thought to facilitate neoplastic progression to cancer (Castellsague, 2008).

1.1.2.3 *The disease burden associated with HPV infection*

Chronic infection with HR HPV is considered necessary for the progression of neoplastic lesions to invasive cancer, with HPV persistence contributing as a major risk factor for cellular

transformation (Schlecht et al., 2001, zur Hausen, 2002, Paavonen, 2007, Ho et al., 1995, Ferenczy and Franco, 2002). HPV 16 is the most prevalent type detected in cervical cancer and along with types 18, 33, and 45, has been classified by the International Agency for Research on Cancer (IARC) Monographs as a human carcinogen (International Agency for Research on Cancer (IARC), 2013). Almost 100% of cervical carcinomas contain HR HPV DNA, between 70-90% in high grade cervical intraepithelial neoplasias (CIN II & III) and 20-50% in low grade CIN (I). HPVs are also associated with malignancies in other mucosal and skin cancers, and with regard to other anogenital cancers, HR HPV types 16 and 18 account for 70-85% anal cancers, ~40% vulval/vaginal/penile cancers, as well as ~40% head and neck cancers (Paavonen, 2007, De Vuyst et al., 2009).

1.1.2.4 *Vaccination: prevention of HPV infection*

Vaccination strategies aim to prevent precancerous and cancerous lesions by targeting the aetiological agent of disease (HPV). Vaccination works by effectively preventing initial infection with HPV in previously unexposed women; it is not effective in women with existing HPV infections (Monsonego et al., 2010).

The immunisation program introduced into the UK in 2008 initially used the bivalent vaccine, Cervarix™, containing Virus Like Particles (VLPs) composed of L1 proteins of HR HPV 16 and 18 (GlaxoSmithKline, 2013). More recently, the UK has switched to Gardisil®, a quadrivalent vaccine, containing VLPs against HPV 16, 18, 6 and 11 (Merck Sharp & Dohme, 2013). Both vaccines protect against HR HPV 16 and 18, which are associated with cancer. Gardisil® also protects against LR HPV types 6 and 11, which cause genital warts.

1.1.3 HPV lifecycle (productive infection)

The classic HPV life cycle is commonly described as productive infection, which entails entry of the virus into the squamous epithelial cells and thereafter the production of new virus

particles (Stanley et al., 2007, Doorbar, 2005), as illustrated in Figure 1.1. Productive infection by HPV may manifest as cutaneous warts from which shedding of infectious viral particles occurs. The HPV life cycle is dependent on the differentiation pattern of the keratinocytes within the stratified layer of squamous epithelia (Kajitani et al., 2012). To establish productive infection HPV requires access to cells comprising the basal cell layer. HPV infects basal cells when they are exposed through micro-abrasions formed during sexual contact.

1.1.3.1 *Attachment and entry*

Once HPV has been exposed to basal cells, L1 proteins bind to heparin sulphate proteoglycans on the epithelial basement membrane causing conformational changes that expose L2. L2 is cleaved and the entire L1 protein becomes exposed to cell surface receptors on keratinocytes that migrate across the basement membrane through the wound healing process (Schiller et al., 2010, Kines et al., 2009). After attaching to keratinocytes, HPV virions enter the cell via endocytosis and become localised within an endosome where HPV uncoats. An L2 dependent mechanism permits escape from the endosome and L2 bound HPV DNA moves through the cytoplasma and enters the nucleus of the cell and co-circularize to form an episome. The L2-DNA complex associates with sub-nuclear domains within the nucleus, and transcription is initiated (Schiller et al., 2010).

Viral genomes establish as episomes within the nucleus, and episome replication is synchronised with the host cell replication machinery. As HPV infected basal cells divide, viral genomes are partitioned into daughter cells and detach and move through layers of stratified epithelia toward the surface where mature virions are shed. Once cells have become infected, tightly controlled sequences of molecular events are initiated which involve expression of viral genes in co-ordination with epithelial cell differentiation using the host cell replication machinery (Figure 1.1) (Doorbar, 2005, Stanley et al., 2007).

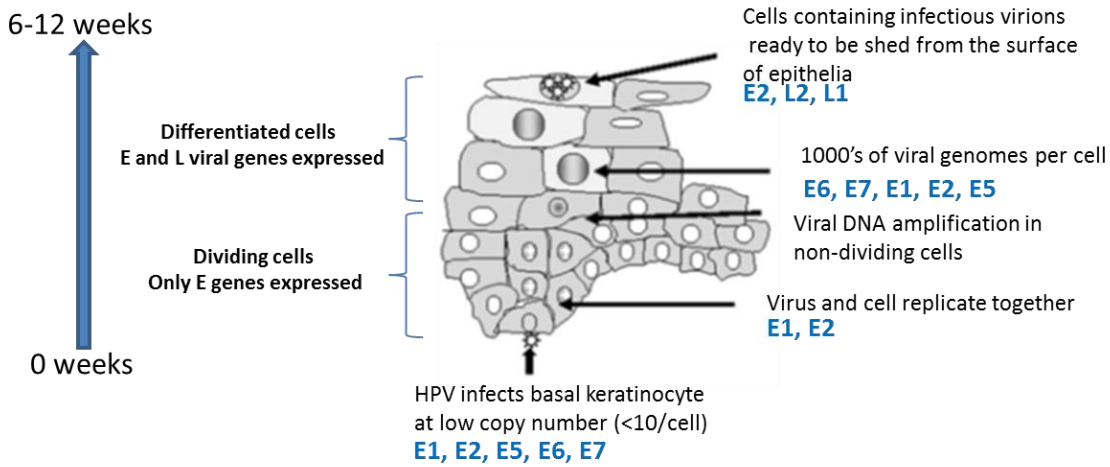

Figure 1.1. HPV genes expressed at different stages of epithelial differentiation.

Early (E) genes permit viral replication and DNA synthesis, after which late (L) genes express structural proteins for viral assembly and encapsidation before release from the epithelial surface. Adapted from (Stanley et al., 2007).

Viral genomes establish as episomes within the nucleus, and episome replication is synchronised with the host cell replication machinery. As HPV infected basal cells divide, viral genomes are partitioned into daughter cells and detach and move through layers of stratified epithelia toward the surface where mature virions are shed. Once cells have become infected, tightly controlled sequences of molecular events are initiated which involve expression of viral genes in co-ordination with epithelial cell differentiation using the host cell replication machinery (Figure 1.1) (Doorbar, 2005, Stanley et al., 2007).

1.1.3.2 *Molecular aspects of HPV 16 productive lifecycle*

The double stranded DNA genome of HR HPV16 consists of 7904bp. Only 1 strand of double stranded DNA functions as the coding strand for transcription. The genome of HPV16 is divided in to early (E) genes (6-7-1-2-4-5) and late (L) genes (1 and 2), as shown in Figure 1.2. Several of the HPV open reading frames (ORF) overlap and protein production is influenced by alternative splicing of mRNAs to allow differential expression of HPV proteins at different times in the HPV lifecycle.

There are at least two promoters within the HPV16 genome; a promoter is a sequence of DNA where transcription is initiated. In HPV16, the p97 promoter region is located upstream of the E6 ORF and regulates expression of E genes (Smotkin and Wettstein, 1986) while the P670 promoter lies within the E7 ORF and is responsible for expression of L genes (Zheng and Baker, 2006).

1.1.3.2.1 Intitiation of viral DNA replication

The LCR is a non-coding sequence of DNA (~1kb) in the HPV genome which is important for viral DNA replication because it contains the origin of replication. It also contains binding sites for numerous viral and cellular transcription factors which function to either activate or

repress the early p97 promoter, which initiates transcription of early (E) genes (Doorbar, 2006, Kammer et al., 2000).

1.1.3.2.2 E1 & 2: viral replication and expression of E genes

E1 and E2 genes encode proteins that associate with and bind to DNA at the origin of viral replication (within the LCR) resulting in recruitment of polymerases and other proteins to initiate viral replication. The E2 protein induces E1 to migrate to the viral origin of replication (Longworth and Laimins, 2004), permitting helicase to allow separation of viral DNA strands so replication can proceed. E2 protein has affinity for promoters located throughout the HPV genome and regulates viral transcription through activation/repression of the early promoter p97 (Hines et al., 1998). Regulation of transcription through E2 occurs in a concentration dependent manner, whereby in low E2 concentrations transcription is initiated through stimulation of HPV promoters and in high concentrations transcription is repressed (Steger and Corbach, 1997). Transcription of HPV oncogenes, E6 and E7, are also regulated by E2. E2 also directs the anchorage of viral episomes to mitotic chromosomes to ensure the correct separation of viral genomes into the resulting daughter cells (Hamid et al., 2009).

1.1.3.2.3 E4 & E5

The functions of E4 and E5 are incompletely understood. However it is thought that E4 is involved in the HPV DNA amplification (Nakahara et al., 2005). Efficient viral release from cornified epithelia at the epithelial surface may be facilitated by E4, since E4 has been found to affect the membranes of cornified squamous epithelia which is related to virus release/viral shedding (Doorbar, 2006). E5 is thought to participate in helping HPV evade host immune responses, by down-regulating communication signals between cells which affect major histocompatability complex class I (MHCI) and growth factor receptors (Ashrafi et al., 2002). It is also thought that E5 enhances the transforming properties of HPV, together with E6 and E7,

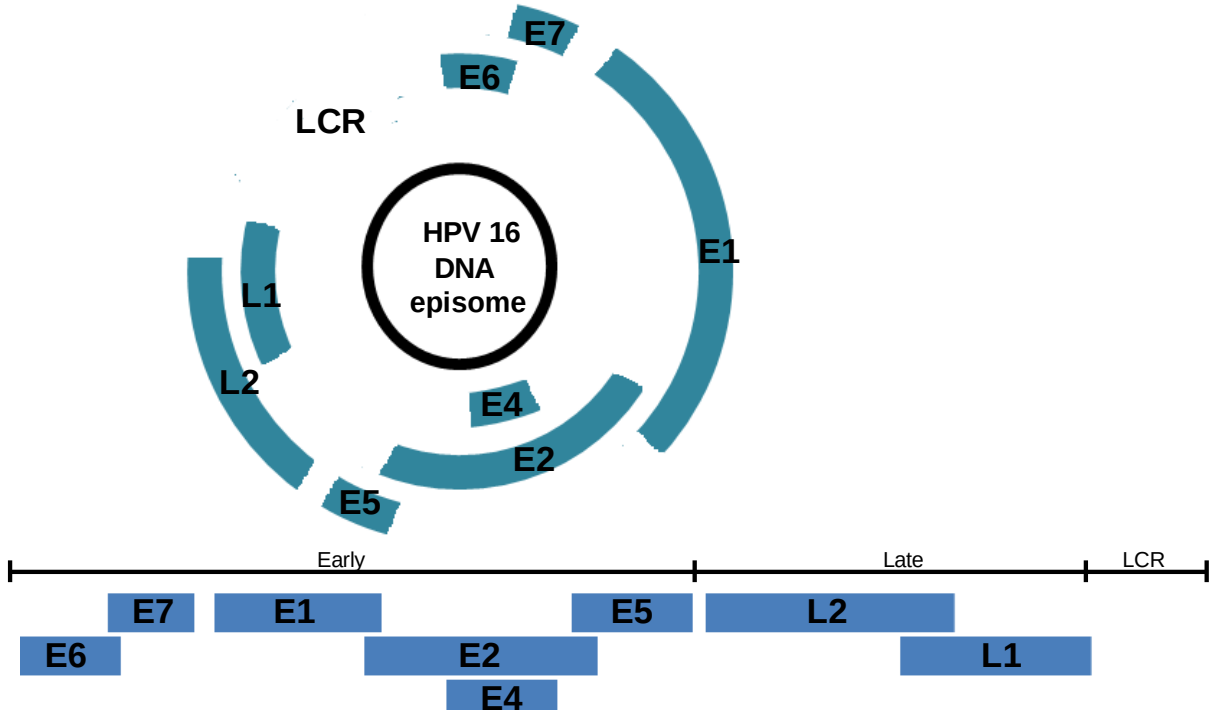

Figure 1.2. Episomal HPV 16 genome.

Schematic representation of circular (episomal) HPV 16 genome showing early (E) and late (L) genes and the lower control region (LCR); corresponding linearised representation of HPV 16 genome also illustrated.

by interacting with epidermal growth factors and cell cycling pathways (Venuti et al. 2011).

1.1.3.2.4 E6 & 7: disruption to the cell cycle and cell transformation

High risk E6 and E7 are the most studied HPV genes and are termed oncogenes due to their association with cellular transformation and cancer. E7 protein maintains cell cycle activity in differentiating cells by interfering with the activity of retinoblastoma (pRB) tumour suppressor protein, and other members of the pocket proteins, e.g. p21 (Munger et al., 2001, Funk et al., 1997). Under normal conditions, pRB forms a complex with transcription factor E2F which regulates the cell cycle by repressing the transcription of genes that allow cell proliferation. However, when E7 is present it binds to pRB causing displacement of E2F which allows expression of genes that promote DNA replication; this leads to constant expression of cell cycle genes and continual cell proliferation.

E6 has been shown to inhibit the action of p53. In normal cells the activity of p53 is low and this is due to mdm2 mediated p53 ubiquitination which flags p53 for proteosomal degradation. During severe DNA damage, mdm2 is inhibited causing levels of p53 to increase to a threshold level which is sufficient to arrest the cell cycle and activate cell death (apoptosis) (Kubbutat et al., 1997). When E6 protein is present it associates with cellular E6 associated protein to form the complex E6-AP which has a high affinity for p53 and causes p53 ubiquitination and degradation; E6-AP induced p53 degradation therefore allows continuous cell proliferation and evasion of apoptosis (Scheffner et al., 1990, Scheffner et al., 1993, Scheffner, 1998). Additionally, E6 permits DNA damage to go unnoticed and allows mutations to accumulate and transfer to subsequent generations of daughter cells, which facilitates cell transformation. Disruption to p53 also causes c-myc and sp1 transcription factors to induce transcription of human telomerase reverse transcriptase (hTERT), an enzyme that maintains telomere length (Gewin and Galloway, 2001, Oh et al., 2001). Telomeres are located at the ends of each

chromosome and shorten with cell proliferation due to the end replication problem. Telomeres function to protect the DNA comprising the chromosome, and stop chromosome ends being recognised as DNA breaks. Erosion of telomeres beyond a critical level leads to cellular senescence. E6 related activation of hTERT therefore prevents telomeres from eroding and enables the cell to continually replicate, which contributes to cellular transformation (Veldman et al., 2001).

In summary, E6 and E7 related deregulation of normal cell cycle and loss of DNA repair mechanisms leads to genomic instability and accumulation of further mutations, which can then lead to cell transformation and carcinogenesis.

1.1.3.2.5 L1 & L2: capsid proteins, virus assembly, and release

Expression of L1 and L2 occurs after HPV genome amplification and facilitates the packaging and assembly of infectious virions in the upper epithelial layers (to avoid host immune surveillance) (Schwartz, 2000). L1 and L2 are capsid proteins and combine in the cytoplasm to form capsomeres; cytoplasmic L1 assembles into capsomeres and migrates to the nucleus once L2 has associated with the nucleus (Florin et al., 2002). The E2 protein is also thought to aid in the formation of the capsid by inducing expression of the late genes (Mole et al., 2009). L2 enhances infectivity of HPV and the efficient packaging of the HPV virions. Together, L1, L2, E2 and E4 are necessary for the assembly of infective virions during the final stage of HPV lifecycle, and also aid in virus release (shedding) when cells reach the surface of differentiated epithelia (Nakahara et al., 2005, Wang et al., 2004)

1.1.4 Pathogenesis

Pathogenesis refers to the chain of events that occur during development and manifestation of disease.

1.1.4.1 *Non-productive infection*

Most individuals that become infected with HR HPV will clear the virus within a matter of months, however there are a small percentage of individuals that do not clear infection (Evander et al., 1995, Ostor, 1993). Persistent infection may be followed by loss of regulation of viral gene expression, such that it is no longer synchronised with epithelial cell differentiation and L1 and L2 proteins are no longer produced; this is referred to as non-productive infection. In non-productive infection, the E6 and E7 oncogenes are still expressed, and interact with tumour suppressor pathways which control the cell cycle. Several factors may underlie loss of control of viral gene expression including viral integration, methylation and mutation of the LCR. The clinical implications of this include the development of neoplasia with the potential to progress to invasive cancer.

1.1.4.2 *Pathology*

Cancers develop through a succession of neoplastic stages that are graded according to the degree of dysplasia and to the proportion of the cross section of biopsied stratified epithelia that contains dysplastic cells (Figure 1.3). The histological classification of biopsies can be through 2 tier Bethesda classification i.e. grouped into low grade or high grade squamous intraepithelial lesions (LSIL and HSIL, respectively), or using the 3 tier system of cervical intraepithelial neoplasia, i.e. grade 1, 2 and 3 (CIN1, CIN2 and CIN3, respectively).

1.1.5 HPV Integration

As previously described, the productive HPV lifecycle and gene expression is synchronised with epithelial differentiation. During productive infection HPV exists as an episome inside the cell nucleus. During non-productive infection, viral gene expression becomes deregulated which allows E6 and E7 proteins to disrupt the cell cycle through the processes previously described; this can lead to genomic instability and neoplastic progression (Doorbar, 2006). Integration of

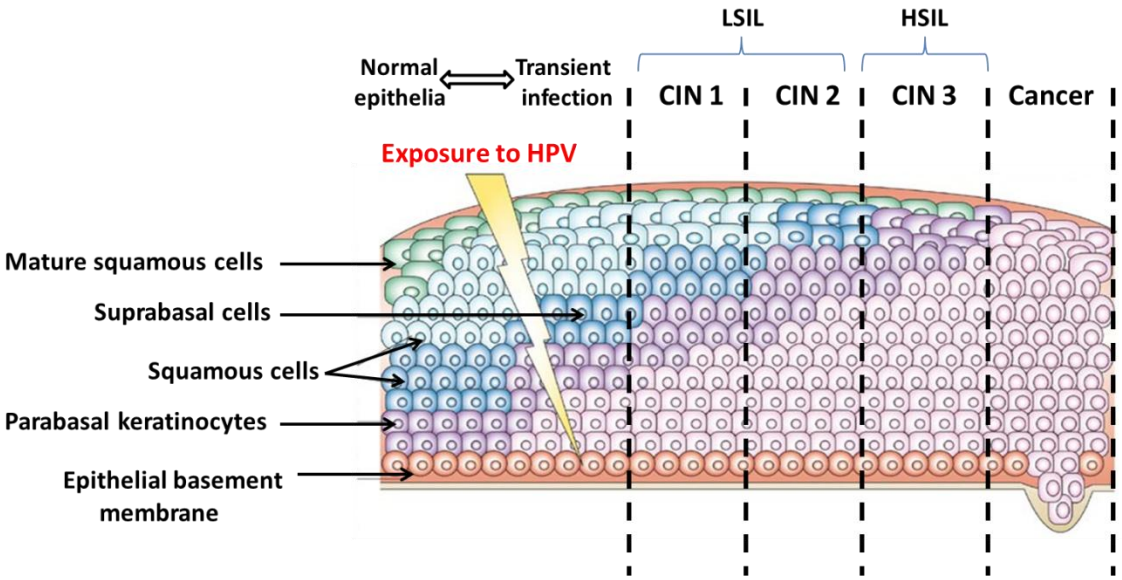

Figure 1.3. Schematic representation of histological classification of HPV infected cells

When basal cells of stratified epithelia are exposed to HPV a series of changes can occur which are classified depending on the degree of dysplasia and proportion of the epithelium affected. CIN 1, 2 and 3 refers to increasing grades of abnormal cells (neoplasia); 1 and 2 are referred to as low grade (low grade squamous intraepithelial lesions = LSIL), and 3 as high grade (high grade squamous intraepithelial lesions = HSIL). Grade 3 can progress to cancer, where cells invade through the epithelial basement membrane. Adapted from (Wheeler, 2007).

HPV in to the host genome often underlies deregulation of viral gene expression and increases the risk of progression to cancer; integrated HPV has been detected in ~80% of cervical cancers (Luft et al., 2001, Walboomers et al., 1999, Klaes et al., 1999, Ziegert et al., 2003). Reports are inconsistent when trying to associate the grade of neoplasia (and cancer) with integration status. It is currently unclear whether integration of HPV is a late or early event. Studies have found purely integrated HPV in CIN 2 and 3 (Peitsaro et al., 2002, Kulmala et al., 2006) and vulval intraepithelial neoplasia (VIN) 2 and 3 (Hillemanns and Wang, 2006) and suggested that integration is a late event. Other studies (Huang et al., 2008) have suggested that integration of HPV is an early event.

1.1.5.1 *Molecular events that contribute to HPV integration*

The mechanism of HPV integration is still not fully described. When episomal HPV integrates it causes disruption to the HPV genome itself but also causes disruption to the host genome. It is generally accepted that HPV integration occurs through a succession of events. First DNA damage occurs to the host and viral DNA, followed by DNA repair mechanisms that insert the HPV DNA in to the genome. Selection of a cell containing integrated HPV forms an immortalised cell that multiplies clonally and progresses to invasive cancer; all of which will be explained in subsequent sections.

1.1.5.1.1 Chromosomal fragile sites

Fragile sites (FS) are regions of genomic instability that are visible as gaps and breaks on metaphase chromosomes due to partial inhibition of DNA synthesis. FS have been identified in many oncogenes, and therefore a link has been recognised between FS and cancer (Gecz et al., 1997, Chan et al., 1994, Hansen et al., 1997).

There are several mechanisms by which FS may induce carcinogenesis. The first describes how FS could directly or indirectly inactivate a gene leading to altered transcripts. The second

describes how FS might allow chromosomal breakage in response to DNA damaging agents (Sutherland et al., 1998). In the context of HPV and carcinogenesis, the latter would probably be most relevant. The reason why DNA at FS is more prone to breakage is still unclear. Over the past few decades studies have shown that HPV integration commonly occurs within regions of FS (Wentzensen et al., 2004).

1.1.5.1.2 DNA damage and repair

DNA damage occurs within the cell as a result of exposure to various endogenous and exogenous chemicals, UV, and ionising radiation. During the cell cycle, check points detect DNA damage and create a delay in response before the cell divides. Integration of HPV may be facilitated by non-homologous end joining. Non-homologous end joining occurs is an error prone DNA repair pathway that predominates when repair by homologous recombination is not possible. A few complementary bases are used to direct repair of the break and this sometimes results in small insertions of deletions at the site of repair (Shrivastav et al., 2008).

In regard to HPV integration, and consistent with non-homologous end joining as a mechanism of DNA repair, overlapping sequences of homology have been detected between HPV and human sequence as well as small sequence insertions that are not homologous with human or HPV sequence, at the site of integration (Ziegert et al., 2003, Durst et al., 1987).

1.1.5.2 *Linking HPV integration with cancer*

During cancer formation, lesions usually consist of populations of several sorts of cells (heterogeneous) which are involved in a battle of competitive growth advantage. In HPV infected cells, HPV integration is considered a selective advantage to a cell, driving carcinogenesis.

1.1.5.2.1 Actively transcribed HPV integrated loci

Transcription of HPV integration loci has been described as a late event in the progression of cancer, although the literature is contradictory as previously described. Integrated transcripts are reportedly most frequent in cervical cancer, with low levels in cervical intraepithelial neoplasia (Klaes et al., 1999, Vinokurova et al., 2008). Similarly, in some reports episomal transcripts are frequently detected in early-late grade cervical intraepithelial neoplasia (CIN I-III), but in cancers episomal transcripts are considerably reduced (Klaes et al., 1999). This is significant because it might suggest that transcription of HPV integration loci confers a selective advantage to the cell which supports neoplastic progression to cancer.

1.1.5.2.2 Expression of HPV oncogenes, E6 and E7

Many studies have shown that when HPV integration occurs, parts of the HPV genome are lost, which results in disruption to E1, E2, E4 and E5 ORFs, however E6 and E7 ORF are retained (Matsukura et al., 1986, Pater et al., 1986). Expression of oncogenes E6 and E7 are detected at higher levels in HPV integrated cells, and through the molecular interactions previously described, increased production of E6 and E7 is vital for ongoing cell proliferation and subsequent transformation (Romanczuk and Howley, 1992). E1 and E2 ORFs can reduce E6 and E7 over-expression and therefore repress cell immortalisation, however due to the disruption of E1 or E2 ORFs upon integration, this cannot occur. This might provide a selective growth advantage to the cell. However, integration into the host DNA alone is not sufficient to drive transformation, as transcription of integrated HPV will be inhibited in cells possessing a mixed population of integrated and episomal HPV (Pett et al., 2006); thus loss of episomal E2 is thought to play a key role.

1.1.5.2.3 Oncogenic genes of the host genome

Integration within a gene or near a gene that has oncogenic properties might disrupt the function of the gene or protein and confer a selective growth advantage to the cell. It is also

possible that deletions near integration sites may cause disruption to human genes and consequently effect the expression of these genes (Thorland et al., 2003). More importantly, integration might occur within a gene but this might not have detrimental structural or functional effects (Dall et al., 2008, Ferber et al., 2003a, Ferber et al., 2003b).

1.2 Vulval Intraepithelial Neoplasia (VIN)

VIN is a premalignant condition and a precursor of vulval cancer. It can be caused by infection with HR HPV, which is referred to as 'usual VIN'. VIN can also be associated with a skin condition called lichen sclerosus, which is referred to as 'differentiated VIN'. Usual VIN accounts for approximately 80% of VIN cases, and differentiated VIN accounts for a smaller percentage (~20%) (van de Nieuwenhof et al., 2011). Differentiated VIN is more common in older women and results in differentiated keratinised squamous cell carcinoma, whereas usual VIN tends to progress to non-keratinising squamous cell carcinoma and occurs in younger women. Regression of 'usual VIN' to normal epithelia is common (van de Nieuwenhof et al., 2008). The two pathways associated with usual and differentiated VIN are illustrated in Figure 1.4. The rest of this chapter will describe usual VIN (HPV related), which will be referred to as VIN.

In 1912 Bowen first described neoplastic squamous epithelial lesions and the disease was subsequently termed 'Bowen's disease (Kaufman, 1995). However, more recent classification of intraepithelial neoplasia by International Society for the Study of Vulvovaginal Disease (ISSVD) has resulted in the preferential use of VIN as terminology for this disease.

HPV DNA was first detected in vulval lesions in 1982 and has been detected in 86.7 % of VIN cases worldwide (de Sanjose et al., 2013). Early studies showed that HPV 16 DNA was found to

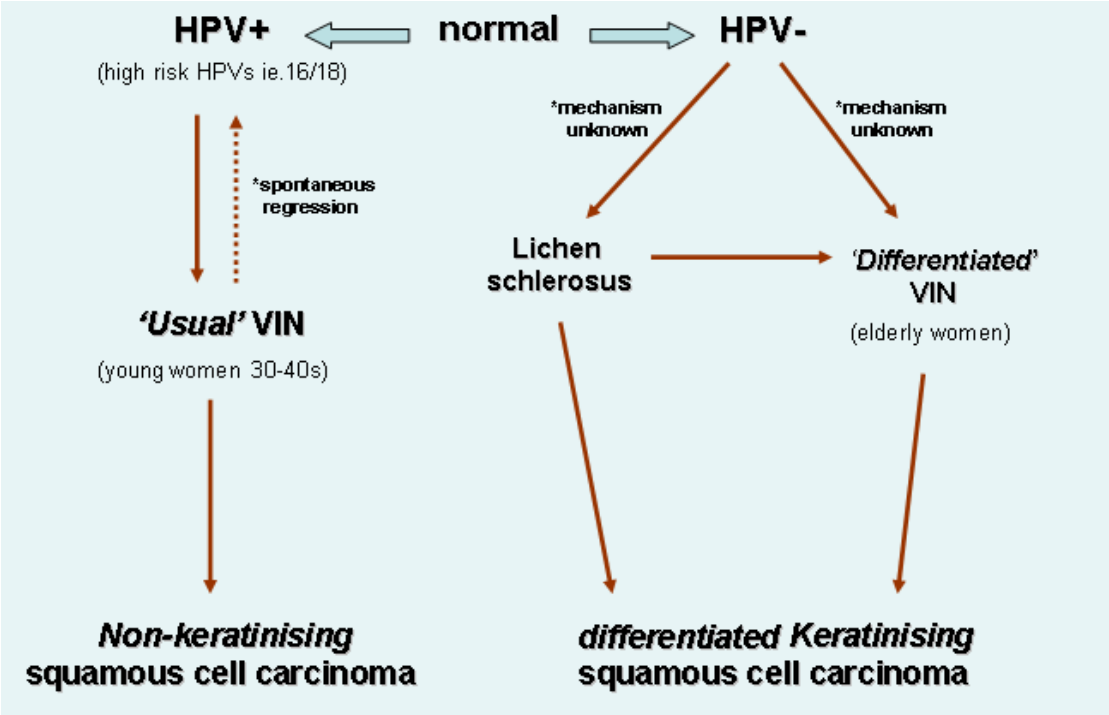

Figure 1.4. Two pathways to vulval intraepithelial neoplasia (VIN) and progression to squamous cell carcinoma

Adapted from (van de Nieuwenhof et al., 2008).

be actively transcribed in multifocal and multicentric VIN lesions, suggesting a role of HPV in pathogenesis of VIN (van Beurden et al., 1995).

1.2.1 Epidemiology of VIN and cancer

In a recent report, HPV DNA was detected in 86.7% (587) of VIN cases and 28.6% (1709) invasive vulval cancers (de Sanjose et al., 2013). In invasive cancers, HPV 16 was found to be the most common type (72.5%) followed by HPV 33 (6.5%) and HPV 18 (4.6%) (de Sanjose et al., 2013). In a meta-analysis by De Vuyst and colleagues, HPV infection was investigated in VIN 1 and 2/3 (De Vuyst et al., 2009). In VIN 1, HPV 16 DNA was detected in 9.8%, and low risk HPV 6 and 11 DNA was detected in 22.4% and 9%. In VIN 2/3, HPV16 (71.9%), 33 (8%) and 18 (5%) were the most frequent HPV types detected (De Vuyst et al., 2009). HPV 16 was also found to be the most prevalent type in a a separate meta-analysis of type distribution study of vulval and vaginal cancers (Smith et al., 2009).

Usual VIN is most common in young women between the ages of 20 and 30. Since usual VIN is highly associated with HPV infection, the increasing prevalence of HPV and HPV related genital infection is thought to contribute to the increasing incidence of VIN worldwide (incidence of 5/100, 000 women per year)(Joura, 2002). Even though the incidence of VIN is increasing, the relationship between incidence of VIN and vulval carcinoma is not directly proportional. Various factors are thought to contribute to this, for example, improved rates of diagnosis and treatment, and the high frequency of spontaneous disease regression. The increase in HPV associated VIN without similar increase in invasive vulvar carcinoma may be explained through the application of diagnostic vulval biopsy, and thus earlier diagnosis and treatment. Treatment is then likely to prevent progression of neoplastic disease to cancer (van de Nieuwenhof et al., 2008) (Kautman 1995).

1.2.2 Risk factors

The risk factors of VIN are similar to those for HPV infection and include; age, tobacco use, history of genital warts, immunosuppression, and a high number of sexual partners (van de Nieuwenhof et al., 2008). In relation to age as a risk factor, HPV is the aetiological agent of disease, and is more prevalent in younger populations that are at the height of sexual activity.

1.2.3 Histology and characterisation of VIN

The system provided by the International Society for the Study of Vulvovaginal Diseases (ISSVD) is the preferred grading system for determining VIN severity, since it is capable of distinguishing between the type of VIN (usual or differentiated), which is not considered when using Bethesda classification. Prior to update by ISSVD, the grading system measured an approximate percentage of dysplastic cells within a cross section of differentiated epithelia from a punch biopsy of suspicious vulval tissue; this is consistent with the grading of CIN (Figure 1.3). Revised terminology in 2006 no longer characterises VIN I due to its poor reproducibility, although this is not universally accepted (McCluggage, 2009).

Usual VIN lesions are easy to recognise microscopically. They demonstrate 'wind-blown' epidermis and disorganised keratinocytes with an array of nuclear abnormalities. There are 2 types of usual VIN lesions which demonstrate thickened epidermis and hyperkeratosis, these are 'warty' (textured surface) and 'basaloid' (flattened surface), and both lesions can occur in the same region (van de Nieuwenhof et al., 2008).

1.2.4 Clinical manifestations and symptoms

Usual VIN primarily affects the labia majora, labia minora and posterior fourchette although it occasionally occurs at the mons pubis, perineal and perianal regions. Dysplastic regions appear raised or asymmetrical and can be discoloured (white/reddened) or pigmented (Figure 1.5). Between 25-66% are multicentric (lesions are present at more than one genital region) which

Figure 1.5. VIN 3 lesion

The VIN 3 lesion extensively affects the labia, which is characteristically raised and discoloured. Taken from (Tristram and Fiander, 2005).

signifies the importance of cervical screening as a precaution when VIN is diagnosed (van Beurden et al., 1998). Additionally, more than one VIN lesion can occur in the same region (multifocal). Eighty one percent of VIN 3 cases were multifocal (van Beurden et al., 1995).

The majority of patients experience pruritus, and other symptoms include pain, ulceration and dysurea. Significant sexual and psychological stress is associated with disease (Shylasree et al., 2008). A substantial portion of sufferers do not have symptoms and discover vulval abnormalities during self-examination or examination related to cervical screening (van de Nieuwenhof et al., 2008).

1.2.5 Treatment options, patient management and disease prevention

Usually VIN is treated with surgery, although other treatments have been assessed with varying degrees of success (van de Nieuwenhof et al., 2008). The clinical objectives of treatment aim to prevent progression to invasive carcinoma, relieve symptoms, eradicate HPV infection, and sustain remission whilst preserving healthy normal tissue and maintaining genital function (van de Nieuwenhof et al., 2008). Treatment strategies that target VIN lesions without affecting healthy tissue are desirable, particularly through topical treatments, which would cause less distress to patients, can be applied easily, and reduce hospital visits.

1.2.5.1 *Surgery*

Surgery involves excision of VIN using a cold knife, diathermy or laser ablation. There are advantages and disadvantages for all surgical techniques and surgical success varies according to recurrence rates demonstrated post-surgery (Bruchim et al., 2007). The preferred route of surgery involves multiple local excisions over an extended time period rather than extensive surgery because this better preserves the remaining vulval tissue and is less significantly associated with physical, psychological and sexual trauma (Campion and Singer, 1987). Extensive, repeat surgery as a result of recurrence has the potential for genital mutilation and

associated morbidity. There is therefore a desire for alternative treatment options (Campion and Singer, 1987).

1.2.5.2 *Photodynamic therapy*

Photodynamic therapy causes cell death through the formation of highly reactive oxygen species; a topical photosensitizer and light of an appropriate wavelength are combined to destroy tissue (van de Nieuwenhof et al., 2008).

1.2.5.3 *Imiquimod*

Imiquimod (Aldara®) is an imidazoquinoline amine which acts as an immune response modifier. It also inhibits viral replication, thereby focusing on the cause of usual VIN (HPV) without having an effect on healthy vulval tissue (van de Nieuwenhof et al., 2008). Small-scale studies using topical applications of imiquimod have shown encouraging results (van Seters et al., 2008) and it is currently registered to treat genital warts

1.2.5.4 *Cidofovir*

Cidofovir is an acyclic nucleoside phosphonate and has antiviral properties against a range of DNA viruses. It has been clinically investigated for topical treatment of VIN (Tristram and Fiander, 2005), and showed promising results (described in more detail in the following section). The use of CDV as a topical treatment for VIN would be desirable because it would be less distressing for patients than surgery, and could be applied by the patient and therefore reduce hospital visits.

1.3 Development of acyclic nucleoside phosphonates (ANPs)

Collaboration between De Clercq and colleagues in 1976 resulted in the exploration of new acyclic nucleoside analogues (ANA) for use as antivirals. The first ANA, called DHPA [9-(2,3-

dihydroxypropyl)adenine], was shown to act as an adenosine analogue and demonstrated inhibition of viral RNA maturation. Early ANAs were then supplanted by Acyclic Nucleoside Phosphonates (ANP) which have a phosphonate group chemically attached to the alkyl side chain of purine or pyrimidine molecules (Ballatore et al., 2001). ANPs display broad-spectrum antiviral activity against a range of DNA and RNA viruses as well as displaying anti-neoplastic activity (De Clercq, 2011). ANPs include (S)-9-(3-hydroxy-2-phosphonylmethoxypropyl) adenine (HPMPA). Discovered in 1986 HPMPA was a prodrug i.e. it required metabolic activation, and displayed a wide spectrum of activity against DNA viruses. However HPMPA was not developed further, but a year later the antiviral properties of (S)-9-(3-hydroxy-2-phosphonylmethoxypropyl) cytosine (HPMPC), also referred to as Cidofovir (CDV), were described (De Clercq, 2011). Similar to HPMPA, CDV is a prodrug and demonstrated antiviral activity against a wide range of DNA viruses (De Clercq, 2011). CDV is currently approved for CMV infection, but is also potentially an effective treatment option for benign and premalignant vulvar and extra-genital HPV lesions, including VIN (Snoeck et al., 2001, Tristram and Fiander, 2005). Currently, CDV is clinically approved and marketed under the branding Vistide®.

1.3.1 Antiviral action of cidofovir

The mechanism of action of CDV in CMV infections is well characterised (Xiong et al., 1997). CDV is a water-soluble polar molecule and is taken into cells passively by endocytosis (Van Pachterbeke et al., 2009). Once inside the cell, CDV undergoes two phosphorylations to yield the active metabolite, Cidofovir diphosphate (CDVpp), through the process illustrated in Figure 1.6 (Cihlar and Chen, 1996). The first phosphorylation is catalysed by GMP kinase/AMP kinase to produce CDVp and the second by nucleoside diphosphate kinase (NDP) to produce CDVpp. The resulting CDVpp is referred to as the active triphosphate form, and termed ‘triphosphate’ since 1 phosphate comprises the phosphonate bridge prior to the first and second

phosphorylation events, so that 3 phosphate molecules in total are present in the active form of the molecule. CDVpp is structurally similar to naturally occurring nucleotides and hence acts as a competitive inhibitor and an alternative substrate for CMV DNA polymerase, as shown in Figure 1.7 (Xiong et al., 1997). CDVpp is then incorporated into a growing strand of DNA complimentary to dGMP; the incorporation of a second CDVpp molecule (i.e. incorporation in tandem) is required to inhibit DNA elongation (Xiong et al., 1997). This is related to the availability of the 3' OH which aids in addition of adjacent nucleotides to the growing nucleotide sequence. Since classical acyclic nucleoside analogues do not exhibit the hydroxyl group, only one insertion into the extending nucleotide chain is required which results in complete termination of nucleotide elongation. CDV also produce a longer lasting viral response than their classical acyclic nucleoside counterparts because CDV phosphorylated metabolites provide a long intracellular half-life.

1.3.2 Current clinical applications

CDV has demonstrated activity against a broad range of DNA viruses, particularly amongst herpes viruses (herpes simplex virus (HSV) 1 and 2, varicella zoster virus (VZV), cytomegalovirus (CMV), Epstein-Barr virus (EBV) and human herpesviruses 6-8) as well as other viruses such as pox viruses, adenovirus and HPV. It is the only licensed antiviral stockpiled for the therapy and short term prophylaxis of small pox (variola) and small pox vaccination (vaccinia) complications (De Clercq and Holy, 2005). CDV is currently licensed for the treatment of CMV related retinitis in AIDS patients, demonstrating antiviral activity by inhibiting CMV DNA synthesis within infected cells via the mechanism previously described.

Over the past decade CDV has demonstrated significant selectivity for adenovirus infected and high risk (HR) HPV immortalised cell lines *in vitro* (Andrei et al., 1998) and shown promising results in a number of clinical trials involving topical and intralesion treatment of patients with

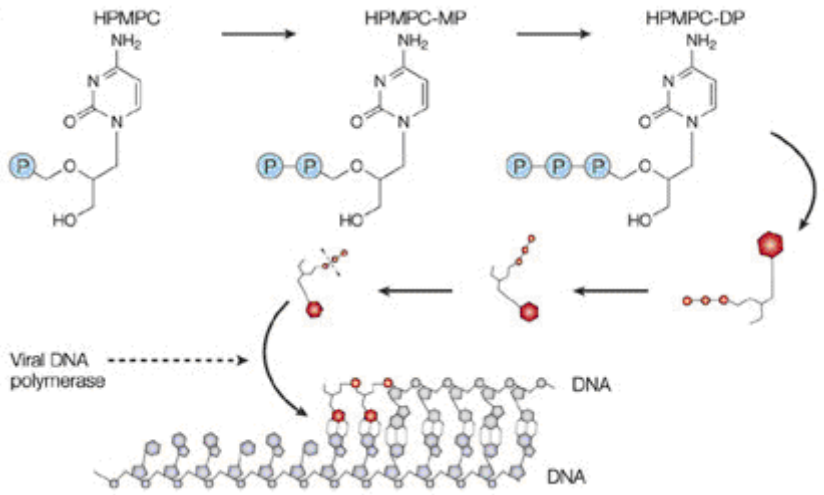

Figure 1.6. Illustration of phosphorylation events required to produce active cidofovir (CDV)

Active CDV acts to competitively incorporate itself 'in tandem' into the growing nucleotide sequence which reduces the rate of viral DNA synthesis. Adapted from (De Clercq and Holy, 2005)

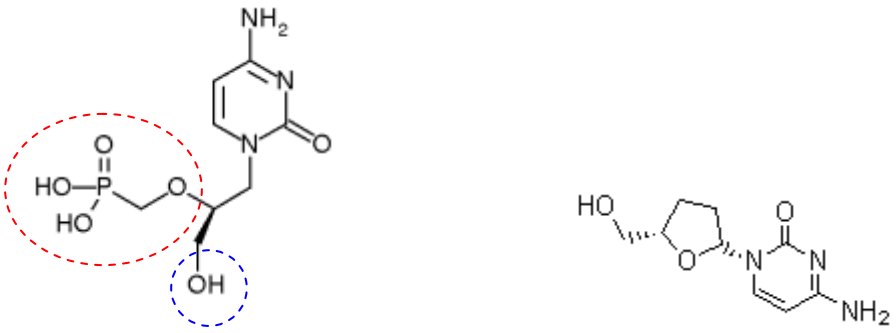

Figure 1.7. Structures of cidofovir and deoxycytidine

(**A**) Structure of Cidofovir: presence of phosphonate bridge (circled red) and available 3'hydroxyl group (circled blue) required for binding of adjacent nucleotide for nucleotide sequence extension during DNA synthesis. (**B**) Structure of deoxycytidine: normal substrate of DNA synthesis (cidofovir represents its analogue).

productive and non-productive HPV infection (Van Pachterbeke et al., 2009, Calista, 2009, Koonsaeng et al., 2001, Snoeck et al., 2000, Stragier et al., 2002).

1.3.2.1 *Molecular effects in HPV infected cells*

In vitro studies using CDV have demonstrated positive effects on HPV infected cells suggesting a potential therapeutic value and providing some molecular rationale. However, the mechanism of action of CDV in HPV infected cells remains elusive and is thought to differ to that described for CMV infection since HPV does not encode its own viral DNA polymerase. In one study, the molecular effects of CDV were examined at concentrations ranging from 0.5 to 200 μg/ml (1.6 - 635 μM) over 7-8 days in several HPV positive tumour cell lines including CaSki, Siha and Hela (Andrei et al., 2000). Higher concentrations of CDV (> 15 μg/ml) were observed to result in induction of apoptosis, which was assessed by DNA fragmentation, caspase activation, Annexin V staining and increased levels of p53 protein.

A study by a different group (Johnson and Gangemi, 1999) treated keratinocytes transformed with HPV16 E6 and E7 and untransformed controls with CDV at doses ranging from 0.1 – 2 μM for 14 days (with treatment 3 times per week). Under these conditions, inhibition of cell proliferation was noted in both transformed and untransformed cells. HPV transformed cells appeared to be more vulnerable to this effect, with a 95% reduction in cell counts in the transformed cells relative to untransformed in the 2 μM sample. The authors did not observe DNA fragmentation but used fluorescent cell sorting to show that cells accumulated in S phase. They hence interpreted CDVs action as cytostatic rather than cytotoxic. These results are consistent with the time and concentration dependence described in Andrei et al. (2000). The authors suggested that the selectivity of CDV for HPV transformed cells was due to altered metabolism of CDV due to modulation of cellular kinases in HPV transformed cells. This was confirmed by assessment of CDV anabolism using radio-labelled CDV and liquid scintillation

counting of HPLC fractionated cell extracts, which showed higher levels of CDVpp in HPV positive cells.

Another *in vitro* study using cervical carcinoma and head/neck squamous cell carcinoma cell lines, suggested that 10 μg/ml CDV over 3-6 days could induce accumulation of p53 and pRB specifically through reducing the expression of E6 and E7 at the transcriptional level, although this effect was modest (50% reduction in E6/E7 transcripts at 3 days post treatment) and was based on experiments performed using semi-quantitative RT-PCR (Abdulkarim et al., 2002). The authors demonstrated nuclear accumulation of p53 after CDV treatment and suggested that reduced E6/E7 expression revived tumour suppressor pathways that regulate the cell cycle resulting in G2/M blockage and accumulation of HPV positive cells in S phase. There was no increase in apoptotic cell death and the absence of apoptosis in response to 10 μg/ml CDV was confirmed by TUNEL assay. In the same study, decreased expression of cyclin A corresponded with accumulation of cells in S-phase of the cell cycle demonstrating inhibition of cell proliferation. This study also suggested that combining radiation and CDV might have therapeutic value; irradiation may cause up-regulation of *E6* and *E7* expression, however in conjunction with CDV, radiation did not cause up-regulation of *E6* and *E7* expression. Abdulkarim and colleagues also suggested that there was a synergistic effect between CDV and ionising radiation and that this effect was greater in HPV positive cells. However this was based on a comparison of HPV positive tumour cell lines with HPV negative tumour cell lines, not on comparison of HPV positive tumour cell lines with non-malignant cells.

In summary, several studies have shown that CDV results in inhibition of cell proliferation, and some studies report selectivity for HPV transformed cells. These results might be explained by a model in which, in HPV infected cells expressing E6 and E7, CDV interferes with *E6/E7* at the transcriptional level causing down regulation of oncogenes which results in revival of protein

suppressor pathways (up-regulation of p53 and p21). This could encourage negative control of cell cycle progression and also induce apoptosis in HPV infected cells.

More recently, CDV has demonstrated anti-metastatic action in an *in vitro* assay by reducing transcription of *E6* and *E7* (Amine et al., 2009). E6 and E7 positive lung carcinoma cells demonstrated upregulation of *CXCR4* gene expression (which is implicated in the signalling mechanism for metastasis), which was reversed by *E6/E7* knockout. CDV also demonstrated inhibition of Rho/ROCK signalling pathways which also contribute to tumour cell invasiveness.

1.3.2.2 *CDV toxicology*

Genotoxicity studies showed that CDV was not mutagenic in the Ames test. However, it showed a dose dependent clastogenic effect (i.e. results in chromosomal breaks) in human peripheral lymphocytes and it was clastogenic at high toxic/lethal doses in the *in vivo* mouse micronucleus assay. The product characteristics for CDV summarised by the European Medicines Agency states that CDV is clastogenic *in vitro* at 100 µg/ml (European Medicines Agency, 2011).

1.3.2.3 *Clinical potential of cidofovir treatment*

Several studies have demonstrated the potential use of CDV as an alternative treatment therapy for HPV/cancer related diseases *in vivo* as well as *in vitro*. Studies on consenting patients have been carried out to gain a better understanding of the effects of CDV treatment on lesions *in vivo*. A study using 1% CDV in Beeler base and 2.5 mg/mL CDV injection successfully treated 3 out of 4 patients presenting with diverse anatomical HPV-associated benign lesions that had relapsed following previous alternative treatments (Stragier et al., 2002).

High risk HPV related cervical intraepithelial neoplasia (CIN) contributes significantly to morbidity in women, particularly as a result of cancer progression. Alternative therapies to surgery are attractive, since many young women with CIN want to preserve their anatomy. The use of topical CDV was investigated in a preliminary study including 15 CIN III patients (Snoeck et al., 2000). Once percent CDV gel was applied to the cervix, 3 times every other day for 1 month after which the cervix was surgically removed and histology examined and HPV-PCR carried out. Complete or partial response occurred in 13/15 patients. There were no toxic effects and normal/uninfected epithelia remained unaffected. Similarly, topical treatment of CIN II and III patients with 2% CDV was carried out in a phase II, double-blind, prospective, placebo controlled trial (Van Pachterbeke et al., 2009). Fifty three women were randomised to receive topical CDV (2% gel) or placebo. Colposcopic analysis of cervical appearance after CDV treatment showed ulceration to infected lesions (consistent with apoptosis) but preservation of surrounding normal epithelia. Complete clearance of the CIN lesion was observed in 60.8% of the treatment arm and in 20% of patients receiving placebo.

Positive responses to CDV have also been reported in small studies involving patients with usual and differentiated vulval intraepithelial neoplasia (VIN) (Calista, 2009, Koonsaeng et al., 2001). The most significant recent study of VIN by Tristram & Fiander (Tristram and Fiander, 2005) assessed the application of CDV (1% gel) in 12 women presenting with biopsy proven VIN III lesions. After written informed consent, a punch biopsy was taken for histology examination and HPV-PCR was performed prior to the start of treatment. Lesions were self-treated on alternate days for 16 weeks with vulvoscopy at 4 week intervals to assess symptoms. At 16 weeks a clinical response, based on recorded symptoms, clinical and photographic evidence and HPV status/histology (via punch biopsy), was obtained. Ten of twelve women completed follow up; 4 demonstrated viral clearance/normal histology (complete regression) and 4 women partially responded (their lesions were reduced by at least

50%). During treatment, symptoms such as pain and ulceration were occasionally recorded and the study also demonstrated that infected hair follicles do not improve after topical treatment (Tristram and Fiander, 2005). This study demonstrated the prospective use of CDV for VIN therapy and justifies further investigation. The study also showed that in clinical practice the effects of CDV appear specific to the VIN lesion and did not cause ulceration of the surrounding normal tissue. Images from this pilot study are shown in Figure 1.8 (kindly provided by Dr Tristram).

1.4 RT3VIN

In areas affected by VIN, preservation of healthy tissue would be an advantage. Current treatment strategies such as excision surgery are invasive and sometimes mutilating. In spite of obvious advantages such as ease of use through self-administration and fewer hospital visits, there is no licensed topical treatment option for VIN (Shylasree et al., 2008). RT3VIN is a multi-centre randomized phase II clinical trial of topical Imiquimod and CDV in women with usual and differentiated high grade VIN (International Standard Randomised Controlled Trial Number (ISRCTN) Register, 2013). Patients were recruited to the trial from October 2009 to January 2013.

Women were eligible if: they were older than 16 years of age at trial commencement; they agreed to using efficient contraception for the duration of the trial; they had a VIN 3 biopsy taken no longer than 3 months previous to entering the trial, which was ≥ 20 mm in diameter. Patients with perianal disease could be included but the disease must not have extended into the anal canal. Finally, patients had to give a three way written informed consent (for screening, trial and cross-over).

Exclusion criteria of the trial included: Patients with current invasive vulval or anogenital carcinoma; Pregnancy, breastfeeding or patients trying to conceive; Patients who were

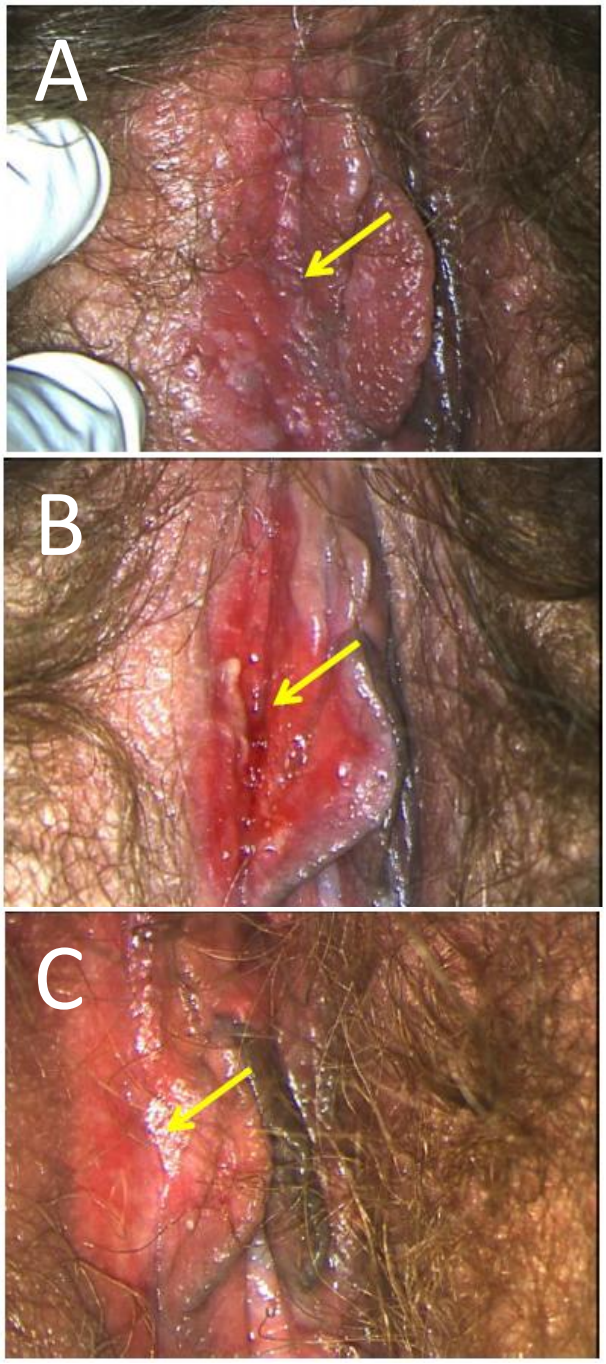

Figure 1.8. Treatment of VIN with CDV

(**A**) VIN lesion before treatment, (**B**) VIN lesion during treatment (ulceration visible), and (**C**) post treatment (lesion cleared). Images kindly provided by Dr Tristram (School of Medicine, Cardiff University).

unresponsive to previous treatment with CDV or Imiquimod; Patients with impaired renal function; Patients who were unable to comply with protocol treatment; Patients who were undergoing treatment or had treatment in the previous 4 weeks. A total of 180 patients were recruited and randomized on a 1:1 basis to either CDV or Imiquimod using a Fleming single-stage design. Topical treatments (CDV or Imiquimod) were applied 3 times a week for up to 24 weeks. A thin layer of CDV gel or Imiquimod cream was spread over the VIN lesion at night and the area was washed using aqueous cream and water the following day. Patients were advised to avoid contact with the treated area until the area was washed the next day.

For the duration of the trial, regular clinical assessments were used to monitor responses. In addition, Response Evaluation Criteria in Solid Tumours (RECIST) assessments were made. These are a standardised set of published criteria to help assess when patients respond, stabilize, or progress during treatments (Eisenhauer et al., 2009). After 30 weeks a biopsy was taken from each patient to examine the histology of the lesion (even if the lesion was cleared) and to determine HPV status of the tissue.

At the end of the trial, patients were assigned to one of four categories determined by their response to the treatment. The categories were:

1. Complete Response (CR) – all treated lesions disappeared within the 24 weeks
2. Partial Response (PR) – at least a 30% decrease was seen in the pathological severity of the lesion
3. Progressive Disease (PD) – at least a 20% increase in the pathological severity of the lesion was seen
4. Stable Disease (SD) – No positive or negative change was seen in the disease state

At the time of submission of this thesis the clinical results of the RT3VIN clinical trial were under analysis.

1.5 Experimental models of HPV associated neoplasia

A variety of experimental models exist which facilitate development of new treatments and diagnostic tools, contributing to the understanding of health and disease in humans. For ethical reasons, potential drug therapies cannot be administered to humans without prior investigation using other biological model systems. After successful validation in this way, drug therapies can be incorporated in to a clinical trial setting. This section will summarise the experimental models which are currently applied in a laboratory setting, their advantages and disadvantages, and their link with investigation of vulval neoplastic disease.

1.5.1 Murine models

Laboratory mice have been used in preclinical drug tests for many years. These commonly consist of mouse xenografts (i.e. human tissue is introduced in to the body of an immunocompromised mouse for experimentation) or genetically engineered mice (i.e. genetic mutations associated with particular human malignancies are introduced in to the mouse for experimentation). Research using mice has led to advances in treating a number of human diseases. Mice share 99% homology with the human genome with obvious similar biological functions, and with the animal's small size it provides the potential for high through-put studies, which makes murine models particularly appealing. Murine models have been used to investigate treatment strategies in a range of diseases such as cancers (Kogan, 2007, Meuwissen and Berns, 2005, Valkenburg and Williams, 2011), as well as inflammatory disorders, bacterial and viral diseases, and dysfunctions of the central nervous system, etc. Particularly in terms of investigating drug therapies for acute promyelocytic leukaemia (APL), work using mice resulted in successful treatments for a disease that was previously untreatable (Kogan, 2007).

Although murine models are used frequently in research, their relevance is still debated. Various studies have shown that particular drugs have worked well in murine models but have been unsuccessful when translated to human clinical trials (Pound et al., 2004, Hackam and Redelmeier, 2006, van der Worp et al., 2010, Rice, 2012). To address this uncertainty, in 2010 the European Commission proposed investigation in to the usefulness of using mice as preclinical models. It was briefly concluded that murine models do not aim to fully model disease or disease mechanisms but rather set out to obtain specific functional information; murine models have previously proven effective in some cases; genetically modified mice need to be validated, reproducible, robust and cost-effective to be considered optimal by the pharmaceutical industry.

Some studies on CDV have been conducted using mouse models (Andrei et al., 1998) using xenografts of cervical cancer cells (Siha) into athymic mice. Intertumoural injections of CDV resulted in reduced growth of tumours but topical and systemic application of CDV was ineffective.

1.5.2 Cell culture models

Cell culture refers to the removal of cells from an animal or plant and their subsequent growth in a favourable artificial environment, usually through aseptic methods within a laboratory setting. Primary cells refer to the outgrowth of migrating cells from a piece of tissue or from homogenised tissue preparation (Freshney, 2005b). Primary culture refers to initial growth of cells after isolation from animal tissue, and after this cultures are referred to as cell lines. Normal cell lines (i.e. those that do not have neoplastic/oncogenic potential) replicate a limited number of times before becoming senescent. Other cell lines with oncogenic potential, as a result of spontaneous, chemical, or viral induction, or from being derived from a cancer, can replicate continuously; these cell lines are referred to as immortalised. The method of culturing cell lines is a selective process; continual replication allows cells in a culture with a

growth advantage to predominate, which eventually results in a cell culture containing cells with a high degree of homology. Clonal cell lines can be derived from cell lines by selecting single cells and culturing them individually so that they establish as a clonal population of cells (Freshney, 2005b).

Cell culture can be used for studying cellular and molecular biology, providing insight in to the normal physiology and biochemistry of cells. It is also useful for assessing the cellular effects of drugs and other toxic compounds, as well as investigations in to diseases and disorders, particularly cancer. Use of cell culture for recombinant DNA technology and genetic manipulations are also important in the field of biotechnology.

The major advantage of using cell culture for any application is the consistency and reproducibility of results that can be obtained from a population of clonal cells, particularly in terms of assessing response to drug treatment where a population of identical cells are desirable. Immortalised cells derived from tumours or transformed intentionally, grow very efficiently in culture and have been successfully used to investigate the biology of certain cancers, as well as therapeutics (Weinberg, 2013). Primary cell cultures are a good *in vitro* representation of disease because they are closely related to the tissue from which they are derived and give a better reflection of disease seen clinically (Burdall et al., 2003). The major disadvantage of primary cells is that they can be fastidious, slow growing, and may not be a renewable resource.

1.5.3 HPV related VIN and VaIN cell culture models

There are few studies in the literature describing the isolation or use of cell culture models of vulval or vaginal neoplastic disease, and both studies to be described were published over a decade ago. The study by Hietanen et al. (Hietanen et al., 1992) describes the explantation of a VaIN cell line (UT-DEC-1) from HPV33 positive VaIN I tissue and a cell line (UT-DEC-2) from

HPV16 positive VaIN II tissue, showing that cells from early neoplastic tissue were capable of continual culture for 40 and 25 passages respectively; this study produced a cell culture model which could be used to investigate early stages of squamous cell carcinogenesis *in vitro.* The study by Schneider-maunoury et al. (Schneider-Maunoury et al., 1987) involved the use of a cell line (SK-v) established from a vulval biopsy infected with HPV16, specifically found to be integrated within the E2 and L2 ORFs. A combination of investigative models contributed to this study; the use of a murine model confirmed that tumours with histological features of vulval carcinoma *in situ* were induced when SK-v cells were injected in to a mouse. Thereafter the SK-v cell culture model itself was used to investigate the biology of HPV integration. However none of the lines mentioned in these two papers appear to have lead to the insights, or a vast array of publications, produced by the W12 cervical line (Stanley et al., 1989).The majority of other studies tend to use HR HPV immortalised cell lines derived from tumours such as SiHa, CaSki, and HeLa to investigate HPV related anogenital disease (Johnson and Gangemi, 1999, Andrei et al., 1998, Andrei et al., 2000, Amine et al., 2009, De Schutter et al., 2013, Johnson and Gangemi, 2003). The derivation and characteristics of these lines are described briefly, as follows:

CaSki: HPV 16 positive (c. 600 copies at multiple sites), derived in 1977 from a small bowel metastases of a cervical tumour in 40 yr old Caucasian female (American Type Culture Collection (ATCC), 2012b). SiHa: HPV 16 positive (single copy), derived in 1970 from a primary cervical tumour in a 55 yr old Asian female. Modal chromosome number = 71 (American Type Culture Collection (ATCC), 2012d). HeLa: HPV 18 positive, derived in 1953 from a primary adenocarcinoma in a 31 year old Black female. Modal chromosome number = 82 ((American Type Culture Collection (ATCC), 2012c). C33A: HPV negative, derived in 1964 from a primary cervical tumour in a 66 yr old Caucasian female (american Type Culture Collection (ATCC), 2012a).

Immortalised cell lines are easily obtainable, since they are distributed widely in the scientific/medical research community, and their non-fastidious growth in culture makes them a desirable option for cell culture. However, in terms of assessing neoplastic disease *in vitro,* there is considerable difference between neoplastic cells and tumour cells and therefore experimental outcomes have limited relevance to pre-cancerous disease presenting in patients.

1.6 Transcriptome sequencing

mRNA sequencing was performed as part of the current study. A brief introduction to the subject is given below.

The transcriptome of a cell is the collection of RNA molecules that are present in a cell at a given time. It is a dynamic entity and is significant because it consists of the transcripts that generate cellular proteins, which determines the biochemical functions of the cell. The field of transcriptome investigation is referred to as transcriptomics.

1.6.1 RNA sequencing of the transcriptome (RNA-seq)

Over the past decade, microarrays have been the primary tool to investigate the transcriptome. More recently the use of next-generation sequencing technology has emerged as a potentially superior technology for obtaining quantitative expression profiles, and is commonly referred to as RNA-Seq. RNA-Seq is an effective method of generating precise measurements of transcript levels and does not limit the detection of transcripts to only those present on a pre-defined chip, hence both known and unknown transcripts can be investigated. RNA-Seq also enables quantification of very large dynamic expression levels, with absolute values rather than relative values (Wang et al., 2009).

1.6.1.1 *AB SOLID RNA-seq*

To date RNA-seq has been performed in various eukaryotic and prokaryotic organisms using different RNA-Seq platforms, such as Illumina IG (Nagalakshmi et al., 2008) Roche 454 Life Science (Emrich et al., 2007) and AB SOLiD (Cloonan et al., 2008). The RNA-Seq platform selected is dependent on the overall objective because each platform has slight variations in error rate, although all methods effectively generate transcriptome data. AB SOLiD and Illumina provide the lowest sequencing error rate and also offer a greater sequencing depth, which allows lowly expressed transcripts to be detected more easily (Metzker, 2010).

1.6.1.2 *Genome wide assessment of gene expression in CDV treated HPV positive cells*

There are limited studies in the literature that have investigated the transcriptomes of HPV infected cells that have undergone treatment with CDV. One other study has previously examined the transcriptional response to CDV using genome wide technology. This was a study by De Schutter and colleagues which examined SiHa (HPV16+), HeLa (HPV18+) and HaCaT (HPV negative) immortalized cell lines and primary human keratinocytes at 24, 48 and 72 hours post treatment with 50 µg/mL (159 µM) CDV using whole genome gene expression microarrays; validation of array data was performed using RT-qPCR (De Schutter et al., 2013). In SiHa cells, 20 genes showed similar changes in expression in both the 48 and 72 hour samples. Expression was also examined in HeLa, HaCaT and normal keratinocytes at 72 hours. Only 2 genes (AOX1 and CLIC3) were differentially expressed in all 4 cell lines. Gene ontology analysis of differentially expressed genes showed 'immune response' and 'inflammatory response' to be the only functional groupings which were significantly up-regulated in all four cell lines. Further functional analysis showed that HPV positive cells showed differential regulation of genes linked to 'cell death of tumour cells' following CDV treatment.

1.7 Chapter introductions

There is a distinct lack of literature surrounding the effects of CDV using a relevant *in vitro* model of VIN. The overall aim of the study was to isolate, characterise and make use of a series of novel VIN/VaIN short term cultures to assess response to CDV treatment.

In this project, interrelated studies were devised and presented as individual chapters. Aspects of each chapter are relevant to other chapters, and the results of earlier studies influenced the design of later studies.

1.7.1 Chapter 3: Phenotypic characterisation of short term VIN and VaIN cell cultures

The initial aim of this investigation was to derive a series of clonal cell lines from naturally occurring HPV16 infected heterogenous cell lines of vulval and vaginal origin. These clonal lines formed the basis of the entire project. The major steps involved single cell cloning and maintaining clonal cell lines in short-term culture. At each passage during this time, a selection of clonal lines were characterised in terms of cell morphology and growth rate, essentially to confirm the stability of the lines. This body of work also incorporated historical data for the parental heterogeneous lines for growth rate comparison.

1.7.2 Chapter 4: Preliminary cell culture and optimisation studies

Preliminary studies are presented secondly because they formed a platform for the standard and consistency of cell culture work carried out throughout the rest of the project. However this work was actually performed before characterisation data was obtained, which is presented in the chapter before (3) and after (5). Preliminary studies were performed using a select few clonal cell lines that were the first to establish in culture (i.e. post isolation from parental lines). It was important to carry out preliminary investigations before progressing to

fully characterising each cell line so that key parameters of cell culture could be established to ensure stability and usability of the cells.

1.7.3 Chapter 5: Molecular characterisation

This chapter linked with chapter 3, whereby clonal cell lines in short-term culture were characterised further at a molecular level. Techniques which had previously been optimised, such as Amplification of Papillomavirus Oncogene Transcripts (APOT) and Detection of Integrated Papillomavirus Sequences (DIPS), were used to determine the status of HPV infection within the different clonal cell lines to investigate whether HPV had integrated in to the host genome (or remained separate in the form of an episome). Relative expression of HPV genes was also investigated through qRT-PCR to obtain expression profiles for each clonal cell line and assess stability over time.

1.7.4 Chapter 6: Optimisation of CDV dosing protocol

There are limited and inconsistent studies in the literature describing *in vitro* CDV dosing protocols in HPV related disease; inconsistency lies at the level of the type of cell culture model, drug concentration and exposure, as well as the dosing protocol time-frame. This section of work describes the design of a dosing protocol which was performed on the novel, fully characterised clonal cell lines, for validation and optimisation purposes. The aim was to produce a final CDV dosing regime that would be used to assess response to CDV treatment in the following chapter (7).

1.7.5 Chapter 7: Response to CDV in clonal cell lines

The final CDV dosing protocol, established through the work carried out in chapter 6, was used on a select group of clonal cell lines and a HPV negative control cell line to investigate response(s) to CDV. The aim here was to identify the molecular mechanism(s) of action of CDV in an *in vitro* cell culture system which closely reflects high grade vulval and vaginal disease

seen clinically. Response(s) to CDV were focussed on assessing changes in cell morphology and gene expression profiles. The literature suggests (in a variety of HPV infected cell models, and dosing strategies) that CDV affects expression of E6 and E7 and may induce apoptosis. It has also been suggested that HPV infected cells are more sensitive to CDV compared to cells which do not contain HPV; these hypotheses were explored in this section of work.

1.7.6 Chapter 8: Whole transcriptome sequencing

Extra funding was provided to perform RNA sequencing of CDV treated and untreated clonal cell lines. This is the first documented description of RNA-seq on HPV16 infected vulval or vaginal keratinocytes. This body of work allowed the entire transcriptome to be explored, which avoided limiting the focus to particular gene transcripts of certain molecular pathways, for example, apoptosis pathways, which were stated in the current literature. Instead RNA-sequencing provided more insight in to the action of the drug by encompassing the differences in all gene transcripts between treated and untreated clonal cell lines (differential gene expression). Whole transcriptome sequencing also provided a means of validating the HPV integration and gene expression data generated in chapter 5.

1.7.7 Central aims

The overall aims of the project are as follows:

1. Revive cryopreserved parental cell lines.
2. Derive vulval and vaginal clonal cell lines from parental lines (produce a novel cell culture system).
3. Maintain clonal cell lines in short-term culture (for at least 5 passages).
4. Characterise clonal cell lines,
    i. in terms of morphology and rate of proliferation
    ii. at a molecular level (HPV integration and gene expression).

5. Design, validate and optimise a CDV dosing protocol using novel cell culture system.
6. Investigate the molecular mechanism(s) of action of CDV.

2 Methods and Materials

2.1 Cell lines

A variety of cell lines were cultured during this PhD: vulval keratinocytes (PC08), vaginal keratinocytes (PC09), PC08 and PC09 derived clonal cell lines, 3T3 mouse fibroblasts, human epidermal keratinocytes (HEKn), and CaSki. Details of these cell lines will be described in this section.

2.1.1 Heterogeneous keratinocyte cell lines: PC08 and PC09

A pilot study was carried out by Dr Ned Powell and Professor Alison Fiander (HPV Research Group, Cardiff University) to investigate the feasibility of deriving and culturing primary cell lines from biopsies taken from a 46 year old female with grade III vulval intraepithelial neoplasia (VIN) and a 31 year old female with grade III vaginal intraepithelial neoplasia (VaIN). Ethical approval was obtained from South East Wales Research Ethics Committee (REC Reference number 08/WSE02/32), and risk reviewed by the Joint Trust/University Peer/Risk Review Committee with approval by Cardiff and Vale NHS Trust Research and Development Office. Primary cell cultures of VIN and VaIN were established via explant procedure, producing 2 heterogeneous keratinocyte cell lines named PC08 and PC09, respectively. PC08 and PC09 primary cells were cultured for 19 and 21 passages (p) respectively, and as a result of their long term replication in culture they are referred to as cell lines throughout this thesis. PC08 and PC09 were found to be infected with HPV16 via PCR immunoassay HPV typing, and southern blot revealed entirely integrated HPV at p19 for PC08, and mixed integrated concatenated HPV and episomal HPV at p21 for PC09.

The pilot study confirmed the feasibility of primary culture of VIN and VaIN, and provided 2 continuously replicating cell lines (PC08 and PC09) which formed the initial foundation for the research carried out as part of this investigation.

2.1.2 Clonal cell lines derived from PC08 and PC09

Clonal keratinocyte cell lines were isolated from heterogeneous PC08 and PC09 cell lines. Clonal cell lines derived from PC08 were named M, P, and Y, and clonal cell lines derived from PC09 were named A-L. These clonal cell lines were fully characterised and also used as vulval and vaginal *in vitro* experimental systems for treatment with cidofovir (CDV).

2.1.3 J2 3T3 mouse fibroblasts (3T3 feeders)

J2 3T3 mouse fibroblasts were originally established during cultivation of mouse embryo fibroblasts (Todaro and Green, 1963). They will be referred to more simply as 3T3 feeder cells throughout this thesis. Irradiated 3T3s were used to supplement the growth of keratinocyte cell lines PC08, PC09, and their derivative clonal cell lines. 3T3 feeder cells were obtained from the University of Cambridge, as referenced in (Stanley et al., 1989)

2.1.4 Neonatal human epidermal keratinocytes (HEKn)

HEKn cells are derived from neonatal foreskin and are not infected with HPV. HEKn cells represented a Human papillomavirus (HPV) negative control for CDV dosing studies carried out during this PhD. HEKn cells were purchased from Life Technologies Corporation (Carlsbad, CA).

2.1.5 CaSki

CaSki cell line originated from a cervical cancer that developed in a 40 year old female (Pattillo et al., 1977) and it has since become widely distributed within the scientific and medical research community. Previous studies have shown that CaSki contains 600 copies of concatenated HPV integrated within several chromosomal sites (2, 3, 6, 7, 11, 12, 14, 20, and 21) (Yee et al., 1985, Mincheva et al., 1987). CaSki was obtained from the American Culture Collection (ATCC-LGC) (Teddington, UK) and cultured within the HPV Research Group, Cardiff University, by Dr Dean Bryant; DNA and RNA extracts of CaSki were used as an experimental positive control in several experiments carried out during this investigation.

2.2 Cell culture

This section will describe cell culture conditions, preparation of cell culture reagents, and the protocols used to culture 3T3 feeder cells, HEKn, and PC08 and PC09. Isolation of clonal cell lines from PC08 and PC09 will also be described.

2.2.1 Terminology

The following terminologies are referred to in this section and are defined according to the World Health Organisation (World Health Organization, 2010).

Primary cell culture: "A culture started from cells, tissues or organs taken directly from one or more organisms. A primary culture may be regarded as such until it is successfully subcultured for the first time. It then becomes a 'cell line' if it can continue to be subcultured at least several times".

Cell line: "Type of cell population with defined characteristics that originates by serial subculture of a primary cell population that can be banked; cloning and subcloning steps may be used to generate a cell line. The term cell line implies that cultures from it consist of lineages of some of the cells originally present in the primary culture".

Passage: "Transfer of cells, with or without dilution, from one culture vessel to another in order to propagate them, and which is repeated to provide sufficient cells for the population process".

2.2.2 Cell culture conditions

Cell culture was carried out using aseptic technique within a class II microbiology safety cabinet. In all instances unless otherwise stated, cultures were incubated at 37^{o}C and 5% Carbon dioxide (CO_2) in a humidified incubator containing Copper(II) sulphate ($CuSO_4$) solution

(Sigma-Aldrich Company Ltd, Dorset, UK). Aspirated media and reagents were discarded in hypochlorite solution (Presept) according to manufacturer's guidelines (Fisher Scientific).

2.2.3 Constituents of cell culture media

A number of reagents were required to supplement media before being used for cell culture, these included: cholera toxin, epidermal growth factor (EGF), hydrocortisone, L-glutamine, trypsin-EDTA, and penicillin/streptomycin (PS). Constituents were prepared as shown in Table 2.1.

2.2.4 Preparation of cell culture media

Media used to culture specific cell lines were prepared according to the following protocols.

2.2.4.1 *PC08, PC09, and 3T3 feeder cells*

Sterile Dulbecco's Modified Eagle's Medium (DMEM) was used to culture 3T3 feeder cells. Glasgow Minimal Essential Medium (GMEM) was used to culture PC08 and PC09 (Sigma-Aldrich Company Ltd, Dorset, UK: #G5154). DMEM and GMEM were supplemented with the reagents shown in Table 2.2. Frozen aliquots of reagents were thawed prior to combining with GMEM or DMEM. GMEM was filter sterilised after preparation using Steritop™ vacuum filter cups (500ml) (Millipore EMD Millipore Corporation, Billerica, MA, USA). After filter sterilising GMEM, EGF was added if required; a combination of GMEM without EGF (EGF-), and GMEM containing EGF (EGF+) was used to culture PC08 and PC09, which will be described in latter sections.

Prepared DMEM and GMEM was stored at 4 ^{o}C and warmed to 37 ^{o}C using a hot water bath prior to being used for cell culture.

2.2.4.2 *HEKn cells*

Sterile EpiLife® medium (Life Technologies Corporation, Carlsbad, CA) was supplemented with sterile Human Keratinocyte Growth Supplement (HKGS) (Life Technologies Corporation, Carlsbad, CA) and used to culture HEKn cells. HKGS (5 ml, 100X) was purchased containing 0.2% v/v bovine pituitary extract (BPE), 5 µg/ml bovine insulin, 0.18 µg/ml hydrocortisone, 5 µg/ml bovine transferrin, and 0.2 ng/ml human epidermal growth factor.

EpiLife® medium (500ml) contained 60 µM calcium chloride, as well as various amino acids, trace minerals, other organic compounds and inorganic salts. Sterile EpiLife® medium (500 ml) was combined with 5ml of HKGS, stored at 4^{o}C, and warmed to 37^{o}Cin a water bath prior to being used for cell culture.

2.2.5 3.2.5. Phosphate buffered saline (PBS)

PBS is an isotonic solution and was used to rinse cells. PBS (10X) was prepared using the compounds shown in Table 2.3 and made up in a 1 L duran to 90% volume at pH 7.4 (using 5 M hydrochloric acid (HCl) or Sodium hydroxide (NaOH). The solution was diluted to 1X concentration within 500 ml durans using deionised water and autoclaved. PBS was cooled to room temperature prior to being used in cell culture.

2.2.6 Initiating cultures from cryopreserved cells

This section will described how cell cultures previously stored in liquid nitrogen were used to initiate new (starter) cell cultures in the laboratory. Cryovials (Thermo Scientific, UK) containing 1 ml of frozen cell cultures were taken out of liquid nitrogen storage, using appropriate personal protective equipment, wrapped in tissue and incubated at room temperature until thawed.

Compound	Preparation details
Cholera toxin 100 nM (1000X) (Sigma-Aldrich Company Ltd, Dorset, UK)	Dissolve 0.5 mg in 0.6 ml sterile water Make up to 60 ml with Glasgow Minimal Essential Medium (GMEM) (Sigma) Aliquot in 5 ml Store at 4 ^{o}C
EGF (from murine submaxillary gland) 1 µg/ml (100X) (Sigma)	Dissolve 0.1 mg in 100 ml GMEM Aliquot in 5 ml Store at -20 ^{o}C
Hydrocortisone 1 mg/ml (2000X) (Sigma)	Dissolve 10 mg in 5 ml 100% ethanol Add 5 ml sterile water Aliquot in 250 µl Store at -20 ^{o}C
L-Glutamine 200 mM (100X) (Sigma)	Add 10 ml GMEM to vial (200 nM) Store at 4 ^{o}C
TE (5.0 g/L porcine trypsin and 2.0 g/L EDTA•4Na in 0.9% sodium chloride) (10X) (Sigma)	Add 100 ml to 900 ml sterile 1X PBS Aliquot in 5 ml Store at -20 ^{o}C
PS (100X) (Sigma)	Aliquot in 5 ml Store at -20 ^{o}C

Table 2.1. Compounds used to formulate reagents for preparing cell culture media

3T3 feeder cells		PC08 and PC09	
Constituent	*Volume*	*Constituent*	*Volume*
Dulbecco's Modified Eagle's Medium (DMEM) (Sigma-Aldrich Company Ltd, Dorset, UK)	500 ml	Glasgow Minimal Essential Medium (GMEM) (Sigma)	500 ml
Penicillin/Streptomycin (PS) (100X) (Sigma)	5 ml	100X PS (Sigma)	5 ml
		Foetal Calf Serum (FCS) (Autogen Bioclea, Witshire, UK)	50 ml
Newborn Calf Serum (NCS) (Autogen Bioclear Ltd, UK)	50 ml	Hydrocortisone (50 µg/ml)(Sigma)	250 µl
		Cholera toxin (Sigma)	500 µl
		L-Glutamine (200 nM) (100x) (Sigma)	5 ml
		*Epidermal Growth Factor (EGF) (Sigma)	1 ml per 100 ml GMEM

Table 2.2. Preparation of DMEM and GMEM used to culture 3T3 feeder cells and PC08/PC09 cell lines, respectively

Compound	Weight (g)
NaCl (Fisher Scientific, UK)	80
KCl (Fisher)	2
Na_2HPO_4 (Fisher)	14.4
KH_2PO_4 (Fisher)	2.4

Table 2.3. Compounds used to prepare 1 L (10X) PBS

2.2.6.1 *3T3 feeder cells*

3T3 cells were previously cryopreserved at various cell densities, generally between 5 x 10^5 and 1 x 10 cells/ml, in 1 ml aliquots. When preparing starter cultures of 3T3 feeders, 1 ml aliquot of 3T3 feeder cells was repeat pipetted to mix and re-suspended in a 75 cm flask containing 25 ml DMEM. 3T3 feeder cells were maintained in culture according to the methods described in the following section.

2.2.6.2 *PC08 and PC09*

PC08 and PC09 cells were previously cryopreserved at 5x10^5-1x10^7 cells/ml in 1 ml aliquots. When preparing starter cultures of PC08/PC09, a 1 ml aliquot was repeat pipetted to mix and re-suspended in 5 ml EGF- GMEM within a 6 cm tissue culture (TC) dish (BD Falcon™); 8 x 10^5 irradiated 3T3 feeder cells were then used to supplement PC08 and PC09 cultures. PC08 and PC09 cultures were maintained in culture according to the method described in the following section.

2.2.6.3 *Human epidermal keratinocytes, neonatal (HEKn)*

Cryovials of HEKn cells were previously cryopreserved at >5 x 10^5 cells/ml in 1 ml aliquots. When preparing starter cultures of HEKn, a 1 ml aliquot was repeat pipetted to mix and re-suspended in 10 ml EpiLife®medium within a 25 cm flask (Sigma-Aldrich Company Ltd, Dorset, UK)) and incubated. HEKn were maintained in culture according to the methods described in the following section.

2.2.7 Culture of 3T3 feeder cells

This section describes the methods used to culture, harvest, and irradiate 3T3 feeder cell cultures, according to the protocol used in Professor Margret Stanley's laboratories (Cambridge, Uk) (Stanley et al., 1989).

2.2.7.1 *Seeding and harvesting cultures*

3T3 starter cultures were prepared in 75 cm flasks containing 25 ml DMEM and cryopreserved cell stocks of 3T3s, as previously described. Cultures were incubated until ~80% confluent; confluence referred to the percentage area of the base of the TC dish that was covered by a monolayer of cells, and was concluded via microscopic analysis. At ~80% confluence, media was discarded and the cell monolayer rinsed several times with 10 ml PBS. Cells were trypsinised using 5 ml TE and incubated for 3-5 minutes, during which time cells were viewed at intervals under a light microscope for cell 'rounding'. When cells within the monolayer appeared more rounded/defined, cells were physically detached from the base of the flask by tapping the flask firmly. DMEM (5 ml) was then added to neutralise TE and cell suspensions were transferred from the flask to a 20 ml universal container (Sterilin™, Thermo Scientific, UK) and centrifuged at 1,500 rpm for 5 minutes. The supernatant was discarded and the cell pellet re-suspended in a known volume of DMEM and a viable cell count performed as described in the following section.

2.2.7.2 *Viable cell counts*

A haemocytometer (Camlab, Cambridge, UK) and separate cover slip were taken out of hypochlorite solution, rinsed with cold running water, and allowed to dry. Condensation was created on the cover-slip and counting grid by breathing onto the surface of each. The cover slip was placed on the counting grid with pressure applied either side to ensure a good seal; the presence of 'Newton's rings' and inability to move the glass slide when pressed using a fingernail demonstrated good contact between both glass surfaces.

Trypan blue stain (Sigma-Aldrich Company Ltd, Dorset, UK) was used to assess cell viability; 100 µl of cell suspension was mixed with 100 µl of trypan blue. The solution was repeat pipetted, to ensure a single cell suspension, and 10 µl dispensed carefully to the edge of the

cover-slip allowing capillary action to draw the suspension underneath the slip and over the surface of the counting grid. The counting grid was viewed under a microscope at 100x total magnification and a cell counter used to record the number of unstained cells within one square of the grid, using the method summarised in Figure 2.1 and Figure 2.2. Cells that did not retain blue stain were those possessing an intact cell membrane and were considered viable; unstained cells within the counting grid were therefore included in the viable cell count.

Each square of the grid was 1 mm height x 1 mm width x 0.1 mm depth which represents a volume of (0.1 mm^3 or 0.1 µl). 0.1 µl is $1/10{,}000^{th}$ of ml, therefore the following formula was used to calculate the number of cells per 1 ml of suspension:

Viable cell count x 10,000 = number cells/ml

In order to calculate the total number of cells in a given cell suspension, the number of cells/ml was multiplied by the total volume of the cell suspension.

2.2.7.3 *Passaging cultures*

Passaging cultures refers to the action of harvesting cells at a particular percentage confluence and re-seeding fresh TC dishes with these cells in order to maintain them in culture. Once a cell count had been obtained for cells harvested, 2 x 10^6 cells were used to seed a new 175 cm flask containing 25 ml DMEM. Cells were maintained in culture until confluence as previously described, and stored for future reference in liquid nitrogen as described in the subsequent section. The remaining 3T3 feeder cells underwent irradiation which will be described in the following section.

2.2.7.4 *Irradiating cells*

3T3 feeder cells were irradiated to sufficiently prevent cellular replication but still maintain secretion of extracellular matrix proteins. A Caesium-137 irradiator was used to dose 3T3

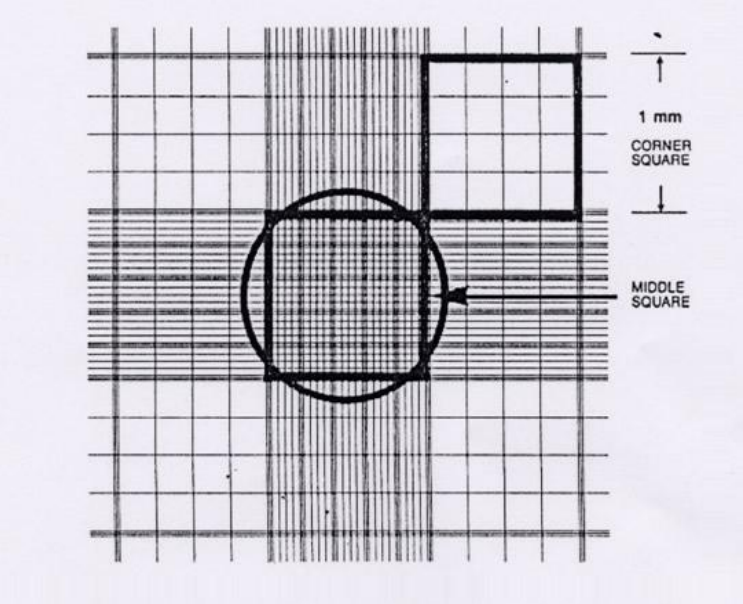

Figure 2.1. Microscopic image of a haemocytometer counting grid

Having undergone trypan blue staining, unstained (viable) cells were counted within the square (highlighted with a circle), according to the method illustrated in Figure 2.2. This image was available from the Health Protection Agency (HPA), cell culture protocols.

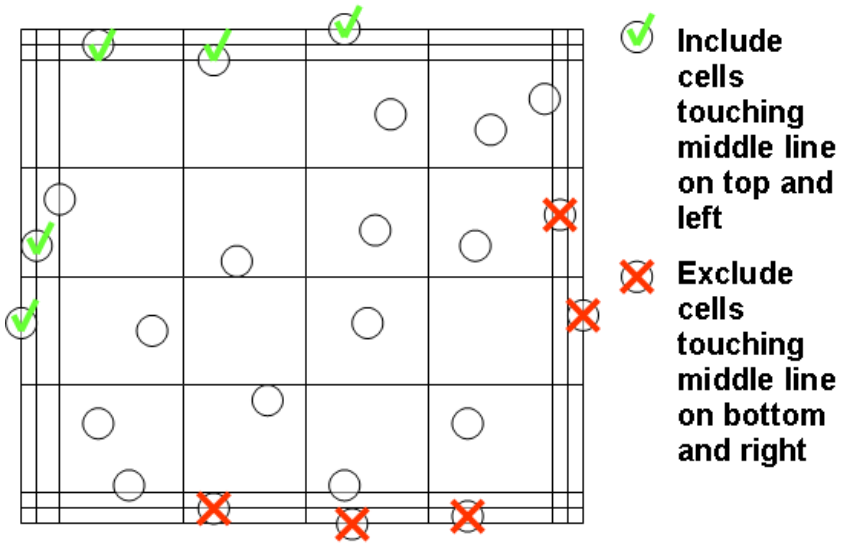

Figure 2.2. Overview of the cell counting technique carried out using a haemocytometer

Cell counts were performed within the central square of a haemocytometer counting grid according to the principle illustrated which ensured accurate and consistent viable cell counts. This cell counting method was available from the Health Protection Agency (HPA), cell culture protocols (http://www.phe-culturecollections.org.uk/technical/ccp/cellcounting.aspx).

feeder cell suspensions with ionising radiation so that cells absorbed the equivalent of 60 gray (Gy) (time = 22 minutes). Irradiated 3T3 feeder cells were then used to supplement PC08 and PC09 cultures in co-culture.

2.2.7.5 *Liquid nitrogen storage*

Un-irradiated 3T3 cell suspensions with a known cell count were prepared for liquid nitrogen storage by centrifuging at 1,500 rpm for 5 minutes. The supernatant was discarded and cell pellet re-suspended in a known volume of DMEM with 5% v/v dimethyl sulphoxide (DMSO) so that each ml of suspension contained between 5 x 10^5 and 1 x 10^7 cells. Aliquots (1 ml) were prepared in appropriately labelled cryovials, stored at -80 ^{o}C for up to 48 hours within a Mr. Frosty™ freezing container (Thermo Scientific, UK), and then transferred to liquid nitrogen for long term storage.

2.2.8 Culture of human epidermal keratinocytes neonatal (HEKn)

This section describes the methods used to culture, passage, and harvest HEKn cell lines, according to the manufacturer's guidelines (Life Technologies Corporation, Carlsbad, CA).

2.2.8.1 *Seeding and harvesting cultures*

HEKn starter cultures were prepared using cryopreserved cell stocks of HEKn in 6cm TC dishes containing Epilife® medium, as previously described. Cultures were incubated and media replenished every other day until cultures reached ~50% confluent; after this time culture media was replenished daily until cultures reached ~80% confluent. At 80% confluence, media was aspirated and cells trypsinised using 3 ml TE and incubated at room temperature for 5-10 minutes. Cultures were viewed microscopically during incubation to inspect for cell 'rounding', when cells appeared rounded/defined TE within the dish was repeat pipetted vigorously over the base of the dish to physically detach HEKn cells and create a single cell suspension. Epilife® medium (3 ml) was added to neutralise TE and the cell suspension transferred to a labelled

universal container and centrifuged at 1,000 rpm for 5 minutes. The supernatant was discarded and the cell pellet re-suspended in a required/known volume of Epilife® medium and gently repeat pipette to ensure a single cell suspension. A haemocytometer was used to perform trypan blue viable cell counts as previously described.

2.2.8.2 *Passaging cultures*

Cultures were passaged by seeding fresh 9 cm TC dishes with 2.5 x 10^4 HEKn cells in 10 ml Epilife® medium. Cells were cultured as previously described, and stored in liquid nitrogen if necessary as described in the following section.

2.2.8.3 *Liquid nitrogen storage*

HEKn cell suspensions with a known cell count were prepared for liquid nitrogen storage by centrifuging at 1,500 rpm for 5 minutes. The supernatant was discarded and cell pellet re-suspended in a known volume of 5% DMSO in Epilife® media so that each ml of suspension contained between 5 x 10^5 and 1 x 10^7 cells. Aliquots (1ml) were prepared in appropriately labelled cryovials, stored at -80 ^{o}C for up to 48 hours within a Mr. Frosty™ freezing container (Fisher Scientific, UK), and then transferred to liquid nitrogen for long term storage.

2.2.9 Culture of heterogeneous PC08 and PC09

This section describes the methods used to culture, passage, and harvest heterogeneous PC08 and PC09 keratinocyte cell lines. This protocol was kindly provided by Professor Margaret Stanley in Cambridge University, and summarised in (Stanley et al., 1989, Freshey and Freshney, 2002). PC08 and PC09 were cultured to obtain sufficient cells for carrying out dilution cloning technique, which will be described in the subsequent section.

2.2.9.1 *Seeding and harvesting cultures*

PC08 and PC09 starter cultures were prepared in 6 cm TC dishes containing EGF- GMEM using crypopreserved cell stocks of PC08 and PC09, supplemented with 8 x 10^5 3T3 feeders, as previously described. Cultures were incubated for 48 hours and replenished with EGF+ GMEM. Cells were viewed microscopically on a daily basis and when gaps appeared in the cell monolayer, cultures were replenished with 8 x 10^5 irradiated 3T3 feeder cells; media was discarded and replaced with 10 ml EGF+ media supplemented with 2 x 10^6 3T3 feeder cells. Cultures were maintained according to this method until keratinocytes reached ~80% confluence. When keratinocytes appeared ~80% confluent, 5 ml PBS was repeat pipetted over the cell monolayer to dislodge 3T3 feeder cells until 3T3 cell were no longer visible under microscopic examination. The remaining keratinocytes were trypsinised using 5 µl TE and dishes were incubated for 10-20 minutes until cells appeared 'rounded' when examined microscopically. The TE was then repeat pipetted vigorously over the base of the dish to physically detach keratinocytes and produce a single cell suspension. TE was neutralised by adding 5 ml EGF- GMEM (5 ml) and the cell suspension transferred to a labelled universal container and centrifuged at 1,000 rpm for 5 minutes. The supernatant was discarded and cell pellet re-suspended in a required/known volume of GMEM and gently repeat pipetted to ensure a single cell suspension. A haemocytometer was used to perform a trypan blue viable count of the cell suspensions, as previously described.

2.2.9.2 *Passaging cultures*

Cultures were passaged by seeding fresh 9 cm TC dishes with 10 ml EGF- GMEM seeded with 8 x 10^5 PC08/PC09 keratinocytes, and ~2 x 10^6 3T3 feeder cells. Cultures were incubated and maintained as previously described; when gaps appeared in the monolayer, 9cm dishes were replenished with 2 x 10^6 3T3 feeder cells. PC08 and PC09 cultures were stored in liquid nitrogen if necessary, as described in the following section.

2.2.9.3 *Liquid nitrogen storage*

Cell suspensions with a known cell count were prepared for liquid nitrogen storage by centrifuging at 1,500 rpm for 5 minutes. The supernatant was discarded and cell pellet re-suspended in a known volume of FCS with 5% v/v DMSO (Autogen Bioclear, Witshire, UK) so that each ml of suspension contained between 5 x 10^5 and 1 x 10^7 cells. Aliquots (1ml) were prepared in appropriately labelled cryovials, stored at -80 ^{o}C for up to 48 hours within a Mr. Frosty™ freezing container (Thermo Scientific, UK), and then transferred to liquid nitrogen for long term storage.

2.2.10 Deriving clonal cell lines from PC08 and PC09

Dilution cloning was carried out to derive a selection of novel clonal cell lines from heterogeneous PC08 and PC09 keratinocyte cell lines. The dilution cloning protocol was conducted according to the method summarised for adherent cells in (Freshney, 2010).

2.2.10.1 *Serial dilution*

PC08 and PC09 keratinocyte cell suspensions were used to create a dilution series using 10^5, 10^4, 10^3 and 10^2 cells in 5 ml EGF- GMEM within universal containers, according to Figure 2.3. Cultures were mixed by repeat pipetting at each step to ensure single cell suspensions, and 5 ml of each dilution was dispensed in triplicate within 6 cm dishes and supplemented with 5 x 10^5 3T3 feeder cells. Cultures were examined microscopically every 24 hours and replenished with EGF+ GMEM 48 hours after seeding. Cultures were viewed microscopically on a daily basis thereafter, and replenished with 5 ml EGF+ GMEM containing 5 x 10^5 3T3s feeders when gaps appeared in the cell monolayer, as previously described.

2.2.10.2 *Selecting keratinocyte colonies for ring cloning.*

Colonies of keratinocytes were viewed microscopically on all dilution plates. Desirable colonies for ring cloning were selected when the following characteristics were visible microscopically which indicated that a keratinocyte colony arose from a single cell:

1. Colony morphology appeared circular and symmetrical
2. Colony occupied <1/4 area of 1 field-of-view at 5X magnification
3. Colony situated >1 field-of-view distance from the location of another colony

Colonies that grew at 10^3 were selected for isolation using ring cloning because colonies met the criteria of the characteristics previously listed. Colony positions were marked with a dot on the base of the TC dish using a permanent marker to identify them for ring cloning.

2.2.10.3 *Ring cloning.*

Dishes marked with colonies were prepared for ring cloning by discarding media and applying a sterile glass ring (Sigma-Aldrich Company Ltd, Dorset, UK) around each colony, as shown in Figure 2.4. In order to create a water tight seal around each glass ring, 5 ml PBS was dispensed in the TC dish surrounding the rings. Cells of the colony within the ring were trypsinised with 100 µl TE and incubated for 10 minutes, then viewed microscopically for 'rounding'. Once cells appeared rounded/defined, the contents of each ring was repeat pipetted to detach all of the cells from the base of the TC dish. Cells isolated within each ring were transferred to individual 6 cm TC dishes; each 6 cm TC dish therefore contained a variety of clonal keratinocyte cells derived from PC08 and PC09. Each clonal cell line was assigned a specific identification comprising a letter (A-Z), the passage number, and the heterogeneous cell line (PC08 or PC09) from which it was derived. Clonal cell lines were maintained in 9 cm TC dishes for short-term culture as described in the subsequent section.

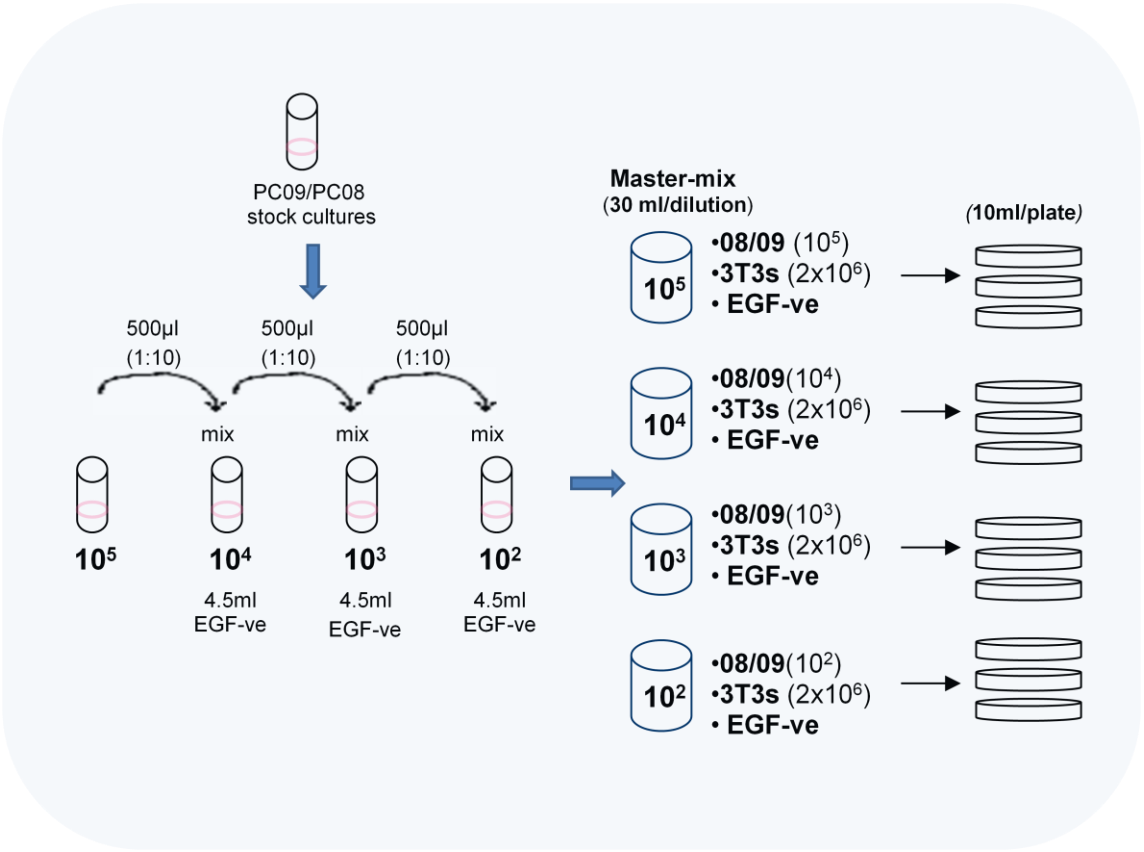

Figure 2.3. Serial dilution technique

Stock cultures of heterogeneous PC08 and PC09 were diluted via serial dilution and plated in triplicate. Cultures were viewed microscopically for circular, symmetrical colonies which were marked for ring cloning technique.

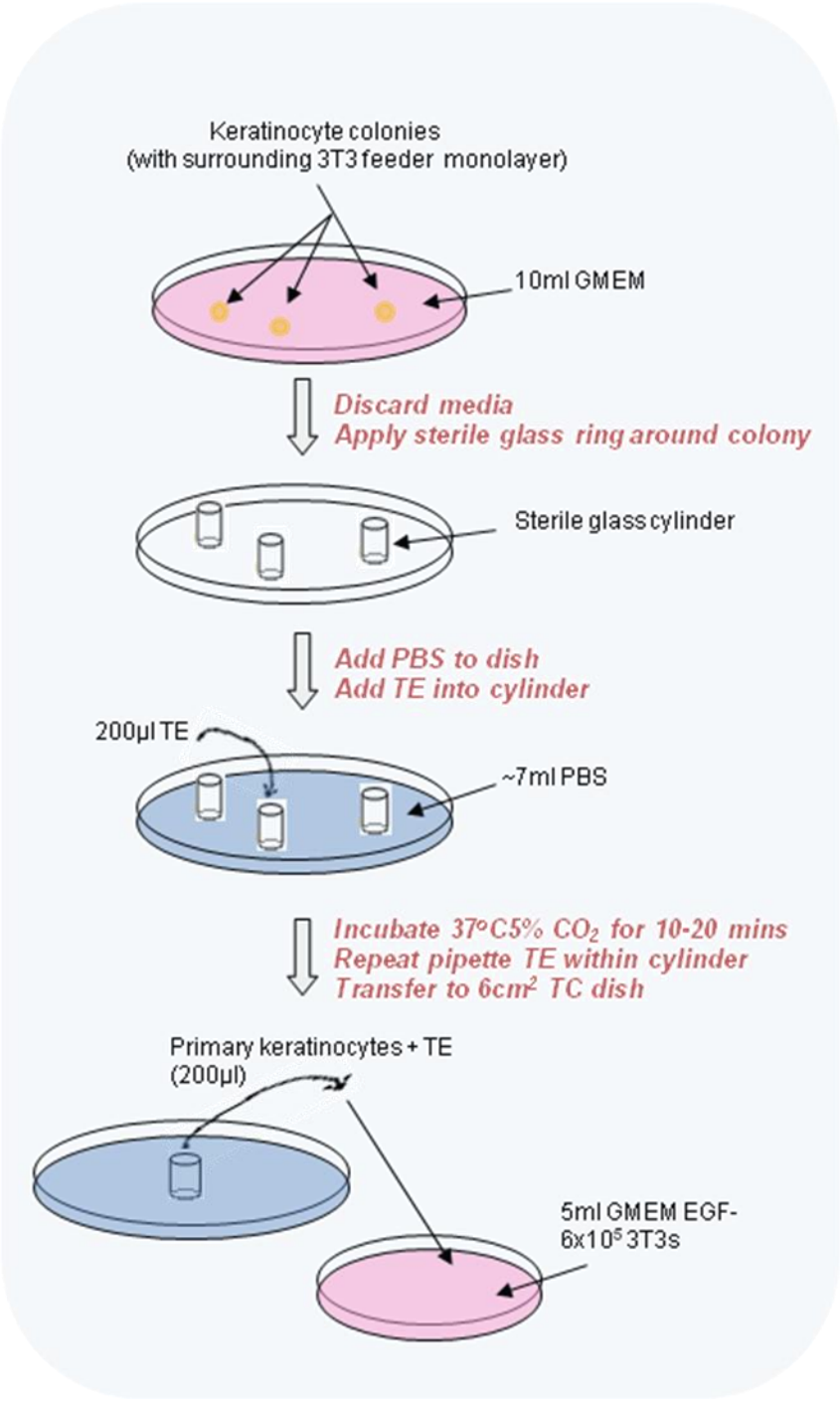

Figure 2.4. Ring cloning technique

Colonies that established on plates seeded at 10^3 were selected and isolated using sterile glass rings. Cells within each ring were trypsinised and transferred to individual 6cm TC dishes, resulting in the isolation and culture of a variety of clonal cell populations derived from PC08 and PC09.

2.2.10.4 *Clonal cell lines selected for use in this project.*

A variety of clonal cell lines were isolated from heterogeneous PC08 and PC09 during this investigation; each clonal cell line was found to replicate in culture at different rates. In order to comply with the project time-frame, and for fulfilling the objectives and investigating hypotheses, several of the most rapid growing clonal cell lines from PC08 and PC09 were used in this project.

2.2.10.5 *Short term culture of clonal cell lines.*

The most rapid growing clonal cell lines underwent short term culture (5-7 passages) according to the seeding, harvesting, and passaging techniques previously described for heterogeneous PC08 and PC09. After harvesting at each passage, 5 x 10^6-1 x1 0^7 cells were retained for DNA and RNA extraction as described in the following section. The slower growing clonal cell lines were not used for continuation in this project and were harvested and stored in liquid nitrogen for future reference.

2.2.11 Calculating population doublings and doubling time

An estimation of the growth rate of each clonal cell line was carried out during short-term culture by calculating population doublings (PD) and doubling time (DT). Terminology was obtained from World Health Organisation (WHO) (World Health Organization, 2010). PD was defined as an estimated measure of the total number of times the initial cell population doubled during one passage to 80% confluence. DT was defined as an estimated calculation of the mean time taken for the population of cells to double in number during culture. PD was calculated according to Equation 2.1, a very similar equation has been published elsewhere (Schaeffer, 1990). Calculation of PD and DT required the following information to be recorded for each passage:

1. The number of viable cells used to seed the dish

2. The number of cells harvested from each dish at ~80% confluence
3. The time taken for each culture to reach ~80% confluence after seeding (one passage)

The number of cells removed at ~80% confluence (N_O) divided by the number of inoculated viable cells (N_i) represents the fold change in cell number during one passage. The fold change in cell number is equivalent to 2 to the power of PD (e.g. 3 population doublings for one cell = 1 X 2^3 = 8 cells = 8 fold change). Mean doubling time was calculated by dividing PD by the time taken for each culture to reach ~80% confluence after seeding and expressed in hours.

2.3 Nucleic acid extraction and quantification

DNA and RNA were extracted from clonal cells that had been harvested at each passage during short term culture. DNA and RNA extracts were required for downstream molecular analyses which contributed to characterising the clonal cell lines. AllPrep DNA/RNA Mini Kit (Qiagen, Hilden, Germany) was used to simultaneously extract DNA and RNA according to the manufacturer's instructions, as summarised in Figure 2.5.

2.3.1 Preparing cells for extraction

Cell suspensions of clonal cell lines were prepared during cell culture, as previously described. Cell suspensions containing 5 x 10^6-1 x 10^7 cells were centrifuged at 1,000 rpm for 5 minutes. Supernatant was poured off gently and RLT buffer containing beta-mercaptoethanol (βME) was added to the cell pellet depending on the number of cells present, as illustrated in Table 2.4; 10 µl βME was required per 1 ml RLT buffer. The sample was mixed by repeat pipetting and transferred into cryovials for storage at -80 ^oC for future reference, or at 4 ^oC to perform extraction on the same day.

RNAseZap® (Sigma-Aldrich Company Ltd, Dorset, UK) was used to spray the working area and equipment used in preparation for RNA extraction to destroy ubiquitous RNases which degrade RNA molecules. Samples were homogenised using 0.9 mm (20 gauge) needle and

$$2^{PD} = \frac{N_o}{N_i}$$

This formula was rearranged to use PD as the subject of the formula.

$$Log_2(2^{PD}) = Log_2\left(\frac{N_o}{N_i}\right)$$

$$PD.Log_2(2) = Log_2\left(\frac{N_o}{N_i}\right)$$

$$PD \times 1 = Log_2\left(\frac{N_o}{N_i}\right)$$

The base of the Log conversion was changed to the more manageable base 10.

$$PD = \frac{Log_{10}\left(\frac{N_o}{N_i}\right)}{Log_{10}(2)}$$

$$PD = Log_{10}\left(\frac{N_o}{N_i}\right) \times \left(\frac{1}{Log_{10}(2)}\right)$$

$$PD = Log_{10}\left(\frac{N_o}{N_i}\right) \times 3.322$$

Equation 2.1: Equation for calculating population doublings from input and output viable cell numbers.

Here, PD represents population doublings, Ni represents the number of viable cells used to inoculate the growth vessel and N_o represents the number of cells in the growth vessel at ~80% confluence and subsequent removal.

syringe by aspirating and dispensing the sample repeatedly, avoiding bubble formation. The resulting homogenate was transferred directly to the membrane of a blue DNA spin column with round-bottom collection tube; sample was dispensed directly on the spin column membrane to prevent sample collection on the lip of the tube. The lid was closed gently to prevent loss of sample to the sides of the tube and centrifuged at 13,000 rpm for 30 seconds to allow binding of DNA to the spin column membrane. The collection tube, containing through-flow RNA, was retained and prepared for RNA extraction which will be described in the following section.

2.3.2 RNA extraction

Ethanol (70%) was added to RNA flow through (according to Table 2.4) and repeat pipetted gently to mix. A maximum volume of 700 µl of sample was transferred directly on to the membrane of a pink RNA spin column within a round-bottom collection tube and centrifuged for 15 seconds; through-flow was discarded and the collection tube re-used.

A DNase step was then carried out to ensure absence of DNA in the sample, using DNeasy Mini Kit (Qiagen, Hilden, Germany) according to the manufacturer's instructions. RW1 (350 µl) was added to the RNA spin column and centrifuged for 15 seconds after which through-flow was discarded and the collection tube re-used. A DNase mixture was then prepared by combining 10 µl DNase with 70 µl buffer RDD (80 µl total per sample) within a sterile microcentrifuge tube. The solution was inverted to mix, centrifuged for a few seconds to collect the solution, and 80 µl dispensed directly on the RNA column membrane. The RNA spin column was incubated at room temperature for 15 minutes after which 350 µl RW1 was dispensed directly to the RNA spin column membrane and centrifuged for 15 seconds; through-flow was discarded and collection tube re-used.

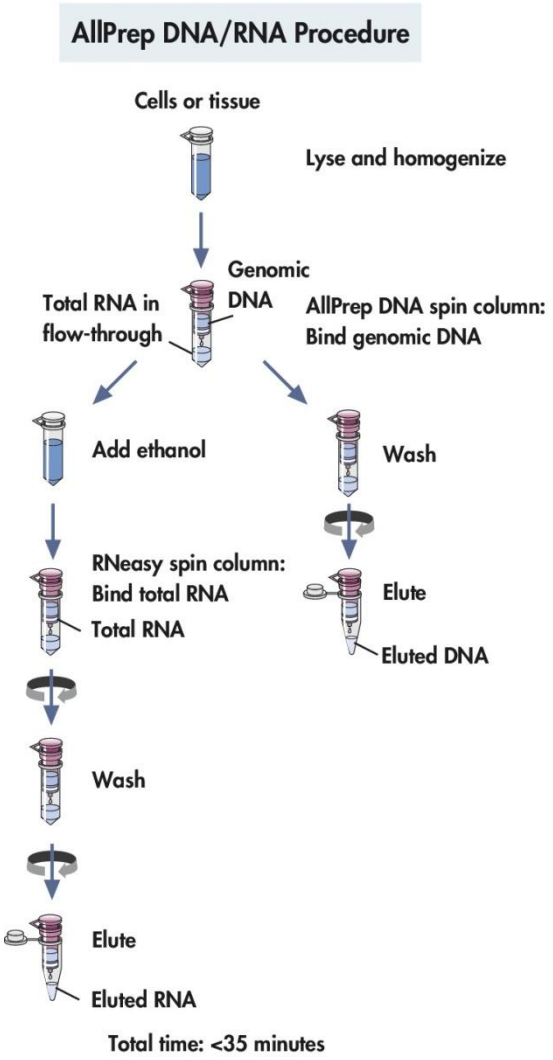

Figure 2.5. Summary of DNA and RNA extraction method via Qiagen® AllPrep DNA/RNA mini kit

Genomic DNA and total RNA were simultaneously purified from cell line material; DNA and RNA were eluted separately from one sample. Cell line material was homogenised using buffer provided with the kit. Firstly DNA was purified using the novel AllPrep DNA spin columns, and RNA purified thereafter using RNeasy mini spin columns. The extraction process involved a series of buffer washes and centrifugation steps resulting in RNA and DNA binding to the spin column membranes, which were captured during the final elution step using specific elution buffers. This image was available in the manufacturer's instructions within the test kit and also online.

RLT buffer*		70% ethanol	
Cell count	Volume (µl)	Volume flow-through (µl)	Volume ethanol (µl)
$<5 \times 10^6$	350	350	350
5×10^6 - 1×10^7	600	600	600

Table 2.4. Volumes of reagents involved in nucleic acid extraction

RLT buffer was required to homogenise cell line material prior to extraction, which was dependent on the number of cells in the sample. Ethanol (70%) was required during RNA extraction and was dependent on the volume of sample through-flow. *Formulation of RLT buffer/βme = 10 µl βME per 1 ml RLT buffer.

After completing the DNase step, 500 µl RPE buffer was added directly to the spin column membrane and centrifuged for 15 seconds; through-flow was discarded and collection tube re-used. This process was repeated with a 2 minute centrifugation at 13,000 rpm. The spin column was then carefully separated from the round-bottom tube containing through-flow (which was discarded) and placed into a fresh round-bottom tube. The spin column was repeat centrifuged for 1 minute to ensure the complete absence of through-flow and the round-bottom collection tube was discarded and replaced with a fresh pointed collection tube. To elute RNA from the column membrane, 50 µl RNase-free water was added directly to the column membrane and centrifuged for 1 minute. RNA elution was repeated using the same volume of fresh RNase-free water or the existing elute.

2.3.3 DNA extraction

Fresh AW1 and AW2 reagents were prepared by adding 100% ethanol to each, according to the preparation instructions on the bottle. After preparing AW1/2, 500 µl AW1 was added directly to the membrane of a DNA spin column with round-bottom collection tube and centrifuged for 15 seconds; through-flow was discarded and collection tube re-used. AW2 (500 µl) was added directly to the membrane of the DNA spin column and centrifuged for 2 minutes; through-flow and collection tube were discarded and replaced with a fresh round-bottom collection tube. The spin column was repeat centrifuged for 1 minute to ensure the complete absence of through-flow, and the round-bottom collection tube discarded and replaced with a fresh pointed collection tube. To elute DNA from the column membrane, 100 µl EB was dispensed directly to the column membrane, incubated at room temperature for 1 minute, and centrifuged for 1 minute. DNA elution was repeated using the same volume of fresh EB or the existing elute.

2.3.4 Nucleic acid storage

A 5 µl aliquot of DNA and RNA extracts were prepared for immediate quantification using a spectrophotometer, according to the method described in the following section. The remaining DNA and RNA extracts were stored for future reference at -18 ^{o}C and -80 ^{o}C, respectively.

2.3.5 Nucleic acid quantification

The concentration and purity of DNA and RNA was determined using a NanoDrop™ 1000 Spectrophotometer (NanoDrop products, Wilmington, DE, USA), according to manufacturer's instructions (v3.7 user's manual). Spectrophotometric measurements, provided a DNA and RNA concentration in ng/µl. The purity of DNA/RNA was assessed through the ratio of absorbance at 260 nm and 280 nm; a ratio of >1.8 and <2.2 was generally accepted as high purity RNA.

An initialisation 'blank' spectral measurement was carried out to initialise the spectrophotometer by loading 2 µl water. To establish a new reference prior to quantifying DNA/RNA extracts, DNA and RNA 'blanks' were carried out using 2 µl of the respective DNA/RNA elution buffers using during nucleic extraction (EB buffer and RNase-free water). 1 µL of DNA or RNA sample was loaded and a spectral measurement of the sample performed.

2.4 *Mycoplasma* Detection

A PCR-based test was used to detect *Mycoplasma* species (spp) in culture media retained from PC08, PC09, and 3T3 feeder cell cultures, at 90-100% confluence. *Mycoplasma* spp frequently contaminate cell cultures because they pass easily through filter sterilisation pores, are not susceptible to general cell wall targeting antibiotics (they lack a rigid cell wall structure), and are easily transmissible from operator to cultures and between cultures thereafter.

Mycoplasma spp modify the physiological aspects of the cell cultures they contaminate. Cell cultures were analysed prior to beginning cell culture experiments and during the period of cell culture (Young et al., 2010b).

VenorGeM® *Mycoplasma* Detection Kit (Minerva Biolabs®, Berlin, Germany) was used to amplify the highly conserved 16S rRNA coding region (267 bp) from *Mycoplasma* species which are most commonly associated with contaminating cell culture systems. Amplified PCR products were electrophoresed and fragment sizes used to determine the presence/absence of *Mycoplasma* spp. This section will describe the method used to detect *Mycoplasma* contamination in cell cultures.

2.4.1 Reagent preparation and rehydration

Reagents included in the test kit were stored at 2-8 ^{o}C prior to use; *Taq* DNA polymerase was purchased separately from Minerva Biolabs® and stored at -18^{o}C until required and on ice during use. Reagents were prepared according to steps 1-6 as illustrated in Table 2.5, and aliquotted and stored at -18 ^{o}C to avoid repeat freezing and thawing.

2.4.2 Sample and mastermix preparation

Media was aspirated from cell cultures at 90-100% confluence and 100 µl dispensed in sterile tubes. Samples were heated at 95 ^{o}C for 5 minutes using a heat block, and centrifuged for 5 seconds at 13,000 rpm to form a pellet of cell debris. Samples were stored at 2-8 ^{o}C for PCR preparation immediately, or at -18 ^{o}C for future reference. The PCR master mix (MM) was then prepared according to Table 2.6, and stored on ice until required.

2.4.3 PCR

PCR tubes were labelled and 23 µl of MM dispensed in each tube followed by 2 µl of sample and repeat pipetted to mix. Lids were closed on tubes after mixing to prevent cross contamination between samples. A negative control (PCR grade water) and a positive control

.

Step	Lyophilised reagents	Preparation details
1	Red cap – primer/nucleotide mix Yellow cap – internal control DNA Green cap – positive control DNA	Centrifuge for 5 seconds at 13,000 rpm
2	Red cap	Add 65 µl PCR grade water (white cap)
3	Yellow cap	Add 300 µl PCR grade water (white cap)
4	Green cap	Add 300 µl PCR grade water (white cap)
5	Red cap Yellow cap Green cap	Incubate at room temperature for 5 minutes
6	Red cap Yellow cap Green cap	Vortex DNA briefly and spin for 5 seconds

Table 2.5. Preparation of reagents included in VenorGeM® Mycoplasma detection Kit

('green cap'- included in the test kit) were also prepared in the same way. PCR tubes were sealed tightly to prevent evapouration, loaded onto a PCR thermocycler, and PCR carried out for 1 cycle at 94 ^{o}C for 2 minutes, 39 cycles consisting of 94 ^{o}C for 30 seconds/55 ^{o}C for 30 seconds/72 ^{o}C for 30 seconds, and a final hold and cool down to 4-8 ^{o}C.

2.4.4 Agarose gel preparation and electrophoresis

Agarose gel (1.5% w/v) was prepared using Tris/Borate/EDTA (TBE) (Life Technologies Corporation, Carlsbad, CA) and agarose (Life Technologies Corporation, Carlsbad, CA) according to Table 2.7. Molten agarose was prepared by heating agarose in a microwave until large bubbles formed. Molten agarose was carefully removed from the microwave with an oven glove and cooled slowly to 60 ^{o}C in a water bath at room temperature. Ethidium bromide (Sigma-Aldrich Company Ltd, Dorset, UK) was added and agarose poured into a gel plate containing a comb to create wells for samples. The agarose gel was left to set at room temperature, the comb was removed carefully when the gel had set, and the agarose gel was placed in to the electrophoresis tank containing 1x TBE. The first well of the gel was filled with 10 µl 100 bp ladder (Sigma-Aldrich Company Ltd, Dorset, UK). The following wells were allocated for 5 µl sample PCR product combined with 5 µl loading dye (Orange G) (Sigma-Aldrich Company Ltd, Dorset, UK) which was carefully dispensed in to each well. The voltage was set to 100 V for 20-30 minutes, and the gel was visualised under UV light within a transilluminator once electrophoresis was complete.

2.4.5 Interpreting Results

Amplified products were visualised within a transilluminator and band sizes determined by comparing with the reference ladder. The internal control DNA produced a band size of 191 bp on the gel which confirmed successful PCR performance. The positive control sample provided with the kit, produced a band size of 265-278 bp. *Mycopl*asma DNA within samples produced a

Reagent	Volume n=1 (µl)
PCR grade water	15.3
10x reaction buffer	2.5
Primer/nucleotide mix (red cap)	2.5
Internal control DNA (yellow cap)	2.5
*Polymerase (5U/µl)	0.2
Total volume	*23*

Table 2.6. Reagents required for Mycoplasma PCR mastermix

*Polymerase was required but not included in the Venor*GeM*® Mycoplasma Detection Kit, and was purchased from Minerva Biolabs GmbH.

Gel size	TBE volume (ml)	Agarose (g)	Ethidium bromide (µl)
Small	100	1.5	2
Medium	300	4.5	5
Large	600	9	10

Table 2.7. Preparation of 1.5% agarose gel for electrophoresis of *Mycoplasma* PCR products

Mycoplasma band size (165-278 bp)	Internal control band size (191 bp)	Interpretation
Positive	Irrelevant	*Mycoplasma* present
Negative	Negative	PCR inhibition
Negative	Positive	*Mycoplasma* absent

Table 2.8. Interpretation of PCR amplified products of Mycoplasma PCR

band size of 265-278 bp, which would be observed in *Mycoplasma* infected samples. A summary of band size interpretation are illustrated in Table 2.8.

2.5 Relative gene expression

The real-time quantitative reverse-transcription polymerase chain reaction (qRT-PCR) protocol in use within the department of HPV Research was a modification to Roche® LightCycler carousel-based qRT-PCR system (Roche Applied Science, Mannheim, Germany) protocol which was set-up and optimised by Dr Dean Bryant. The qRT-PCR protocol was performed using LightCycler DNA Master SYBR Green I reagent kits and LightCycler reaction capillary tubes (Roche Applied Science, Mannheim, Germany) to detect PCR amplified products which were viewed in real-time using the LightCycler® carousel-based qRT-PCR system and associated software.

qRT-PCR was carried out using RNA extracts of clonal cell lines to determine relative gene expression of HPV early (E) genes, E2, E4, E5, E6, and E7, and cellular housekeeping genes, hypoxanthine phosphoribosyltransferase (*HPRT*) and TATA-box-binding protein (*TBP*). Relative HPV gene expression profiles for samples were obtained using CaSki HPV gene concentration standard curves (which were previously obtained by Dr Dean Bryant) and then calculating the relative expression ratio between HPV genes and housekeeping genes.

Relative expression of HPV genes was carried out to characterise clonal cell lines at a molecular level.

2.5.1 qRT-PCR

This section of writing will describe the method used to perform qRT-PCR.

2.5.1.1 *Reverse transcription polymerase chain reaction (RT-PCR)*

PCR hoods were routinely cleaned with 70% ethanol and subjected to 30 minutes UV light treatment before commencing. RNAseZap® (Sigma-Aldrich Company Ltd, Dorset, UK) was also used to spray the working area and any equipment being used when handling RNA.

RNA extracts from clonal cell lines were subjected to RT-PCR within a designated area of the laboratory. RT-PCR was performed to obtain complimentary DNA (cDNA) using reagents provided in SuperScript III Reverse Transcriptase kit (Invitrogen, Paisley, UK) and random hexamer primers (Invitrogen, Paisley, UK), as shown in Table 2.9.

Group A reagents were added to a microcentrifuge tube, heated at 65 ^{o}C for 5 minutes, and incubated on ice for 1 minute. An RT positive (RT+) and negative (RT-) mastermix (MM) was prepared using 'group B' reagents; each sample was prepared in duplicate using reverse transcriptase (RT+) and RNase free water (RT-) as an internal control for assessing the success of RT-PCR. 'group B' were combined with 'group A' on ice and mixed by repeat pipetting. Samples were incubated for 5 minutes at 25 ^{o}C, 60 minutes at 50 ^{o}C, and 15 minutes at 70 ^{o}C

Group	Reagent (n=1)
A	RNA sample (0.5 µg) 1 µl random primers (200 ng) 1 µl dNTP mix (10 mM) Sterile distilled water to 13 µl
B	4 µl 5x first strand buffer 1 µl DTT (dithiothreitol) (0.1 M) 1 µl RNAse-out *1 µl SuperScript III reverse transcriptase **1 µl RNase free water

Table 2.9. Reagents (Group A and B) used to prepare RT mastermix

Group A reagents were used for the initial RT step and group B reagents used in the latter step. *Superscript III reverse transcriptase was used in Group B reagents for preparing RT+ mastermix. ** RNase free water was used in Group B reagents for preparing RT- mastermix.

using a thermocycler. The resulting cDNA was stored at -20 ^{o}C for future reference or prepared immediately for real time quantitative PCR, as described in the following section.

2.5.1.2 *Real-time quantitative PCR*

The resulting cDNA was diluted 1:10 using PCR grade water. A HPV+ control sample was prepared using CaSki cell line DNA diluted to 1:100 using PCR grade water, and a PCR negative control sample prepared using PCR grade water.

LightCycler® Capillaries were placed in LightCycler® Centrifuge Adapters within the LightCycler® aluminium cooling block (all from Roche Applied Science, Mannheim, Germany) in numerical order; the cooling block was stored at 4 ^{o}C several hours before commencing the protocol.

The MM was prepared using FS DNA Master SYBR Green reagents (Roche Applied Science, Mannheim, Germany) and HPV specific primers or house-keeping gene primers, as illustrated in Table 2.10; details of forward and reverse primer sets are shown in Table 2.11.

LightCycler® capillaries were supported in their adapters within the chilled cooling block, and 18 µL MM and 2 µl cDNA dispensed into each capillary. Capillaries within their adapters were centrifuged for 3 seconds at 5k rpm to deposit the sample, and then returned to the cooling block in numerical order. Capillaries were taken out of adapters and stored in numerical order within a capillary holder and transferred to a separate laboratory to perform qPCR using LightCycler® quantitative real-time PCR Carousel-Based System and associated PC software.

Capillaries were loaded into the carousel of the LightCycler® qPCR machine, and pressed down lightly to ensure they were fully seated. The lid was lowered gently and the specific programme selected using LightCycler® PC software; programme details for PCR amplification cycles were set according to the primer set being used (Table 2.12).

	Primer pair						
	E2	E4	E5	E6	E7	HPRT	TBP2
Reagent	µl per reaction						
F primer (5 µM)	2	2	2	2	2	2	2
R primer (5 µM)	2	2	2	2	2	2	2
*FS mix	2	2	2	2	2	2	2
$MgCl_2$ (25 mM)	2	1.6	1.2	1.6	2	1.6	2.4
H_20	10	10.4	10.8	10.4	10	10.4	9.6
Template cDNA	2	2	2	2	2	2	2
Total volume	*20*	*20*	*20*	*20*	*20*	*20*	*20*

Table 2.10. Reagents used to prepare mastermixes of each primer set for real-time qPCR

*FS mix was produced by adding 10 µl of reagent 1a to a full vial of defrosted reagent Ib; FS was stored at 4 ^{o}C within an opaque storage container for up to 1 month, according to the manufacturer's instructions.

	Primer set details
Name	Hypoxanthine guanine phosphoribosyl transferase (*HPRT*)
Forward primer	TGACACTGGCAAAACAATGCA
Reverse primer	GGTCCTTTTCACCAGCAAGCT
Amplified DNA	4982 bp (nt 133627546-133632438 of Chromosome X)
Amplified RNA	94 bp (nt 496-589 of M31642.1)
Reference	(Allen et al., 2008)
Name	TATA binding protein, 2nd pair of primers (*TBP*2)
Forward primer	TCAAACCCAGAATTGTTCTCCTTAT
Reverse primer	CCTGAATCCCTTTAGAATAGGGTAGA
Amplified DNA	803 bp (nt 170880539-170881341 of Chromosome 6)
Amplified RNA	122 bp (nt 1128-1224 of M55654.1)
Reference	(Minner and Poumay, 2009)
Name	E6
Forward primer	CTGCAATGTTTCAGGACCCA
Reverse primer	TCATGTATAGTTGTTTGCAGCTCTGT
Amplified DNA/RNA	80 bp (nt 99-178 of NC001526.1)
Reference	(Wang-Johanning et al., 2002)
Name	E7
Forward primer	AAGTGTGACTCTACGCTTCGGTT
Reverse primer	GCCCATTAACAGGTCTTCCAAA
Amplified DNA/RNA	78 bp (nt 739-816 of NC001526.1)
Reference	(Wang-Johanning et al., 2002)
Name	E4
Forward primer	AACGAAGTATCCTCTCCTGAAATTATTAG
Reverse primer	CCAAGGCGACGGCTTTG
Amplified DNA/RNA	82 bp (nt 3362-3426 of NC001526.1)
Reference	(Roberts et al., 2008)

Name	E2
Forward primer	TAACTGCACCAACAGGATGT
Reverse primer	TTGCATATGTCTCCATCAAACTGC
Amplified DNA/RNA	82 bp (nt 3362-3426 of NC001526.1)
Reference	Designed in-house
Name	E5
Forward primer	CCGCTGCTTTTGTCTGTGTC
Reverse primer	GCAGAGGCTGCTGTTATCCA
Amplified DNA/RNA	82 bp (nt 3362-3426 of NC001526.1)
Reference	Designed in-house

Table 2.11. Details of qPCR primer sets used and gene products amplified

M31642.1 = GenBank accession no. Homo sapiens HPRT mRNA. M55654.1 = GenBank accession no. Homo sapiens TBP2 mRNA. NC001526.1 = GenBank accession no.: HPV 16.

	Temperature (°C)	Time (s)	Cycles
Initial denaturation	95	600	1
Denaturation	95	10	60
Primer annealing	58/60/62*	5	
Extension	72	5	
	Temperature (°C)	Rate of change (°C/s)	Cycles
Melting curve	65-95	0.1	1

Table 2.12. Details of qPCR conditions for each primer set .

Details are provided for both the qPCR reaction and the melting curve. *Annealing temperatures were primer pair specific. E5/E4 (58 °C), E2/E6/*HPRT*/*TBP* (60 °C) and E7 (62 °C).

2.5.1.3 *Data analysis*

Relative expression of HPV genes was determined by quantifying clonal cell line cDNA using LightCycler® software and analysing data through qbase^{PLUS} (Biogazelle Zwijnaarde, Belgium) according to the manufacturer's instructions, and documented in the literature (Hellemans et al., 2007); absolute quantification of HPV gene expression was not performed. Data manipulation and analysis was carried out using qbase^{PLUS} because this function was limited in LightCycler® software.

Real-time PCR using LightCycler® system provided a Ct value (cycle threshold) translating to the number of cycles required for fluorescent signal to accumulate to a level where it intersects with the threshold (exceeds the background signal). Thresholds were calculated automatically in the LightCycler® software using second derivative maximum.

HPV genes and cellular house-keeping gene concentrations were imported in to qbase^{PLUS} software and used to calculate the ratio between HPV genes and cellular housekeeping genes to establish relative gene quantifications within each sample. Expression ratios were calculated using CaSki as a calibrator sample, such that expression ratios are expressed relative to CaSki RNA.

2.6 HPV Integration Analysis

Molecular techniques used to investigate HPV16 integration status in cell line material were previously optimised by Dr Rachel Raybould within the department of HPV Research.

This section describes the protocols used to detect integrated HPV in clonal cell lines through two different molecular techniques. Detection of transcriptionally active HPV integrations in clonal cell line RNA extracts was performed using amplification of papillomavirus oncogene

transcripts (APOT) assay, a reverse transcription PCR-based amplification method (Klaes et al., 1999). Detection of genomic HPV integrations in clonal cell line DNA was performed using detection of integrated papillomavirus sequences (DIPS) assay, an adapter ligation PCR method (Luft et al., 2001).

HPV integration status was investigated to characterise clonal cell lines at a molecular level.

2.6.1 APOT assay

2.6.1.1 *Reverse transcription polymerase chain reaction (RT-PCR)*

Clonal cell line RNA samples were subjected to RT-PCR to obtain complimentary DNA (cDNA) using the reagents illustrated in Table 2.13; details of primer sequences used in RT-PCR step and at other steps throughout APOT protocol are shown in Table 2.14.

PCR hoods were cleaned with 70% ethanol and subjected to 30 minutes UV light treatment before commencing the protocol. RNAseZap® (Sigma-Aldrich Company Ltd, Dorset, UK) was used to spray the working area and any equipment being used when handling RNA.

Microfuge tubes (Sigma-Aldrich Company Ltd, Dorset, UK) were set-up in duplicate for samples to represent a RT+ (reverse transcriptase) and RT- (RNase free water) version of each sample; this was carried out as an internal control for assessing the success of RT-PCR. Group A reagents were dispensed in microcentrifuge tubes and 1 µg RNA sample added and repeat pipette to mix. Samples were heated to 70 ^{o}C for 10 minutes using a thermocycler, and then stored on ice for 1 minute and centrifuged for 2 seconds to collect sample. Group B reagents were prepared as 2 separate mastermixes (MM) representing an RT+ MM and an RT- MM; RT+ MM contained 1 µl (200 units) of Superscript™ II Reverse Transcriptase (Invitrogen, Paisley, UK), which was added last and stored on ice, and RT- MM contained 1 µl RNase free water. A total volume of 7 µl RT+ MM was added to each RT+ sample; this was repeated using RT- MM

Group	Reagent	Volume (µl) (n=1)
A	(dT)17-p3 primer (500 ng/µl)	1
	10mM dNTP	1
	Total volume	*2*
B	First strand buffer	4
	DTT	2
	SuperScript II RT*	1
	RNase free water**	1
	Total volume	*8*

Table 2.13. Reagents used in APOT RT-PCR to obtain cDNA

Group A reagents were prepared initially and added to RNA samples (in duplicate). Group B reagents were prepared in duplicate to account for an RT+ mastermix (*) and an RT- mastermix (**).

Protocol	Primer name	Sequence
APOT	HPV 16-p1 forward	CGGACAGAGCCCATTACAAT
	HPV 16-p2 forward	CTTTTTGTTGCAAGTGTGACTCTACG
	p3 reverse	GACTCGAGTCGACATCG
	(dT)17-p3 reverse	GACTCGAGTCGACATCGATTTTTTTTTTTTTTTT

Table 2.14. Details of primer sequences used in APOT protocol

for RT- samples. Samples were incubated at 42 ^{o}C for 2 minutes, repeat pipetted to mix, and -incubated at 42 ^{o}C for 1 hour, followed by 70 ^{o}C for 15minutes. The resulting cDNA was stored at -20 ^{o}C for future reference, or prepared immediately for primary PCR as described in the following section.

2.6.1.2 *Primary PCR*

The resulting cDNA samples were dispensed in 1µl aliquots in labelled microfuge tubes. A HPV+ control was included which consisted of CaSki cell line DNA diluted to 1:100 using sterile water, and a PCR negative control consisting of PCR grade water.

Primary PCR mastermix (MM) was prepared in a microfuge tube as shown in Table 2.15. Each cDNA sample was combined with 24 µl MM and mixed by repeat pipetting. *Taq* was stored on ice and added last. Tubes were sealed using adhesive film (Fisher) and primary PCR carried out according to the conditions illustrated in Table 2.16. Primary PCR products were prepared immediately for nested PCR, as described in the following section.

2.6.1.3 *Nested PCR*

The resulting PCR products were dispensed in 5 µl aliquots within labelled microfuge tubes. Nested PCR mastermix (MM) was prepared in a microfuge tube as shown in Table 2.17; *Taq* was added last and was stored on ice prior to use. Samples were combined with 45 µl MM and mixed by repeat pipetting. Tubes were sealed with adhesive film and nested PCR carried out according the conditions illustrated in Table 2.18. The resulting nested PCR products were stored at 4-20 ^{o}C for future reference, or prepared immediately for gel electrophoresis as described in the subsequent section.

Reagent	Concentration	Volume (µl) (n=1)
10X buffer		2.5
dNTP	10 mM	0.5
$MgCl_2$	50 mM	0.75
F HPV16-p1	10 uM	0.5
p3 reverse	10 uM	0.5
Taq polymerase	5 U/µl	0.2
Water		19.05
Total volume		*24*

Table 2.15. Reagents used to prepare APOT primary PCR mastermix

Temperature (°C)	Time (seconds)	
94	180	
94	30	30 cycles
61	120	
72	120	
72	600	

Table 2.16. Conditions for APOT primary PCR

Conditions for APOT originated from the literature (Klaes et al. 1999) and were optimised previously by Dr Rachel Raybould during her research studies.

Reagent	Concentration	Volume (µl) (n=1)
10X buffer		5
dNTP	25 mM	1
$MgCl_2$	25 mM	5
F HPV16-p2	10 uM	5
(dT)17-p3 reverse	10 uM	5
Taq polymerase	5 U/µl	0.2
Water*		23.8
Total volume		*50*

Table 2.17. Reagents used to prepare APOT nested PCR mastermix

* Mastermix was made up to 45 µl with water.

APOT	Temperature (°C)	Time (seconds)	
Nested PCR	94	180	
	94	30	30 cycles
	67	120	
	72	120	
	72	600	

Table 2.18. Conditions for APOT nested PCR

Conditions for APOT originated from the literature (Klaes et al. 1999) and were optimised previously by Dr Rachel Raybould during her research studies.

2.6.2 DIPS assay

2.6.2.1 *Genomic DNA digestion*

Clonal cell line DNA samples underwent a digestion step to fragment DNA; DNA samples were prepared in duplicate to account for digestion by two restriction endonuclease enzymes, *TaqI* and *Sau3AI.* A HPV+ control was included using CaSki cell line DNA diluted to 1:100 wIth sterile water, and a PCR negative control was included using PCR grade water.

DNA samples (1.2 µg) in duplicate were added to tubes and made up with PCR grade water to a total volume of 17.3 µl (for *TaqI* digestion), and 15.3 µl (for *Sau3AI* digestion). *TaqI* and *Sau3AI* mastermixes (MM) were then prepared according to Table 2.19, and 4.7 µl *Sau3AI* mastermix or 2.7 µl *TaqI* mastermix, were combined with samples. Samples were sealed using adhesive film, incubated at 37 ^{o}C for 15 hours and then heat inactivated at 65 ^{o}C for 20 minutes (*Sau3AI* digestion), or 80 ^{o}C for 20 minutes (*TaqI* digestion). Products of digestion were prepared for ligation, as described in the following section.

2.6.2.2 *Preparation of TaqI and Sau3AI specific adapters*

TaqI and *Sau3AI* specific adapters (25 µM) were prepared in microfuge tubes using the reagents shown in Table 2.20, details of adapters and primers are illustrated in Table 2.21. Adapter mixes were cooled from 90 ^{o}C to 4 ^{o}C over a 16 hour period using a thermocycler, and aliquots were stored at -20 ^{o}C.

2.6.2.3 Ligation

The resulting sample digestion products were dispensed in 20µl aliquots in labelled microcentrifuge tubes and stored on ice. *TaqI* and Sau3AI mastermixes (MM) were made up separately in microfuge tubes according to Table 2.22, and 4µl of *TaqI* or Sau3I MM were

Mastermix	Reagent	Concentration	Volume (µl) (n=1)
Sau3AI	*Sau3AI*	10 U	2.5
	Sau3AI buffer	10X	2
	BSA	100X	0.2
	Total volume		*4.7*
TaqI	*TaqI*	10 U	0.5
	TaqI buffer	10X	2
	BSA	100X	0.2
	Total volume		*2.7*

Table 2.19. DIPS reagents used in Sau3AI and *TaqI* genomic digestion

Reagent	Concentration	Volume (µl)
ALI primer	100µM	25
AS primer (*TaqI* or *Sau3AI*)	100µM	25
Sterile TrisHCl (pH 7.4)	66mM	50
Total volume		*100*

Table 2.20. Reagents used to prepare *TaqI* and Sau3AI specific ligation adapters

	Abbreviations	sequence
DIPS control* (primers and adapters)	DIPS_CON_1	TTCTCTATGTGCGTTCTCTCCCTG
	DIPS_CON_2	CAAACTCCAGGTCTCCAACCAG
	DIPS_AP1	GGCCATCAGTCAGCAGTCGTAG
DIPS (adapters)	DIPS_AL1	GGGCCATCAGTCAGCAGTCGTAGCCCGGATCCAGACTTACACGTTG
	DIPS_AS *Taq*	PO_4-CGCAACGTGTAAGTCTG-NH_2
	DIPS_AS *SauAI*	PO_4-GATCCAACGTGTAAGTCTG-NH_2
DIPS** (linear amplification primers)	DIPS_PCR1_16F1	ACAAAGCACACACGTAGACATCG
	DIPS_PCR1_16F2	AGTAATAAATCAACGTGTTGCGATTG
	DIPS_PCR1_16F3	TTTGGTTACAACCATTAGCAGATGC
	DIPS_PCR1_16F4	GTGCCAACACTGGCTGTTCAAAG
	DIPS_PCR1_16F5	TACCAATTCTACTGTACCTAATGCCAG
	DIPS_PCR1_16F6	ACTTATTGGGGTCAGGTAAATGTATTC
	DIPS_PCR1_16F7	AGTAGATATGGCAGCACATAATGAC
	DIPS_PCR1_16F8	GTTGGCAAGCAGTGCAGGTCAG
DIPS** (nested PCR primers)	DIPS_PCR2_16F1	CGTACTTTGGAAGACCTGTTAATGG
	DIPS_PCR2_16F2	GGACTTACACCCAGTATAGCTGACAG
	DIPS_PCR2_16F3	AATAGGTATGTTAGATGATGCTACAG
	DIPS_PCR2_16F4	ACAAGCAATGAACTGCAACTAACG
	DIPS_PCR2_16F5	GAGGTTAATGCTGGCCTATGTAAAG
	DIPS_PCR2_16F6	CCCTGTATTGTAATCCTGATACTTTAGG
	DIPS_PCR2_16F7	TGCGTGCTAGTATACAACAACAGTAAC
	DIPS_PCR2_16F8	TTAAACCATAGTTGCTGACATAGAAC

Table 2.21. Details of primer and adapter sequences used in DIPS.

* In control experiment, DIPS_CON_1 was used in linear PCR and DIPS_CON_2 used in nested PCR. ** In linear and nested PCR, 8 different sets of HPV specific primers were required to span the HPV16 genome; each primer was used in a separate PCR reaction.

Mastermix	Reagent	Concentration	Volumeµl (n=1)
Sau3AI	Ligase buffer	10X	2.4
	T4 Ligase (NEB)	400 U/µl	1
	Sau3AI adapter*		0.48
	Water		0.12
	Total volume		*4*
TaqI	Ligase buffer	10X	2.4
	T4 Ligase (NEB)	400 U/µl	1
	TaqI adapter*		0.48
	Water		0.12
	Total volume		*4*

Table 2.22. DIPS reagents used in Sau3AI and *TaqI* ligation reaction

*Mastermix contained a *TaqI* and Sau3AI adapter final concentration of 50pmol.

added to each corresponding *TaqI* or *Sau3I* sample digestion product and repeat pipetted gently to mix. Tubes were sealed withadhesive film and the ligation reaction performed at room temperature for 2 hours followed by heat inactivation of ligase at 65^{o}C for 10 minutes. The resulting sample ligation product was then made-up to a total volume of 40µl by adding 16µl of sterile PCR grade water. Samples were prepared for DIPS linear amplification, as described in the following section.

2.6.2.4 *DIPS linear amplification*

A 1.4kb genomic loci on chromosome 21 (accession no. AP001068) was amplified using the ligation product of each sample to ensure DIPS assay was performing correctly. This was carried out using the control primers illustrated in Table 2.21 for control DIPS linear amplification and nested PCR steps, and then repeated using HPV16 specific primers also illustrated in the same table.

PCR plates consisting of 96 microfuge wells were used to prepare samples for linear amplification. Plates were labelled with the sample and primer set being used and 2µl sample ligation product was added to wells of the plate in duplicate (accouting for sample ligation products derived from both *TaqI* and *SauA3I* digestions). This was set up 8 times (8 primer sets were required to analyse each sample product) for both *TaqI* and *Sau3AI* ligation products (therefore 16 in total); primer sets are shown in Table 2.21. Mastermixes (MM) were made up individually in microfuge tubes for each primer set as illustrated in Table 2.23; Hot Star *Taq* (Qiagen, Hilden, Germany) was added last and stored on ice. Sample ligation products were combined with 23µl MM and mixed gently by repeat pipetting. Plates were sealed and linear amplification carried out in the post PCR laboratory using a thermocycler according to the conditions shown in Table 2.24. The resulting linear amplification products were maintained at 4^{o}C in the post PCR laboratory to prevent cross contamination.

Mastermix	Reagent	Concentration	Volumeµl (n=1)
Linear PCR	10X buffer + 15mM $MgCl_2$	1X	2.5
	dNTPs	10 mM (each)	0.5
	HPV_PCR1_16 (1-8)*	10 µM	0.5
	Hot Star *Taq*	1 U	0.125
	Water		19.375
	Total volume		*23*
Nested PCR	10X buffer + 15mM $MgCl_2$	1x	2.5
	dNTPs	10 mM (each)	0.5
	HPV_PCR2_16 (1-8)*	10 µM	1
	Hot Star *Taq*	1 U	0.125
	AP1 primer	10 µM	1
	Water		17.875
	Total volume		*23*

Table 2.23. Reagents used to prepare DIPS linear and nested PCR mastermix

*HPV specific primers used in linear and nested PCR are illustrated in Table 2.21, and were prepared in individual mastermixes for separate reactions.

DIPS	Temperature (°C)	Time (s)
Linear amplification	95	900
	94	30
	66	30
	72	180
	72	420
Nested PCR	95	900
	94	30
	66	30
	72	180
	72	420

Table 2.24. Conditions for DIPS linear and nested PCR.

2.6.2.5 *DIPS nested PCR*

Within the main laboratory, PCR plates were labelled and divided as described previously for linear amplification. Nested PCR mastermixes (MM) were set up individually in microfuge tubes according to Table 2.23, using 8 primer sets previously illustrated in Table 2.21; Hot Start *Taq* was combined with the MM last. MM (23µL) was added to the corresponding microfuge well of the plate and sealed using adhesive film. PCR plates were transferred to the post PCR laboratory and 5µl of linear amplification product for each sample was added to corresponding wells of the plate. Plates were resealed firmly, placed in a thermocycler, and nested PCR performed according to the conditions in Table 2.24. Nested PCR products were stored at at -20^{o}C for future reference, or prepared immediately for gel electrophoresis as described in the subsequent section.

2.6.3 Identifying amplified products of DIPS and APOT

Two gel staining and visualisation methods were utilised to detect PCR products from APOT and DIPS. The first method involved the addition of Ethidium Bromide (EB) (Sigma-Aldrich Company Ltd, Dorset, UK) directly to molten agarose containing 1X Tris-borate-EDTA (TBE) (Geneflow Ltd,Lichfield, UK); EB gels identified DNA bands by visualising gels under UV light within a transilluminator, which required the use of personal protective equipment due to the toxic nature of EB. The second method involved the addition of BlueView (TAE with methylene blue) (Sigma-Aldrich Company Ltd, Dorset, UK) directly to molten agarose containing distilled water, and DNA bands were visualised by the naked eye.

Sample DNA was electrophoresed simultaneously on ethidium bromide and BlueView gels so that the resulting DNA band patterns could be compared. Band patterns were visualised initially on EB gels because band images were more enhanced under UV light exposure, and were used as a reference to compare with band patterns viewable on BlueView gels. Bands of

interest were then excised from BlueView gels rather than EB gels because exposure of DNA to UV light during visualisation of EB gels could adversely affect DNA, making it unsuitable for down-stream purification, sequencing and analysis.

2.6.4 Gel electrophoresis: APOT amplified products

This section of writing will describe the preparation of EB and BlueView agarose gels for electrophoresis of APOT derived PCR products; these protocols share a high degree of similarity with the protocols carried out to prepare gels for electrophoresis of DIPS derived PCR products, and for some parts will be referenced back to this section.

2.6.4.1 . *Preparation of ethidium bromide (EB) agarose gel*

EB gel at 1.2% w/v agarose was prepared for separating APOT PCR products using the reagents illustrated in Table 2.25.

EB gels were made up in 500ml durans by dissolving agarose (Life Technologies Corporation, Carlsbad, CA) in 1X TBE using a microwave on full power until agarose appeared clear, froth disappeared, and large bubbles formed. Durans were placed in a water bath at 60 ^{o}C to reduce molten agarose temperature (without allowing agarose to set), after which EB was added carefully and swirled gently to mix. A gel plate was prepared by sealing the perimeter of the plate with autoclave tape and a comb fitted to produce wells within the gel. Agarose was gently swirled to avoid generating bubbles, poured into the gel plate, and left to cool and solidify on the bench top. Once the gel had solidified, combs and autoclave tape was carefully removed and the gel was placed in a gel tank containing 1X TBE in preparation for electrophoresis, which will be described in subsequent sections.

2.6.4.2 *Preparation of BlueView agarose gel*

BlueView gels were prepared at 1.2% w/v agarose as shown in Table 2.25, via the same method described previously for EB gels. However, agarose was dissolved in distilled water by making up to 90% of the volume and the remaining 10% made up with 10X BlueView when agarose was molten. The solidified BlueView gel was placed in a gel tank containing 1X BlueView solution in preparation for electrophoresis, which will be described in the following section.

2.6.4.3 *Electrophoresis*

A 100bp ladder (Geneflow Ltd, Lichfield, UK) (10 µl) was loaded in to the first well of the gel as a reference for DNA band sizes. Nested PCR product (5 µl) was combined with 10µl loading dye (Orange G, Sigma) and loaded into a well of the gel. The voltage was set to 150 and electrophoresis carried out for half an hour (small gel) or for 1 hour (large gel). EB gel bands were visualised under UV light within a transilluminator; a snapshot of the band patterns were printed and saved. The corresponding BlueView gel bands were visualised with the naked eye and compared with band patterns present on the EB gel.

2.6.4.4 *Analysis of band patterns*

DNA band patterns were examined on both gels, and DNA band sizes between 250 bp and 1050 bp were selected on BlueView gels; these DNA fragments represented possible HPV-human fused sequences and underwent DNA purification, sequencing and analysis, which will be described in subsequent sections. DNA bands visualised at 250 bp and 1050 bp were avoided; 250 bp bands were generated due to mis-aanealing of the oligo$(dT)_{17}$ primer to an adenosine rich region of the HPV genome, and 1050 bp bands represented episomal derived HPV transcripts.

Gel size	TBE/distilled water* (ml)	Agarose (g)	Ethidium bromide (µl)	10X BlueView (ml)
Small	100	1.2	2	10
Medium	300	3.6	5	30
Large	600	7.2	10	60

Table 2.25. Preparation of 1.2% w/v agarose gel required for separating APOT and DIPS PCR products via electrophoresis

*BlueView agarose gels were prepared to 90% of the volume using distilled water and the remaining 10% made up with 10X BlueView after molten agarose had cooled enough to handle safely.

2.6.5 Gel electrophoresis: DIPS amplified products

2.6.5.1 *Prepartion of EB and BlueView agarose gel*

EB and BlueView agarose gels were prepared as described previously for APOT amplified products (Table 2.25) except that EB and BlueView gels were prepared at 2% w/v agarose using the reagents.

2.6.5.2 *Electrophoresis*

Electrophoresis of DIPS nested PCR products was carried out as described previously for APOT nested PCR products.

2.6.6 DNA purification and elution

Illustra GFX PCR DNA and Gel Band Purification Kit (GE Healthcare) was used to purify and concentrate DNA from PCR BlueView agarose gels.

DNA bands selected for purification were counted and the corresponding number of 1.5 ml DNase-free tubes were weighed and recorded. A sterile scalpel was used to cut DNA bands from agarose and each slice placed in individual tubes of known weight; a new scalpel was used for each band slice to prevent cross contamination between samples. Tubes containing agarose slices were reweighed, and the weight of the agarose was calculated by subtracting the initial weight of the tube from the combined weight of the tube and the agarose slice. Capture buffer 3 (10 µl) was added per 10mg of agarose slice; if the gel slice weighed less than 300 mg, 300 µl capture buffer 3 was added. Samples were mixed by gently inverting tubes, and incubated at 60 ^{o}C in a hot water bath for 15-30 minutes; samples were mixed by inversion every 3 minutes until the agarose appeared completely dissolved. Sample mixtures were visualised for a yellow/pale orange colour change, which ensured that the mix was at optimal pH for efficient DNA binding to the silica membrane of the GFX MicroSpin columns. Tubes were them centrifuged briefly for sample collection. GFX MicroSpin columns were set-up

within round bottom collection tubes for each sample and a maximum volume of 800µl sample mixture dispensed in each column. Columns were incubated at room temperature for 1 minute, centrifuged at 16,000 x g for 30 seconds, flow through discarded, and collection tube reused; this process was repeated until all of the sample mixtures had been loaded, incubated, and centrifuged. Wash buffer 1 (500 µl) was added to each column and centrifuged at 16,000 x g for 30 seconds after which collection tubes were discarded and columns added to fresh 1.5 ml DNase-free pointed bottom collection tubes. Between 10 and 50 µl of elution buffer 6 was added to the centre of the GFX MicroSpin membrane and incubated at room temperature for 1 minute. Samples were then centrifuged at 16,000 x g for 1 minute to elute purified DNA. Purified DNA was prepared immediately for sequencing or stored at -20 ^{o}C for future reference.

2.6.7 Sequencing and analysis

The approximate concentration of purified DNA for each sample was estimated by comparison with a standard of known concentration included during electrophoresis. Samples were labelled and prepared to be sent for sequencing at the Sequencing Core, Cardiff University School of Biosciences; 200ng DNA in a total volume of 20µl was required, therefore sample DNA was diluted to 10ng/µl and a total of 20µl dispensed in DNase free microfuge tubes. DNA was sequenced using BigDye (Applied Biosystems,Foster city, CA) chemistry on an ABI 3130xl using primers previously used to carry out nested PCR (Table 2.21).

2.6.7.1 *Assessing sequence data quality*

DNA sequences for each sample were obtained from the Sequencing Core in a Microsoft Word file. Sequence data was imported into BioEdit Sequence Alignment Ibis Biosciences An Abbott company, Carlsbad, CA) and used to check the quality of the sequence data. Nucleotide bases were represented in capital letters, and uncalled bases were represented

with the letter ‘N’. Uncalled bases were compared with the frequency histogram produced automatically within the software and corrected in edit mode by manually replacing with the correct base in lower-case letters; samples containing numerous uncalled bases suggested poor quality sequence and were highlighted for reference. The entire sequence was saved, copied, and pasted into Notepad in FASTA format.

2.6.7.2 *Bioinformatics*

The algorithm BLAST (a Basic Local Alignment Search Tool) was used to compare the sequence to a list of sequences in the GenBank database maintained by NCBI (the National Centre for Biotechnology Information). In this instance it was used to align the DNA sequence obtained for each sample against the HPV16 reference genome and the human reference genome. This provided a way of identifying HPV and human fused sequences within the sample sequence, in order to detect integrated HPV within the human genome.

BLAT (the BLAST-Like Alignment Tool) is an alignment tool like BLAST but works by storing an index of an entire genome and comparing the sequence input to this, rather than a set of GenBank sequences (which occurs for BLAST). In this instance, BLAT was used to analyse sequences found to contain HPV fused to human genome, and research the location of the HPV sequence within the human genome. Sequences were pasted in to the data base and the region of HPV and the location of integration was obtained.

2.6.8 Primer design

Clonal cell lines containing HPV-human fused sequences were re-explored in order to verify the presence of integrated HPV in samples. Primers were designed to specifically flank the HPV-human boundary at integration sites, and were used to interrogate samples to confirm that the integration events previously detected were genuine. Cross examination of samples

was also performed to identify whether integration loci were shared between clonal cell lines or whether they were unique to individual clones.

2.6.8.1 *Designing flanking primers*

PRIMER 3 was used to design primers that flank the site of HPV integration in clonal cell lines. Clonal cell line DNA sequences were entered in to PRIMER 3, and a variety of forward and reverse primer sequences (complimentary to the fused HPV-human sequence input) were generated. Flanking primers are illustrated in Table 2.26; primers were purchased from Sigma-Aldrich Company Ltd, Dorset, UK.

2.6.8.2 *Rehydration and preparation of flanking primers*

Lyophilised primers were diluted according to the manufacturer's instructions using sterile DNase free water to produce a 100 µM solution; 50 µl aliquots were stored at -80 ^{o}C and diluted to 5 µM using DNase free water when required for use.

2.6.8.3 *Touch-down PCR*

The designed flanking primers were used to interrogate the corresponding cDNA or DNA from which they were initially detectable. Each primer set was also used to cross-test other clonal cell line cDNA or DNA. Touch-down PCR was used as a one-step method for obtaining optimal amplification of products by varying the annealing temperature with progressive cycles to increase the specificity of the PCR product and prevent non-specific priming.

Mastermix (MM) was prepared for each primer set as shown in Table 2.27; Hot-start *Taq* (Qiagen, Hilden, Germany) was stored on ice and added to the MM last. Sample cDNA/DNA at 50 ng/µl and 15 µl MM was added to microfuge tubes and a touch-down PCR performed according to the conditions in.

Protocol	Primer name	Sequence
APOT	5D forward	GCTCACACAAAGGACGGATT
	5D reverse	AGTGTGGAGAGGAAGACACCA
	11D1 forward	CCATAGTACATTTAAAAGGTGATGC
	11D1 reverse	TGCCTGTATTTTTCTGGAAGG
	11D2 forward	GCTCACACAAAGGACGGATT
	11D2 reverse	AGTGTGGAGAGGAAGACACCA
	5H forward	AATTGTGTGCCCCATCTGTT
	5H reverse	TCATGAGGCTGAAGGAGGTT
	11H1 forward	CACCGAAGAAACACAGACGA
	11H1 reverse	CAGAAAGCAAAAACACCAAGC
	11H2 forward	CCTGTTAATGGGCACACTAGG
	11H2 reverse	TCATGAGGCTGAAGGAGGTT
	5M1 forward	AATTGTGTGCCCCATCTGTT
	5M1 reverse	CCTCCACAGTCAAAGGGAAA
	5M2 forward	CCTGTTAATGGGCACACTAGG
	5M2 reverse	CACAGTCTTAGCATCCATCTCTG
	5M3 forward	AATTGTGTGCCCCATCTGTT
	5M3 reverse	ATCATGCGCCCACATTTT
	5M4 forward	AATTGTGTGCCCCATCTGTT
	5M4 reverse	CGCCCACATTTTGGTTTTAT
	9Y forward	TAGGAATTGTGTGCCCCATC
	9Y reverse	TGAGCTCATCCTCAGGGAAG
	13Y1 forward	TAGGAATTGTGTGCCCCATC
	13Y1 reverse	TGAGCTCATCCTCAGGGAAG
	13Y2 forward	CCTGTTAATGGGCACACTAGG
	13Y2 reverse	CACCCTCAAACACAGACTCG
DIPS	5D forward	CACCTATAGATTTTCCACTACG
	5D reverse	ACAAGGTCGCTGCTTAGGG
	11D forward	GCACCTATAGATTTTCCACTACG
	11D reverse	ACAAGGTCGCTGCTTAGGG
	5H forward	TGAAATTTCTGCAAGGGTCTG
	5H reverse	CTCTCTGCCCACGGAAAATA
	11H forward	TGAAATTTCTGCAAGGGTCTG
	11H reverse	CTCTCTGCCCACGGAAAATA
	11H1 forward	ATGTTCATGGGGAATGGTTG
	11H1 reverse	CCTATGGGGCAGCATGATTA
	5M1 forward	CTGCACAGGAAGCAAAACAA
	5M1 reverse	ATGTTCCAGGGAGAACAGGA
	5M2 forward	CTGCACAGGAAGCAAAACAA
	5M2 reverse	ATGTTCCAGGGAGAACAGGA
	5M3 forward	CTGCACAGGAAGCAAAACAA
	5M3 reverse	ATGTTCCAGGGAGAACAGGA
	5M4 forward	CTGCACAGGAAGCAAAACAA
	5M4 reverse	ATGTTCCAGGGAGAACAGGA
	5M n.c. forward	TGCCAGTACGCCTAGAGGTT
	5M n.c. reverse	CGTGCCAAATCCCTGTTTT
	5P n.c. forward	AAGGATTGTGCAACAATGTG
	5P n.c. reverse	TGCACAAAATATGTTCGTATTCC
	9Y forward	ATGCACAATTGGCAGACACT
	9Y reverse	ATCCCACCACGGTTGATTT
	13Y forward	TTTAACTGCACCAACAGGATG
	13Y reverse	GTTGCCTCAATTCTGGGTGT

Table 2.26. Details of flanking primer sequences designed via PRIMER 3 to interrogate clonal cell lines previously found to contain integrated HPV.

n.c: abbreviation of non-contiguous; refers to fragmented sequences of integrated HPV.

Reagent	Concentration	Volume* (µl) (n=1)
10x buffer		2
dNTP	2 mM	2
$MgCl_2$	15 mM	2
F primer*	10 µM	2
R primer*	10 µM	2
Hot-start *Taq*	5 U/µl	0.2
Water		4.8
Total volume		*15*

Table 2.27. ***Reagents used to prepare mastermix for touch-down PCR.***

*Details of F and R flanking primer sequences are referred to in Table 2.26.

. **Temperature (°C)**	**Time (seconds)**
94	180
94	30
66-1 °C/cycle*	30
72	60
	30 cycles
94	30
55	30
72	60
	30 cycles
72	600

Table 2.28. ***Conditions for touch-down PCR.***

*The temperature for annealing in the first cycle was 5-10 °C above the melting temperature (*T*m) of the primers (T*m* values provided by Sigma-Aldrich). In the cycles thereafter, the annealing temperature was decreased in stages by 1 °C until the final temperature fell 2-5 °C below the *T*m of the primers.

2.6.8.4 *Gel electrophoresis and interpretation of results*

Touch-down PCR products were separated on a 2% w/v EB agarose gel, which was prepared as shown previously in Table 2.25, and electrophoresis was carried out as previously described. The DNA band patterns produced were analysed; to confirm amplification of the HPV-human integration loci, a single band would be observed for each sample with a size that correlated with the number of base pairs in the initial sequence of interest indicating that the selected sequence had been amplified.

2.7 Cidofovir (CDV) dosing studies

Cell culture and drug/compound optimisation experiments were performed to develop a CDV dosing protocol; optimisation experiments were carried out in collaboration with Miss Áine Flynn, HPV Research Group, Cardiff University. The final dosing protocol entailed treating vulval and vaginal clonal cell lines with cidofovir (CDV) under optimised conditions; CDV was purchased from Shanghai Sun-Sail Pharmaceutical Science & Technology Corporation Limited (Shanghai, China).

This section describes the optimisation protocols carried out and the final CDV dosing protocol produced. The overall aim of the dosing regime was to assess cellular and molecular response(s) to CDV treatment and therefore give insight in to the mechanism(s) of action of CDV in VIN/VaIN disease.

2.7.1 Preparation of CDV

2.7.1.1 *CDV assessment and formulation*

Compound verification and assessment of purity was performed by Davide Carta, Fabrizio Pertusati, and Karen Hinsinger (McGuigan Group, Cardiff University, Welsh School of

Pharmacy) using nuclear magnetic resonance (NMR). Synthesis of CDV was also carried out by the McGuigan Group according to the procedure outlined in the literature (Kern et al., 2002).

Prior to preparing concentrations of CDV, stock CDV underwent repeat vortexing and warming to disperse the consistency and turbidity of the compound; this was carried out after verbal communication with colleagues of the McGuigan Group.

2.7.2 Optimisation studies

Optimisation studies were carried out to determine optimal experimental variables that would comprise the final CDV dosing protocol. This section describes the optimisation experiments carried out.

2.7.2.1 *CDV concentration and cell density: 96 well plates*

PC08 and PC09 clonal cell lines were cultured with irradiated 3T3 feeder cells in two 9cm TC dishes until ~80% confluent. Cultures were then passaged and trypan blue viable cell counts performed using a haemocytometer, as previously described. Single cell suspensions were used to seed three 96 well plates with 5,000, 7,000, and 10,000 cells/well in triplicate using EGF- GMEM without being supplemented with irradiated 3T3 feeder cells, according to the format illustrated in Figure 2.6. PBS was dispensed in wells of the perimeter to prevent evaporation of cultures within central wells of the plate. A CDV dosing protocol was then carried out as illustrated in Figure 2.7. Plates were incubated for 24 hours to allow cells to attach to the base of each well. After 24 hours (day 1) media was aspirated gently from wells of plate 1, which represented an initial cell count without CDV treatment; a rubber tube connected to an air suction pump was used to aspirate media, taking care not to disrupt the cell monolayer. Aspirated media was diverted into a discard bottle containing hypochlorite solution (Presept). Cells were then washed with PBS and trypsinised using 5 µl TE and incubated for 5-10 minutes. During incubation cells were visualised

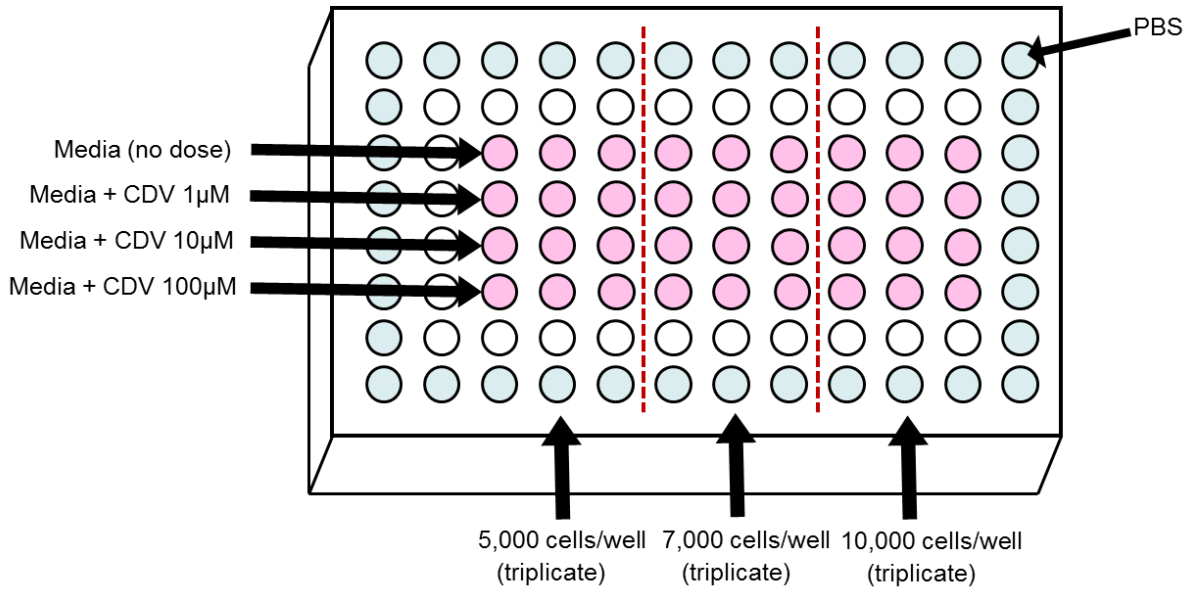

Figure 2.6. 96 well plate format for optimisation of cell density and CDV concentration

Wells were inoculated with 5, 000, 7, 000, and 10, 000 cells/well in triplicate which were subjected to different concentrations of CDV prepared in GMEM (0, 1, 10, and 100 µM) and a no dose control.

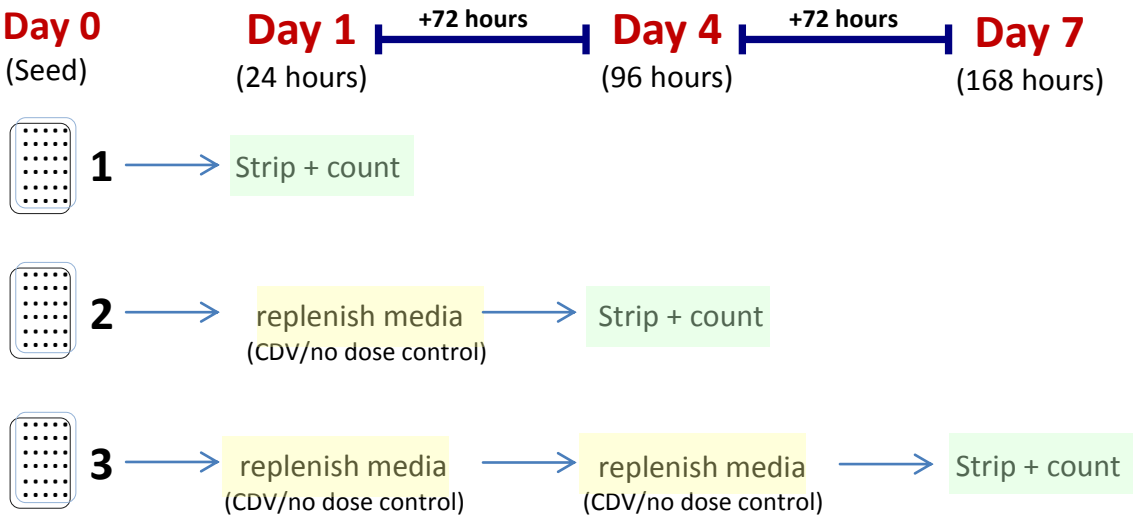

Figure 2.7. Dosing regime carried out for optimisation of cell density and CDV concentration in 96 well plate format.

Wells of plates 1, 2, and 3, were seeded on day 0 and incubated for 24 hours. After 24 hours (day 1) cells were stripped from plate 1 and cell viability assessed by performing viable cell counts, and the first dose of CDV applied to wells of plates 2 and 3 by replenishing with EGF+ GMEM supplemented with 0, 1, 10, and 100 µM CDV and incubated for 72 hours. After 72 hours (day 4) plate 2 was stripped and cell viability assessed, and the second dose of CDV was applied to wells of plate 3 and incubated for 72 hours. After 72 hours (day 7) plate 3 was stripped and the final assessment of cell viability performed.

microscopically for cell rounding, and wells were repeat pipetted to physically detach cells. The resulting cell suspensions were transferred from each well into individual, labelled 1ml tubes and combined with 5 µl GMEM to neutralise TE; plate 1 was then discarded. Media was also aspirated and discarded from wells of plates 2 and 3 in the same way, and replenished with EGF+ GMEM supplemented with 0, 1, 10, and 100 µM CDV and re-incubated for 72 hours. After 72 hours (day 4), media was aspirated from wells of plate 2 and viable cell counts performed as described previously; plate 2 was then discarded. After 72 hours (day 7), media was aspirated from wells of plate 3 and viable cell counts performed as described previously, plate 3 was then discarded.

2.7.2.2 *Cell density: 6 cm TC dishes*

To cultivate sufficient cell numbers for optimising cell density in 6cm TC dishes, PC08 and PC09 clonal cell lines were cultured with irradiated 3T3 feeder cells in four 9cm TC dishes until ~80% confluent. Cultures were then passaged and trypan blue viable cell counts performed as previously described. The resulting clonal single cell suspensions were used to seed 6cm TC dishes in triplicate with 1 x 10^5, 5 x 10^5, and 1 x 10^6 cells (nine 6 cm TC dishes in total) using EGF- GMEM, without supplementing with 3T3 feeder cells. Cultures were replenished with EGF+ GMEM at 24 hours (day 1), viewed microscopically to analyse cell/colony morphology and assess percentage confluence, and re-incubated for an additional 72 hours. After 72 hours (day 4) cells were viewed microscopically to analyse cell/colony morphology and assess percentage confluence for the final time.

2.7.3 Developing the final CDV dosing protocol

A preliminary CDV dosing protocol was designed prior to the final CDV dosing protocol to ensure that a dose response was detectable under the conditions. The preliminary CDV dosing

protocol is illustrated in Figure 2.8. After performing this protocol, the time points for assessing cell viability were modified and the final CDV dosing protocol was devised.

2.7.3.1 *Final CDV dosing protocol*

The final CDV dosing protocol was carried out as shown in Figure 2.9. TC dishes (A-E) were set up in duplicate to account for two separate down-stream applications, i. viable cell counts, and ii. DNA and RNA extraction. When viable cell counts had been carried out, the remaining cell suspensions were prepared for apoptosis analysis via flow cytometry, which will be described in the following section.

To cultivate sufficient cell numbers for the dosing protocol, each PC08 and PC09 clonal cell line was cultured with irradiated 3T3 feeder cells in eight 9 cm TC dishes until ~80% confluent. Cultures were then passaged and viable cell counts performed using a haemocytometer, as previously described. Five 6cm TC dishes (A-E) in duplicate (10 dishes in total) were set up and the resulting clonal single cell suspensions of PC08 and PC09 were each used to seed dishes with 5×10^5 cells in 5ml of EGF- GMEM, without supplementing with 3T3 feeder cells, and incubated for 24 hours.

After 24 hours incubation, cells of dish A were viewed microscopically and an initial viable cell count was carried out to assess cell viability using a haemocytometer as previously described; dish A was then discarded. The remaining cell suspensions were prepared for analysis of apoptosis via flow cytometry. Cells of duplicate dish A was prepared for DNA and RNA extraction, according to the method previously described, and then discarded. Cells of dish D and E were viewed microscopically, media was aspirated and replenished with 5ml EFG+ GMEM supplemented with 10µM CDV, and Dish D and E were incubated for 12 hours and 36 hours respectively. Cells of dish B and C were prepared in the

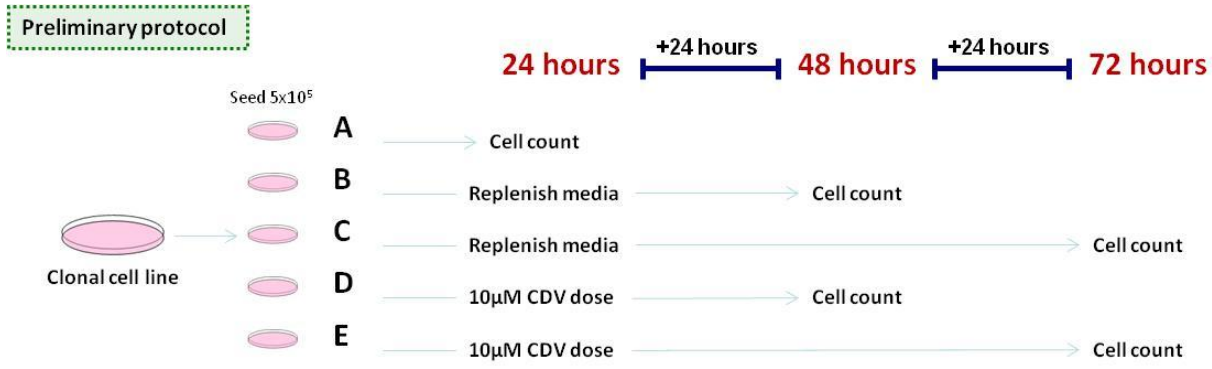

Figure 2.8. The preliminary CDV dosing protocol

Dishes A-E were seeded with $5x10^5$ cells and incubated for 24 hours. After 24 hours an initial cell viability reading of dish A was carried by counting viable cells using a haemocytometer; dishes D and E were treated with GMEM supplemented with 10µM CDV (CDV treated), and dishes B and C were replenished with GMEM only (no treatment). Dish B (no treatment) and D (CDV treated) were incubated for a further 24 hours and assessed for cell viability. Dish C (no treatment) and E (CDV treated) were incubated for a further 48 hours and assessed for cell viability.

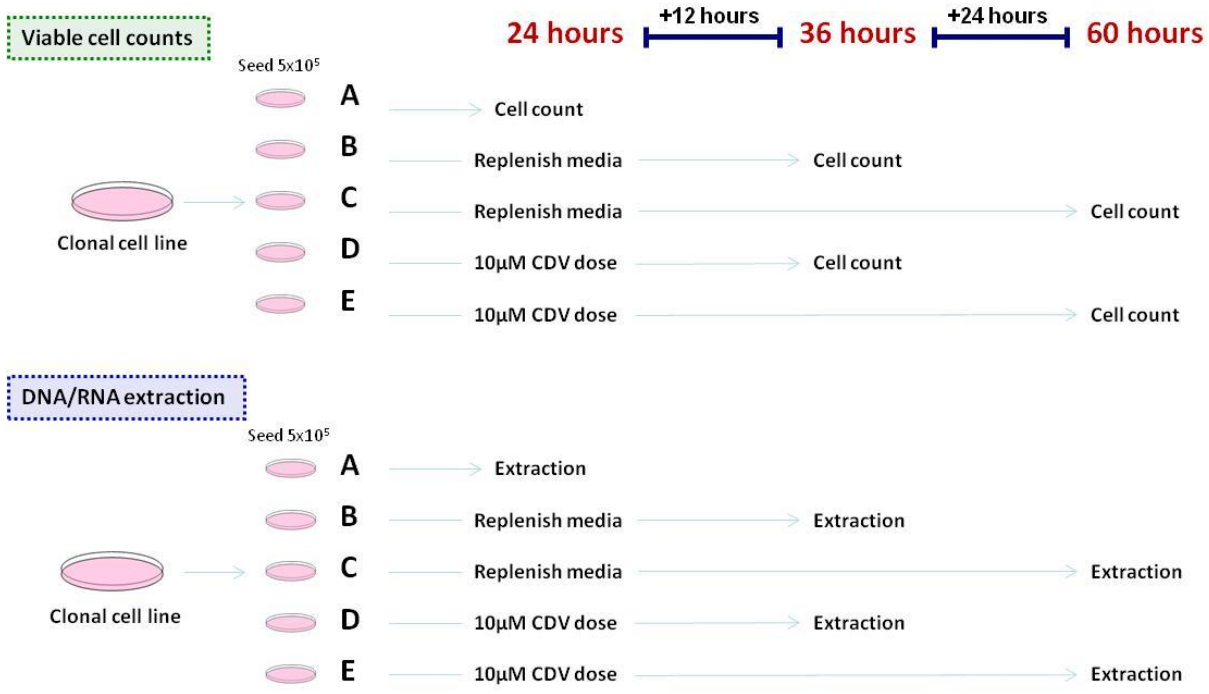

Figure 2.9. The final CDV dosing protocol

Dishes were seeded with $5x10^5$ cells and incubated for 24 hours. After 24 hours, an initial reading of plate A was carried out to assess cell viability and extract DNA/RNA; plates D and E were treated with GMEM supplemented with 10µM CDV (CDV treated), plates B and C replenished with GMEM only (no treatment control), and all plates incubated for a further 12 hours. After 12 hours, plates B (no treatment control) and D (CDV treated) were assessed for cell viability, and DNA/RNA extracted. After 36 hours, plates C (no treatment) and E (CDV treated were assessed for cell viability and DNA/RNA extracted. Nb. After cell viability counts, remaining cell suspensions underwent preparation for flow cytometry (apoptosis analysis).

same way, replenishing with 5ml EGF+ GMEM and incubating for 12 and 36 hours respectively.

After 12 hours incubation with 10µM CDV, cells of dish B were viewed microscopically and prepared for a viable cell count and cell suspensions retained for flow cytometry. Cells of duplicate dish B were prepared for DNA and RNA extraction. Both dishes were discarded. Dish D cell cultures were prepared in the same way, representing 12 hours incubation without CDV treatment,

After 36 hours incubation with 10µM CDV treatment, cells of dish C were viewed microscopically and prepared for a viable cell count and cell suspensions retained for flow cytometry. Cells of duplicate dish C were prepared for DNA and RNA extraction. Both dishes were discarded. Dish E was then prepared in the same way, representing 36 hours incubation without CDV treatment.

2.8 Detection and quantification of apoptosis

During the CDV dosing protocol, CDV treated and untreated cells were retained and underwent apoptosis analysis using annexinV-Cy5/7-aminoactinomycin D (7-AAD) staining (eBioscience, Incorporated, San Diego, CA.) and flow cytometry. Stained cells were analysed for signs of apoptosis by detecting fluorescence absorptions of AnnexinV-Cy5 and 7-AAD between 650-670 nm and 543-625 nm, respectively, using Accuri™ Flow Cytometer C6 (BD Biosciences, USA) according to the manufacturer's instructions.

Reagents used to prepare cells were stored on ice for the duration of the experiment. Once cell suspensions had been prepared, they were immediately transported on ice to Accuri™ C6 flow cytometer (BD Biosciences, Belgium) for analysis.

2.8.1 Cell preparation and staining

Clonal cell lines were were cultured and dosed with CDV according to the dosing regime previously described. Cells were then trypsinised, resuspended and trypan blue viable cell counts performed. Cells suspensions were centrifuged at 12,000 rpm for 5 minutes and supernatant discarded gently. The cell pellet was resuspended in 1 ml staining buffer (Life Technologies), transferred to a microfuge tube and re-centrifuged. 1X annexinV-Cy5 binding buffer (Life Technologies) containing 1/100 of stock AnnexinV-Cy5 solution (Life Technologies) and 1µg/ml 7-AAD (Life Technologies) was made up in 50 µl total volume and used to resuspend cells. Tubes were tapped gently to ensure that cells were resuspended, and incubated at room temperature in the dark for 5 minutes. After incubation, AnnexinV binding buffer containing 1µg/µl of stock AnnexinV-Cy5 solution was prepared in a total volume of 150 µl and used to resuspend cells. Cells were centrifuged at 12, 000 rpm for 5 minutes. After centrifugation, cells were resuspended in 100 µl AnnexinV binding buffer containing 1 µg/µl of stock AnnexinV-Cy5 solution and transferred to miniFACS tubes (BD Biosciences, Belgium). Tubes were transferred immediately on ice for flow cytometry analysis.

2.8.2 Flow cytometry

The Accuri C6 flow cytometer was operated according to manufacturer's instructions and laboratory standard operational procedure within the department of Haematology, Cardiff Univeristy, School of Medicine. Prior to running cell suspensions through the system, the machine was initialised and prepared for a series of washing cycles. Samples were run separately at medium speed until 50,000 cells had been counted; gating, speed settings and cell count limits were selected using the software icons. Once a sample had been processed it was discarded and the machine prepared for one washing cycle using water for 30 seconds; a 30 second water rinse was carried out between samples to clean the tubes and prevent carry-over of the previous sample. At the end of use and the machine required preparation for the

next user, the machine was prepared for another series of washing cycles and the machine left on. If the software and machinery was not required, an extended wash was performed prior to closing down the software and shutting off the machinery.

2.9 Whole transcriptome sequencing and analysis

RNA sequencing of the transcriptome is a recently developed method which enables accurate and complete transcript profiling of cells (Wang et al., 2009). Whole Transcriptome Analysis Kit was used to convert the full set of RNA transcripts expressed within a cell into a cDNA library for sequencing analysis on the Applied Biosystems SOLiD™ Sequencing system, as described in manufacturer's instructions (Applied Biosystems, CA, USA). RNA sequencing was carried out out by Dr James Colley and colleagues at Wales Gene Park (Cardiff University), supported by additional funding from the Tom Owen Scholarship fund.

The basic principles of SOLiD™ transcriptome sequencing comprised 3 stages, i. sample preparation, ii. substrate preparation, and iii. SOLiD analyser barcoding. Each stage was carried out as follows:

I. *Sample preparation*. A mate-paired library was created by sheering sample DNA to a specified size and ligating adapters to the ends to produce 2 DNA fragments at a known distance apart in the target sample. The resultant mate-paired library comprised millions of unique molecules which represented the entire target sequence.
II. *Substrate preparation*. Mate-paired libraries underwent emulsion PCR to hybridise libraries to beads; libraries were then clonally amplified. Bead enrichment was carried out to capture beads containing amplified library templates, which were then covalently attached to a glass slide.
III. *Barcoding on SOLiD™ analyser*. Template beads bound to the glass slide were combined with universal sequencing primer, ligase, and a pool of fluorescently labelled

probes (4 dyes representing 4/16 dinucleotide sequences). A complimentary probe was hybridised to the template sequence and ligated, after which fluorescence was measured and the dye cleaved off for further reactions. A new primer was hybridised off-set by 1 base and the ligation cycle repeated; this primer reset process was repeated for 5 rounds to provide dual measurement of each base separated by several cycles, to increase sequence accuracy.

The resultant raw sequence data underwent down-stream analysis in conjunction with Dr Peter Giles and Dr Kevin Ashelford at Wales Gene Park (Cardiff University), according to the flow chart illustrated in Figure 2.10.

2.9.1 Statistical and data analysis

2.9.1.1 *Quality control of RNA and sequence data*

Concentration and quality of cell line RNA extracts was assessed using Nanodrop 2000 spectrophotometer and Agilent to ensure RNA was suitable for SOLiD™ sequencing, as previously described. Data yield and mapping success of the resulting SOLiD™ sequence data was prepared for all samples to ensure transcript data quality was sufficient for down-stream gene expression analysis.

2.9.1.2 *Quantification of gene expression*

RPKM values (Reads per Kilobase exon Model per million mapped reads) (Mortazavi et al., 2008) the common method for quantifying expression levels for RNA-sequence datasets, were calculated for individual transcripts using in-house software. To define the transcript locations used in the analysis, the RefSeq gene model RefGene, as provided by the UCSC human reference hg19 site, was used along with the gene model for HPV16 downloaded from NCBI (accession no: NC_001526). Integrative Genomics Viewer (IGV) was used to visualise mapped transcript reads to reference these reference genomes.

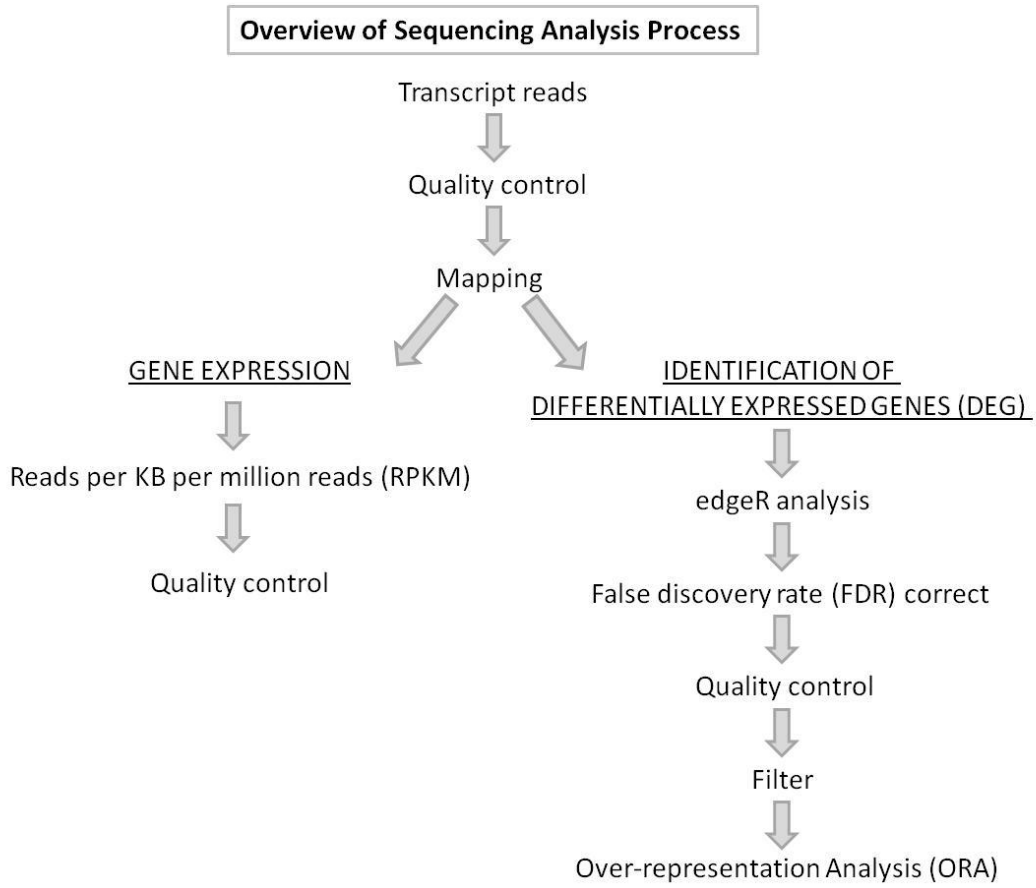

Figure 2.10. Summary of SOLiD™ sequencing and data analysis.

Clonal cell line total RNA extracts underwent SOLiD™ Whole Transcriptome sequencing and the resultant raw data analysed. Raw data in the form of transcript reads underwent quality control (QC) to ensure data was suitable for down-stream analysis. Transcripts were then mapped to the human and HPV genomes; this provided an estimation of mapping yield and success to determine whether sequence data was suitable for further down-stream analyses. Sequence data was then subjected to i. gene expression analysis, and ii. differentially expressed gene (DEG) analysis followed by over-representation analysis (ORA) and gene ontology (GO). Gene expression was assessed by converting sequence data to reads per KB per million reads (RPKM values), the common method for quantifying gene expression in this instance. Transcripts were then visualised through IGV and mapped to the RefSeq gene model RefGene, as provided by the UCSC human reference hg19 site, along with the gene model for HPV16, downloaded from NCBI (NC_001526). As part of DEG analysis, corrected p-values were filtered for transcripts presenting with a high degree of confidence as being significantly different between 2 data sets. This data was filtered by FDR multiple testing correlation and a cut-off of $p<0.05$ applied. ORA GO analysis was then applied to the significantly expressed ($p<0.05$) transcripts to sort them in to different GO categories; GO ORA identified changes in expression for a number of genes in an ontology group and allowed a selection of genes to be identified as having some differential expression which all map to the same category.

2.9.1.3 *Quality control of transcript count data*

To check any issues with the underlying transcript data distributions for each sample, the smallest value, lower quantile, median, upper quantile, and largest value, were calculated and illustrated in a box plot for easy visual representation using R statistical software. MvA plots were also produced using R statistical software to check samples for irregularities in transcript data in a pairwise comparison with other samples.

2.9.1.4 *Identification of differentially expressed genes (DEG) using edgeR*

To identify differentially expressed genes in response to CDV treatment, edgeR analysis (Robinson et al., 2010) was carried out on normalised transcript count data. The resultant p-values were corrected for multiple testing and false discovery issues using the false discovery rate (FDR) method (Benjamini and Hochberg, 1995). This provided a list of significant transcripts found to be over or under-expressed after treatment with CDV. Heat maps of significant transcripts were constructed using R statistical software in order to reveal patterns within the dataset which could be visualised more easily.

2.9.1.5 *Over representation analysis (ORA) of gene transcripts against Gene Ontology (GO) annotations*

GO ORA was carried out using goseq method (Young et al., 2010c) to standardise the representation of significant gene transcripts using a controlled vocabulary of terms. Transcripts were grouped into associated functions (GO ID and term) which were then categorised under 3 general themes, 1. Biological processes (BP), 2. Molecular functions (MF), and 3. Cellular component (CC). GO ORA of the top 500 significant gene transcripts was carried out against GO annotations and the resulting data was corrected for multiple testing and false discovery using the FDR method.

3 Phenotypic characterisation of short term vulval intraepithelial neoplasia (VIN) and vaginal intraepithelial neoplasia (VaIN) cell cultures

3.1 Results

Heterogeneous cell lines PC08 and PC09 were derived in a pilot study from tissue biopies of VIN III and VaIN III; PC08 and PC09 were cultured for 19 and 21 passages respectively. Cryopreserved cell stocks of early passage PC08 and PC09 were revived and used to produce a selection of clonal cell lines, which will be described in this Chapter. Early passage PC08 and PC09 were selected because they were closely related to the parental biopsy tissue from which they were explanted and so provide a good representation of neoplastic disease *in vitro*. The clonal cell lines were used in a series of preliminary experiments to optimise cell culture conditions (described in Chapter 4). Clonal cell lines also underwent short-term culture for 5-7 passages during which time they were characterised; characterisation was carried out to determine whether the individual lines differed from one another and whether they were stable with regard to morphology, growth rates and HPV gene expression.

This chapter describes phenotypic characterisation of early passage PC08 and PC09, and clonal cell lines during short-term culture; PC08 and PC09 cell culture records over 19 and 21 passages are also included from the pilot study (kindly provided by Dr Ned Powell). Phenotypic characterisation refers to the observable characteristics of the cells and was carried out by examining cell cultures microscopically to assess cell and colony morphology (shape and appearance). Exploring cell and colony morphology was important because it gave an indication of the health of the cells, allowed an initial assessment of potential cell culture contaminants, and allowed differences in cell and colony characteristics to be identified among clonal cell lines.

Characterisation also included estimation of the total number of population doublings (PD) over the entire cell culture period, and doubling time (DT) at each passage, which were defined previously. Investigation of the growth characteristics was important because it accurately showed how robust the clonal cell lines were in culture, identified potential growth rate variants amongst the clonal cell lines, and also gave an indication of the health of the cells when linked to morphology.

3.1.1 Aims and objectives

The central aim was to derive a series of clonal cell lines from heterogenous (parental) cell lines and phenotypically characterise them during short-term culture; this comprised assessing morphology and growth characteristics.

The following objectives structured this section of work:

1. Revive crypreserved heterogenous cell lines (PC08 and PC09) and maintain for 1 passage in culture.
2. Isolate clonal cell lines from PC08/PC09 and maintain in short-term culture for 5-7 passage.
3. Assess cell and colony morphology for each clonal cell line during short-term culture.
4. Investigate the rate of cell proliferation for each clonal cell line during short-term culture (through calculating doubling time (DT)).
5. Investigate rate of cell proliferation through calculating DT in PC08 and PC09 using historical cell culture records.

3.1.2 Study sample.

Phenotypic characterisation was carried out for:

i. Passage (P) 2 PC08 and PC09 cultures initiated from cryopreserved cell stocks at P1.

ii. P4 clonal cell lines isolated from P3 PC08 and PC09 cultures.

iii. Clonal cell lines (>P4) that underwent short term culture (5-7 passages).

Growth characteristics were assessed in:

i. A selection of clonal cell lines (>P4) during short term culture (5-7 passages).

ii. Heterogeneous PC08 and PC09 using cell culture records originating from the previous pilot study (19 and 21 passages).

3.2 Early passage PC08 and PC09 cell cultures

3.2.1 Morphological characteristics

Early passage heterogeneous PC08 and PC09 cell lines were fastidious in culture which was very challenging and labour intensive. Initial cultures of P2 PC08 and PC09 were highly contaminated with dermal fibroblasts from the original biopsy tissue, as shown in Figure 3.1; fibroblasts originated from the biopsy tissue where they generate connective tissue in the dermis of the skin. Fibroblasts overpopulated both cultures quickly and were problematic because they restricted keratinocyte establishment and growth. During initial stages of P2 cultures, fibroblasts were discouraged by growth with 3T3 feeder cells and were removed by washing vigorously with phosphate buffered saline (PBS). This did not appear to affect the growth of 3T3 feeder cells or keratinocytes and fibroblasts were not transferred into future cultures.

PC09 established and grew quicker than PC08. Both cell lines grew well amongst a background of irradiated (non-proliferating) 3T3 feeder cells, as illustrated in Figure 3.2; 3T3 feeder cells did not possess a characteristic cell shape and it was not difficult to distinguish between keratinocyte colonies and 3T3 feeder cells under microscopic examination. Colonies of keratinocytes were roughly circular in shape and contained a population of polygonal

keratinocytes that tessellated (i.e. polygonal shaped keratinocytes covered the base of the TC dish in an interlocking manner, without gaps or overlapping) as shown in Figure 3.3. Keratinocyte colonies grew outwards as a result of peripheral cell division causing surrounding 3T3 feeder cells to dislodge from the monolayer, forming a 'ridge' on the periphery of expanding keratinocyte colonies as illustrated in Figure 3.4. This was also evident when expanding keratinocyte colonies in close proximity converged.

3.2.1.1 *Main findings*

Culturing of early passage (P2) PC08 and PC09 was labour intensive and problematic particularly during the initial stages of P2 cultures. PC09 appeared to establish more rapidly in culture than PC08. Nevertheless both heterogeneous cell lines grew in culture at early passage and were considered suitable for dilution cloning to isolate a selection of clonal cell lines.

3.2.2 A selection of colony morphologies exist in early passage heterogeneous PC08 and PC09 cultures

Two types of colony variants were observed in P2 PC08 and PC09 cell cultures, as illustrated in Figure 3.5; type 1 contained laterally growing keratinocyte cells forming 'flat' colonies, and type 2 contained differentiating keratinocyte cells forming colonies that appeared to resemble 'peaks'. By comparison type 2 colonies were smaller than type 1, and were more frequently observed at lower cell densities. For example, post seeding where cultures approached ~40% confluence, type 1 colonies were predominant over type 2 colonies, and once cultures exceeded ~40% confluence type 1 colonies dominated cultures.

3.2.2.1 *Main findings*

Heterogeneous PC08 and PC09 early passage (P2) cell cultures comprised colonies representing 2 different morphological variants which appeared to be related to percentage confluence of the cell culture.

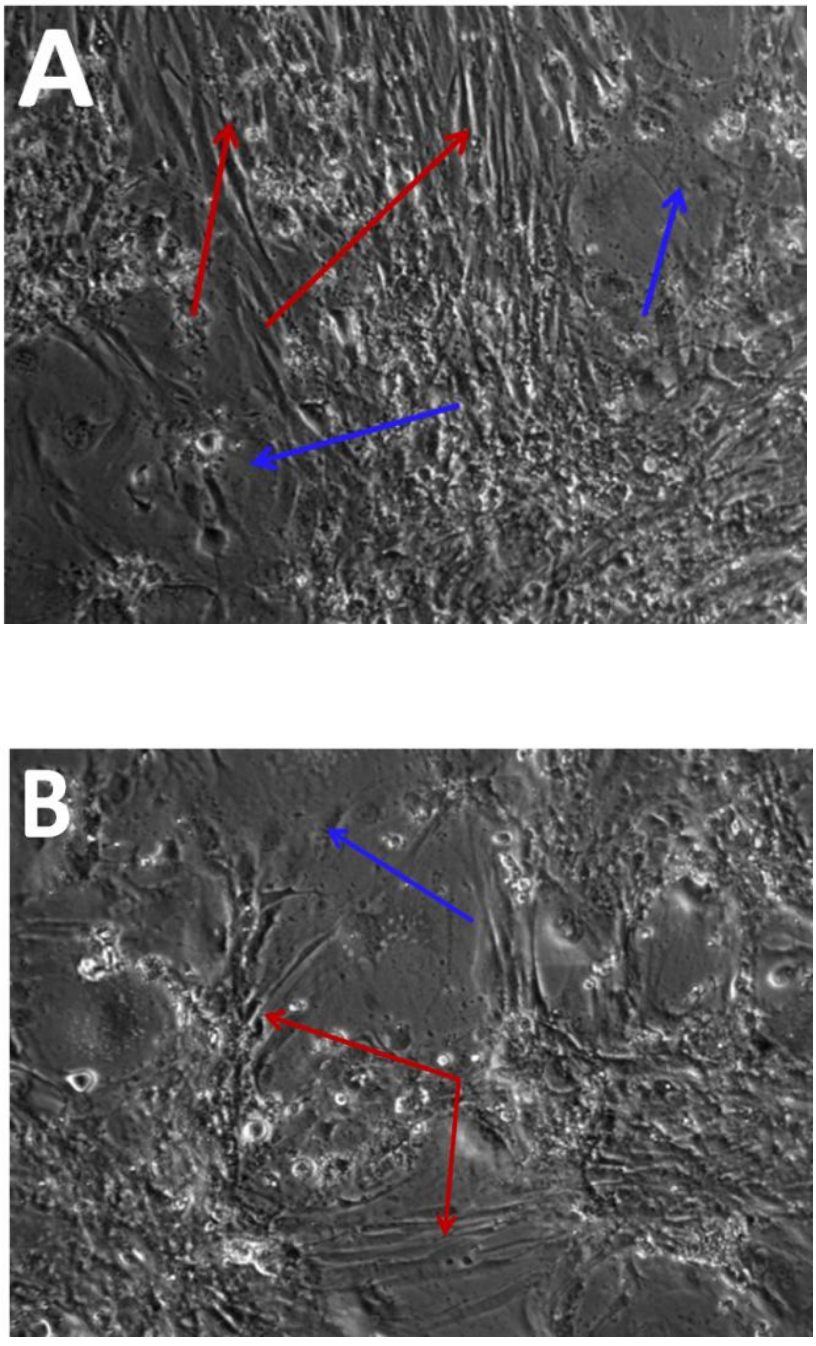

Figure 3.1. Dermal fibroblast contamination in P2 PC08 and PC09 heterogeneous cultures

A. P2 PC09 cell culture in 6 cm TC dish and, **B**. P2 PC08 cell culture in 6 cm TC dish (100x total magnification). The cultures consisted of 3T3 feeder cells (blue arrow), which did not display characteristic cell shape, and fibroblasts (red arrow) which demonstrated elongated morphology.

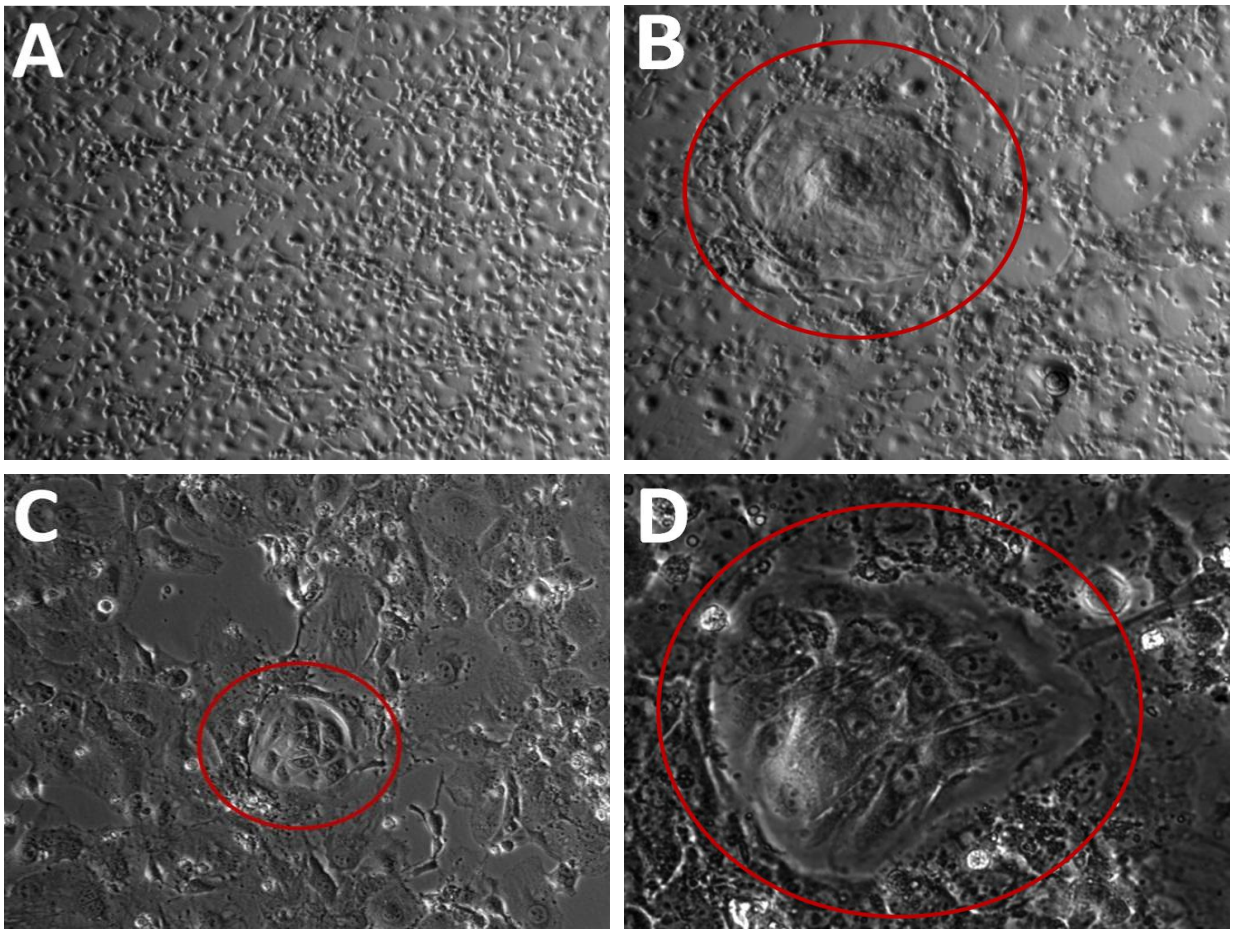

Figure 3.2. Morphological characteristics of P2 PC09 and 3T3 feeder cells in culture

A. A background of irradiated 3T3 feeder cells (50x total magnification) used to support keratinocyte cell cultures in 6 cm TC dish. Irradiated 3T3s were not capable of replicating and did not demonstrate characteristic cell morphology. **B**. One keratinocyte colony (circled in red) surrounded by 3T3 feeder cells in 6 cm TC dish (50x total magnification). Keratinocyte colonies were roughly circular in shape, and were easily distinguishable next to 3T3 feeder cells. **C**. One keratinocyte colony (circled in red) consisting of approximately 10 dividing keratinocyte cells (100x total magnification) with surrounding 3T3 feeder cells in 6 cm TC dish. **D**. One keratinocyte colony (circled in red) consisting of approximately 20 dividing keratinocytes (320x total magnification) with surrounding 3T3 feeder cells in 6 cm TC dish.

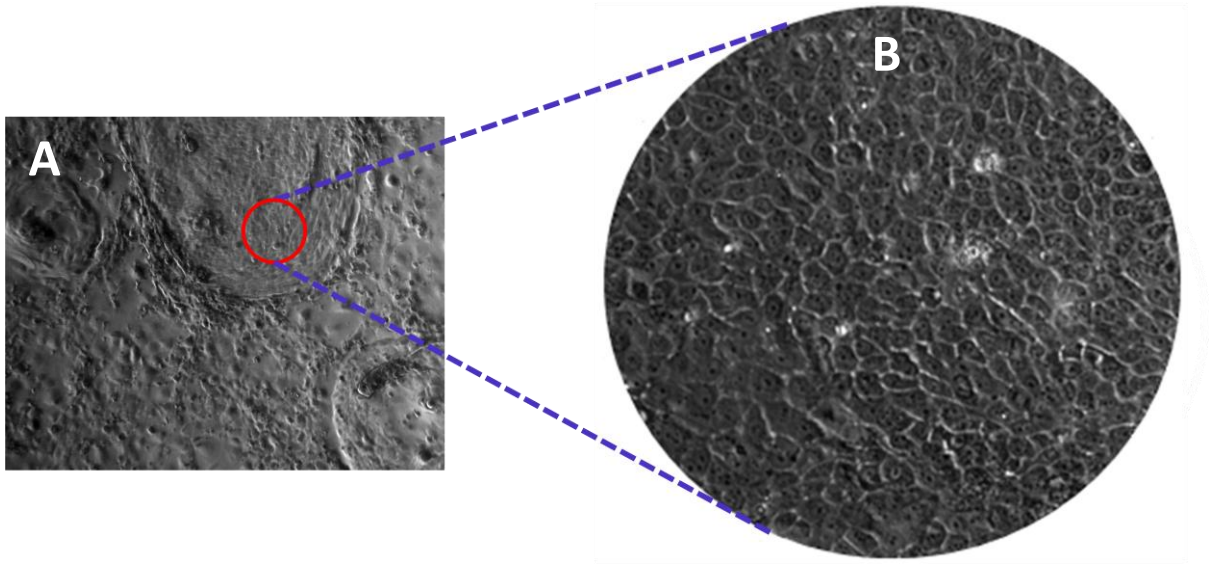

Figure 3.3. Characteristic morphology of P2 PC09 keratinocyte cells within a colony

A. Keratinocyte colonies surrounded by 3T3 feeder cells in 6 cm TC dish (50x total magnification). The red circle highlights an area of laterally growing keratinocytes within a colony which has been magnified as shown in B. **B**. Characteristic polygonal morphology and tessellating pattern of keratinocytes within a colony (100x total magnification).

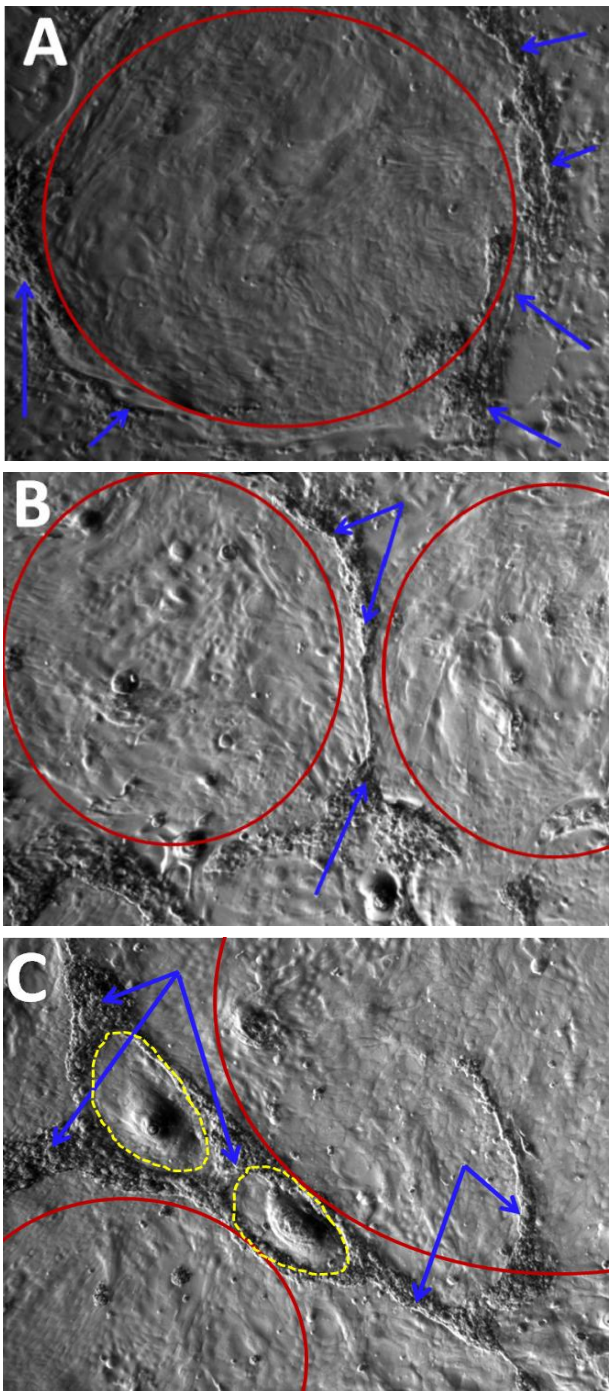

Figure 3.4. Characteristics of 3T3 feeder cells surrounding expanding keratinocyte colonies in P2 PC09 cultures

A. One keratinocyte colony containing lateral keratinocytes (circled in red) in 6 cm TC dish (50x total magnification). 3T3 feeder cells formed a 'ridge' (blue arrows) on the periphery of expanding keratinocyte colonies, which eventually detached from the base of the dish and into media suspension. **B**. Convergence of two lateral keratinocyte colonies (circled in red) formed a 3T3 feeder cell 'ridge' (blue arrows) in 6 cm TC dish (50x total magnification). **C**. Multiple converging keratinocyte colonies in 6 cm TC dish; two of which were larger and contained lateral keratinocytes (circled in red) and two of which were considerably smaller and contained differentiating keratinocytes that resembled 'peaks' (circled in yellow) (50x total magnification).

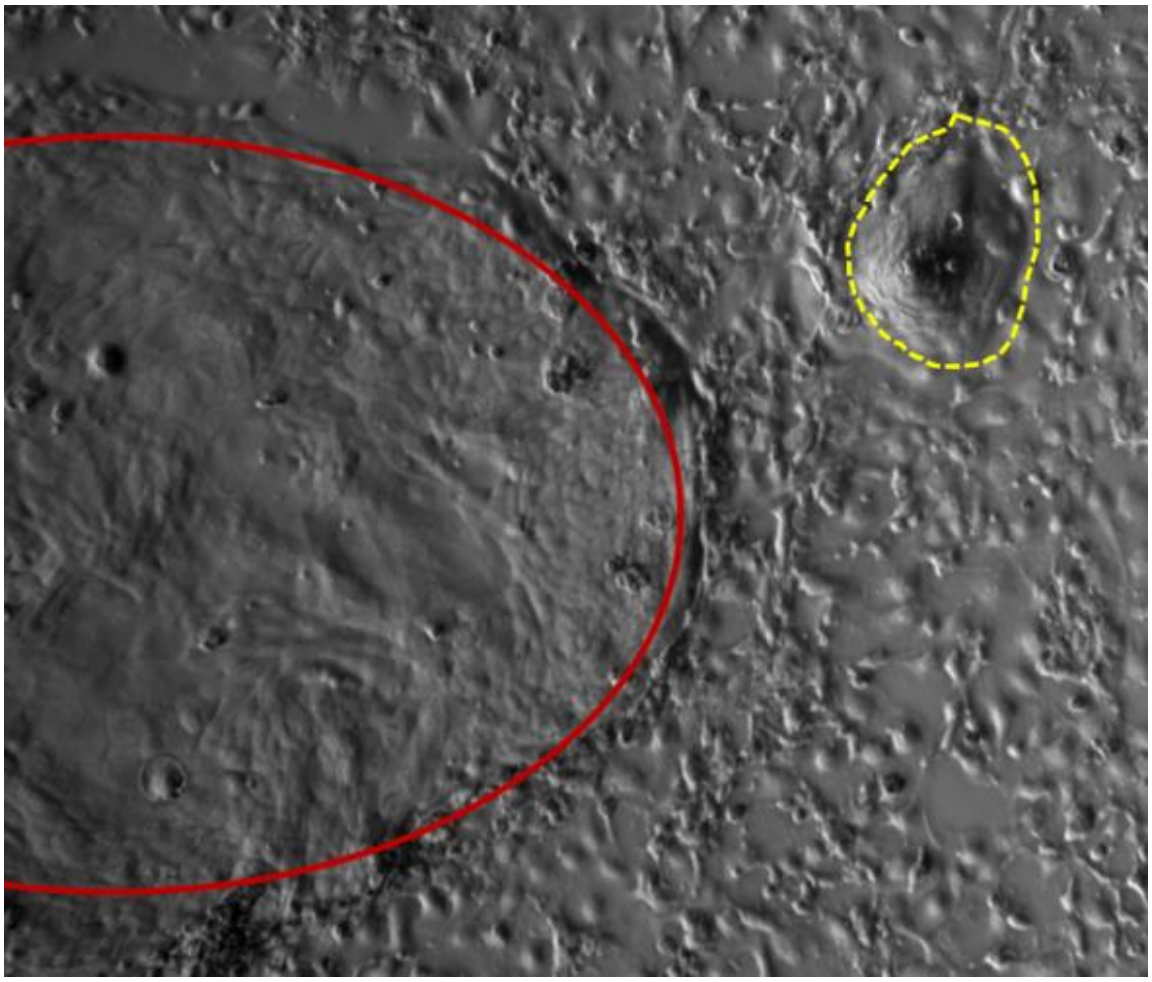

Figure 3.5. Variation in keratinocyte colony morphology in P2 PC08 cell cultures

An example of type 1 (circled in red) and type 2 colonies (circled in yellow) identified in PC08 cultures in 6 cm TC dishes. Type 1 colonies contained lateral keratinocytes that appeared 'flat' and were significantly larger than 'type 2' colonies which contained differentiating keratinocytes, resembling 'peaks' (50x total magnification).

3.3 Clonal cell lines

3.3.1 Overview of clonal cell lines isolated from PC08 and PC09

In the literature, previous investigations to derive cell lines from VaIN and VIN biopsy tissue have been documented to evaluate early stages of neoplasia (Hietanen et al., 1992), and to analyse HPV16 transcription patterns (Grassmann et al., 1996). However, isolation and characterisation of clonal cell lines with VIN and VaIN origin have not previously been achieved or documented.

In this study a selection of clonal cell lines were isolated from early passage (P2) heterogeneous PC08 (VIN) and PC09 (VaIN) cells lines. Early passage (P2) rather than later passage PC08 and PC09 were used because they were likely to be more representative of the original biopsy tissue from which they were explanted, and so were likely to be good models of neoplastic disease *in vitro*. When selecting a suitable *in vitro* model for assessing response to drug treatment, it is ideal that the cells being treated comprise of a homogeneous cell population so that response to treatment can be assessed without interference from multiple cell types. The clonal cell lines isolated in this study consisted of homogeneous cell populations which could be used as *in vitro* experimental systems of vulval and vaginal neoplastic disease, to investigate response to CDV treatment and potentially other therapeutic agents in the future.

3.3.1.1 *Clonal cell lines isolated from PC08 and PC09*

To produce the P2 cultures, cryopreserved P1 PC08 and PC09 cell lines were thawed and used to seed 6 cm TC dishes with 3T3 feeder cell support. To isolate clonal cell lines, P2 PC08 and PC09 were allowed to reach ~80% confluence then trypsinised and used for dilution cloning in 9 cm TC dishes (in triplicate). Well dispersed keratinocyte colonies arose on TC dishes seeded with 10^3 cells (P3) and were selected for ring cloning. Cells isolated within each ring were

trypsinised and transferred to individual 6 cm TC dishes. Each resulting clonal cell population was assessed independently in culture.

Twelve clonal cell lines were isolated as shown in Table 3.1. Each clonal cell line was given a letter of identification; PC08 clonal cell lines = M-X, and PC09 clonal cell lines = A-L. Each letter was linked with the parental heterogeneous cell line, therefore clonal cell lines were referred to as M08-X08, and A09-L09.

After initial isolation, 2/12 PC08 clones and 11/12 PC09 clones survived. Due to the relatively poor success for PC08, a second attempt was made to isolate more clonal cell lines; higher passage (P5) cryopreserved cell stocks of PC08 and PC09 were set up in culture at P6 and dilution cloning was carried out in the same way. Two clonal cell lines (Y08 and Z08) were isolated from P8 PC08 and only Y08 survived culture after initial isolation. Overall, 10 clonal cell lines from PC09 and 3 clonal cell lines from PC08 survived initial isolation and were maintained in culture. With regard to the project time-frame and due to the fastidious nature of the cell cultures thus far, for PC08 and PC09 the 3 clonal cell lines that established and reached confluence most rapidly after initial isolation were selected and underwent short-term culture of between 5 and 7 passages; these were PC08 clonal cell lines M08, P08, and Y08, and PC09 clonal cell lines A09, D09, and H09. The remaining clonal lines were maintained in culture and achieved between 1 and 4 passages; at each passage they were stored in liquid nitrogen for future reference but were not included in future analyses constituting this project.

Clonal cell lines M08, P08 and Y08, were cultured for 5 passages which lasted 63, 63, and 51 days, with an estimated total number of population doublings (PD) during this time of 25.0, 24.0, and 23.7, respectively. Clonal cell lines A09, D09, and H09, were cultured for 7 passages which lasted 84, 86, and 84 days, with an estimated 36.2, 38.5, and 33.5, respectively.

Biopsy tissue	Heterogeneous cell line	Clonal cell line	Survival post isolation	Short term culture (passage)		Total time in culture (days)	Total PD
				Start	Finish		
Vulval	PC08	M	✓	5	9	63	25.0
		N	-				
		O	-				
		P	✓	5	9	63	24.0
		Q	-				
		R	-				
		S	-				
		T	-				
		U	-				
		V	-				
		W	-				
		X	-				
		Y	✓	9	13	51	23.7
		Z	-				
Vaginal	PC09	A	✓	5	11	84	36.2
		B	✓	5	8		
		C	✓	5	7		
		D	✓	5	11	86	38.5
		E	✓	5	8		
		F*					
		G	✓	5	6		
		H	✓	5	11	84	33.5
		I	✓	5	5		
		J	✓	5	9		
		K	✓	5	9		
		L	✓	5	9		

Table 3.1. Isolation and short-term culture of clonal cell lines derived from PC08 and PC09

The 3 most rapid clonal cell lines to establish from PC08 and PC09 were selected for short-term culture (5-7 passages) during which time they were characterised phenotypically and growth characteristics also assessed. The star (*) highlights clonal cell line F which was discarded immediately due to fungal contamination, and the dash (-) denotes colonies that were isolated and given ID but did not survive when cultured independently.

3.3.1.2 *Main findings*

Clonal cell lines were successfully isolated from heterogeneous PC08 and PC09 cell lines. PC09 produced more lines that survived the cloning procedure and proliferated.

3.3.2 Morphological characteristics

Once clonal cell lines had been isolated and transferred to TC dishes for their first initial passage, they were viewed daily microscopically to assess cell and colony morphology and allowed to reach ~80% confluence.

Microscopic images of clonal cell lines derived from PC08 (M, P and Y) and PC09 (A, B, C, D, E, G, H, I, J, K and L) are shown at first passage after isolation in Figure 3.6, Figure 3.7, and Figure 3.8. During this initial passage, variations in keratinocyte size and tessellation patterns within the cell monolayer were visible for each clonal cell line.

3.3.2.1 *Main findings*

Variations in keratinocyte cell morphology and tessellation patterns in the monolayer were observed between clonal cell lines after initial isolation and remained unchanged for the length of time each clone was maintained in culture. Also, morphological differences were observed between clonal cell lines which confirmed that they are distinctly different (clonal).

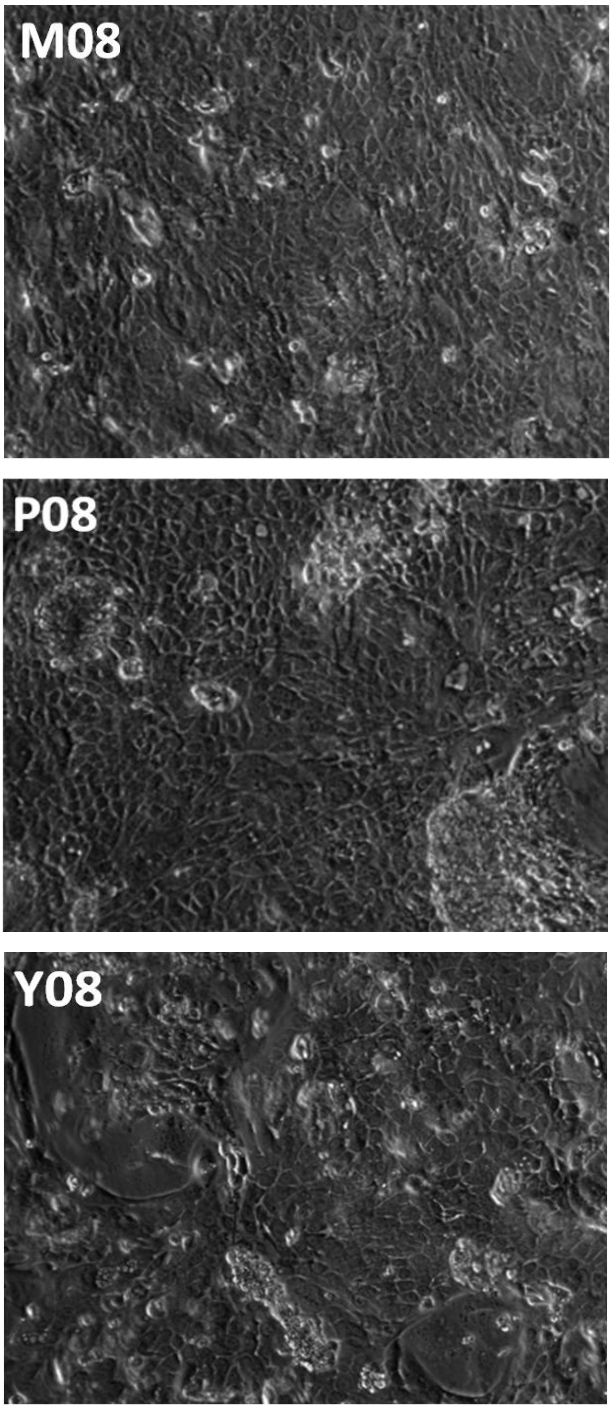

Figure 3.6. Morphology of clonal cell lines isolated from PC08 at first passage post isolation

Clonal cell lines were cultured in 6 cm TC dishes and images taken at 80% confluence (100x total magnification); initial cultures of clonal cell lines M08 and P08 were at P4, and Y08 at P8.

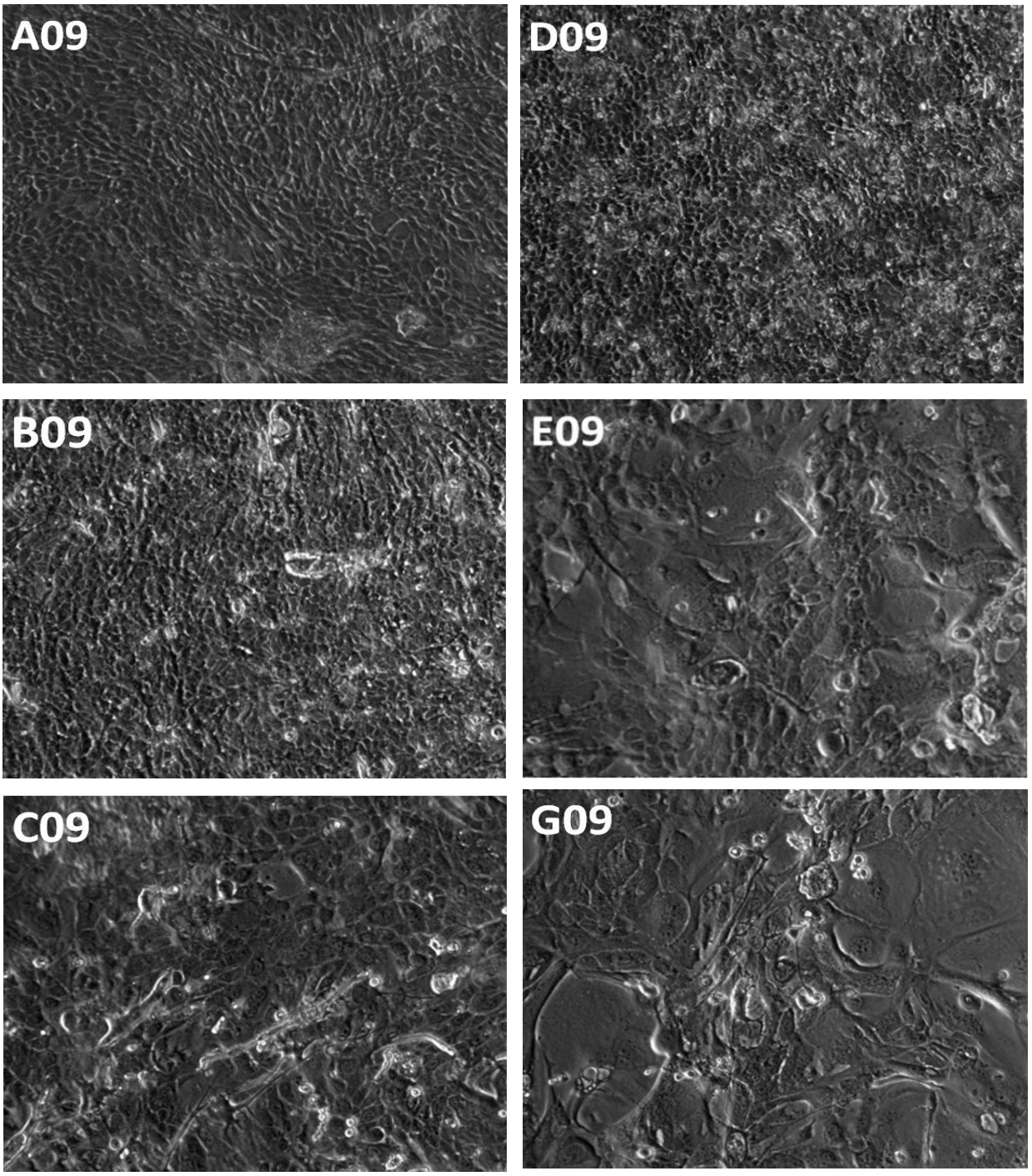

Figure 3.7. Morphology of clonal cell lines A09-G09 isolated from PC09 at first passage post isolation

Clonal cell lines were cultured in 6 cm TC dishes and images taken at 80% confluence (100x total magnification). Initial cultures of clonal cell lines A09-L09 were at P4.

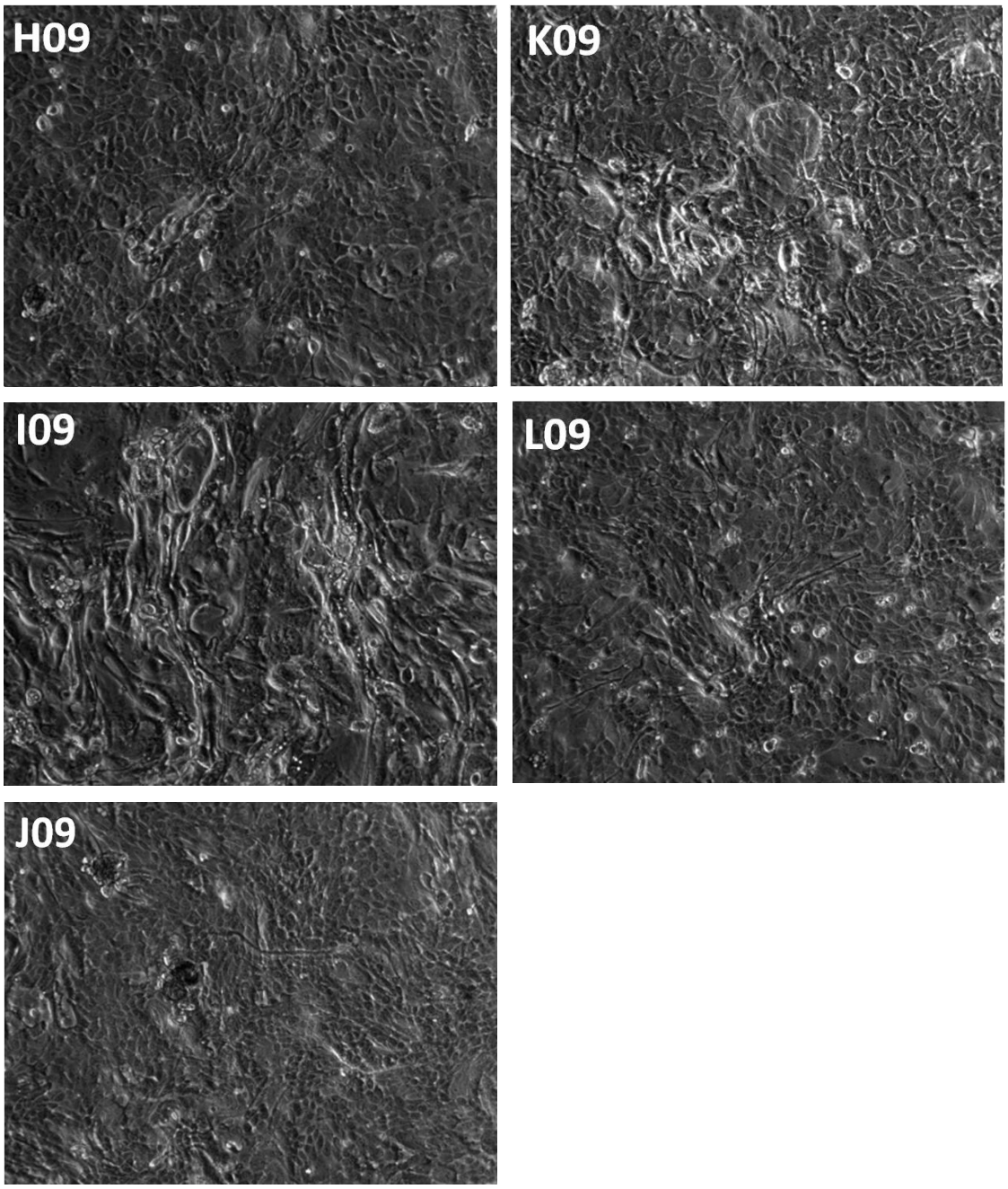

Figure 3.8. Morphology of clonal cell lines H09-L09 isolated from PC09 at first passage post isolation

Clonal cell lines were cultured in 6 cm TC dishes and images taken at 80% confluence (100x total magnification). Initial cultures of clonal cell lines A09-L09 were at P4.

3.3.3 Keratinocyte morphology correlates with growth during culture

Cell morphology and tessellation pattern appeared to vary amongst clonal cell lines in culture. The association between keratinocyte morphology and the number of population doublings for each clonal cell line during the period of culture, was assessed by correlating cell morphology (Figure 3.6, Figure 3.7, and Figure 3.8) and cell culture data presented (Table 3.1). Clonal cell lines M08, P08 and Y08, and A09, D09, H09, J09, K09 and L09, all demonstrated relatively smaller, tightly tessellating polygonal keratinocytes and were passaged most frequently in culture (between 5-7 passages were performed). Clonal cell lines B09, C09 and E09, demonstrated relatively larger keratinocytes with a more loosely forming tessellation, and were passaged 3-4 times during culture. Clonal cell lines G09 and I09 lacked typical polygonal keratinocyte morphology, with cells of varying size and shape (particularly enlarged cytoplasm) and and no obvious tessellation pattern; G09 was passaged twice and clone I passaged once over the culture time period. Clonal cell lines comprising relatively smaller keratinocytes appeared to proliferate more rapidly during this initial passage.

3.3.3.1 *Main findings*

A relationship was identified between the morphology of keratinocytes and a crude estimate of the rate of proliferation during the first passage in culture. It appears that the morphology of clonal keratinocytes is linked to their rate of proliferation, and supports the suggestion that there are distinct differences among the lines. Rates of proliferation were confirmed more accurately through assessment of doubling time (DT), which will be described in the following section.

3.3.4 Time in culture and population doubling time

Cells were consistently seeded at 8 x 10^5 cells in 9 cm TC dishes and passaged when 80% confluence was reached (with the exception of one occasion when passage was delayed due to

contamination of feeder cells), hence the number of population doublings was consistent across the culture series; values for cell counts, population doubling and doubling times are included in Appendix I. Population doubling times were calculated to assess the rate of proliferation for clonal cell lines M08, P08, and Y08, and A09, D09, and H09. The DT at each passage is illustrated in Figure 3.9.

The DT values for all clonal cell lines appeared to be fairly stable during short-term culture, with a trend for doubling time to decrease for all cell lines except D09, for which doubling time appeared to increase; this suggested that rate of cell proliferation increased with duration in culture for all clonal cell lines excluding D09. However, anomalous DT values were obtained at the third passage for M08 and P08, fourth passage A08 and H09, and fifth passage for D09 (highlighted with red star symbol in Figure 3.9). This problem was related to the 3T3 feeder cells which were found to be contaminated prior to irradiation and could not be used. This resulted in delayed passage of the clonal lines. Excluding these anomalies, the mean doubling times are shown in Table 3.2

3.3.4.1 *Main findings*

The DT decreased with time in culture for all clonal cell lines except D09, showing all clones (excluding D09) exhibited increased rate of cell proliferation during culture.

3.4 Historical PC08 and PC09 cell culture records

3.4.1 Time in culture affects PD and DT

PC08 and PC09 were cultured for 17 and 19 passages over 101 and 129 days respectively, as described previously. During this time it was calculated that PC08 achieved a total of 96.7 population doublings and PC09 achieved 111.6 population doublings. Mean doubling times for

PC08 and PC09 were 1.1 and 1.2 days respectively. Variation of doubling time with passage number is shown in Figure 3.10.

There appeared to be a trend for shorter doubling times with increasing passage number. There was no significant difference between the mean doubling times for the PC08 and 09 cell population (T Test, 2 tailed, unpaired samples with unequal variances: P = 0.21). The mean doubling times for the heterogeneous populations were however significantly shorter than for the clonal populations (Table 3.2).

3.4.1.1 *Main findings*

The mean doubling times for PC08 and PC09 were 1.1 and 1.2 days and were significantly shorter than for clonal cell lines. Doubling times in PC08 and PC09 appeared to decrease with time in culture showing that rate of cell proliferation increased with time in culture.

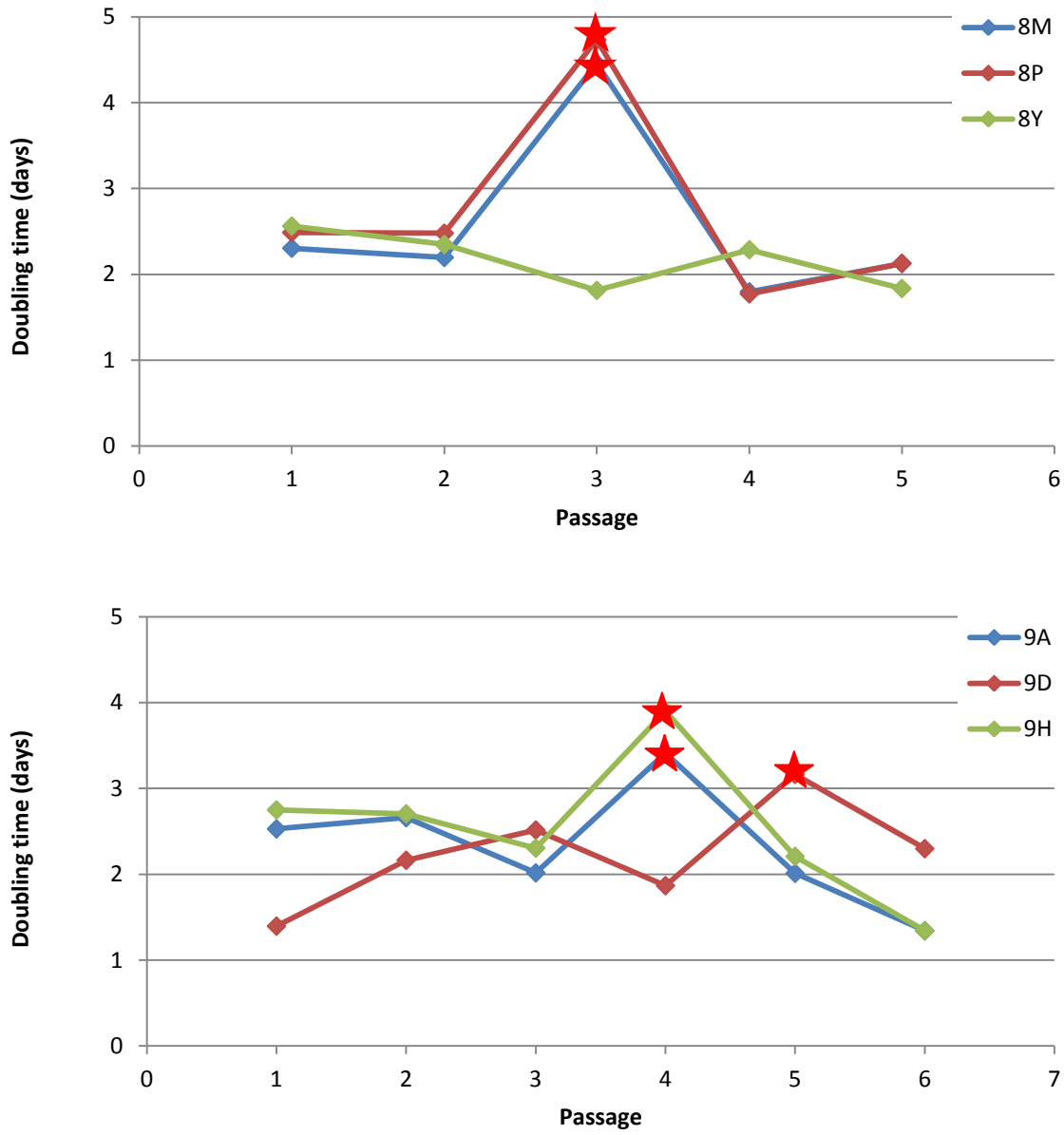

Figure 3.9. Doubling time versus passage in clonal cell lines M08, P08 and Y08, and A09, D09 and H09.

'Passage' illustrated on the x axis refers to the number of times the clonal cell line had been passaged since being derived from the parental line. The red star highlights anomalous DT values which were a result of delayed passage due to contamination of 3T3 feeder cells.

Clonal cell line	Mean DT (days)	Linear regression (R^2)	Comparison with parental population (PC08/PC09) (P values)
M08	1.69	0.4	0.00028
P08	1.77	0.59	0.00260
Y08	1.81	0.52	0.00051
A09	1.76	0.81	0.03735
D09	2.23	0.38	0.01933
H09	1.88	0.83	0.02276

Table 3.2. Mean doubling times for clonal cell lines derived from PC08 and PC09 in short-term culture

Doubling times were calculated without including the starred values in Figure 3.9. R^2 values were calculated by linear regression, without including the starred values in Figure 3.9. Doubling times were also compared (T Test, 2 tailed, unpaired, unequal variances) with the doubling times for the parental heterogeneous cultures (PC08 and PC09).

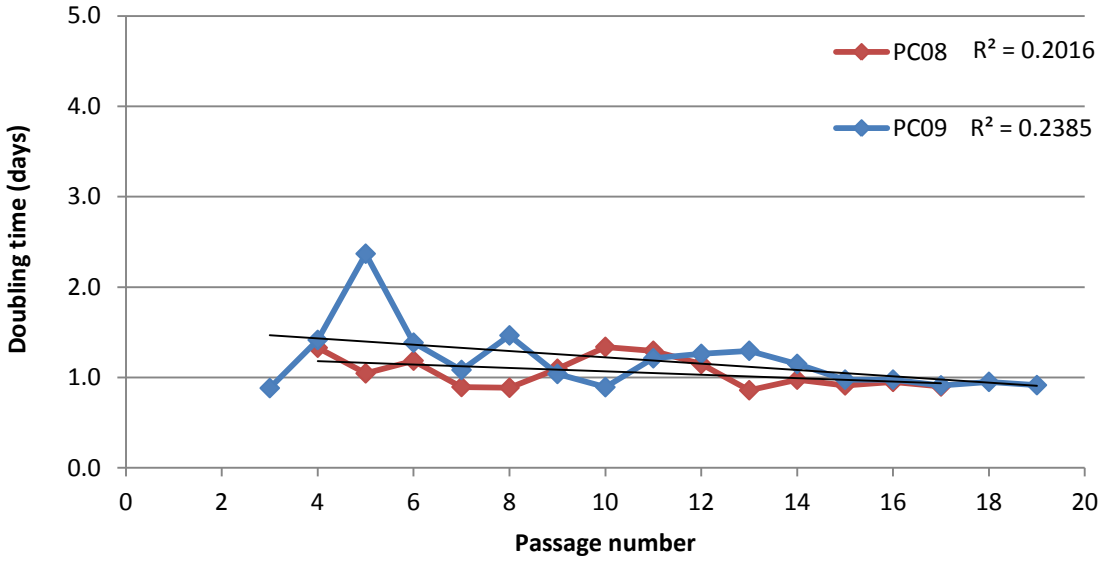

Figure 3.10. Doubling time versus passage number for heterogeneous PC08 and PC09 cell lines

R^2 values were calculated by linear regression and linear regression lines are shown for extended passage.

3.5 Discussion

The main conclusions of the experiments described in this chapter were:

1. Early passage (P2) heterogeneous cell cultures of PC08 (VIN) and PC09 (VaIN) were successfully revived and cultured.
2. Early passage (P2) heterogeneous cell cultures produced colonies with diverse morphologies.
3. Clonal cell lines were successfully isolated from heterogeneous PC08 and PC09 cell lines.
4. Differences were observed in cell and colony morphology between keratinocytes of clonal cell lines.
5. For 5/6 clones, rate of cell proliferation (assessed as DT), increased with increasing passage number.
6. For heterogeneous PC08 and PC09 cultures, rate of cell proliferation also increased with increasing passage number.
7. Rate of cell proliferation was significantly different between PC08/PC09 and clonal cell lines.

Clonal cell lines were isolated, assessed in terms of morphology and growth characteristics, and intended for use as an *in vitro* experimental culture system representing VIN and VaIN.

3.5.1 Morphology of cultures and isolation of clonal cell lines

Early passage cultures of PC08 and PC09 were fastidious in culture and this was thought to be because cultures were only 1 passage away from their parental biopsy tissue. Colony morphology variants observed at these early passages might be expected in primary/secondary cell cultures as cultures include a variety of cell types reflecting the composition of the epithelia. Colonies were identified which resembled 'peaks' under

microscopic analysis, and these were thought to represent differentiating epithelial cells. Colonies of laterally growing cells were also observed in the monolayer, and their morphology appeared more similar to transformed cells such as CaSki and SiHa. Laterally growing keratinocytes dominated over differentiated keratinocytes when cultures became more confluent, and this observation suggested that cells conferring a selective growth advantage eventually replace cells within the culture population.

The data show that very early passage (P2) PC08 and PC09 cultures were slow growing, contaminated with fibroblasts, and included cells with diverse morphologies, which is a common feature of explanted early passage cell lines (Stanley, 2002). Nonetheless, several lines were derived by single cell cloning from the parental population. Laterally growing keratinocytes that produced 'flat' colonies appeared more likely to produce lines capable of sustained growth, while colonies that formed peaks, were perhaps more likely to differentiate and grew less well.

Early cultures of PC09 established better than PC08 and a higher proportion of PC09 single cell isolates survived cloning. These observations may suggest that the heterogeneous PC09 population may have included a greater proportion of cells with a 'more transformed' phenotype than was present in PC08. Alternatively the differences between PC08 and PC09 might relate to their distinct anatomical origins (vaginal and vulval) and that they were biopsied from two different women; hence individual genetic factors might contribute to how well the resulting cell lines established and grew in culture. To try to increase the number of PC08 clones available, the dilution cloning was repeated using higher passage cells. The rationale for using higher passage cells was that during culture, heterogeneous cell populations undergo selection for cells most suited to growth in culture. Therefore PC08 heterogeneous cells of higher passage might be able to thrive better in culture and therefore increase the success rate of dilution cloning. This repeat was not as successful as expected, and

in hindsight there was not a great difference in passage number between the first attempt (P1) and the repeat (P5) (only 4 passages higher).

Morphology and growth of clonal cell lines was initially assessed post isolation. Clonal cell cultures that comprised enlarged cells, lacked polygonal morphology and tessellation patterns, and took longer to reach ~80% confluence during first passage; G09 and I09 in particular exhibited these features. Previous studies have reported the morphology of senescent keratinocytes (Kang et al., 2000, Rheinwald et al., 2002). Cellular senescence was first described by Hayflick (Hayflick, 1965), and defined as viable and metabolically active cells that exhibit permanent arrest of cell proliferation, which occurs in response to various stressors (Campisi and d'Adda di Fagagna, 2007, Loughran et al., 1996). Keratinocytes undergoing cellular senescence are irregularly shaped (not polygonal), with enlarged cytoplasm, and reduced cellular organelle density. Freshly isolated cultures of G09 and I09 could have become growth arrested through senescence due to the stress inflicted on cells post cloning in a culture environment, resulting in the morphological phenotype and limited proliferative potential previously described.

3.5.2 Growth characteristics

There were significant differences between the mean doubling times for the parental heterogeneous cell populations and the clonal lines derived from them, with the clonal lines showing doubling times approximately 50-100% longer than the parental cell lines. There are several possible reasons for this, including loss of cellular diversity within the culture environment or selection of slow growing clones. Heterogeneous cell populations comprise a diverse selection of cells, all of which respond differently to the external cell culture environment. The likelihood of a cell arising with a growth advantage over other cells is increased in a diverse (heterogeneous) population of cells, and these might then quickly overpopulate the culture. In clonal cell lines, cells respond similarly because they are identical

and this reduces the likelihood of cells with a selective growth advantage arising and might therefore limit rate of change within a cell population. This might be the best explanation for why PC08 and PC09 doubled more frequently than the clonal cell lines. Selection of slow growing clones appears less likely, given that the most rapidly growing clones were selected, and doubling time appears fairly consistent between clones. The difference could also have been caused by differences in the handling of the cell cultures, but this appears unlikely as heterogeneous and clonal lines were cultured according to standardised protocols.

Both the heterogeneous and 5/6 of the clonal populations showed a tendency for doubling time to reduce with increasing passage number. This is consistent with selection of faster growing clones with increasing time in culture. The behaviour of clone D09, which showed the opposite trend, is more difficult to explain but might be attributed to changes in expression of HPV encoded genes which will be discussed in later chapters.

3.5.3 Strengths and weaknesses

The clonal lines have several strengths as potential models of VIN and VaIN. They were derived from early passage heterogeneous cell lines explanted from biopsy tissue, and are likely to provide a good in vitro representation of vulval and vaginal neoplastic disease because they still closely represent the physiology of the human tissue from which they were derived. At these very early passages, cells have not had sufficient time to accumulate genetic modifications which occur as a result of selective pressures through long-term cell culture process. Additionally the clonal cell lines provide a homogeneous population of cells which can be used experimentally; identical cells comprise the cell culture model and cellular response is therefore consistent i.e. results should not be influenced by selection of subclones from within a heterogeneous population. The majority of documented studies that have investigated HPV related disease and potential therapeutics have used immortalised cell lines as an experimental system, such as CaSki, SiHa and HeLa (Divya and Pillai, 2006, De Schutter et al.,

2013). Immortalised cell lines are either derived directly from late metastatic tumours or have established in long-term culture and undergone selective pressures conferring growth advantages resulting in cell transformation. Hence immortalised cell lines can lack biological relevance especially in relation to early neoplastic disease. The clonal cell lines isolated during this study originated from grade III VIN and VaIN biopsy tissue and have replicated successfully during short-term culture; this has not been accomplished or documented previously and is therefore novel.

Only one previous study has reported successful derivation of cell lines from VIN (Grassmann et al., 1996); the HPV16 positive KG line was derived using an explant procedure from a VIN3 lesion and was used in organotypic raft culture to investigate the activity of the HPV P670 differentiation dependent promotor. The heterogeneous line was cultured for >80 population doublings and was described as an immortalised line, however no further publications have reported use of this line. Similarly a single publication has reported isolation of keratinocyte lines from vaginal lesions (Hietanen et al., 1992); two cell lines, UT-DEC-1 (HPV33) and UT-DEC-2 (HPV16), were derived from VaIN 1 and 2 lesions. Both lines grew for >24 passages and were described as potentially immortal, but no further publications describing use of these lines have been identified. By contrast, the HPV16 positive W12 cell line derived by Margaret Stanley in 1989 (Stanley et al., 1989) from a low grade cervical lesion has provided the basis for numerous insights into the biology of HPV infection and the significance of viral integration in particular (Pett and Coleman, 2007); the W12 heterogeneous population has given rise to several defined clones with distinct integration events (Gray et al., 2010).

The experiments described above do have several limitations. During short-term culture, confluency was determined under microscopic analysis, and clonal cell lines were passaged at 80% confluence which is the simplest and most common method described in the literature. However it must be acknowledged that this is a subjective measure.

A further limitation was the somewhat crude method used for calculation of doubling time. Doubling times can be more accurately determined by analysis of the log phase of a fully defined growth curve based on multiple replicates of daily cell counts from seeding to plateau phase (Freshney, 2005a), however this was not appropriate here where the main aim was to study multiple lines over an extended period of culture.

Clonal cell populations can be obtained in several ways. For cells that are usually in suspension (e.g. blood cells) FACS can be used to directly isolate single cells. In this study these methods were not suitable due to the adherent nature of keratinocytes and their sensitivity to cell density i.e. at low cell densities cell survival was reduced as a result of cell density dependent regulation of growth, and as a result dilution cloning was performed according to a standardised protocol (Freshney, 2010). This process creates single cell suspensions and allows single cells to divide and replicate to form colonies in TC dishes; colonies are then isolated and transferred to separate vessels. The limitations of this technique included the possibility of cells establishing in close proximity on the base of the TC dish and then replicating and cell types combining, which would form a colony comprising two different cell types. To ensure that the colonies selected were those that arose from a single cell, single cell suspensions were seeded at a variety of cell densities, and the exclusion criteria listed in Methods and Materials implemented when selecting individual colonies for isolation.

4 Preliminary cell culture and optimisation studies

4.1 Results

Clonal cell lines were derived from PC08 (vulval) and PC09 (vaginal) heterogeneous cell lines, as described in Chapter 3. The clonal cell lines were intended for use as *in vitro* experimental models of HPV related vulval and vaginal neoplastic disease; specifically for assessing responses to cidofovir (CDV) treatment described in Chapters 7 and 8. Before they could be used for CDV dosing studies, clonal cell line cultures were assessed during short-term culture (between 5 and 7 passages) to identify phenotypic and molecular characteristics of each clonal cell line, as described in Chapter 5 and 6.

Prior to characterisation and CDV dosing studies, a series of preliminary studies were performed using early passages of two clonal cell lines. Firstly to optimise the growth conditions for short-term culture of clonal cell lines, and secondly to determine key parameters within the culture system that might affect growth of cells and expression of HPV oncogenes. The aim of these experiments was to ensure that clonal cell lines could be used dependably for investigating response to CDV.

In culture, keratinocytes are often supplemented with irradiated 3T3 feeder cells (this is referred to as co-culture i.e. culturing mixed cell types together). 3T3s are thought to provide extracellular proteins to support the growth of keratinocytes and provide paracrine factors that enhance epithelial cell survival (Parkinson and Yeudall, 2002, Alitalo et al., 1982, Rheinwald and Green, 1975) and therefore clonal cell lines were prepared in co-culture with 3T3 support. It has been suggested that specific 3T3 clones support growth better than others (i.e. the J2 clone), and that 3T3s should not be used beyond passage 20, as extended culture results in selection for fast-growing variants that do not survive as long after irradiation and are inferior as feeders (Stanley, 2002). The clonal cell lines isolated during this project were

novel, thus to optimise the co-culture system, the effect of irradiated 3T3 passage number on the time taken for clonal cell lines to reach 100% confluence was investigated. The main aims of this experiment was to determine a passage limit past which 3T3s would no longer be useful for supplementing clonal cells in culture.

The next experiment investigated the effects of growing clonal cell lines without 3T3 feeder cells. This was undertaken because for CDV dosing studies, a mixed population of cells would be undesirable and this could potentially confound cell counts and quantification of nucleic acids. This experiment investigated whether clonal cell lines could establish and grow independently without co-culture with 3T3 feeder cells.

Published studies suggest that CDV may affect expression of HPV oncogenes, E6 and E7 (Amine et al., 2009, Abdulkarim et al., 2002). To explore this, the effect of clonal cell confluence on E6 and E7 expression was investigated. The outcome would then guide the standardisation of percentage confluence to be used in future cell culture experiments.

Lastly, cell cultures were also examined for M*ycoplasma* infection. *Mycoplasma* species are the smallest free-living prokaryotic microorganisms. Contamination of cell culture is a common and serious problem (Young et al., 2010a) causing biochemical and metabolic changes in infected cell lines resulting in altered physiology and metabolism of nucleoside analogues (Taylor-Robinson and Bebear, 1997). *Mycoplasma* detection was carried out to ensure that cultures were uncontaminated.

4.1.1 Aims and objectives

The central aim was to optimise and assess variables within the novel cell culture systems to standardise the cell culture process for the rest of the project.

The following objectives structured this section of work:

1. Investigate whether the passage number of irradiated 3T3 feeder cells affects the establishment and growth of clonal cells in co-culture.
2. Assess whether clonal cell lines could establish and grow adequately without irradiated 3T3 cells.
3. Investigate whether confluence of clonal cell lines affects HPV oncogene expression.
4. Assess whether presence/absence of 3T3 feeders affects HPV oncogene expression.
5. Examine cell cultures for *Mycoplasma* contamination.

4.1.2 Study sample

Clonal cell lines M08 and D09 established and replicated most rapidly after initial isolation, as described in chapter 4, and were therefore used to carry out the preliminary studies at passage (P) 6. Irradiated 3T3 feeder cells at P≤20 were used to supplement M08 and D09 in all instances except for when variability in 3T3 passage number was being assessed (P17, 22, 29, and 36 were used).

4.1.3 Passage number of 3T3 feeder cells affects the growth of clonal cell lines

The effect of 3T3 passage number on the growth of clonal cell lines in co-culture was investigated by exploring how long it took for cultures to reach 100% confluence in co-culture with irradiated 3T3 feeder cells of variable passage. 3T3 feeder cells were prepared in culture in four rounds at P17, 22, 29 and 36, and stripped and irradiated as previously described. Irradiated 3T3 feeder cells (2×10^6) were then used to supplement D09 and M08 cultures in 9 cm tissue culture (TC) dishes seeded with 8×10^5 cells. Cultures were viewed microscopically twice daily until cultures reached 100% confluence.

The relationship between time taken for D09 and M08 to reach 100% confluence and 3T3 passage number is shown in Figure 4.1. There was clearly a strong positive correlation between 3T3 passage number and time taken to reach confluence for both cell lines. There

were also substantial differences in the morphology of cultures observed microscopically. 3T3s at higher passages (P29 and 36) tended to detach from the base of the dish more easily. This was identified by the presence of increased numbers of 3T3 cells in media suspension and 'gaps' observed in the cell monolayer under microscopic analysis (summarised in Table 4.1).

4.1.3.1 *Main findings*

This experiment clearly established that there was a relationship between the passage number of the 3T3 cells and keratinocyte proliferation. From this, a passage limit for irradiated 3T3 feeders was established for co-cultures in future experiments.

4.1.4 Clonal cell lines can establish and grow independently

In order to investigate whether clonal cell lines could be cultured effectively in the absence of 3T3 feeder cells, M08 was prepared in culture at 8 x 10^5 in 9 cm TC dishes, with and without 3T3 feeder cells (in duplicate). Cultures were analysed microscopically on a daily basis until cells reached 100% confluence; cell morphology was also assessed during this time.

Cultures of M08 supplemented with 3T3 feeder cells appeared to establish better within the first 48 hours of culture in comparison to cultures of M08 without 3T3 feeder cells. However, cells with and without 3T3 feeder cells reached 100% confluence in a comparable time frame (10 days). With and without 3T3 feeder cells, the keratinocytes maintained polygonal morphology, however keratinocytes tended to establish and replicate as circular colonies in a background of 3T3 feeder cells whereas colony formation was less defined in cultures without 3T3s (Figure 4.2).

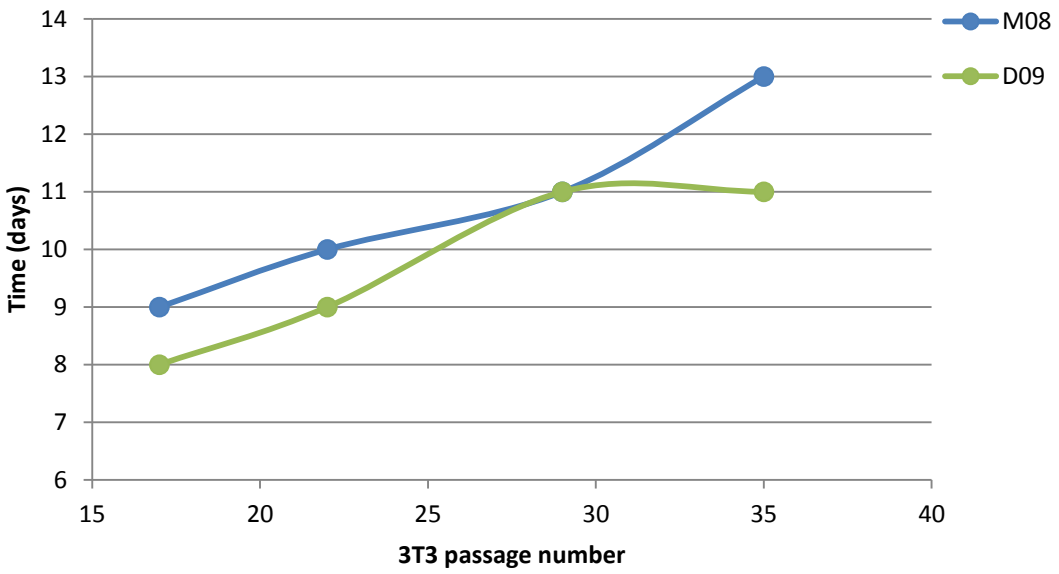

Figure 4.1. Time taken for clonal cell lines M08 and D09 to become confluent in co-culture with 3T3 feeder cells of varying passage

M08 and D09 at P6 were seeded with 8 x 10^5 cells in 9 cm TC dishes with 2 x 10^6 irradiated 3T3 feeder cells at P17, 22, 29 and 36. The time taken for keratinocytes to reach 100% confluence was assessed microscopically. Cultures were prepared in triplicate; microscopic analysis of triplicate cultures showed that replicates for each condition reached confluence on the same day (error bars are not shown).

Clonal cell line	3T3 passage no.	Time to confluence (days)	Observations during culture
D	17	8	3T3s attached and few in suspension
	22	9	3T3s attached with increased numbers of cells in suspension with increasing time in culture
	29	11	3T3s establish poorly and detach easily with increased numbers of cells in suspension and 'gaps' in the monolayer
	36	11	3T3s establish poorly and detach easily with increased numbers of cells in suspension and 'gaps' in the monolayer
M	17	9	3T3s attached and few in suspension
	22	10	3T3s attached with increased numbers of cells in suspension with increasing time in culture
	29	11	3T3s establish poorly and detach easily with increased numbers of cells in suspension and 'gaps' in the monolayer
	36	13	3T3s establish poorly and detach easily with increased numbers of cells in suspension and large 'gaps' in the monolayer

Table 4.1. Microscopic observations of clonal cell lines M08 and D09 supplemented with irradiated 3T3 feeder cells of varying passage

M08 and D09 at P6 were seeded with 8 x 10^5 cells in 9 cm TC dishes with 2 x 10^6 irradiated 3T3 feeder cells at P17, 22, 29 and 36. Co-cultures were examined microscopically and observations recorded throughout culture upon reaching 100% confluence. Cultures were prepared in triplicate and the same observations were made in each replicate.

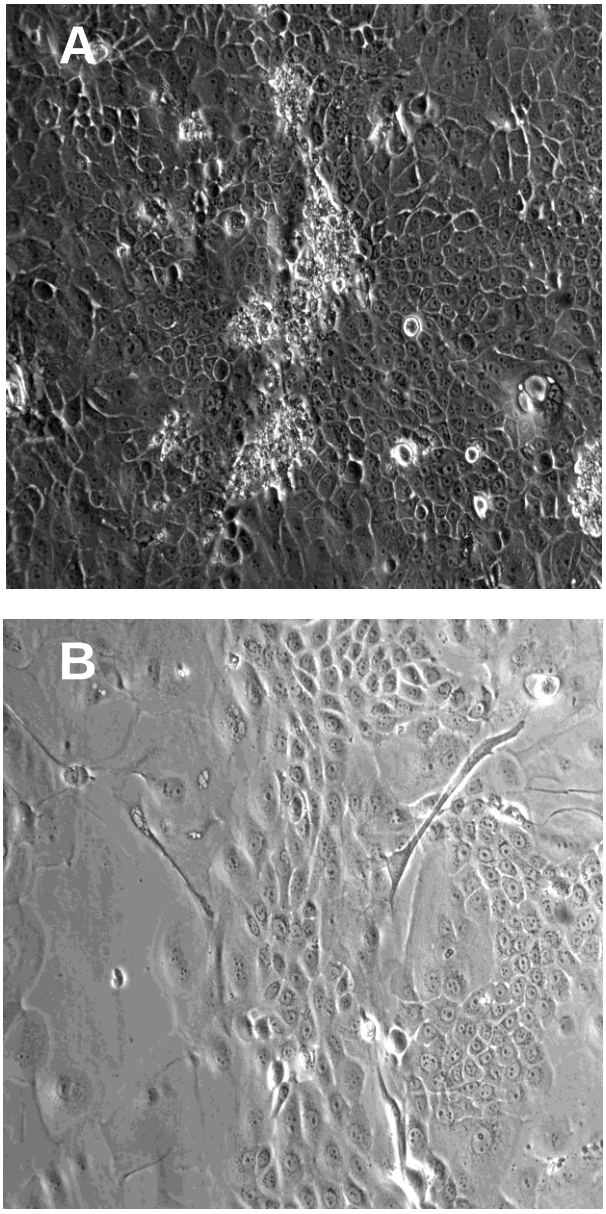

Figure 4.2. Morphology of M08 keratinocytes in culture with and without 3T3 feeder cell support

M08 at P6 was seeded with 8 x 10^5 cells in 9 cm TC dishes with or without 2 x 10^6 irradiated 3T3 feeder cells and no feeder cells. **A**. M08 cells grown with 3T3 feeder cells at 100% confluence, and **B**. M08 cultures without 3T3 feeder cells at ~80% confluence (100x total magnification).

4.1.4.1 *Main findings*

Clonal cell cultures proliferated independently of co-culture with 3T3 feeder cells.. This suggested that clonal cell lines without co-culture with 3T3 feeder cells could be used for future drug treatment and response experiments.

4.1.5 Confluence of clonal cell lines affects HPV oncogene expression

The effect of confluence on E6 and E7 expression in M08 was analysed at 50%, 75%, 100% and 100% + 1 week confluence whilst in co-culture with and without 3T3 feeder cells. Cells were maintained in culture until the desired degree of confluence was reached, and then trypsinised and nucleic acids extracted. RNA was used for qRT-PCR and relative E6 and E7 expression values were obtained according to the methods previously described.

The effect of cell density on mRNA levels for HPV oncogenes E6 and E7 is shown in Figure 4.3. Examples of real time fluorescent traces and melt curves are shown in Appendix II. There was no significant difference in mRNA levels for HPV E6 and E7 in cultures with and without 3T3 feeder cells, as shown in Figure 4.4.

4.1.5.1 *Main findings*

Expression of E6 and E7 was clearly affected by cell density, with highest expression observed in cells at approximately 75% confluence. This demonstrated the importance of standardisation of culture conditions when analysing oncogene expression. In subsequent experiments cells were passaged consistently at ~80% confluence. There was no significant difference between relative expression ratios of E6 and E7 in M08 cultures supplemented with and without 3T3 feeders at 75% confluence (E6: $p = < 1.1821.$, E7: $p = < 0.9223$, at $p < 0.05$, 2-tailed t-test).

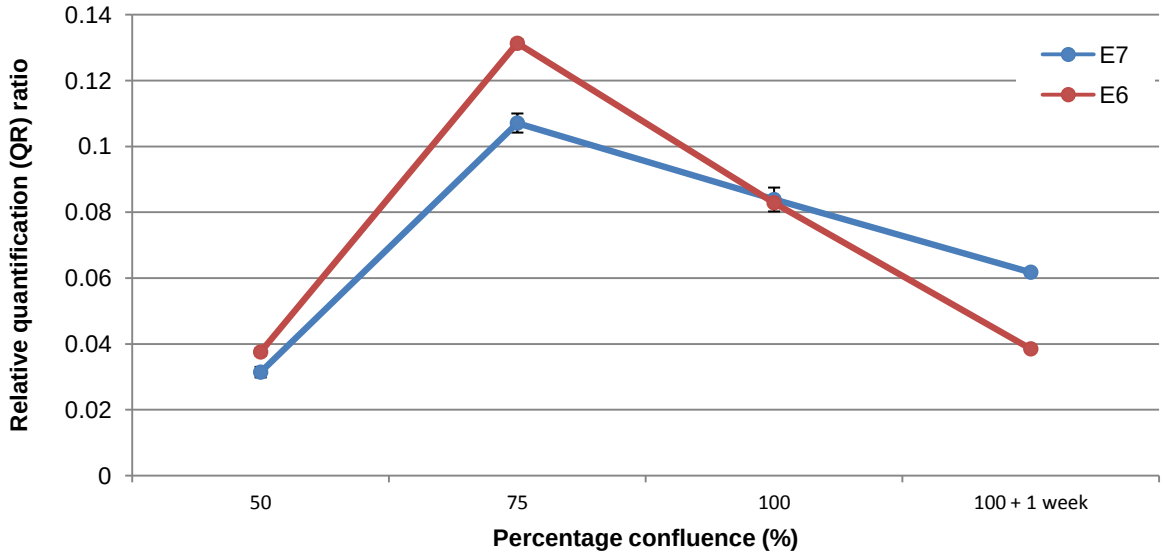

Figure 4.3. Effect of percentage confluence on mRNA levels of E6 and E7 in P6 clonal cell line M08

M08 co-cultures containing irradiated 3T3 feeder cells were investigated using qRT-PCR to determine relative E6 and E7 mRNA levels when cultures reached 50%, 75%, 100%, and 100% plus 1 week confluence. Expression was normalised to stable house-keeping genes TBP2 and HRPT. Expression was quantified relative to CaSki cDNA as a standard. Cultures were prepared in triplicate and error bars denote the standard deviation.

	E7	E6
Without feeders	0.056217	0.054881
With feeders	0.059026	0.040682

Figure 4.4. Mean relative quantification ratios of E6 and E7 mRNA levels in P6 clonal cell line M08 cultured with and without 3T3 feeders at 75% confluence.

M08 cultures with and without irradiated 3T3 feeder cells underwent qRT-PCR to determine relative E6 and E7 expression levels. Cultures were prepared in triplicate. There was no significant difference between E6 and E7 mRNA levels in clonal cell line M08 cultures supplemented with and without 3T3 feeders (E6: $p = < 1.1821$, E7: $p = < 0.9223$, at $p < 0.05$, 2-tailed t-test).

Mycoplasma contamination

3T3 feeder and clonal cell line cultures were examined by PCR for *Mycoplasma* contamination, as previously described. An example of the data generated is shown in Figure 4.5.

4.1.5.2 *Main findings*

Mycoplasma contamination was not detected in any of the cell cultures tested.

4.2 Discussion

The main conclusions of these preliminary studies were:

1. There was a clear relationship between the passage number of the 3T3 feeder cells used to constitute the feeder layer and keratinocyte proliferation assessed as time taken to reach confluence.
2. Keratinocytes did proliferate in the absence of feeder cells.
3. mRNA levels for HPV E6 and E7 were affected by cell density.
4. mRNA levels for HPV E6 and E7 at 75% confluence was not affected by the presence or absence of 3T3 feeders in culture.
5. Cultures were free from *Mycoplasma* contamination.

These experiments provided useful information to guide the planning of future experiments. On the basis of this data it was decided that keratinocytes would usually be prepared using co-culture with 3T3s at less than P22, but would not be used in CDV dosing studies to avoid using multiple cells in culture (particularly since the presence/absence of 3T3s in culture did not appear to affect HPV E6 and E7 expression levels). Passaging cultures would also be standardised to ~80% confluence.

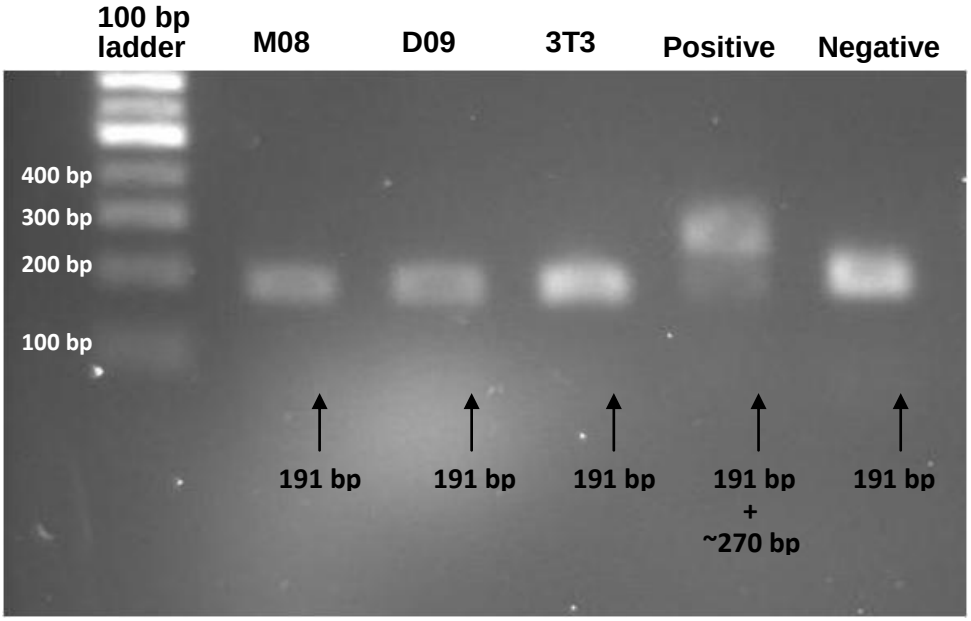

Figure 4.5. *Mycoplasma* testing using Venor*GeM*® PCR

Clonal cell cultures M08 and D09, 3T3 feeder cell cultures, and test kit positive and negative control samples underwent PCR, electrophoresis on a 1.5% ethidium bromide agarose gel, and were visualised using a UV transilluminator. The test kit negative control and positive control generated band sizes of 191 bp and 265-278 bp, respectively. Each sample included an internal control that generated a band size of 191 bp, which confirmed successful PCR; samples with an absent band at 191 bp indicated PCR inhibition. *Mycoplasma* species DNA within samples (i.e. samples that were contaminated with *Mycoplasma*) also generated a band size of 265-278 bp with or without a 191 bp internat control band. All cell culture samples generated amplicons of 191bp confirming that the PCR had worked and samples were not contaminated with *Mycoplasma*.

4.2.1 Cell culture with and without 3T3 feeder support

Some of the data on the effects of culture with 3T3s were difficult to interpret; the time taken for M08 cells to become confluent with P36 3T3s was 13 days, while without 3T3s, cultures reached confluence in 10 days. This suggests that the presence of late passage 3T3s was more detrimental to the growth of keratinocytes than their complete absence. 3T3s produce extracellular matrix proteins such as basal lamina glycoproteins which may promote keratinocyte cell attachment and growth (Alitalo et al., 1982, Rheinwald and Green, 1975), although Peehl and colleagues (Peehl and Ham, 1980) suggest that keratinocyte cells do not necessarily require co-culture with 3T3 feeder cells to grow effectively. The use of epidermal growth factor (EGF) as a media supplement might contribute to enhancing the growth of keratinocytes cultures that are not supported by 3T3 feeder cells (Rheinwald and Green, 1977), and clonal cell lines in this study were supplemented with GMEM containing EGF.

The data suggested that the M08 cell line could be cultured effectively without feeder cells. However, the potential convenience of culture without feeder layers had to be balanced against the potential effects on the cultures. Using W12 cells, a naturally HPV transformed cell line derived from a cervical intraepithelial neoplasia, Dall *et al*. have previously shown that culture without feeder cells for 15 to 25 population doublings may promote HPV episome loss via induction of stress response pathways (Dall et al., 2008). However, as the planned drug treatment studies would only involve short term culture without feeders, episome loss appeared an acceptable risk.

4.2.2 The effect of confluence on HPV oncogene expression

The effect of confluence on E6 and E7 emphasised the importance of comparing cell cultures of the same percentage confluence, particularly in CDV dosing studies where HPV oncogene expression is investigated, in order to avoid bias and produce reliable results. The effects of confluence on expression of HPV E6 and E7 have previously been investigated by Wechsler *et*

al. (Wechsler et al., 2012). HPV16 genomes were transformed into the NIKS keratinocyte line to generate clones which in organotypic raft culture phenocopied low and high-grade squamous intraepithelial lesions (LSIL and HSIL). In monolayer culture, the LSIL-like clones did not appear to continue to divide effectively post 100% confluence and showed reduced E6 and E7 expression, which suggested that they were sensitive to contact inhibition. However, the HSIL-like clones displayed an increase in E6 and E7 when they reached confluence and continued to divide. This demonstrates the importance of standardisation of culture conditions. Considering that the M08 and D09 cells both showed reduced E6 and E7 mRNA in cells at confluence, and appeared to show contact inhibition, it might also suggest that despite being derived from high grade lesions (VIN3 and VaIN3) they may be more representative of low grade disease. This could be confirmed by organotypic raft culture of these lines, but these experiments were not undertaken during this project.

4.2.3 Mycoplasma infection and cellular metabolic activity

Mycoplasma testing confirmed that the cell lines were not infected. It was especially important to perform this testing as mycoplasma infection can affect the metabolism of nucleoside analogues, such as Cidofovir, which is used in treatment of VIN. Bronckaers *et al*. demonstrated that several nucleoside analogues are degraded to their inactive base forms by *Mycoplasma hyorhinis* encoded thymidine phosphorylase in MCF-7 breast carcinoma cells (Bronckaers et al., 2008). The mycoplasma encoded enzyme dramatically reduced the cytostatic activity of the compounds causing a reduction in the formation of active metabolites and/or reduced drug incorporation into nucleic acids in infected cells compared with uninfected cells.

4.2.4 Strengths and weaknesses

The strengths of the preliminary studies were that all experiments were performed in replicates, and the results generated were highly consistent between replicates and between

clonal cell lines M08 and D09, which originated from different anatomical sites (vulval and vaginal respectively). Although the data output was not entirely quantitative, the analyses identified important parameters to guide design of future experiments.

There were some weaknesses in the experimental design; clonal cell lines M and D were selected for preliminary studies because they were the most rapid clonal cell lines to establish and replicate in culture after being isolated. Early passage keratinocytes were slow growing in culture, as previously described in chapter 3, and using the first clonal lines to establish meant that the project time frame could be optimised and the preliminary studies could be carried out before a variety of clonal cell lines were available. However, picking the most rapid growing clonal cell lines for use in these studies introduced selectivity in to the experiment because these cell populations were those with genetic traits that conferred a cellular growth advantage, and might not be fully representative of the other clonal lines. Selectivity was unavoidable in this instance as the preliminary data had to be completed before clonal cell lines were characterised to ensure that the cell culture environment was optimal for future experiments.

The preliminary studies considered percentage confluence of cell cultures as a standard for assessing variables within the culture system, and also as a variable under investigation. Confluence was determined under microscopic analysis, which is the simplest, most common method described in the literature, although it is subjective. This subjectivity was considered a weakness, however this technique is commonly accepted as a method of determining confluence.

5 Molecular characterisation

5.1 Results

Clonal cell lines were characterised at a molecular level by investigating HPV integration status and HPV gene expression over a range of passages during short-term culture. DNA, but not RNA, from heterogeneous PC08 and PC09 was also available from the previous pilot study (kindly provided by Dr Ned Powell) and underwent limited HPV integration analysis.

HPV integration status was investigated using two PCR based assays, 1. Detection of Integrated Papillomavirus Sequences (DIPS), and 2. Amplification of Papillomavirus Oncogene Transcripts (APOT). DIPS detected genomic integrated HPV and APOT explored whether HPV integrants were actively transcribed. E2 PCR was also performed to confirm disruption to E2, by Dr Rachel Raybould (HPV Research Group, Cardiff University). Incorporation of historical PC08 and PC09 was useful for assessing the origin of HPV integrants detected in clonal cell lines previously derived from PC08 and PC09, i.e. to assess whether HPV integrated loci were present in the parental cell line or induced as a result of clonal cell line isolation and cell culture. HPV integration status was explored for several reasons, i. to determine whether distinct HPV integration profiles were present in the clonal cell lines, ii. to determine when integration of HPV occurred (before or after isolation *in vitro*), and iii. to explore whether the cell culture process can induce integration of HPV. It has been suggested that integration of HPV into the host genome can cause activation of endogenous proto-oncogenes or inactivation of tumour suppressor genes (Einstein et al., 2002, Ferber et al., 2003a, Ferber et al., 2003b, Couturier et al., 1991). Hence the exact sites of integration were identified to see if they coincided with known oncogenes or tumour suppressor genes.

HPV gene expression was also investigated during short-term culture to fulfil the objective of characterising clonal cell lines at a molecular level. Relative expression of HPV genes E2, E4, E5,

E6 and E7, was assessed at each passage using qRT-PCR to obtain transcription profiles for each clonal cell line. HPV gene expression was also explored because CDV has previously been shown to affect expression of HPV oncogenes E6 and E7 (Abdulkarim et al., 2002). Since clonal cell lines were intended for use as an *in vitro* experimental system for future CDV dosing protocols, it was necessary to assess the stability of E6 and E7 expression over a succession of passages in culture.

5.1.1 Aims and objectives

The central aim was to characterise clonal cell lines during short-term culture at a molecular level; this involved investigating HPV integration status and relative HPV gene expression. The following objectives structured this section of work:

1. Investigate integration of HPV in to the host DNA (genome) in all clonal cell lines at early and late passages of short-term culture.
2. Investigate transcriptionally active HPV integrants in all clonal cell lines at early and late passages of short-term culture.
3. Investigate if there is a link between genes disrupted by HPV integration and carcinogenesis (through researching gene function).
4. Investigate relative HPV gene expression in all clonal cell lines at each passage of short-term culture.

5.1.2 Study sample

5.1.2.1 *HPV integration status*

DNA and RNA extracts of earliest and latest passages of clonal cell lines M08 (P5 & 9), P08 (P5 & 9), Y08 (P9 & 13), A09 (P5 & 11), D09 (P5 & 11) and H09 (P5 & 11) underwent DIPS and APOT analysis, respectively. DNA of heterogeneous PC08 (P19) and PC09 (P21) also underwent DIPS analysis.

5.1.2.2 *HPV relative gene expression*

RNA extracts of all passages of clonal cell lines M08 (P5 - 9), P08 (P5 - 9), Y08 (P9 - 13) A09 (P5 - 11), D09 (P5 - 11) and H09 (P5 - 11) underwent qRT-PCR and gene expression analysis.

5.1.2.3 *E2 PCR*

DNA extracts of earliest and latest passages of clonal cell lines M08 (P5 & 9), P08 (P5 & 9), Y08 (P9 & 13), A09 (P5 & 11), D09 (P5 & 11) and H09 (P5 & 11), and heterogeneous PC08 (P19) and PC09 (P21), underwent E2 PCR.

5.2 HPV integration status

HPV integration was determined using several different assays. DIPS ligates adapters to common restriction endonuclease cut sites in the HPV and human genome. PCR with adapter specific primers is then used to amplify HPV:human DNA fusions (Luft et al., 2001). APOT amplifies HPV mRNAs in order to detect and differentiate HPV:human fusion transcripts (Klaes et al., 1999). E2 PCRs are a series of overlapping PCRs that cover the entire E2 gene (Collins et al., 2009). Missing fragments indicated disruption or loss whilst complete coverage of E2 suggested the presence of episomal HPV, integrated HPV with intact E2, or HPV genomes integrated as concatamers (as observed in the CaSki cell line) (Meissner, 1999).

5.2.1 E2 disruption

DNA extracts of PC08, PC09, and clonal cell lines, underwent PCR amplification of the HPV E2 gene as described by Collins and colleagues (Collins et al., 2009). The results of E2 PCRs are summarised (along with DIPS data) in Table 5.1. In all clonal cell lines, E2 PCR data was consistent at early and late passage. E2 was intact in PC08 and its derivative clonal cell line Y08, which suggested the presence of episomal HPV or integration of full length, possibly concatenated, HPV. E2 was not amplified in clonal cell line M08 which suggested E2 disruption due to integration of HPV into the host genome. In P08 a truncated E2 fragment was

produced; sequencing of this fragment revealed a section of E2 spanning nt 2201 to 3147 had been deleted (Figure 5.1). PC09 and its derivative clonal cell lines A09, D09, and H09 all contained intact E2 which suggested the presence of episomal HPV or integration of full length, possibly concatenated, HPV.

5.2.1.1 *Main findings*

E2 PCR data suggested that clonal lines representing integrated and potentially episomal HPV infections had been isolated. E2 PCR data was consistent in early and late passage (which were independent samples), validating the status of E2 in each clonal cell line.

5.2.2 Genomic integration loci

DIPS was performed using DNA extracts of PC08, PC09, and clonal cell lines, to detect genomic HPV integration. The resulting sequence data underwent BLAST and BLAT analysis, as previously described, to identify the site of integration in the human genome and also the region of the HPV genome that was disrupted. All integration and non-contiguous events detected by DIPS were confirmed by PCR and sequencing using primers that flanked the host viral junction. Viral disruption and genomic integration loci that were detected in PC08, PC09, and clonal cell lines are shown in Table 5.1. Integrated HPV was detected in M08 and Y08 but not in P08 or heterogeneous PC08, which suggests that these events occurred during culture or were present at undetectable levels in heterogeneous PC08. HPV integration was also detected in heterogeneous PC09 and D09 and H09, but not in A09. Integration loci were different in each clonal cell line, and were consistent at early and late passage; an additional integration loci was detected in late passage of H09.

Biopsy	Cell line	Passage no.	E2 PCR	Viral disruption (ORF)	Integration loci	Orientation
PC08	Hetero.	19	Intact	Not detected	-	-
	M08	5	Disrupted	nt 1194 (E1)	3q28	Antisense
		9	Disrupted	nt 1194 (E1)	3q28	Antisense
	P08	5	Disrupted	nt 2201-3147 (E1-E2)	None	NA
		9	Disrupted	nt 2201-3147 (E1-E2)	None	NA
	Y08	9	Intact	nt 2116 (E1)	3p21.31	Antisense
		13	Intact	nt 3167 (E2)	3p21.31	Antisense
PC09	Hetero.	21	Intact	nt 6033 (L1)	2q36.1	Sense
	A09	5	Intact	Not detected	-	-
		11	Intact	Not detected	-	-
	D09	5	Intact	nt 5003 (L2)	18p11.31	Antisense
		11	Intact	nt 5003 (L2)	18p11.31	Antisense
	H09	5	Intact	nt 2490 (E1)	11p15.3	Sense
		11	Intact	nt 2490 (E1)	11p15.3	Sense
		11	intact	nt 1848 (E1)	22q12.3	Antisense

Table 5.1. Genomic integration loci determined by DIPS and E2 PCR, for PC08, PC09 and clonal cell lines at early and late passages

'None (non-contiguous)' refers to viral disruption causing non-contiguous (fragmented) HPV sequence. The percentage consensus of sequence data with NCBI database was >95% for all samples. 'Hetero.' denotes the heterogeneous cell population, and 'nt' specifies the nucleotide number in the HPV16 genome.

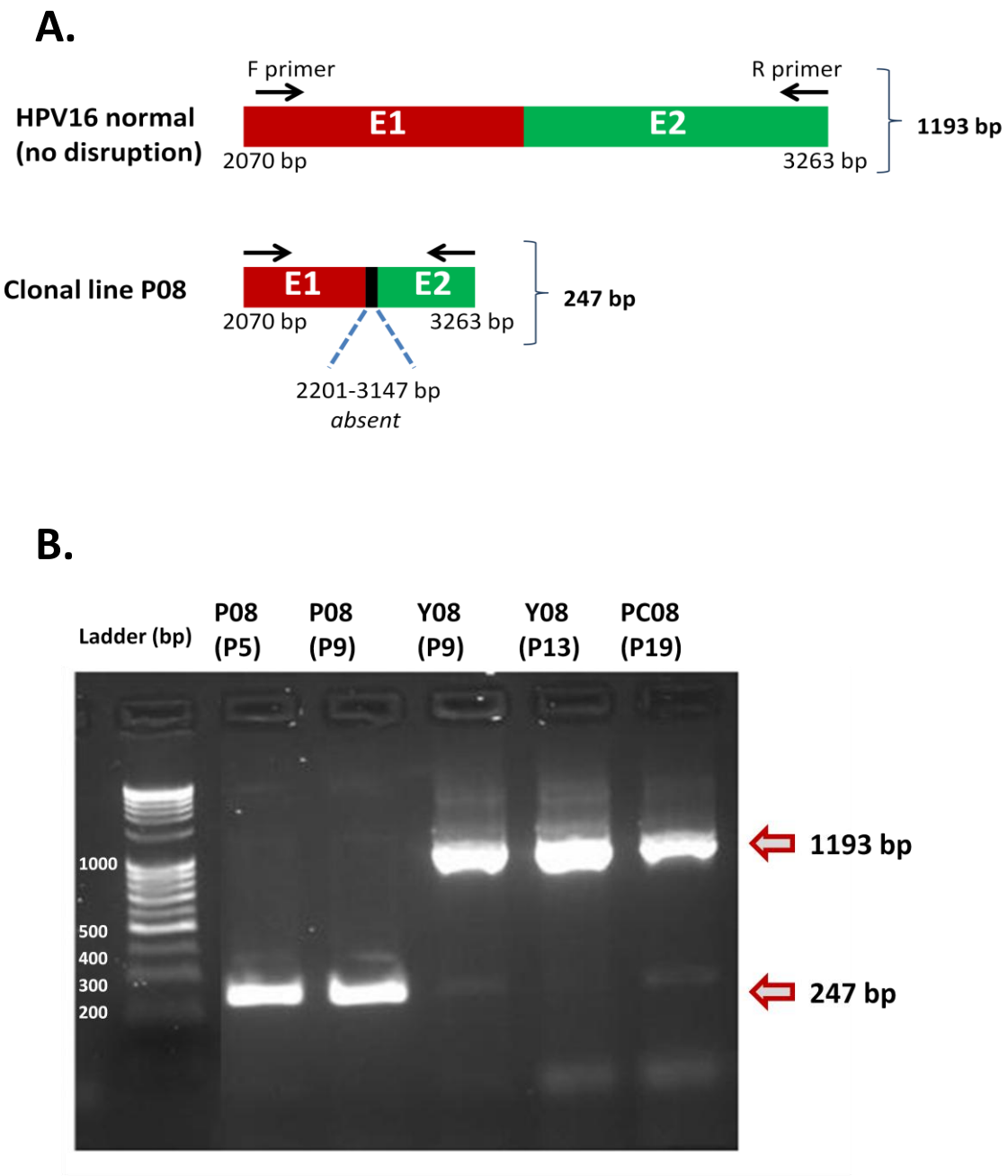

Figure 5.1. Disruption to E2 detected in P08

A. A schematic representation of wildtype (no disruption) and clonal cell line P08 HPV16 E1 and E2 amplicon. In wildtype, forward (F) and reverse (R) primers span 2070-3263 bp producing a fragment with a total size of 1193 bp. In P08, primers spanning the same region produced a fragment with a total size of 247 bp and sequencing identified an absent region between 2201-3147 bp. **B**. Gel electrophoresis image of amplicons generated using forward (F) and reverse (R) primers flanking E1 and E2 in P08, producing a fragment of 247 bp in size. Amplicons for Y08 and heterogeneous PC08 are also illustrated at 1193 bp, consistent with wildtype (no disruption). Gel electrophoresis image was kindly provided by Dr Rachel Raybould and adapted for this illustration.

5.2.2.1 *Main findings*

DIPS analysis suggested that a selection of integrated and episomal HPV existed in the clonal cell lines. Genomic integration loci were different in each clonal cell line.. Integration loci were consistent at early and late passage and this validated the integration events identified in independent samples of each clonal cell line. As integration was not detected in heterogeneous PC08, this might highlight limitations of DIPS as a technique or indicate that HPV integration may have occurred during culture. An additional genomic integration loci was detected in clonal cell line H09 at late passage which might indicate that HPV integration was induced during short-term culture.

5.2.3 Transcriptionally active integration loci

APOT was performed using RNA extracts of clonal cell lines to explore whether genomic integration loci were actively transcribed. RNA was not available for heterogeneous PC08 or PC09 and as such these were not tested. The resulting sequence data underwent BLAST and BLAT analysis, as previously described and integrated and episomal transcripts were identified.

Electrophoresed APOT fragments and the resulting sequenced transcripts for clonal cell lines are shown in Table 5.2 and Figure 5.2. Four different transcript patterns were detected in the clonal cell lines investigated (Figure 5.3):

- Type 1: integrated transcript consisting of E7-E1 fused directly to human sequence.
- Type 2: integrated transcript consisting of E7-E1 spliced to E4 fused to human sequence.
- Type 3: episomal transcript consisting of E7-E1 spliced to E4.
- Type 4 transcripts: episomal transcript consisting of E7-E1 spliced to E4-E5.

HPV integrated transcripts were detected in D09, H09, M08 and Y08; HPV episomal transcripts were detected in A09 and P08. Different integrated transcripts were identified in each clonal

Biopsy	Cell line	Passage no.	Viral disruption (ORF) (type)	Integration loci	Orientation
PC08	M08	5	nt 880 (E1) (type 1)	3q28	Antisense
		9	nt 880 (E1) (type 1)	3q28	Antisense
	P08	5	NA (type 3)	NA (episomal)	
		9	NA (type 3)	NA (episomal)	
	Y08	9	nt 882 (E1) (type 1)	3p21.31	Antisense
		13	nt 882 (E1) (type 1)	3p21.31	Antisense
PC09	A09	5	NA (type 3)	NA (episomal)	
		11	NA (type 3)	NA (episomal)	
		11	NA (type 4)	NA (episomal)	
	D09	5	nt 3716 (E4) (type 2)	18p11.31	Sense
		11	nt 3716 (E4) (type 2)	18p11.31	Sense
	H09	5	nt 882 (E1) (type 1)	5q11.2	Sense
		11	nt 882 (E1) (type 1)	5q11.2	Sense
		11	nt 3494 (E4) (type 2)	1p36.13	Antisense

Table 5.2. APOT derived transcripts (integrated and episomal) detected in clonal cell lines at early and late passages

'NA' denotes instances where episomal transcripts were detected. The percentage consensus of sequence data with NCBI database was >98% for all cell lines. 'Nt' specifies the nucleotide number within the HPV16 genome.

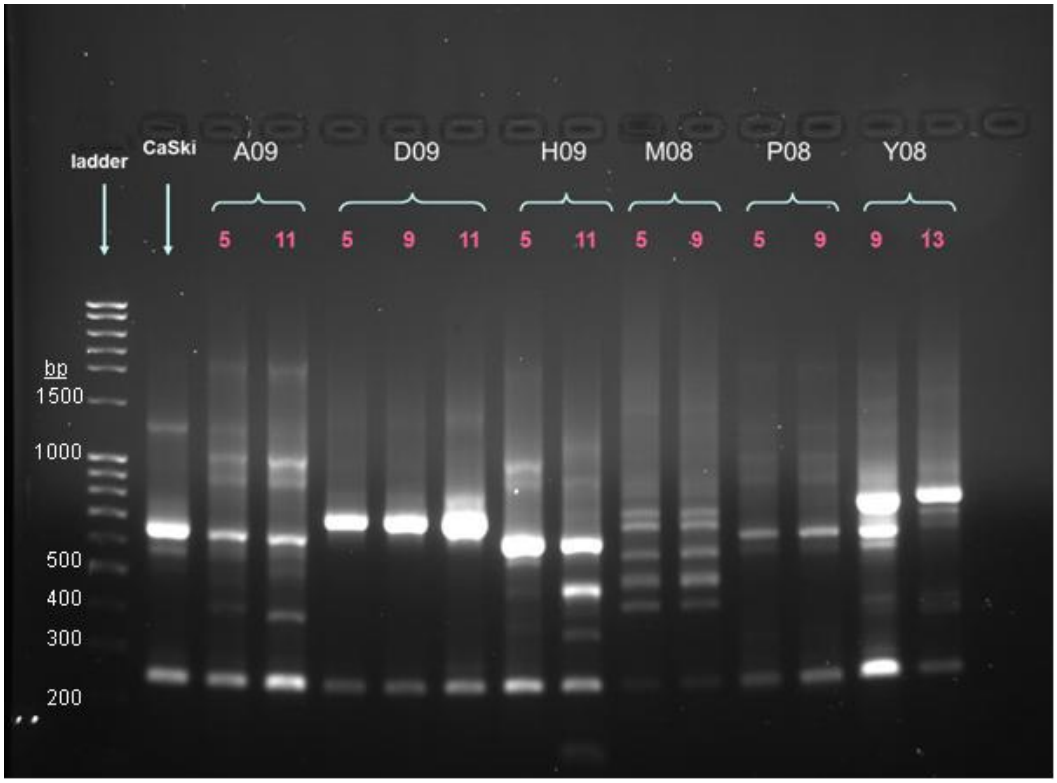

Figure 5.2. APOT amplified transcripts of early and late passage clonal cell lines

Amplicons were electrophoresed on a 2% w/v agarose gel for early and late passages of clonal cell lines A09 (P5 & 11), D09 (P5 & 11), H09 (P5 & 11), M08 (P5 & 9), P08 (P5 & 9), and Y08 (P9 & 13).

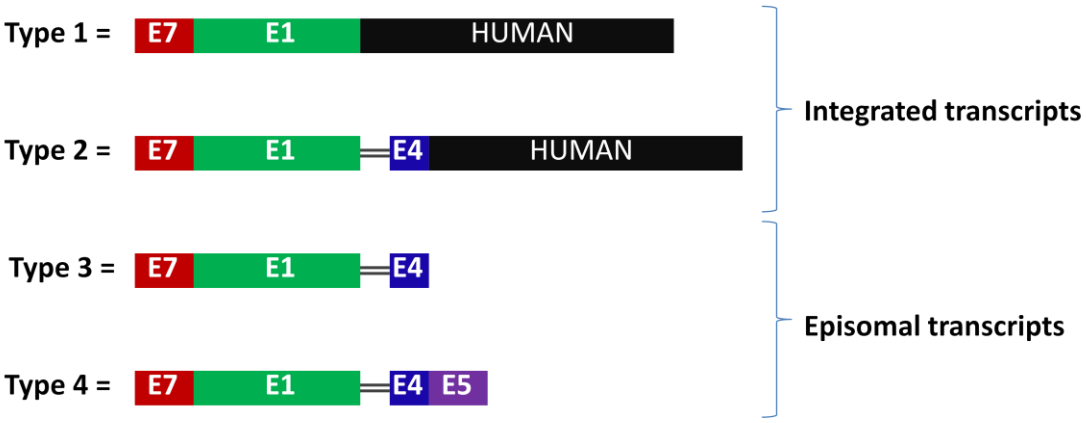

Figure 5.3. Schematic representation of transcript types detected via APOT for clonal cell lines

Four transcript types were detected for clonal cell lines; types 1 and 2 are integrated transcripts since they contain human sequence, and types 3 and 4 are episomal since they did not contain human sequence. Type 1 transcripts tend to arise when HPV integration disrupts HPV genes E2/E4, and type 2 when integration disrupts HPV genes L2/L1. = represents splicing within a transcript.

cell line, and were consistent at early and late passage; however H09 had acquired an additional integrated transcript at late passage.

To confirm the presence of integrated transcripts in each clonal cell line, flanking primers were designed, using PRIMER 3 software, to span the HPV-human junction of each integration site detected by APOT. The clonal cell line cDNA used for APOT was investigated using these primer sets to confirm the presence of specific integrated transcripts; PCRs were also performed using integrant-specific primers to investigate whether these integrated transcripts were present in clonal cell lines derived from the same parental heterogeneous cell line (PC08 or PC09).

Amplified fragments for each clonal cell line are illustrated in Figure 5.4. The electrophoresis image shows that the flanking primers amplified the expected fragment in the relevant clonal cell lines. When the primer sets were used for PCR with other clones from the same heterogeneous line (e.g. D09 primers with H09 cDNA) an amplicon was not produced. This validated the results of the APOT analysis, and also confirmed that integrated transcripts were unique to each individual clonal cell line. An additional integrated transcript was detected in late passage H09 which might indicate that a HPV integration event occurred during short-term culture.

5.2.3.1 *Main findings*

APOT analysis showed that integrated HPV was present in several of the lines and suggested that episomal HPV in others. Integrated transcripts were distinct in each clonal cell line, confirming that they represent independent clones. Integrated transcripts were consistently detected at early and late passage, which were independent samples and were confirmed using flanking primers. An additional integrated transcript was detected in one clonal cell line which might indicate that an integration event was acquired during culture.

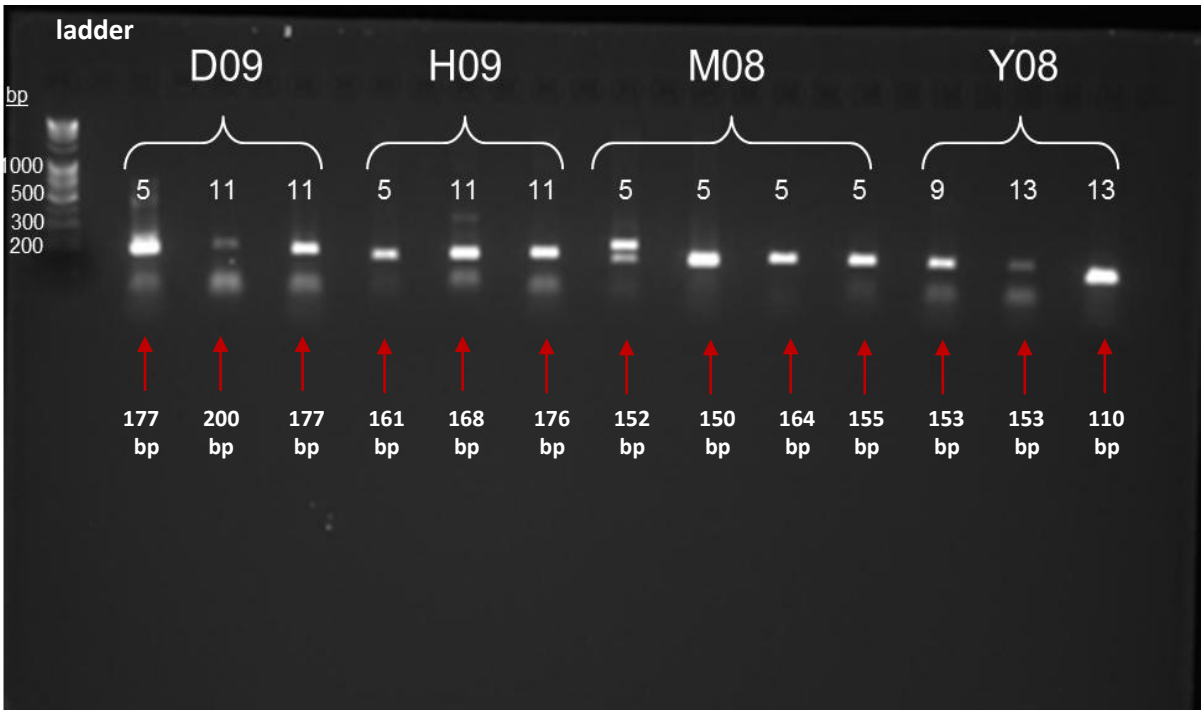

Figure 5.4. Confirmation of integrated transcripts identified by APOT using flanking primers for HPV-human integration loci

Unique primer sets were designed to interrogate HPV-human fused sequences within each sample. Amplicons of various sizes (see below) were therefore expected depending on the location of the primers during the design process. Amplicons were electrophoresed on 2% agarose gels, and fragment sizes for each clonal cell line and passage number were confirmed as follows: D09 at P5 (177 bp) and P11 (200 bp, 177 bp), H09 at P5 (161 bp) and P11 (168 bp, 176 bp), M08 at P5 (152 bp, 150 bp, 164 bp, 155 bp), and Y08 at P9 (153 bp) and P13 (153 bp, 110 bp).

5.2.4 Host genes disrupted by integration

BLAST searches were used to identify host cell genes that were disrupted by HPV integration (Table 5.3). The functions of these genes were as follows:

LEPREL1, also known as P3H2, encodes a member of the prolyl 3-hydroxylase subfamily of 2-oxo-glutarate-dependent dioxygenases. These enzymes play a critical role in collagen chain assembly, stability, and cross-linking by catalyzing post-translational 3-hydroxylation of proline residues. Mutations in this gene are associated with nonsyndromic severe myopia with cataract and vitreoretinal degeneration, and downregulation of this gene may play a role in breast cancer (*http://www.genecards.org/cgi-bin/carddisp.pl?gene=LEPREL1*). *LEPREL1* expression has been reported to be down-regulated in breast cancer cell lines due to hyper-methylation of CpG islands around exon 1 (Shah et al., 2009). Loss of collagen is an early event in the development of some epithelial cancers (Ikeda et al., 2006).

CDCP1 encodes a transmembrane protein which contains three extracellular CUB domains and acts as a substrate for Src family kinases. The protein plays a role in the tyrosine phosphorylation-dependent regulation of cellular events that are involved in tumor invasion and metastasis (*http://www.genecards.org/cgi-bin/carddisp.pl?gene=CDCP1)*. *CDCP1* is up-regulated in colon cancer (Scherl-Mostageer et al., 2001) and increased expression correlates with poor prognosis in lung cancer patients (Ikeda et al., 2009).

TGIF1 encodes a member of the three-amino acid loop extension (TALE) superclass of atypical homeodomains. TALE homeobox proteins are highly conserved transcription regulators. The TGIF1 protein binds to a previously characterized retinoid X receptor responsive element from the cellular retinol-binding protein II promoter. In addition to its role in inhibiting 9-cis-retinoic acid-dependent RXR alpha transcription activation of the retinoic acid responsive element, the protein is an active transcriptional co-repressor of SMAD2 and may participate in the

Clonal cell line	Passage no.	Integration loci (chromosome and gene)	
		DIPS	APOT
M08	5	3q28.7 *LEPREL1*	3q28.7 *LEPREL1*
	9	3q28.7 *LEPREL1*	3q28.7 *LEPREL1*
P08	5	NA (episomal)	NA (episomal)
	9	NA (episomal)	NA (episomal)
Y08	9	3p21.31 *CDCP1*	3p21.31 *CDCP1*
	13	3p21.31 *CDCP1*	3p21.31 *CDCP1*
A09	5	NA (episomal)	NA (episomal)
	11	NA (episomal)	NA (episomal)
	11	NA (episomal)	NA (episomal)
D09	5	18p11.31 *TGIF1*	18p11.31 *TGIF1*
	11	18p11.31 *TGIF1*	18p11.31 *TGIF1*
H09	5	11p15.3 *MICAL2*	5q11.2 no gene
	11	11p15.3 *MICAL2*	5q11.2 no gene
	11	22q12.3 *LARGE*	1p36.13 *CLCNKB*

Table 5.3. Comparison of integration loci detected via DIPS and APOT

The location of HPV integration within the host cell chromosome and the gene disrupted are shown for each clonal cell line. H09, highlighted in yellow, illustrates discrepant DIPS and APOT integration loci.

transmission of nuclear signals during development and in the adult. Mutations in this gene are associated with holoprosencephaly type 4, which is a structural anomaly of the brain (*http://www.genecards.org/cgi-bin/carddisp.pl?gene=TGIF1*). SMAD proteins are tumour suppressors that inhibit cell proliferation and are reported to be down-regulated in colorectal cancer (Xie et al., 2003). TGIF1 has been found to be expressed in several cancers (oesophagus, stomach, liver and leukaemia) (Hamid et al., 2008, Nakakuki et al., 2002, Borlak et al., 2005). TGIF1 located at 18p11.3 is a region commonly involved with head and neck squamous cell carcinoma (van den Broek et al., 2007, Noutomi et al., 2006). Reis and colleagues carried out detailed mapping of tumoural and non tumoural tissue through a Brazilian head and neck cancer project and found that TGIF1 transcripts were expressed (Reis et al., 2005). Expanding on this head and neck cancer project, Matizonkas-Antonio and colleagues studied the expression of TGIF1 transcripts and found that gain or loss of function might play a role in oral cancer cell differentiation (Matizonkas-Antonio et al., 2011).

MICAL2 (microtubule associated monooxygenase, calponin and LIM domain containing 2) is a protein-coding gene, associated with visceral leishmaniasis, and prostate cancer (*http://www.genecards.org/cgi-bin/carddisp.pl?gene=MICAL2*). The *MICAL2* gene product acts as a cytoskeletal regulator and is involved in axon guidance. The development of the nervous system is an invasive process and it is thought that overexpression of *MICAL2* may contribute to invasiveness in prostate cancer (Ashida et al., 2006).

LARGE is one of the largest genes in the human genome and encodes a glycosyltransferase which participates in glycosylation of alpha-dystroglycan, and may carry out synthesis of glycoprotein and glycosphingolipid sugar chains. Mutations in this gene cause MDC1D, a novel form of congenital muscular dystrophy with severe mental retardation and abnormal glycosylation of alpha-dystroglycan (*http://www.genecards.org/cgi-bin/carddisp.pl?gene=LARGE*).

CLCNKB encodes a member of the family of voltage-gated chloride channels. Chloride channels have several functions, including the regulation of cell volume, membrane potential stabilization, signal transduction and transepithelial transport. This gene is expressed predominantly in the kidney and may be important for renal salt re-absorption. Mutations in this gene are associated with autosomal recessive Bartter syndrome (a congenital kidney condition) (*http://www.genecards.org/cgi-bin/carddisp.pl?gene=CLCNKB*).

5.2.4.1 *Main findings*

The genes disrupted by HPV integration were in most cases previously documented to be associated with carcinogenesis.

5.3 Relative expression of HPV genes

Relative expression of HPV genes E2, E4, E5, E6 and E7 were assessed and normalised to stable house-keeping genes TBP2 and HRPT, which are constitutively expressed in keratinocyte cells. Expression was quantified relative to CaSki cDNA as a standard. Relative expression of HPV genes was investigated using RNA extracted from clonal cell lines at each passage during short-term culture. RNA was reverse transcribed to cDNA prior to performing qPCR and analysis, as previously described. Relative expression levels of house-keeping genes, TBP2 and HPRT, were analysed initially to ensure that expression levels were of equivalent difference for each passage of short-term culture; an example is illustrated for A09 in Figure 5.5.

Each clonal cell line exhibited unique patterns of E gene expression, as shown in Figure 5.6; examples of real-time fluorescent traces are presented in Appendix III. In all clonal cell lines, unless found to be completely absent, transcripts of E2, E6, and E7 tended to be stable over a range of successive passages in culture, however E4 and E5 expression fluctuated more frequently, particularly in D09 and Y08, and were completely absent in clonal cell line M08. E2,

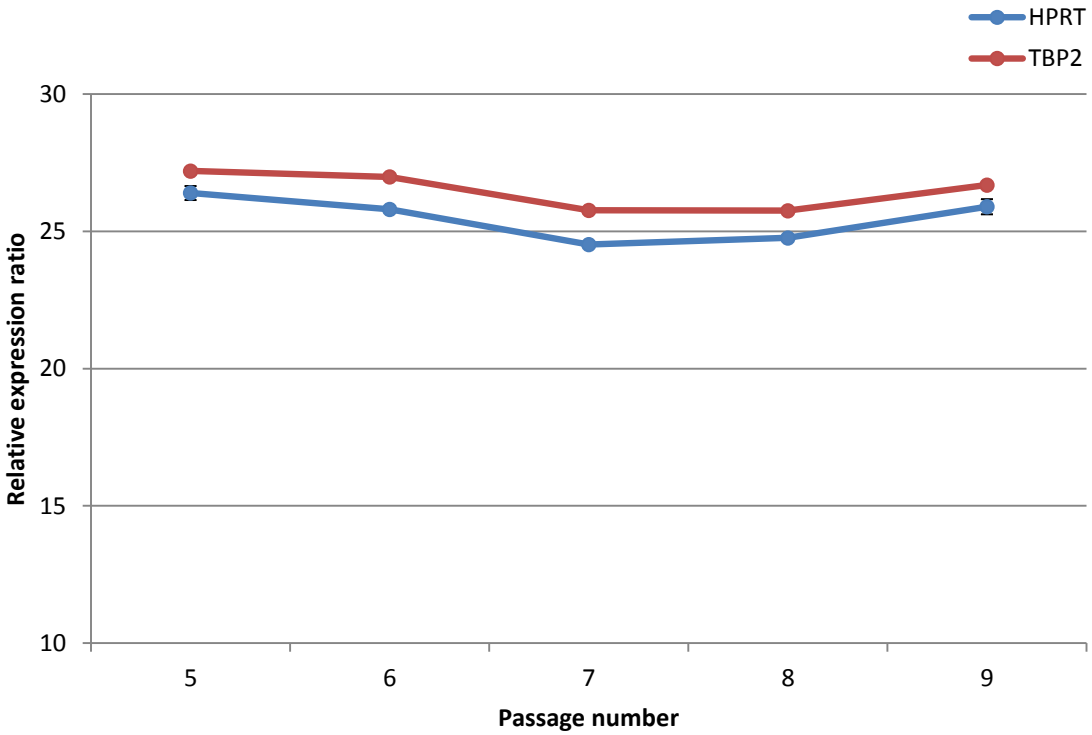

Figure 5.5. Mean relative expression ratios of house-keeping genes TBP2 and HPRT in A09

Mean relative expression of HPRT was normalised to TBP2, and vice versa, at a range of passages during short term culture. Expression was calculated relative to standards produced for CaSki cell line. Error bars signify standard deviation.

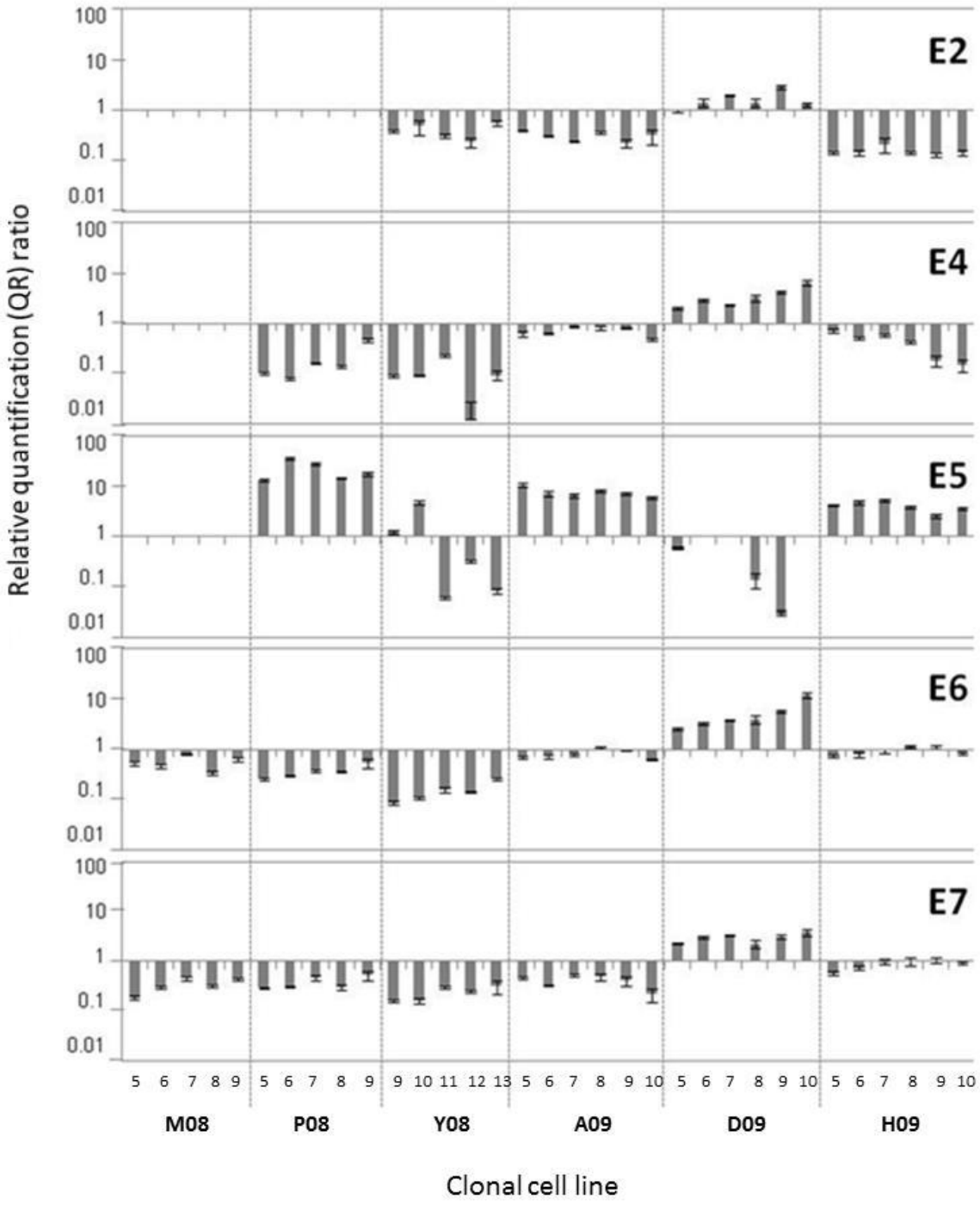

Figure 5.6. Relative expression of HPV E2, E4, E5, E6, and E7 during short-term culture of clonal cell lines

Relative expression was investigated in clonal cell lines at a range of passages: M08 (P5-9), P08 (P5-9), Y08 (P9-13), A09 (P5-10), D09 (P5-10), and H09 (P5-10). Expression is relative to CaSki; a value of 1 indicates the same level of expression detected in the CaSki cell line. No data signifies that transcripts were not detected for a particular gene. Error bars signify standard deviation.

E6, and E7 were expressed at low levels relative to CaSki in all clonal cell lines except for D09, where E2, E4, E6 and E7 were expressed at higher levels than in CaSki.

5.3.1.1 *Main findings*

The clonal cell lines exhibited diverse patterns of HPV gene expression over multiple passages in culture. This reinforces the suggestion that the clones are distinct from one another. HPV oncogenes E6 and E7 were expressed in all clonal cell lines, but E2 expression was absent in 2/6 lines (M08 and P08) and mRNA for E4 and E5 was undetectable in M08. Expression of HPV encoded genes was relatively stable in 4/6 lines but was less stable in lines Y08 and D09.

5.4 Summary of HPV integration and expression profiles

This section will bring together HPV integration status and relative gene expression patterns to create an overview for each clonal cell line.

5.4.1 Heterogeneous PC08 and PC09

PC08 cell line: E2 was found to be intact and no integration was detected. This data suggested that PC08 contained episomal HPV only, or an integrated HPV which was not detectable by APOT or DIPS.

PC09 cell line: E2 was found to be intact and genomic integration was detected. This data suggested that PC09 contained either a mixed population of episomal and integrated HPV, or contained only integrated HPV, but with an intact E2 gene. The later scenario is consistent of a break site in the L1 region identified by DIPS (Table 5.1).

5.4.2 Clonal cell lines M08, P08 and Y08

M08: E2 was found to be disrupted which was confirmed by absent expression of E2. Consistent genomic integration and integrated transcripts were also detected. This data suggested that M08 contained integrated HPV only. HPV E6 and E7 expression appeared stable during short-term culture at levels approximately half those present in the CaSki cell line. E4 and E5 expression was absent, which is consistent with the breaksite detected by DIPS at nt 1194 in the E1-E2 region upstream of E4 and E5. This data indicated that clonal cell line M08 could be used as a suitable *in vitro* experimental model for integrated HPV in vulval neoplastic disease in future CDV dosing experiments.

P08: HPV was initially believed to be episomal in this line, as integration was not suggested by DIPS or APOT analysis. This suggested that P08 could be used as a suitable *in vitro* experimental model for episomal HPV in vulval neoplastic disease in future CDV dosing experiments. However E2 PCRs later established that the E2 ORF was disrupted. Sequencing of the truncated E2 PCR product revealed a deletion of the E2 ORF from nt 2201 to 3147. This was consistent with the absence of E2 expression in qRT-PCR analyses (which were also conducted towards the end of the project). HPV E6 and E7 expression appeared stable during short-term culture at levels approximately half those observed in CaSki. E4 mRNA levels were approximately 1/10 of levels in CaSki, while E5 mRNA levels were over 10 fold higher.

Y08: E2 was found to be intact and E2 expression was detected, however consistent genomic integration and integrated transcripts were also detected. This suggested that clonal cell line Y08 contained either a full length, possibly concatenated insertion, or a mixed population of episomal and integrated HPV. HPV E6 and E7 expression appeared stable during short-term culture at levels approaching 1/10 those of CaSki. However, E4 and E5 appeared to fluctuate markedly between passages, and for this reason Y08 was not considered for use as an *in vitro* model, since it exhibited characteristics which suggested molecular instability.

5.4.3 Clonal cell line A09, D09, and H09

A09: E2 was found to be intact and E2 expression was detected. Genomic integration and integrated transcripts were not detected, however episomal transcripts were identified. This data suggested that clonal cell line A09 contained episomal HPV only. HPV E2, E6, and E7 expression appeared stable during short-term culture at levels similar to CaSki; E4 and E5 expression was also detected which is consistent with the presence of episomes. This data indicated that clonal cell line A could be used as a suitable *in vitro* experimental model for episomal HPV in vaginal neoplastic disease in future CDV dosing experiments.

D09: E2 was found to be intact and E2 expression was detected. Consistent genomic integration and integrated transcripts were also detected. This data suggested that clonal cell line D09 contained either a full length, possibly concatenated, insertion or a mixed population of episomal and integrated HPV. HPV E2 and E7 expression appeared stable during short-term culture, however expression levels were higher than observed in CaSki. Additionally E4 expression was detected which is consistent with episomal HPV. E4 and E6 levels showed a possible trend to increase with time in culture. E5 expression levels were very low or absent. Clonal cell line D was not considered for use as an *in vitro* model of mixed episomal/integrated HPV in vaginal neoplastic disease because it exhibited unstable molecular characteristics at levels comparable with CaSki (which is a cell line derived from a late metastatic tumour) and therefore considered to be a poor representation of neoplasia.

H09: E2 was found to be intact and E2 expression was detected. Genomic integration and integrated transcripts were detected although integration loci were inconsistent; interestingly at late passage an additional genomic integration and integrated transcript was detected, however the genomic and transcript loci were inconsistent. This data suggested that clonal cell line H09 contained either a full length, possibly concatenated, insertion or a mixed population of episomal and integrated HPV. HPV E6 and E7 expression appeared stable during short-term

culture at similar levels to those in CaSki. E2 expressed at approximately 1/10 of the level of CaSki. E4 and E5 were also found to be expressed which is consistent with the presence of episomes. This data indicated that clonal cell line H could be used as a suitable *in vitro* experimental model for mixed episomal/integrated HPV in vaginal neoplastic disease in future CDV dosing experiments.

5.4.3.1 *Main findings*

Stable M08, P08, A09 and H09 were selected for use as in vitro models of neoplastic disease for future CDV dosing studies, and comprised a selection of naturally occuring HPV integrated and episomal infected clonal cell lines representing vulval and vaginal neoplasia.

5.5 Discussion

The main conclusions of these investigations were:

1. Different patterns of HPV integration were identified among clonal cell lines;
    i. E2 PCRs suggested integration had occurred in M08 and possibly in P08.
    ii. DIPS identified genomic insertion of HPV in heterogeneous PC09, and clonal cell lines M08, Y08, D09 and H09.
    iii. APOT identified human:HPV fusion transcripts in M08, Y08, D09 and H09.
2. There was consensus between E2 PCR, DIPS, and APOT in all clonal cell lines except H09.
3. The majority of genes found to be disrupted through HPV integration had previous association with carcinogenesis.
4. Different patterns of HPV gene expression were identified in different clonal cell lines.

The main aim of the experiments described in this chapter was to determine whether the clonal cell lines showed different patterns of HPV integration state and gene expression. A secondary aim was to investigate the stability of these characteristics in short-term culture, over at least five passages. The isolation of clonal cell lines with different patterns of integration and gene expression meant that they could be used to model a range of naturally occurring HPV infections, and that integration state and HPV gene expression could potentially be correlated with response to drug treatment.

5.5.1 Relationships between integration and gene expression

The data also allows some observations to be made on the relationships between HPV integration and gene expression. In some cases the relationship was straight forward to interpret. For example, in M08 the absence of E2, E4 and E5 transcripts was consistent with the presence of integration disrupting the E1 gene at nt 1194 resulting in loss of transcription of downstream ORFs. Similarly in P08, DIPS identified a deletion of the E1-E2 region which included the E2 qRT-PCR amplimer, which is consistent with detection of E4 and E5 transcripts but absence of E2. However the data for other lines was more ambiguous; for Y08, full length E2 was amplifiable and E2, E4 and E5 were transcribed, however integration in E1 was also consistently detected by both DIPS and APOT. This data was suggestive of the presence of episomes or concatenated full length insertion of HPV, or a mixed infection with both episomes and integrants. There are examples of all of these possibilities in other cell lines; the CaSki cell line contains integrated full length concatenated HPV (Meissner, 1999) while the W12 cell line can contain episomal or integrated HPV, or a mixture of both (Pett et al., 2006).

There is a widely accepted model of cervical carcinogenesis in which E2 loss, attributable to viral integration, leads to upregulation of the E6 and E7 oncogenes (Pett and Coleman, 2007). It was notable therefore that an inverse relationship was not observed between E2 and E6/E7 expression in cultured cells. In fact the highest levels of E2 mRNA were in clonal line D09,

which also showed the highest levels of E6 and E7 expression. This suggests that in cultured cells this relationship does not hold true. Likewise there was no obvious correlation between HPV integration and gene expression; the A09 line was the only line showing no evidence of viral integration, and E6/E7 mRNA levels were similar to the other clonal lines. This may suggest that E6/E7 has been upregulated by other means in the A09 line, although it should be noted that the relationship between integration and HPV gene expression has been challenged in at least one publication (Hafner et al., 2008)

5.5.2 HPV integration during culture

Since integration analyses were not performed on early passage heterogeneous PC08 and PC09, it is not clear whether these integration events already existed in the heterogeneous populations and were selected out of it, or whether integrants were induced through the cell culture process. The data are possibly more consistent with the presence of the integrated clones in the parental heterogeneous population and selection during the dilution cloning step. This is because the integrated transcripts were detected in the very earliest passages and confirmed again at latest passage. The identification of new integration events in later passage cultures, as seen in H09 where a new integration event at 1p36.13 was identified in at P11, demonstrates that integration during the culture process is possible. The additional integration event in H09 at P11 was detected by both DIPS and APOT however the loci were inconsistent as previously described. Flanking primers were designed to span the HPV-human fused transcript detected in H09 at P11 only, and applied to cDNA from H09 at P5 and P11. The integrated transcript was detectable at P11 only.

Intact E2 was also detected at early and late passage of H09, suggesting the presence of episomal HPV. Since H09 appears to have acquired an integration event which was confirmed in late passage only, integration of HPV may have occurred during short term culture which suggests that culturing cells might have induced episomal HPV to integrate in to the host DNA.

5.5.3 Gene disruption and link to carcinogenesis

The genes disrupted via HPV integration were researched to identify previous literature which might suggest a role in promoting or enabling cell proliferation, providing cells with a selective growth advantage and possibly resulting in cell immortalization. Several of the genes disrupted had some reported association with cancer, but this was often when overexpressed rather than disrupted.

5.5.4 Non-random integration events

According to DIPS and APOT assays, HPV integration disrupted *LEPREL1* (specifically at 3q28.7) in clonal cell line M08. Over the past few decades studies have shown that HPV integration occurs within regions of fragile sites (FS) and in cluster formations at chromosome loci which might reflect chromosomal regions that are generally unstable (Wentzensen et al., 2004). Schmitz and colleagues provided further support for a clustering of HPV integration sites in chromosomal 'hot spot' regions, of which 3q28 *LEPREL1* was described (Schmitz et al., 2012). Thus, detection of integration also at *LEPREL1* in M08 might contribute to supporting the theory of non-random integration of HPV within FS that is described in the literature.

5.5.5 Order of assays and integration status of P08

It is important to note that the assays were not performed in the same order in which the data is presented. APOT and DIPS were performed early in the project, and E2 PCRs were developed and applied towards the end of the project. Similarly, the E2 specific qRT-PCR assays were not developed and applied until the latter phases of the project. This was because a published E2 primer set was initially used (Roberts et al., 2008), however it was later noted that this primer set was located within the region of the E2 ORF that overlapped with the E4 ORF, and this primer set actually amplified cDNA corresponding to both E2 and E4. A second primer set was hence designed corresponding to the upstream region of the E2 ORF; this primer set is specific

to the E2 sequence only and is referred to in this thesis as “E2” while the original E2/E4 primer set is referred to as “E4”.

This is highly relevant to the integration state of P08 as data from the assays performed first (DIPS and APOT) both suggested that HPV was episomal in this clone, i.e. no evidence for integration was found. Therefore for the majority of this project, P08 was thought to contain episomal HPV. When the E2 PCRs were performed it became apparent that P08 contained a truncated E2 gene with a 1077bp deletion from nt 2070 to 3147 (illustrated previously in Figure 5.1). This region covers the upstream region of the E2 gene including the E2 specific qRT-PCR amplimer. This finding was consistent with the qRT-PCR data derived using the newer primer sets which showed complete absence of E2 in P08 but detectable E4 (at 1/10 the levels detectable in CaSki).

These findings changed the assessment of the integration state of HPV in P08. E2 is a multifunctional protein (McBride, 2013). It is the main transcriptional regulator for many papillomaviruses (Phelps and Howley, 1987) but also has other essential functions in the viral life cycle. E2 initiates replication by loading the E1 helicase on to the viral origin of replication (Sanders and Stenlund, 2000, Mohr et al., 1990), and is also involved in genome partitioning by joining viral genomes to host chromosomes (Bastien and McBride, 2000, Ilves et al., 1999, Lehman and Botchan, 1998, Skiadopoulos and McBride, 1998). E2 is also almost certainly required for productive viral DNA replication (McBride, 2013). It therefore seems very unlikely that the truncated E2 present in P08 would be consistent with stable replication and maintenance of episomal HPV. This question could be resolved by Southern blotting extracted DNA and probing with full length HPV sequences as described by Alazawi and colleagues (Alazawi et al., 2002). Unfortunately time constraints prevented this experiment from being undertaken but would be informative future work.

5.5.6 Strengths and Weaknesses

The data illustrate several of the strengths and weaknesses of the assays employed, which can be summarised as follows:

The E2 PCR assay is quick and relatively simple to perform and uses only a small quantity of DNA (Collins et al., 2009). However it can only conclusively show integration when the integration event results in disruption of the E2 sequence and no full length E2 is present, either as a full length insertion or as episomes.

The APOT assay is useful to identify transcriptionally active integration events (Klaes et al., 1999), but it is complex, labour intensive and expensive. It also doesn't identify transcriptionally silent integrants or integration events that occur too far from a relevant restriction site, i.e. the assay depends on there being a restriction site within a PCR amplifiable range of the integration site. APOT will identify integrated HPV, but detection of integrants does not rule out the presence of episomal HPV (i.e. a mixed population of integrated and episomal HPV).

The DIPS assay is useful to identify the exact sites of chromosomal integration and can identify transcriptionally silent integration events (Luft et al., 2001). It shares several of the limitations of APOT; it is relatively complex and labour intensive, will not identify integration sites that are too distant from restriction sites used in the initial digestions, and identification of integrated HPV does not exclude the presence of episomal HPV.

Nevertheless a combination of these molecular based assays (E2 PCR, APOT and DIPS) are sensitive and have been reported in the literature to determine HPV integration status.

5.5.7 Discrepencies between APOT and DIPS

APOT and DIPS failed to detect the same integration loci in clonal cell line H09, with several possible explanations.

Multiple integration loci might exist within cells, and therefore DIPS or APOT might detect the most frequently occurring (or dominant) integration event. It is therefore plausible that a 'dominant' genomic integrant detected via DIPS is not transcriptionally active and therefore not detectable via APOT. Similarly, the 'dominant' integrated transcript detectable via APOT may not have been a 'dominant' genomic integrant and therefore not detectable via DIPS. However in H09, 2 integration loci were detectable in the same sample which does not support this theory unless both integrants were equally dominant.

There are limitations associated with both assays, as previously discussed. Both assays depend on there being a restriction endonuclease site within a PCR amplifiable range of the integration site for it to be detected. It could be that one integrant but not the other was detectable in each assay.

6 Optimisation of cidofovir (CDV) dosing protocol

6.1 Results

A selection of clonal cell lines were characterised previously. Of these, clonal cell lines M08 and P08 (vulval), that represented integrated and episomal states of HPV infection with stable E6 and E7 expression, were used to optimise the CDV dosing protocol. A series of optimisation experiments were carried out, which will be described in this chapter, with the primary objective of establishing a final CDV dosing protocol. The final CDV protocol was used to assess cellular and molecular response to CDV treatment using several clonal cell lines as experimental models of vulval and vaginal neoplastic disease, which will be described in chapter 7.

Initially, optimisation experiments were performed using cells cultured in 96 well plates, which required fewer cells, smaller volumes of reagents, and was a less labour and resource intensive method of obtaining replica data sets. Experiments were then translated to 6 cm diameter TC dishes, which would ultimately be used, in order to generate a sufficient quantity of cells for downstream analyses.

Previous studies have evaluated the effects of CDV in HPV positive cell lines through dosing cells with 10 µM CDV (Amine et al., 2009). Thus cell viability was assessed in M08 and P08 cell culture models using a range of CDV concentrations surrounding this value. The fraction of cells that survived CDV treatment was also determined, and the concentration of CDV causing inhibition of 50% of the cell population (or inhibitory concentration = IC_{50}) was also calculated. The confluence of cell cultures seeded at a variety of cell densities was also assessed over a period of 4 days. The seeding density was optimised so that cultures would establish during the first 24 hours but would not exceed >80% by the final day of the experiment; this ensured that cells were proliferating for the entirety of the dosing protocol.

6.1.1 Aims and objectives

The central aim was to design and optimise a dosing protocol through establishing suitable CDV dosing parameters.

The following objectives structured this section of work:

1. Investigate whether seeding cell density affects response to CDV treatment.
2. Investigate whether 10 µM CDV dose will result in reduced growth, ideally approximating IC_{50}.
3. Explore the potential for scaling-up culture vessels from 96 well plates to 6cm TC dishes.

6.1.2 Study sample

Clonal cell lines M08 and P08 at P8 were cultured for optimisation studies. Cultures were not supplemented with irradiated 3T3 feeders in order to maintain a homogeneous cell population to accurately assess dose response, which was previously justified in chapter 4.

6.2 Optimisation in 96 well plate format

6.2.1 Cell density did not affect the toxicity of CDV

A 7 day (168 hour) dosing regime was set up in 96 well plates. The aim of this initial dosing regime was to analyse dose response using a range of seeding cell densities (5,000, 7,000 and 10,000 cells/well) combined with a range of CDV concentrations (1, 10, and 100 µM). Cultures were treated with CDV at 24 hours (day 1) and 96 hours (day 4). Response to CDV was assessed at 96 hours (day 4) and 168 hours (day 7) by performing trypan blue viable cell counts.

Error! Reference source not found. Figure 6.1 illustrates M08 viable cell counts on days 0, 4 and 7 of the dosing protocol. Viability cell counts were mostly inversely proportional to CDV concentration at all seeding cell densities. This suggested that, within the range examined, response to CDV was not dependent on the number of cells being dosed.

The surviving fractions on day 7 were plotted against CDV concentration in Figure 6.2, and data was linearised by Log transformation; the IC_{50} was then calculated from the resulting linear regression equations using the formula in Equation 6.1 (where is Y = 0.5, M is slope, and C is constant).

The surviving fraction was around 0.5 using 10 µM CDV for all seeding cell densities (Table 6.1). The IC_{50} was more variable, falling at approximately 10 µM at seeding densities of 5,000 and 10,000 cells/well; however the IC_{50} was four fold higher for cell cultures seeded at 7,000 cells/well.

6.2.1.1 *Main findings*

Within the range investigated, surviving fraction after treatment with CDV was affected by seeding cell density. IC_{50} for CDV was close to 10 µM on the final day for cultures seeded at 5,000 and 10,000 cells, except for cultures seeded with 7,000 cells/well.

6.3 Optimisation in 6 cm diameter TC dish format

6.3.1 Seeding cell density affected time taken to reach confluence

Preliminary dosing studies were also performed in 6 cm diameter TC dish format. The advantage of culturing cells in a larger vessel, were the generation of greater quantities of cells which would be useful for down-stream analyses in later experiments to assess molecular

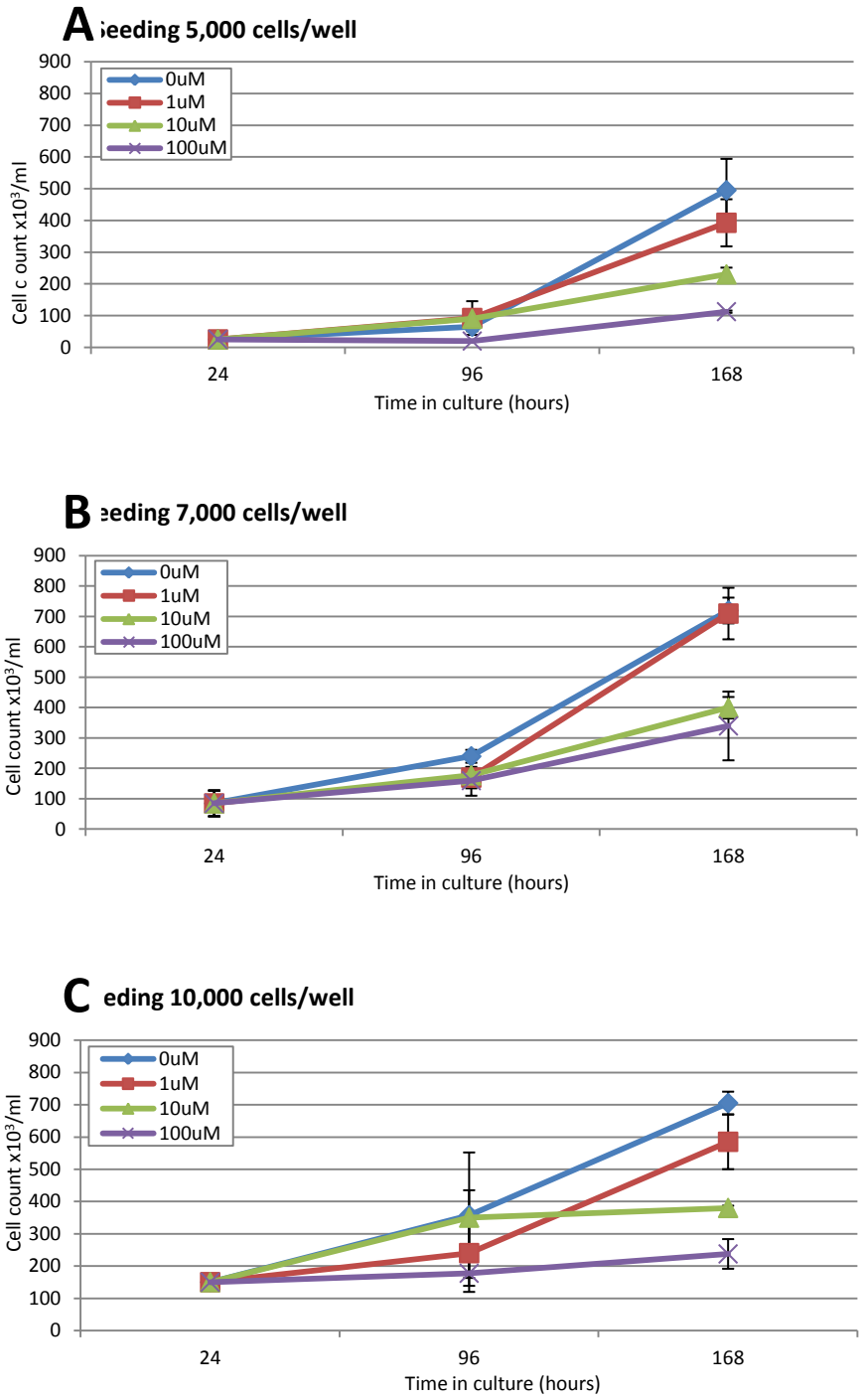

Figure 6.1. Viable cell counts of clonal cell line M08 with CDV

M08 cultures were prepared by seeding a 96 well plate with (**A**) 5,000 cells/well, (**B**) 7,000 cells/well, (**C**) 10,000 cells/well and carrying out x2 CDV doses of 0, 1, 10 and 100 µM CDV at 24 hours and 96 hours of a 168 hour regime. Response to CDV was assessed by viable counts performed at 96 hours and 168 hours. The embedded key shows [CDV]. Error bars signify standard deviation.

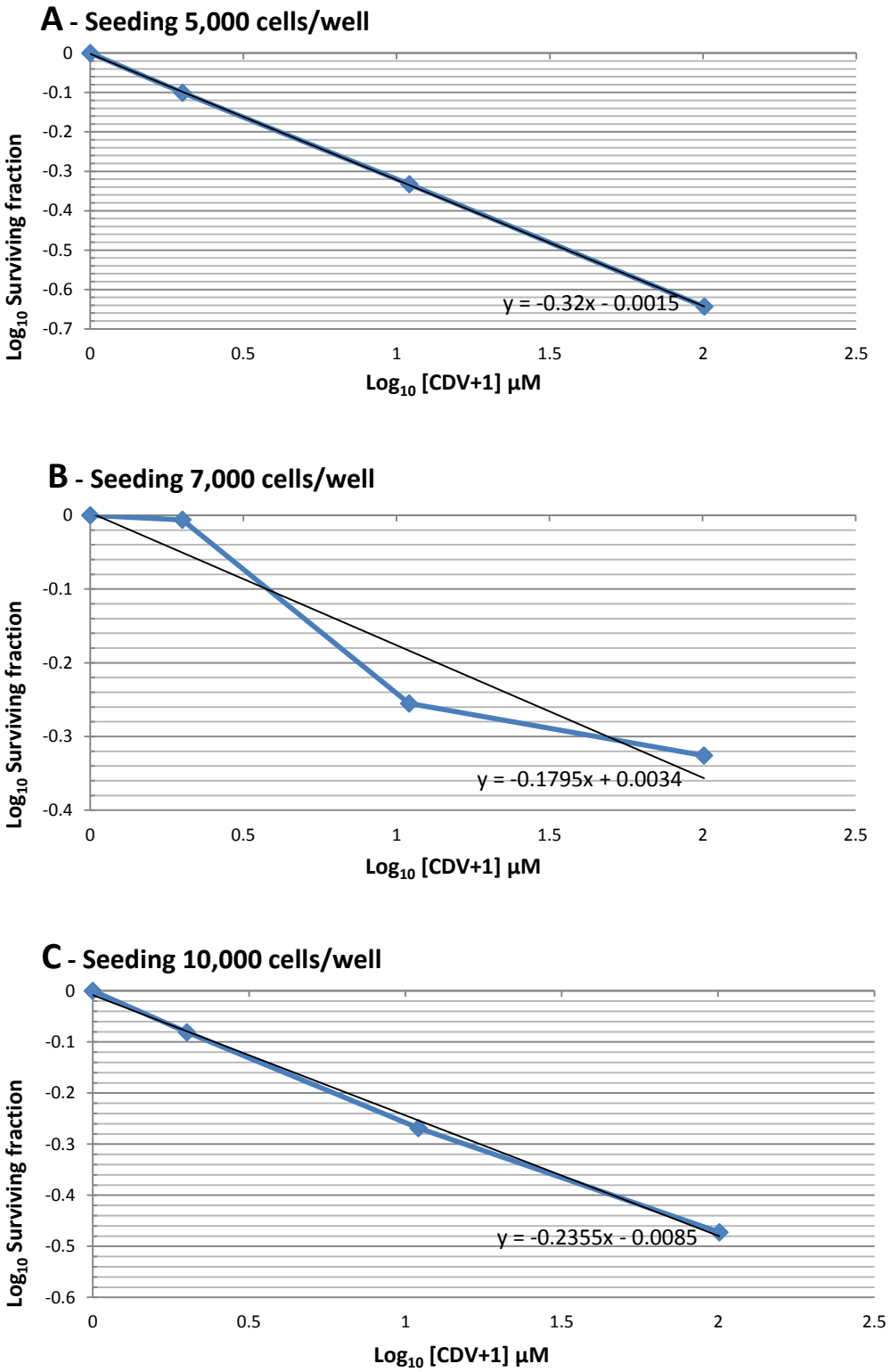

Figure 6.2. Surviving fraction vs. [CDV] at 168 hrs (day 7) for clonal cell line M08

Correlation of Log transformed cell surviving fraction and CDV concentration in M08 cultures seeded at (**A**) 5,000 cells/well, (**B**) 7,000 cells/well, and (**C**) 10,000 cells/well. Linear regression equations have been included in the format of $Y = M.X + C$.

$$X = \left(10^{\frac{log_{10}(Y)-C}{M}}\right) - 1$$

Equation 6.1. The formula used to derive IC_{50} values from linear regression equations.

Cells seeded (cells/well)	Surviving fraction at 10 µM	IC_{50} (µM)
5,000	0.46	7.63
7,000	0.56	44.51
10,000	0.54	16.46

Table 6.1. Surviving fraction of M08 cells at 10 µM and IC_{50} of CDV at 168 hours (day 7) at varying seeding densities

Response(s) to CDV. The aim of this experiment was to determine optimal seeding cell density for cultures in a 6 cm TC dish, so that cultures would establish within the first 24 hours but not exceed >80% confluence before the end of the experiment.

The seeding densities required for a 6 cm TC were guided by scaling from the relative surface area of 1 well of a 96 well plate, to a 6 cm plate. M08 was used to seed 6 cm TC dishes in triplicate at $1x10^5$, $5x10^5$, and $1x10^6$, and maintained in culture for 96 hours. Cultures were viewed microscopically 24 hours (day 1) after cell establishment and at the end of the experiment at 96 hours (day 4), to assess keratinocyte/colony morphology and percentage confluence.

Dishes seeded at $1x10^5$ established poorly during the first 24 hours and 'craters/gaps' were observed in the monolayer and cells were present in media suspension; cultures reached 40% confluence after 4 days. Plates seeded at $5x10^5$ established after 24 hours and reached ~80% confluence after 4 days without any unusual observations within the cell monolayer. Dishes seeded at $1x10^6$ established after 24 hours, however by day 4 cell cultures were already 100% confluent.

6.3.1.1 *Main findings*

The experimental format was scaled up to 6 cm TC dishes and a seeding density of $5x10^5$ in 6 cm TC dishes was selected for the final CDV dosing protocol. Cells established well after 24 hours and reached the required percentage confluence of ~80% in the desired time-frame (4 days).

6.4 Preliminary CDV dosing protocol

Based on the previous optimisation studies, a preliminary CDV dosing protocol was devised lasting 72 hours and consisting of cultures seeded at $5x10^5$ in 6 cm TC dishes, as described and illustrated previously in Figure 2.8. A time period of 72 hrs rather than 96 hours was selected to avoid any chance of cells reaching confluence. A single 10 µM CDV dose was given 24 hours after seeding. Trypan blue viable cell counts and cell morphology were assessed 24 and 48 hours after dosing. The preliminary protocol was performed to ensure that response to CDV could be detected under similar conditions intended for use in the final CDV dosing protocol.

6.4.1 Response to CDV: cell viability

Viable cell counts of M08 and P08 decreased slightly 24 hours after seeding, as shown in Figure 6.3. In both M08 and P08, viable cell counts were lower in the CDV dosed arm compared to the no dose control. At 24 hrs post treatment in M08, cell numbers were reduced by approximately two thirds in the CDV treated plates, while for P08 they were reduced by approximately half. There was a statistically significant difference 24 hours after treatement for M08 and P08 (M08 and P08: $p = >0.0001$ at $p < 0.05$ using 2-tailed t-test). After 48 hours of CDV treatment, viable cell counts increased in M08 but continued to decrease in P08; for both lines at this time point, there was a statistical significance between treated and untreated samples (M08 and P08: $p = >0.0001$ at $p < 0.05$ using 2-tailed t-test). There were some notable differences between the cell lines; especially that despite the same number of cells being used for the initial inoculum, higher cell counts were recorded in M08 at 72 hours in both the treated and untreated samples.

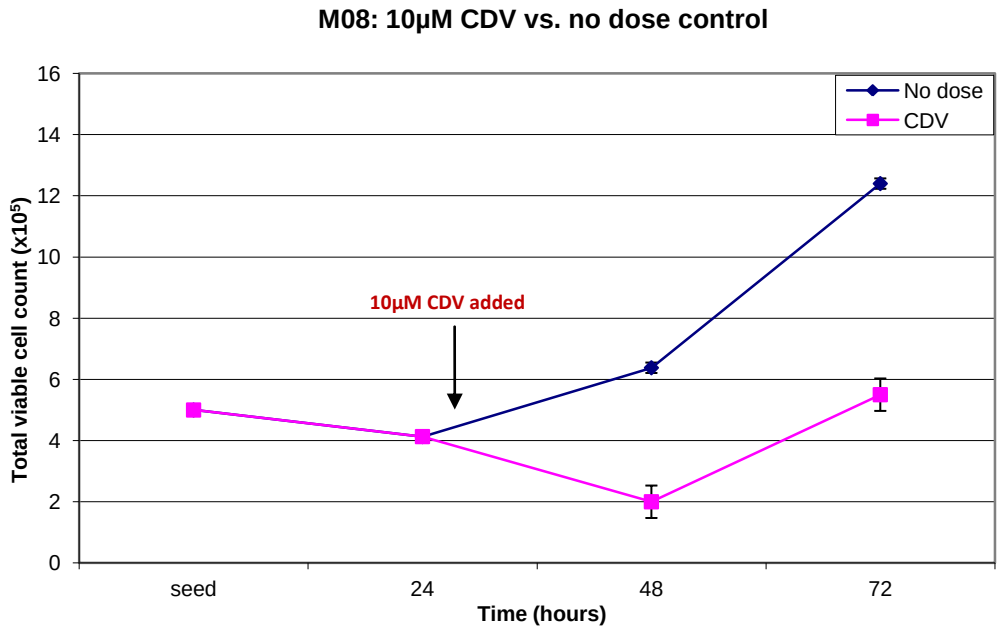

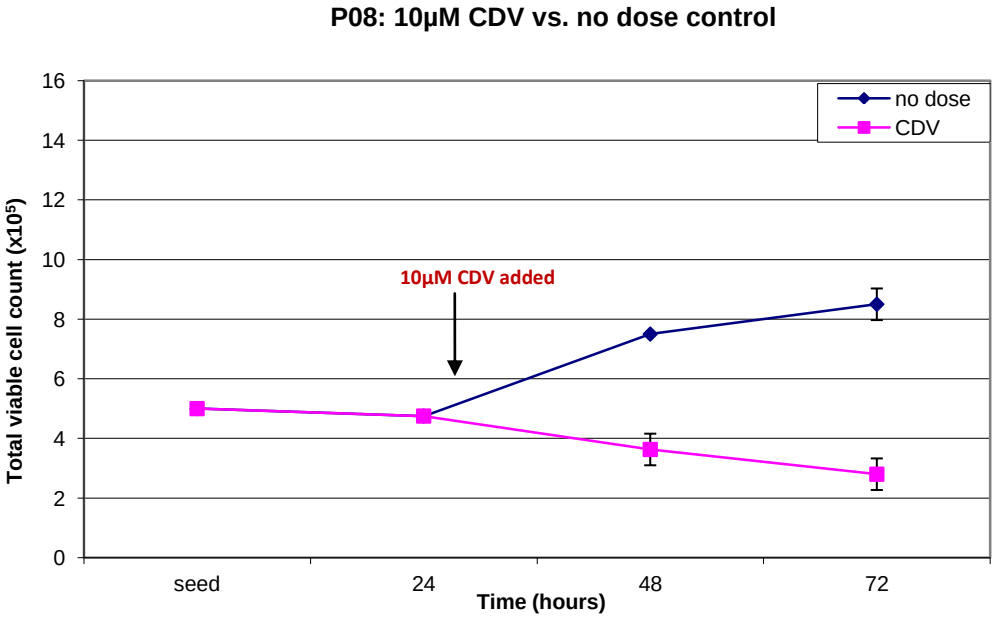

Figure 6.3. Cell viability counts of M08 and P08 during preliminary CDV dosing protocol.

M08 and P08 were seeded at $5x10^5$ in 6 cm TC dishes in duplicate. Cultures were treated with 10 µM CDV 24 hours after seeding (as indicated in figure). An initial viable cell count was performed 24 hours after seeding. Viable cell counts were also performed 24 and 48 hours after cultures were treated with and without CDV. Error bars signify standard deviation. A statistically significant difference was found 24 and 48 hours after CDV treatment in M08 and P08 (M08 and P08, 24 hrs: $p = > 0.0001$., 48 hrs: $p = > 0.0001$ (at $p < 0.05$ (2-tailed t-test)).

6.4.1.1 *Main findings*

A response to CDV treatment was identified by reduced viable cell counts at 24 and 48 hours after treatment in both cell lines, which were shown to be statistically significant. At both time points CDV treatment appeared to reduce viablilty by approximately 50-70%.

6.4.2 Response to CDV: cell morphology

Cell cultures of M08 and P08 were viewed microscopically 24 hours after being treated with and without CDV (Figure 6.4 and Figure 6.5). Keratinocytes of M08 appeared enlarged at 24 and 48 hours post CDV dose when compared to no dose controls. Keratinocytes of P08 appeared enlarged and resembled 'fried egg' morphology within the monolayer at 24 and 48 hours after CDV treatment which was not observed in no dose control cultures. 'Craters' were also visible in the cell monolayer 48 hours after CDV treatment in P08.

6.4.2.1 *Main findings*

Keratinocyte morphology of M08 and P08 was obviously different in response to CDV treatment when compared to no dose controls. Keratinocytes became enlarged, more noticeably 48 hours after CDV treatment in both cell lines.

6.5 Discussion

The main conclusions of these experiments were that:

1. Within the range investigated, seeding density did affect response to CDV.
2. 10 µM was an appropriate dose, as it approximated an IC_{50} dose at 7 days (i.e. it produced a quantifiable response).
3. The experiments were scaled up to higher volumes, and appropriate seeding densities were determined.

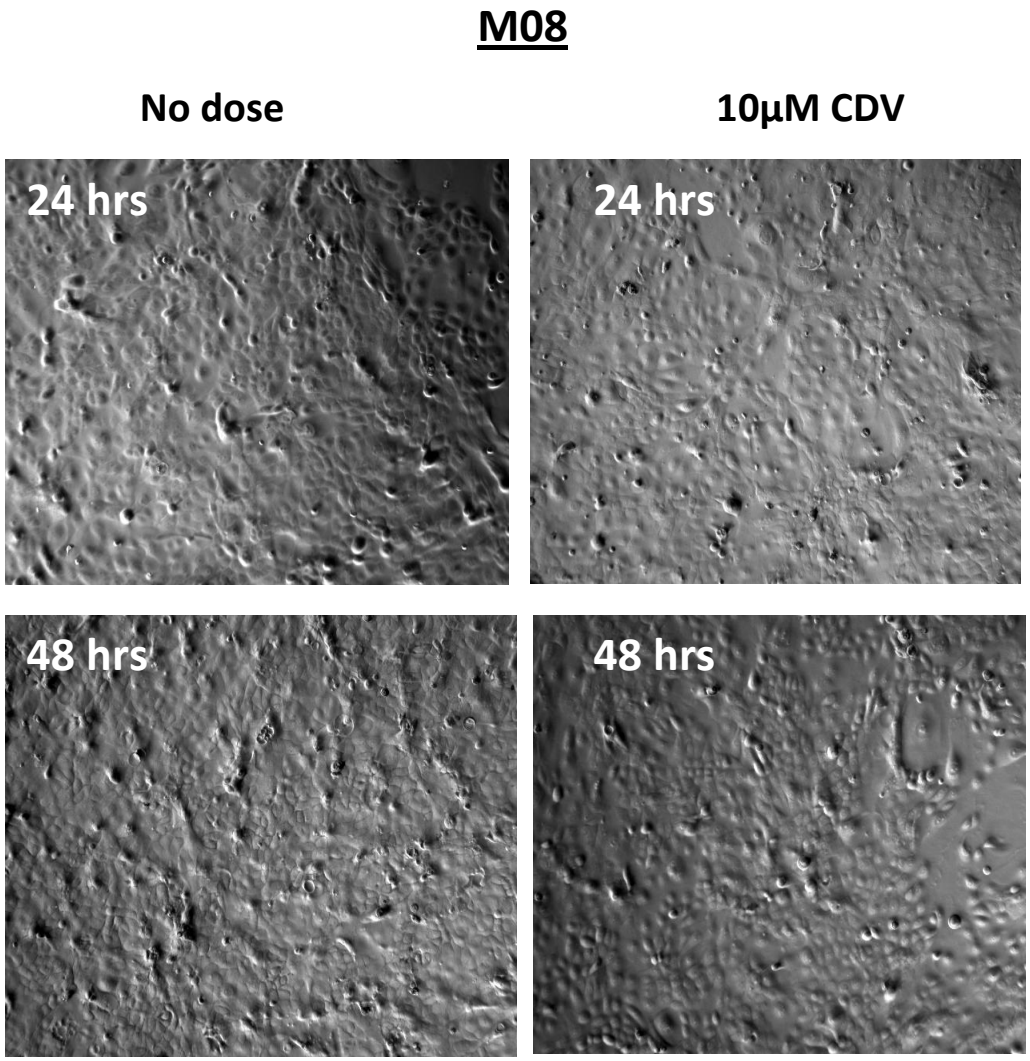

Figure 6.4. Morphology of M08 during preliminary CDV dosing protocol

Cultures of M08 were visualised at 50x total magnification 24 and 48 hours after being dosed with and without CDV.

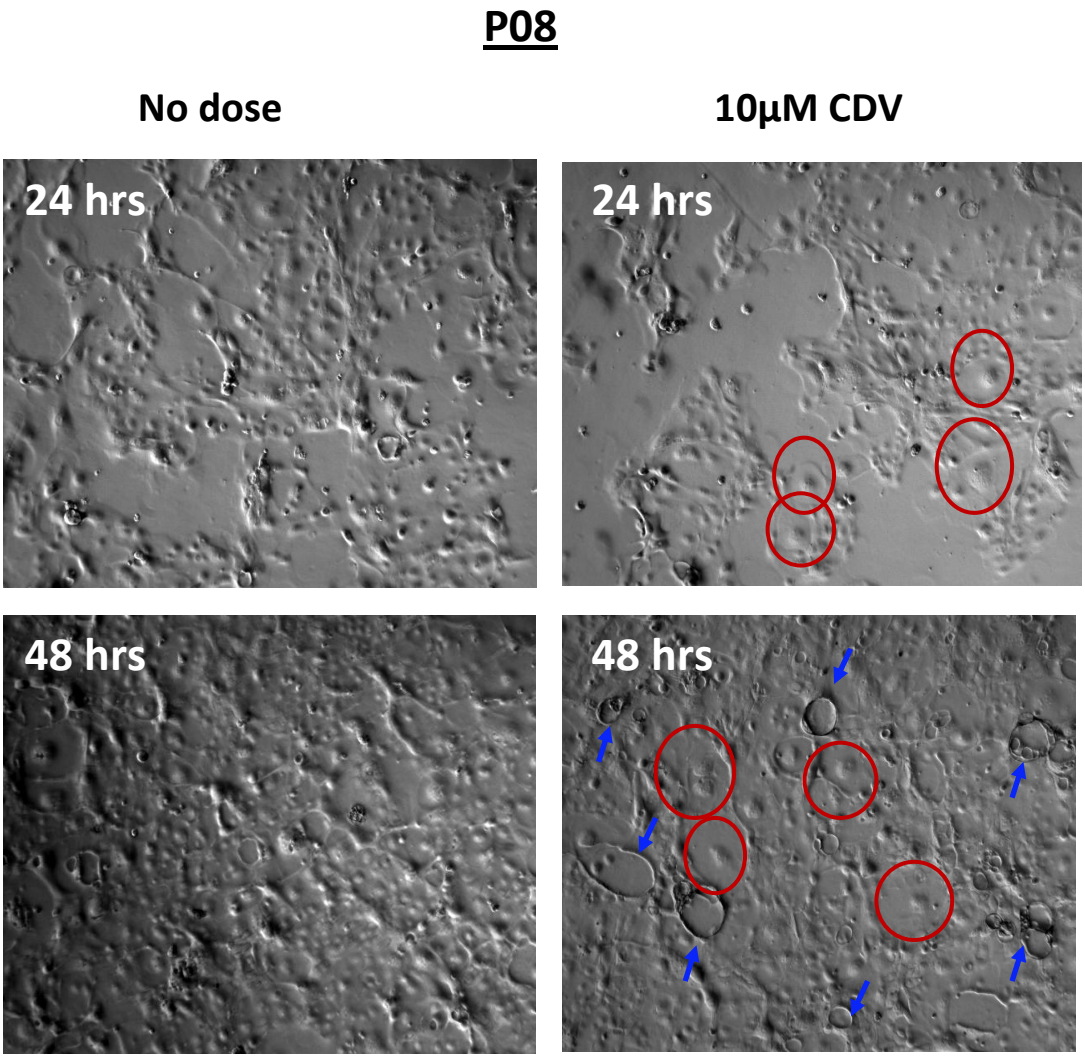

Figure 6.5. Morphology of P08 during preliminary CDV dosing protocol.

Cultures of P08 were visualised at 50x total magnification 24 and 48 hours after being dosed with and without CDV. Red circles highlight enlarged cells which resembled 'fried egg' morphology, and blue arrows point to 'craters' observed in the monolayer which might represent areas where keratinocytes have detached from the monolayer.

4. In 6 cm TC dishes 10 µM CDV reduced viable cell counts by 50-70% at 24 and 48 hrs.

These experiments provided useful information to develop variables constituting the final CDV dosing protocol in this experimental cell culture system.

The IC_{50} doses calculated from the experiments conducted in 96 well plates were consistent for the wells seeded with 5000 and 10000 cells (7.63 and 16.46 µM) but a higher value was obtained for the wells seeded with 7000 cells. From Figure 6.2B, it seems that a slightly different dose response relationship was seen compared to the Figure 6.2A and C, with less effect at lower concentration and more effect at higher concentrations. Given that values closer to 10 µM were found in the other two experiments, it seems likely that this higher IC_{50} may be anomalous.

The results of the initial experiments conducted in 6 cm plates suggested that it was possible to scale the experiments up to larger volumes. This was required to produce sufficient material (nucleic acids) for downstream analysis in the final protocol. These experiments also demonstrated the importance of optimising seeding density, because at lower densities cells displayed altered morphology while cultures at higher densities reached confluence within the experimental timeframe (which was undesirable as it would impose an artificial limit on proliferation and could alter gene expression patterns). These studies also determined the optimal seeding density to be used in the final study. A density of $5x10^5$ cells in 6 cm TC dishes was selected since it provided sufficient cell numbers for successful establishment and growth, without becoming over-confluent by the final day of the dosing experiment (earlier preliminary cell culture studies (chapter 4) had demonstrated that cells seeded at too low a cell density exhibited cell density-dependant growth inhibition identified by detachment of cells from the monolayer during the first 24 hours of culture and poor growth thereafter).

The time period for this study was reduced from 168 hours in the initial experiments, to 96 hours and then further to 72 hours. This was considered necessary to avoid any chance of cells reaching confluence. It also accounted for the desired experiments to follow (to investigate molecular effects of CDV) which would have a shorter time course. For example, for transcriptional responses to be detected cultures would be assessed 12-24 hours after dosing. Additionally, a relatively high seeding cell density would be required to provide sufficient cellular material, which would be inconsistent with longer time courses. The shorter time course also allowed treatment with a single dose of CDV rather than multiple doses.

The first attempt at dosing M08 and P08 in 6 cm TC plates showed that 10 µM CDV was effective in reducing viable cell count. There were some differences in the data obtained with 96 well plates and 6 cm plates; these related mainly to the time taken to achieve a quantifiable effect. In 96 well plates (Figure 6.3) it did not appear that 50% inhibition was achieved within 24-48 hours post dosing, whereas this effect was evident in the larger plates (Figure 6.3).

The data shown in Figure 6.3 also confirmed earlier indications that M08 was the more vigorously growing of the two clonal cell lines examined. This is perhaps consistent with the subjective impression from Figure 6.4 that the morphology of P08 is more variable and that CDV dosing appeared to have a more visible effect in this line.

6.5.1 Strengths and weaknesses

The strengths of these experiments were that growth conditions were optimised to direct the development of a dosing protocol, without haphazard investigation. The optimisation and dosing experiments performed were conducted in two cell lines in a variety of formats with largely consistent results. The weaknesses include the small number and coverage of CDV concentrations in optimisation, and in hindsight the range of concentrations could have been spread more evenly around the 10µM concentration.

More detailed growth curves, again with a greater range of concentrations, would have allowed more exact IC_{50} calculations to be performed. However for the purpose of determining an appropriate concentration to investigate CDV mechanism of action, these experiments were adequate.

7 Response to CDV in clonal cell lines

7.1 Results

A series of cell culture and CDV optimisation studies were previously performed to develop a final dosing protocol, which will be described in this chapter. A selection of clonal cell lines, which comprised integrated and episomal versions of HPV with neoplastic vulval and vaginal origin, underwent the dosing protocol. Response to CDV treatment was investigated to give insight in to the molecular mechanism(s) of action of CDV in these clonal cell lines, which might be indicative of response to CDV observed in clinical disease.

Our current understanding is limited as only a few studies have specifically investigated the mechanism of action of CDV in HPV related anogenital disease. CDV has previously been shown to be specific to cells containing HPV when normal neonatal foreskin keratinocytes were compared to non-tumourigenic d-2C HPV16-transformed keratinocytyes (Johnson and Gangemi, 1999). CDV has been found to reduce E6 and E7 transcription although this effect was modest (50% reduction in E6/E7 transcripts at 3 days post treatment with 10µg/ml CDV) and based on experiments performed using semi-quantitative RT-PCR in the HEP2 cell line which was derived from an HPV18 positive head and neck squamous cell carcinoma (Abdulkarim et al., 2002). The authors demonstrated nuclear accumulation of p53 after CDV treatment and suggested that reduced E6/E7 expression revived tumour suppressor pathways that regulate the cell cycle resulting in G2/M blockage and accumulation of HPV positive cells in S phase. There was no increase in apoptotic cell death and the absence of apoptosis in response to 10µg/ml CDV was confirmed by TUNEL assay. A more recent study examined the effect of CDV treatment on E6 protein levels using western blots and suggested that following 6 days of treatment with an unspecified dose of CDV E6 levels were reduced (although the

degree of reduction was not quantified) (Amine et al., 2009). The same authors also suggested that treatment with CDV did result in apoptosis in HPV positive cells.

These studies have used immortalised cell lines as investigational models of HPV related disease. HPV infected immortalised cell lines such as CaSki (Pattillo et al., 1977), SiHa (Friedl et al., 1970) and HeLa (Gey et al., 1952, Jones et al., 1971), originate from metastatic tumours and have accumulated a selection of mutations and rearranged genomic structures (Meissner, 1999) contributing to a cell phenotype which proliferates uncontrollably and poorly represents disease seen clinically. In contrast, this project focused on the action of CDV in the treatment of neoplastic disease using the relatively early passage HPV16 positive VIN3/VaIN3 clonal cell lines. These lines resemble precancerous neoplasia better than alternative immortal models as they were derived from neoplastic biopsies and are used at early passages.

The primary objective of this chapter was to determine whether the action of CDV currently described in the literature, was reproducible in clonal cell culture models. Other attributes of the clonal cell lines that might affect response to CDV treatment were also considered (i.e. anatomical origin of cell lines (vulval or vaginal) and HPV integration status (episomal or integrated)). An initial assessment of cell death, without distinguishing between cell apoptosis or necrosis, was performed through manual trypan blue viable cell counts and microscopic analysis of cell morphology. To specifically investigate induction of apoptosis as a mechanism of cell death, cell populations were assessed for apoptosis markers using fluorescence-activated cell sorting (FACS) and annexin V/7-Aminoactinomycin D (7-AAD) staining, and the percentage of cells engaged in early and late apoptosis assayed by flow cytometry. Apoptosis data was not generated through flow cytometry due to the adherent nature of keratinocytes that caused problems for flow cytometry machinery which was currently in use for haemopoetic (non adherent) cells (kindly provided by Haematology department, University Hospital of Wales); repetitions were carried out but the problem persisted and an alternative

option was not performed due to the project timeframe. Relative expression of HPV oncogenes E6 and E7 was investigated using qRT-PCR.

The results were assessed to determine whether there were differences in response between cells from the two different anatomical sites (vulva vs. vagina) and to investigate whether HPV integration status (episomal or integrated) might affect response to CDV. Whole transcriptome sequencing via RNA-Seq of CDV treated and untreated cell lines was also performed. This allowed differential gene expression to be determined using the complete set of gene transcripts within a cell, thereby eliminating the selectivity of analysing specific gene transcripts; transcriptome sequencing is described in chapter 8.

7.1.1 Aims and objectives

The central aim was to determine whether the action of CDV currently described in the literature was reproducible in the clonal cell culture models, thereby giving insight in to the molecular mechanism(s) of action of CDV in neoplastic disease.

The following objectives structured this section of work:

1. Investigate whether CDV treatment will result in fewer viable cells.
2. Investigate whether a more marked effect will be seen in HPV16 infected clonal cell lines compared to HPV negative HEKn cell line.
3. Investigate whether fewer viable cells may be a result of cellular apoptosis.
4. Investigate whether HPV oncogene expression will decrease in response to CDV treatment.
5. Explore whether there is a difference in dose response between vulval and vaginal clonal cell lines, and cell lines containing integrated and episomal HPV.

7.1.2 Study sample

Clonal cell lines derived from VaIN 3; A09 (HPV16 episomal) and H09 (HPV16 integrated), and clonal cell lines derived from VIN3; M08 (HPV16 integrated) and P08 (HPV16 status unconcluded (chapter 5) were prepared for the CDV dosing study at P11 in both experiments. Neonatal human epidermal keratinocytes (HEKn) at P3 were also prepared for the CDV dosing study, representing a HPV negative primary keratinocyte cell line. Clonal cell cultures were not supplemented with irradiated 3T3 feeders to maintain a homogenous cell population for accurate assessment of dose response, as justified in chapter 4.

7.2 The final CDV dosing protocol

The final CDV dosing protocol was carried out as previously described and illustrated in Figure 2.9 and described in chapter 6. To summarise, the protocol was carried out in 6 cm TC dishes seeded with $5x10^5$ cells (in duplicate). The protocol lasted 2.5 days (60 hours) and consisted of 1 CDV dose using 10 µM CDV which was given 24 hours after seeding. Response to CDV was assessed in treated cultures and in no dose controls 12 and 36 hours after dosing.

Cells underwent down-stream analyses (experiment 1 and 2), as summarised in the flow-chart (Figure 7.1). In experiment 1, cell cultures were viewed microscopically to assess changes in cell morphology, trypsinised and trypan blue viable cell counts taken (in triplicate) to give an indication of cell death (without distinguishing between cell apoptosis or necrosis). FACS and cytometric assay was then performed to investigate the percentage of cells undergoing apoptosis. In experiment 2, cell cultures were also viewed microscopically at each time point. Cells were rinsed with PBS and lysed directly from the cell monolayer using RLT buffer and beta-mercaptoethanol (βME) (without trypsinisation), and DNA and RNA extraction performed simultaneously. RNA was used to assess HPV E6 and E7 oncogene expression via qRT-PCR. RNA was also used to perform SOLiD™ RNA sequencing, which will be described in chapter 8.

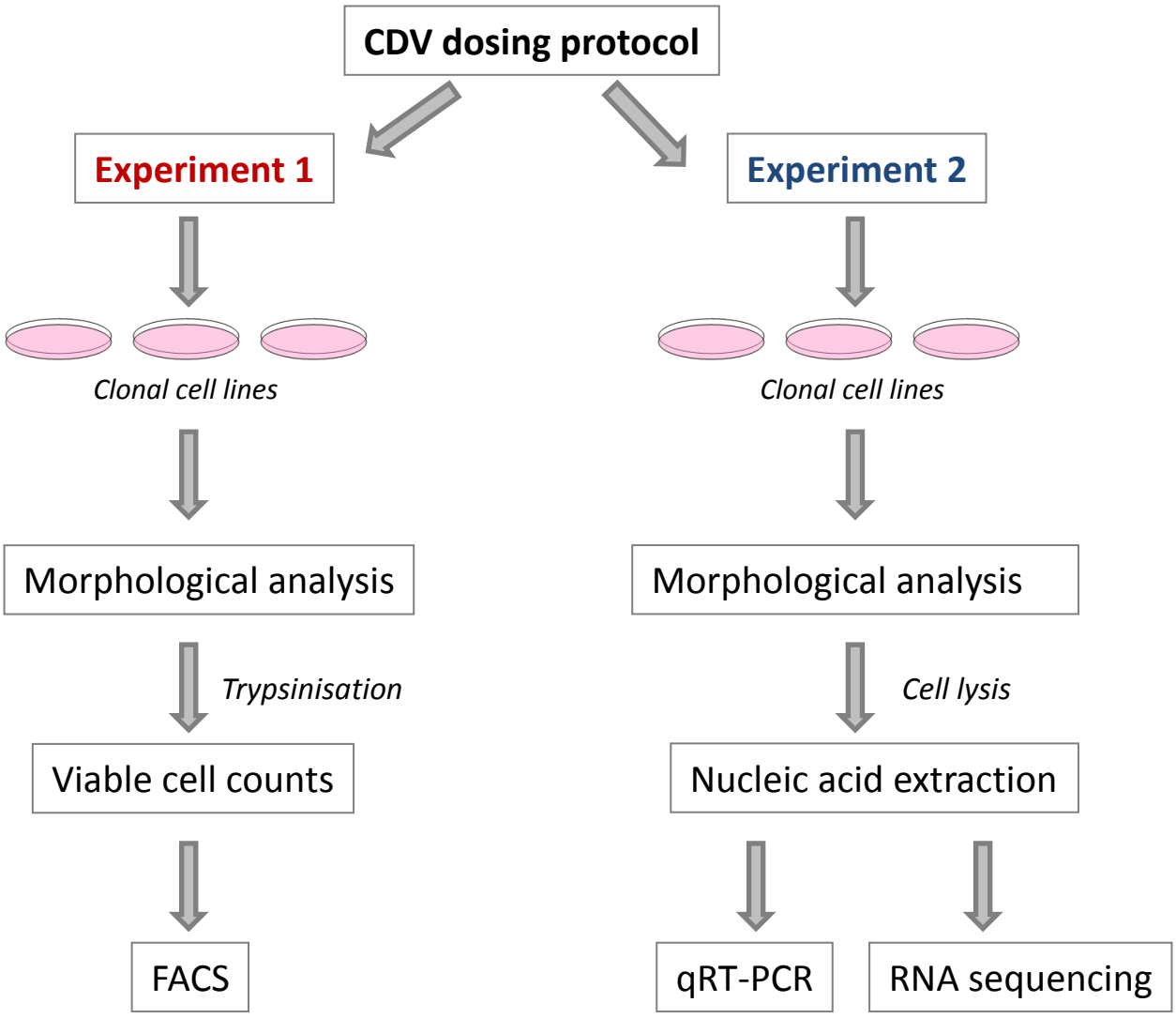

Figure 7.1. Overview of down-stream analyses performed using cells after CDV dosing

Following the CDV dosing protocol, down-stream analyses (experiment 1 and 2) were performed using clonal cell lines M08, P08, A09 and H09 at P11. Cell cultures were analysed microscopically to assess keratinocyte morphology, viable cell counts were performed, and fluorescence-activated cell sorting (FACS) were performed to investigate apoptosis (experiment 1). Duplicate cell cultures were also analysed microscopically to assess cell morphology, and lysed for nucleic acid extraction. RNA extracts were quantified and used to investigate relative expression of HPV oncogenes (E6 and E7) using qRT-PCR, and also underwent RNA-sequencing.

7.3 Response to CDV

Response to CDV treatment was assessed through trypan blue viable cell counts, morphological analysis of keratinocytes, and investigating relative expression of HPV oncogenes (E6 and E7) as previously described.

7.3.1 CDV reduces the number of viable cells

At all time points during two independent repeats of the CDV dosing protocol, treated and untreated cells were rinsed with PBS and trypsinised to obtain single cell suspensions, and trypan blue viable cell counts performed using a haemocytometer; triplicate viable cell counts were performed and combined.

A reduction in mean viable cell count was seen in response to CDV treatment in all clonal cell lines and in HEKs. The surviving fraction of cells 12 and 36 hours after 10μM CDV treatment for clonal cell lines and HEKs are illustrated in Figure 7.1. Twelve hours after being treated with CDV, 50% and 59% of cells remained viable in vulval lines M08 and P08 respectively, 85% and 89% in vaginal lines A09 and H09 respectively, and 60% in HEKs. Thirty six hours after being treated with CDV, the number of viable cells remained relatively stable in M08 (2% decrease), but increased by 9% in P08. In vaginal lines A09 and H09, the number of viable cells had decreased by 13%. The number of viable cells remained relatively stable in HEKs (2% decrease). After 12 hours of treatment, there was a significant difference between surviving fraction of vulval cell lines (M08 and P08) and vaginal cell lines (A09 and H09) ($p = 0.0194$ at $p < 0.05$ (2-tailed t-test)). There was no significant difference between surviving fraction of vulval and vaginal lines 36 hours after treatment ($p = 0.2514$). After 12 hours of treatment, surviving fractions of vulval lines with HEK lines were not found to be significantly different ($p = 0.3061$), and vaginal lines with HEK lines were found to be significantly different ($p = 0.0061$), at $p < 0.05$. After 36 hours of treatment, vulval lines and HEKs were not found to be significantly

different (p = 0.7493), and vaginal lines with HEKs were found to be significantly different (p = 0.0332).

Viable counts at all time points of the dosing study, for untreated cells, were used to create growth curves for clonal cell lines and HEKs (Figure Figure 7.2). From this, the growth of M08 and H09 appeared to be more rapid than A09 and P08, followed by HEKs. Viability counts 24 hours after seeding were also much lower than the initial seeding cell density (= $5x10^5$ cells) in A09 and P08.

7.3.1.1 *Main findings*

A reduction in viable count was seen in response to CDV in all cell lines. Surviving fractions 12 hours post CDV treatment showed a more considerable response to 10µM CDV in vulval clonal lines (M08 and P08) than vaginal lines (A09 and H09), which was statistically significant, suggesting that vaginal lines are less sensitive to the effects of CDV treatment. After an additional 24 hours in CDV, the surviving fraction of cells for M08 remained relatively stable, but increased in P08, and decreased the same percentage in A09 and H09. The difference in survival fraction of A09 and H09 suggested that these vaginal lines were more sensitive to CDV 24 hours after treatment than vulval lines. In terms of comparison with HEK (HPV negative), after 12 hours of treatment, survival fractions of vulval and HEk lines were not significantly different, but vaginal and HEK lines were; this was reflected at 36 hours also. This suggested that HPV negative HEK lines were also sensitivie to CDV treatment, with a response that was more comparable with the vulval lines.

Cell line	Surviving fraction		Difference
	12 hrs	36 hrs	
M08	0.51 (51%)	0.49 (49%)	-0.02 (-2%)
P08	0.59 (59%)	0.68 (68%)	0.09 (9%)
A09	0.85 (85%)	0.72 (72%)	-0.13 (-13%)
H09	0.89 (89%)	0.76 (76%)	-0.13 (-13%)
HEKs	0.6 (60%)	0.62 (62%)	0.02 (2%)

Table 7.1. Survival fractions at 12 and 36 hours after treatment with CDV.

Mean viable cell counts of P3 HEKs, P 11 vulval cell lines (M08 and P08), and P11 vaginal cell lines (A09 and H09), were used to calculate the surviving fraction of cells at 12 and 36 hours post treatment. The surviving fractions illustrated are calculated from the mean viable counts (in triplicate) from 2 separate CDV dosing experiments. Surviving fractions of vulval cell lines and vaginal cell lines were significantly different 12 hours after treatment at $p < 0.05$ (2-tailed t-test ($p=0.0194$)), and were not significantly different 36 hours after treatment ($p=0.2514$). After 12 hours of treatment, surviving fractions of vulval and vaginal lines in comparison to HEK lines were not found to be significantly different and not significantly different, respectively (vulval: $p = 0.3061$., vaginal: $p = 0.0061$). After 36 hours of treatment, vulval and vaginal lines with HEKs were not found to be significantly different and found to be significantly different, respectively (vulval: $p = 0.7493$., vaginal: $p = 0.0332$).

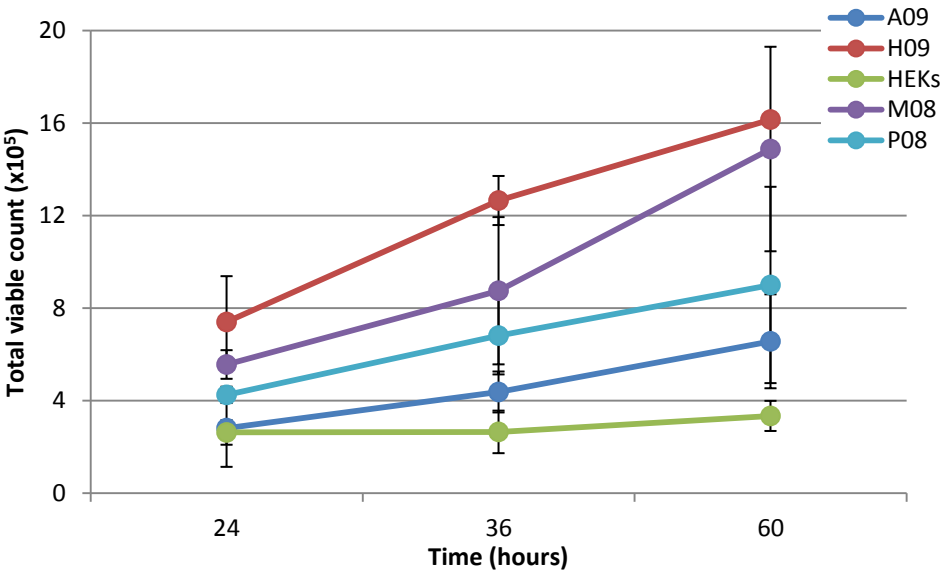

Figure 7.2. Viability cell counts at each time point of the CDV dosing protocol

Mean viable cell counts of untreated P3 HEKs and P11 clonal cell lines M08, P08, A09, and H09, at 24, 36, and 60 hours; data was calculated from triplicate cell counts of 2 separate CDV dosing experiments. Error bars signify standard deviation.

7.3.2 CDV affects keratinocyte morphology

HEKs and clonal lines were examined microscopically to assess keratinocyte morphology in two independent repeats of the CDV dosing protocol. Keratinocyte morphology of M08 (Figure 7.3, Figure 7.4), P08 (Figure 7.5, Figure 7.6), A09 (Figure 7.7, Figure 7.8), H09 (Figure 7.9Figure 7.10), and HEKS (Figure 7.11, Figure 7.12), at 12 and 36 hours after CDV treatment (and no dose control) are shown. Figure 7.13, taken from (Li et al., 2012), is included to illustrate the morphological appearance of apoptosing keratinocytes. Treatment with CDV had a distinct effect on keratinocyte morphology, with larger cytoplasmic compartments, and more rounded keratinocytes lacking tessellation pattern in the monolayer; this effect was not evident for HEKS (Figure 7.11, Figure 7.12). For vulval cell line M08, the effect was evident at 12 hours post treatment and was increased at 36 hours (Figure 7.3, Figure 7.4). These effects were less visible in the P08 cells, with an increased effect observed 12 hours after treatment which reverted to relatively smaller (but still enlarged) cells after 36 hours (Figure 7.5, Figure 7.6). In the vaginal A09 keratinocytes, a less distinct effect on keratinocyte morphologically was observed at 12 hours but more so 36 hours (Figure 7.7, Figure 7.8). The same trends were more visible in H09 where large polymorphic keraintocytes were observed 12 hours after CDV treatment and more considerably 36 hours after treatment (Figure 7.9, Figure 7.10).

7.3.2.1 *Main findings*

CDV appeared to distinctly affect keratinocyte morphology of clonal cell lines but a distinct effect was not observed in HEKs. Morphological changes did not appear to be consistent with apoptosis. Changes in morphology became more considerable with increasing time after CDV treatment in M08 and H09. In P08, substantial changes to keratinocyte morphology were observed 12 hours after treatment that appeared to revert after 36 hours. In A09, morphological changes in response to CDV treatment were mostly apparent 36 hours after treatment.

. **M08**

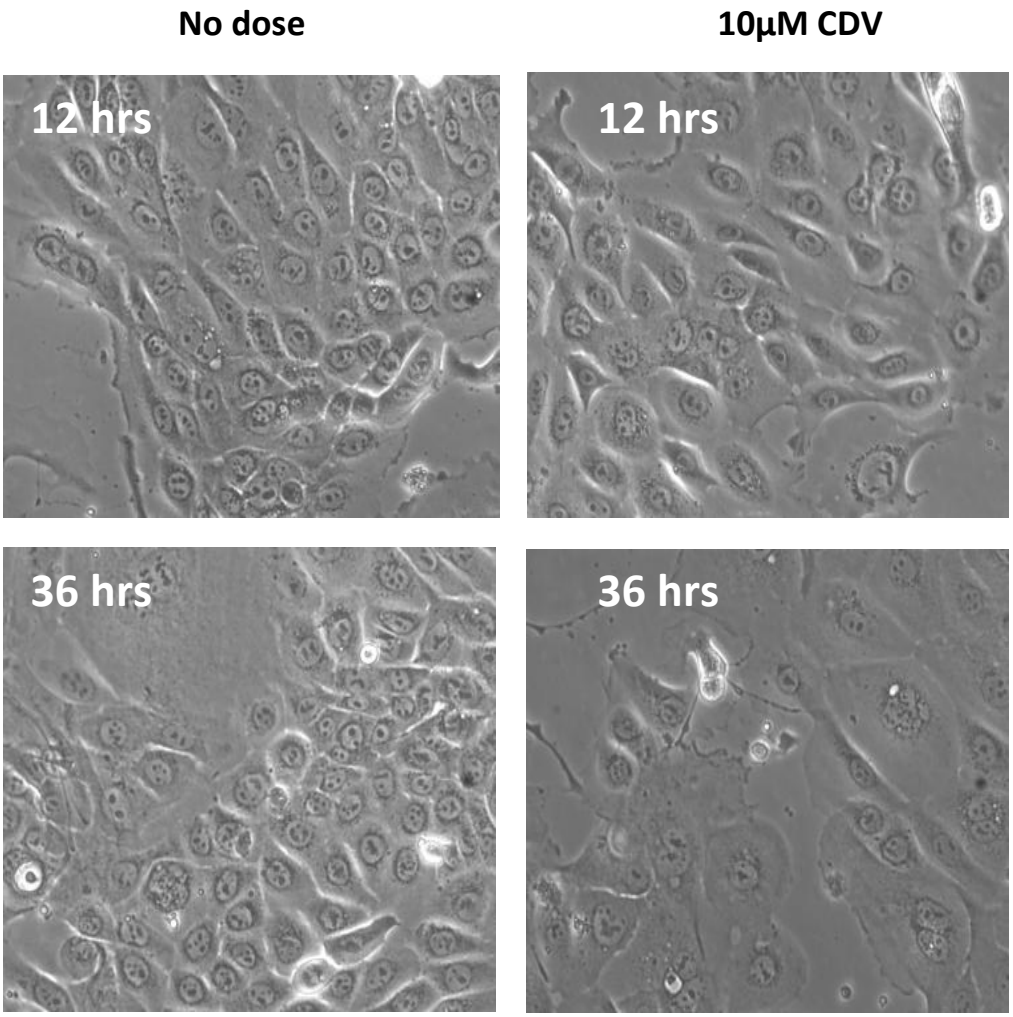

Figure 7.3. Morphology of M08 during CDV dosing protocol (experiment 1)

Cultures of M08 at P11 were visualised at 320x total magnification under light microscopy and a snap shot taken 12 and 36 hours after being dosed with and without CDV in CDV dosing protocol experiment 1.

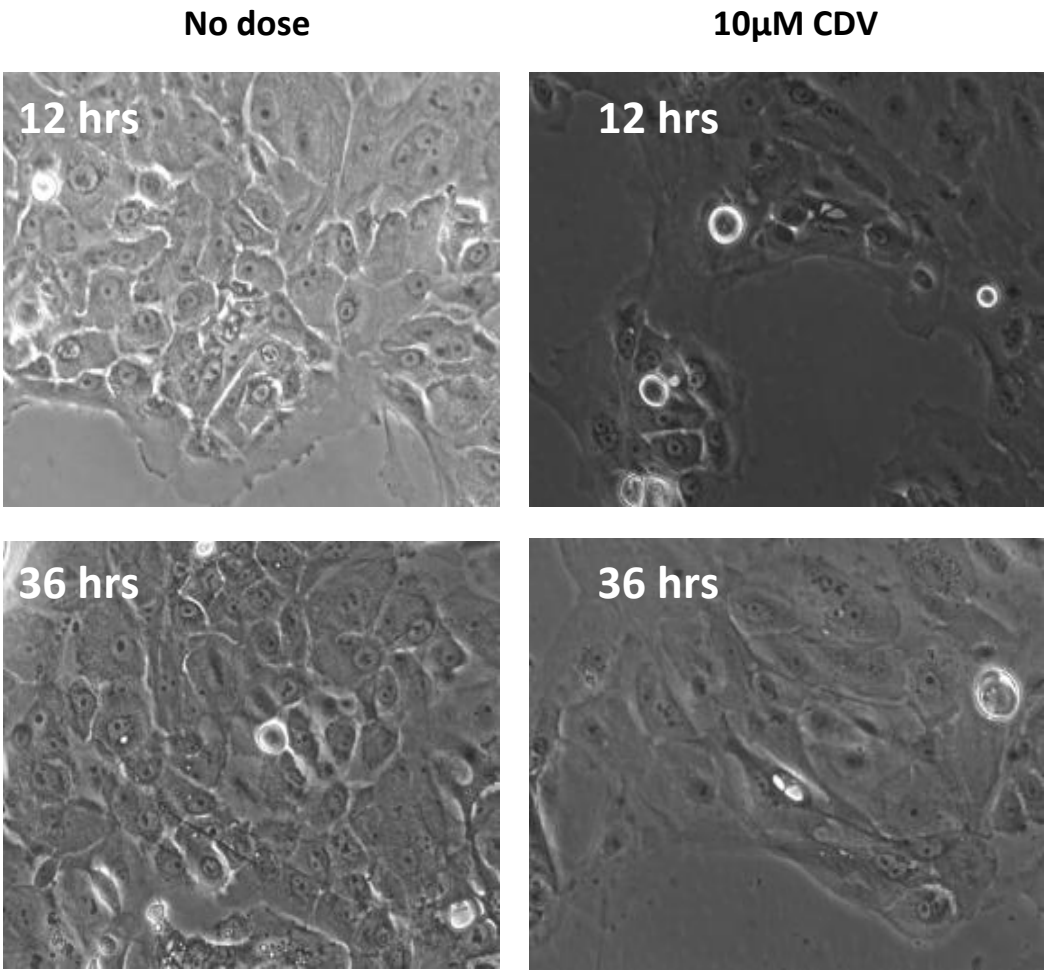

Figure 7.4. Morphology of M08 during CDV dosing protocol (experiment 2)

Cultures of M08 at P11 were visualised at 320x total magnification under light microscopy and a snap shot taken 12 and 36 hours after being dosed with and without CDV in CDV dosing protocol experiment 2.

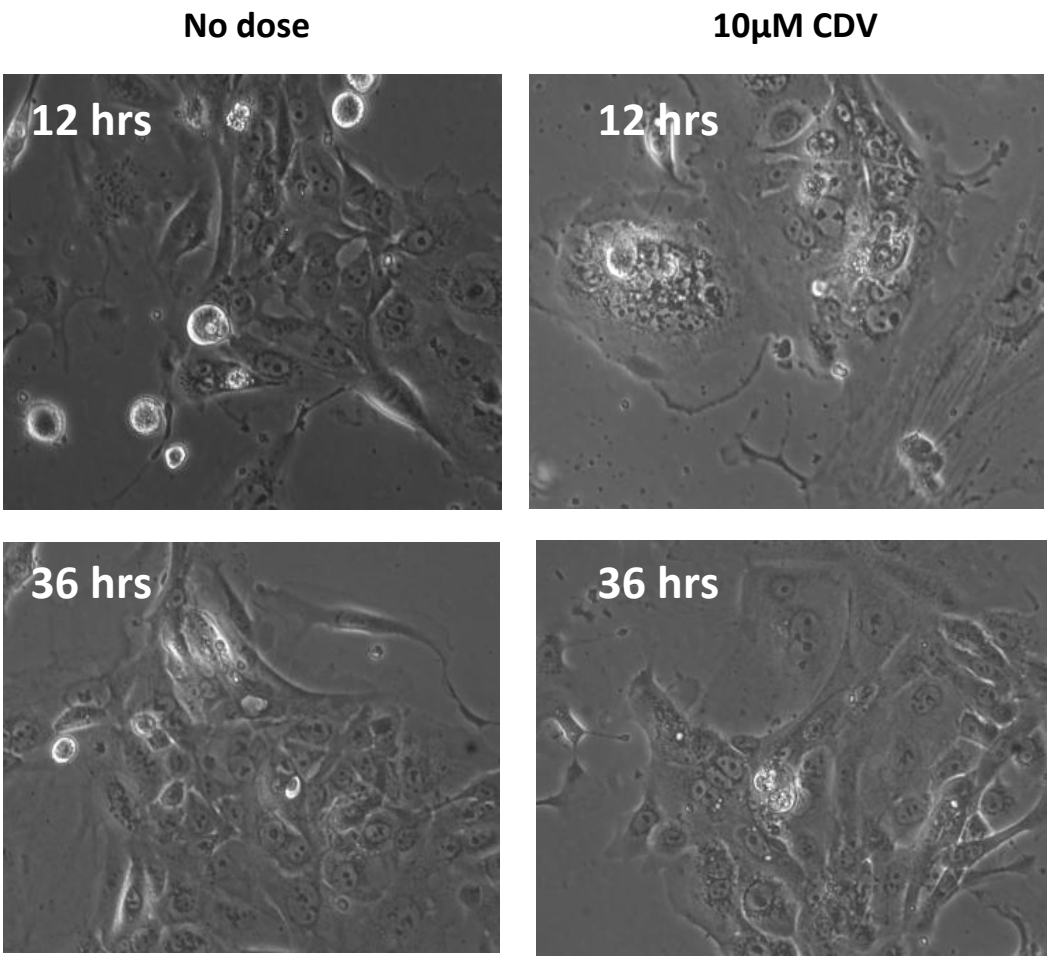

Figure 7.5. Morphology of P08 during CDV dosing protocol (experiment 1)

Cultures of P08 at P11 were visualised at 320x total magnification under light microscopy and a snap shot taken 12 and 36 hours after being dosed with and without CDV in CDV dosing protocol experiment 1.

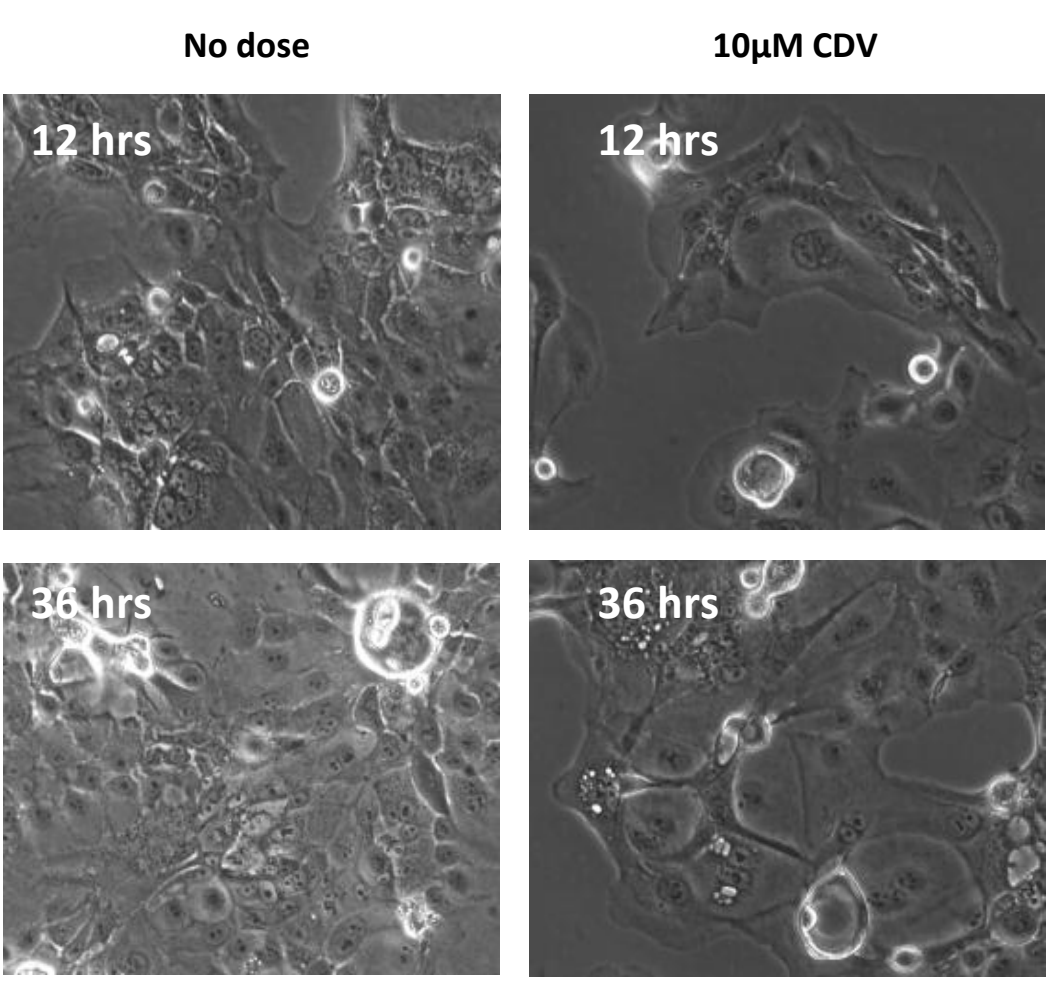

Figure 7.6. Morphology of P08 during CDV dosing protocol (experiment 2)

Cultures of P08 at P11 were visualised at 320x total magnification under light microscopy and a snap shot taken 12 and 36 hours after being dosed with and without CDV in CDV dosing protocol experiment 2.

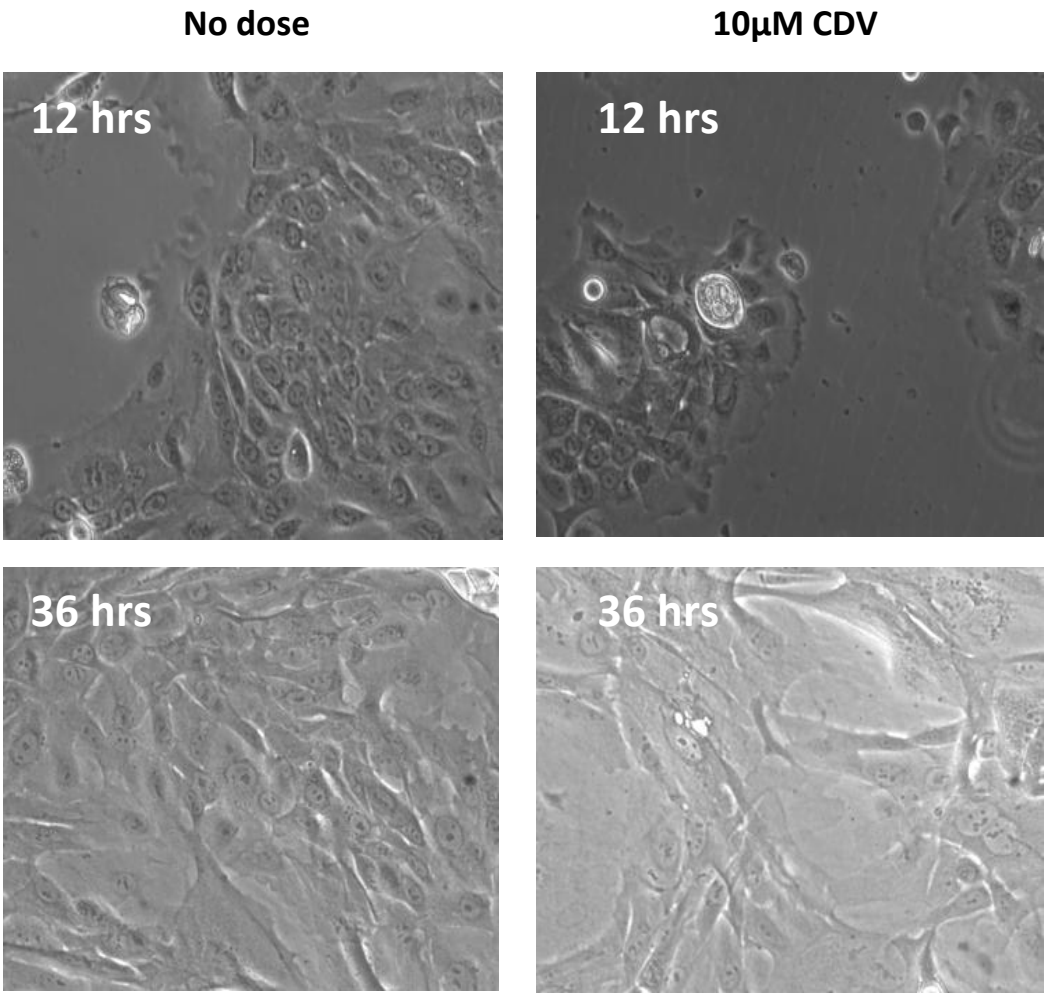

Figure 7.7. Morphology of A09 during CDV dosing protocol (experiment 1)

Cultures of A09 at P11 were visualised at 320x total magnification under light microscopy and a snap shot taken 12 and 36 hours after being dosed with and without CDV in CDV dosing protocol experiment 1.

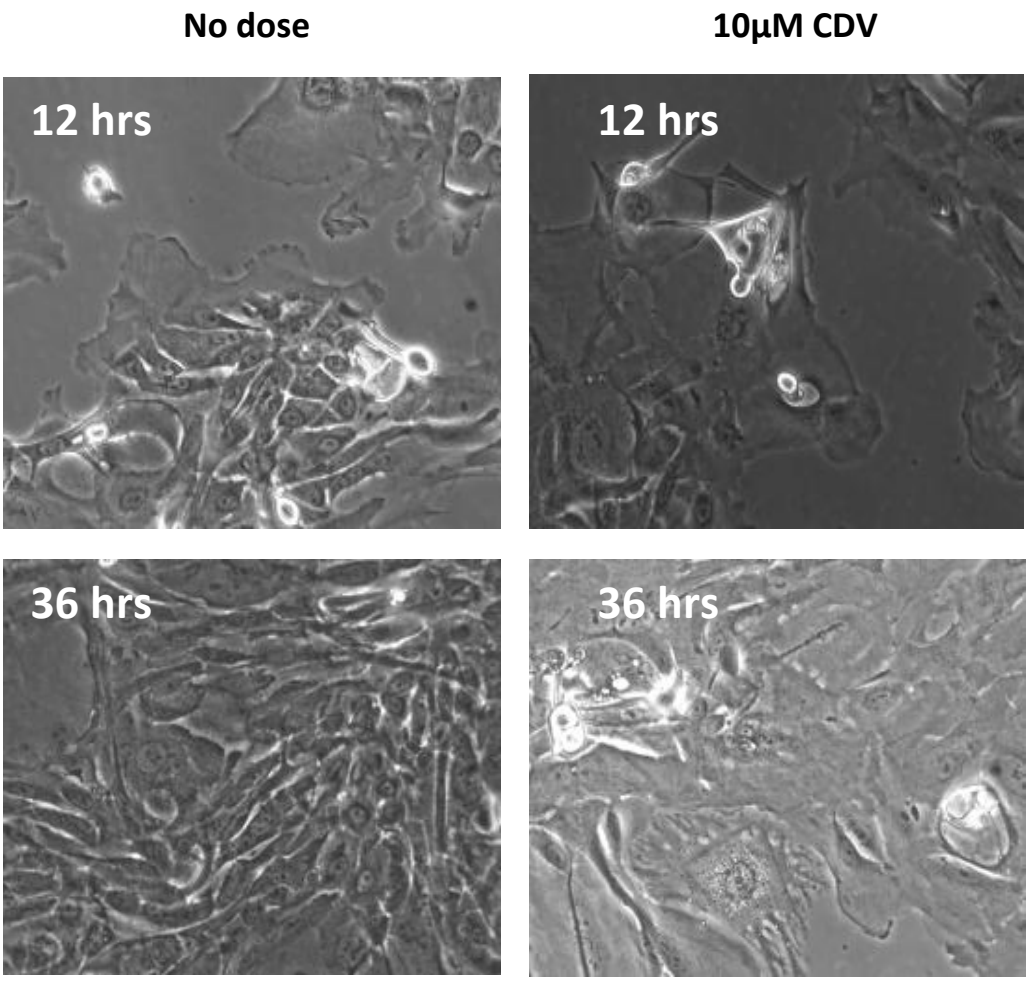

Figure 7.8. Morphology of A09 during CDV dosing protocol (experiment 2)

Cultures of A09 at P11 were visualised at 320x total magnification under light microscopy and a snap shot taken 12 and 36 hours after being dosed with and without CDV in CDV dosing protocol experiment 2.

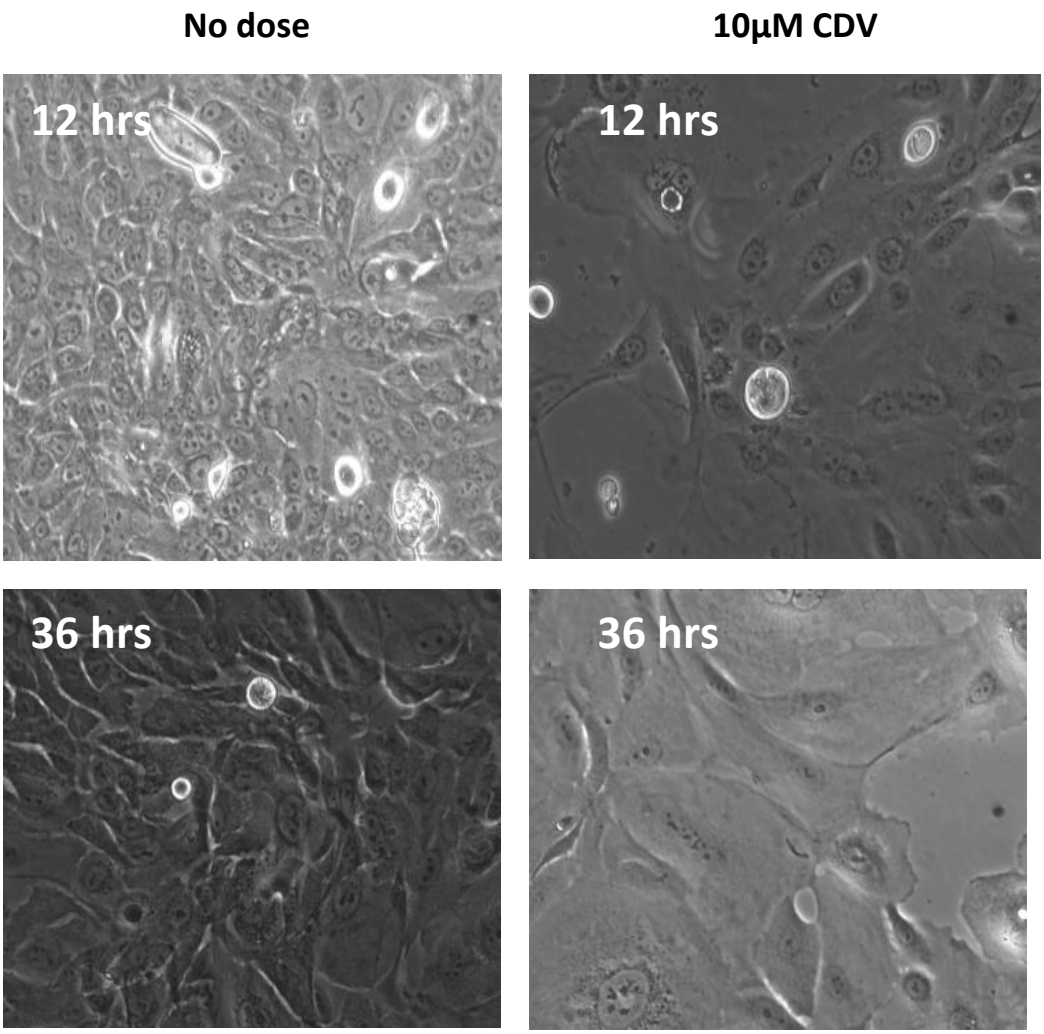

Figure 7.9. Morphology of H09 during CDV dosing protocol (experiment 1)

Cultures of H09 at P11 were visualised at 320x total magnification under light microscopy and a snapshot taken 12 and 36 hours after being dosed with and without CDV in CDV dosing protocol experiment 1.

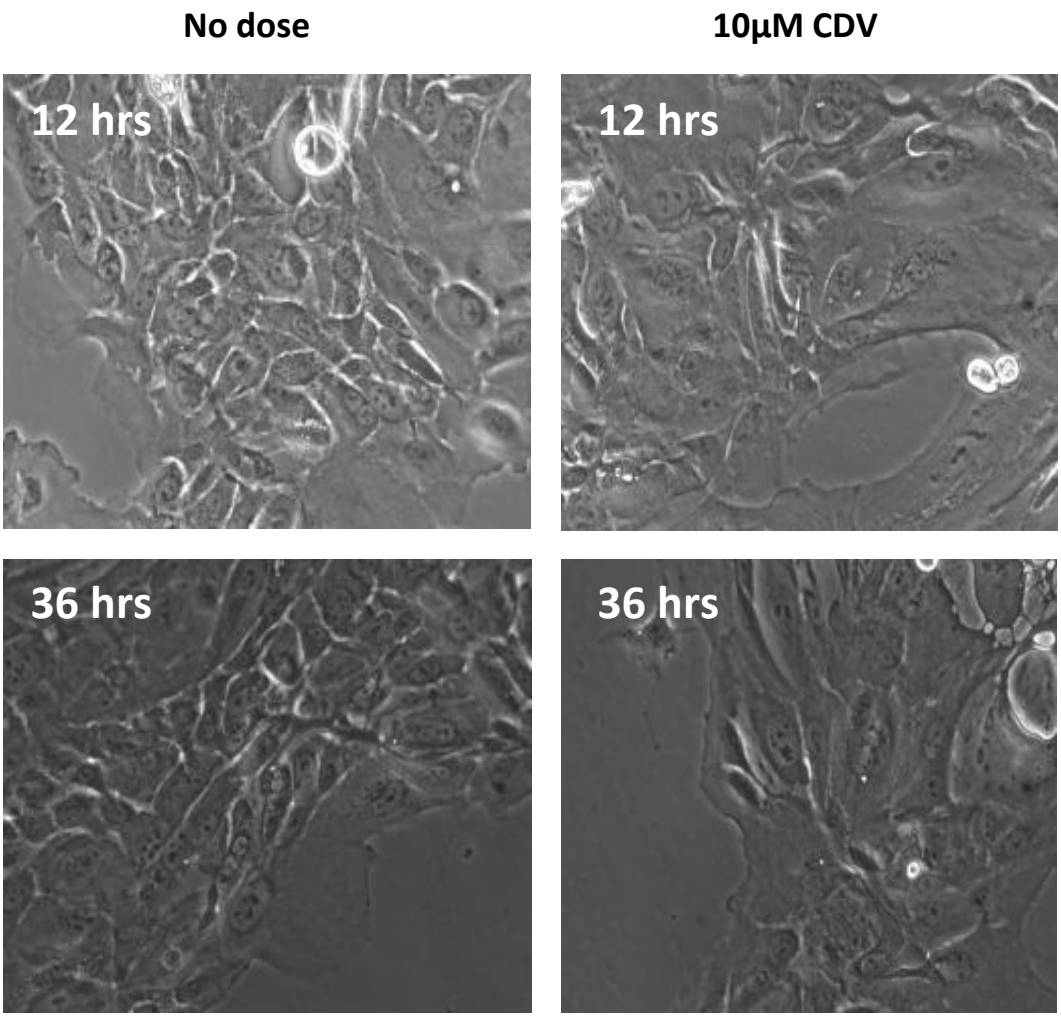

Figure 7.10. Morphology of H09 during CDV dosing protocol (experiment 2)

Cultures of H09 at P11 were visualised at 320x total magnification under light microscopy and a snapshot taken 12 and 36 hours after being dosed with and without CDV in CDV dosing protocol experiment 2.

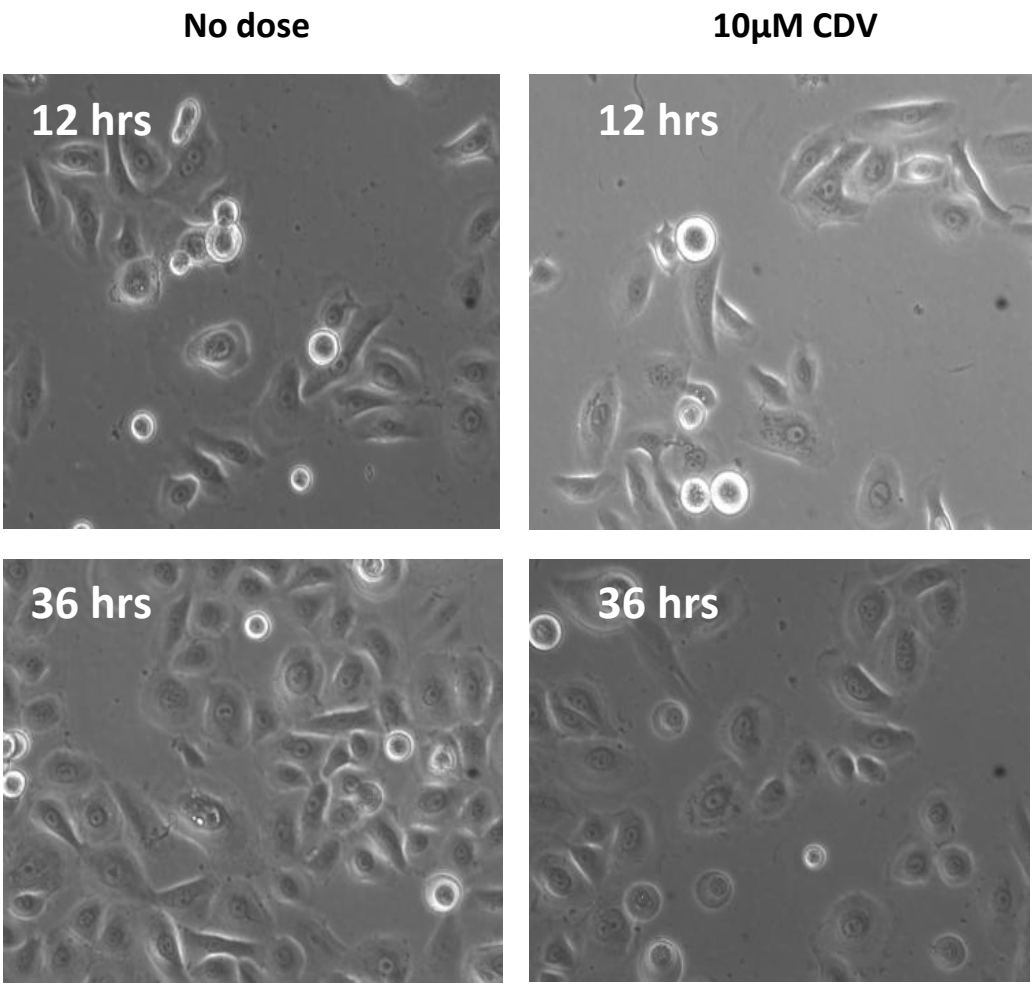

Figure 7.11. Morphology of HEKs during CDV dosing protocol

Cultures of HEKs at P3 were visualised at 320x total magnification under light microscopy and a snapshot taken 12 and 36 hours after being dosed with and without CDV in CDV dosing protocol experiment 1.

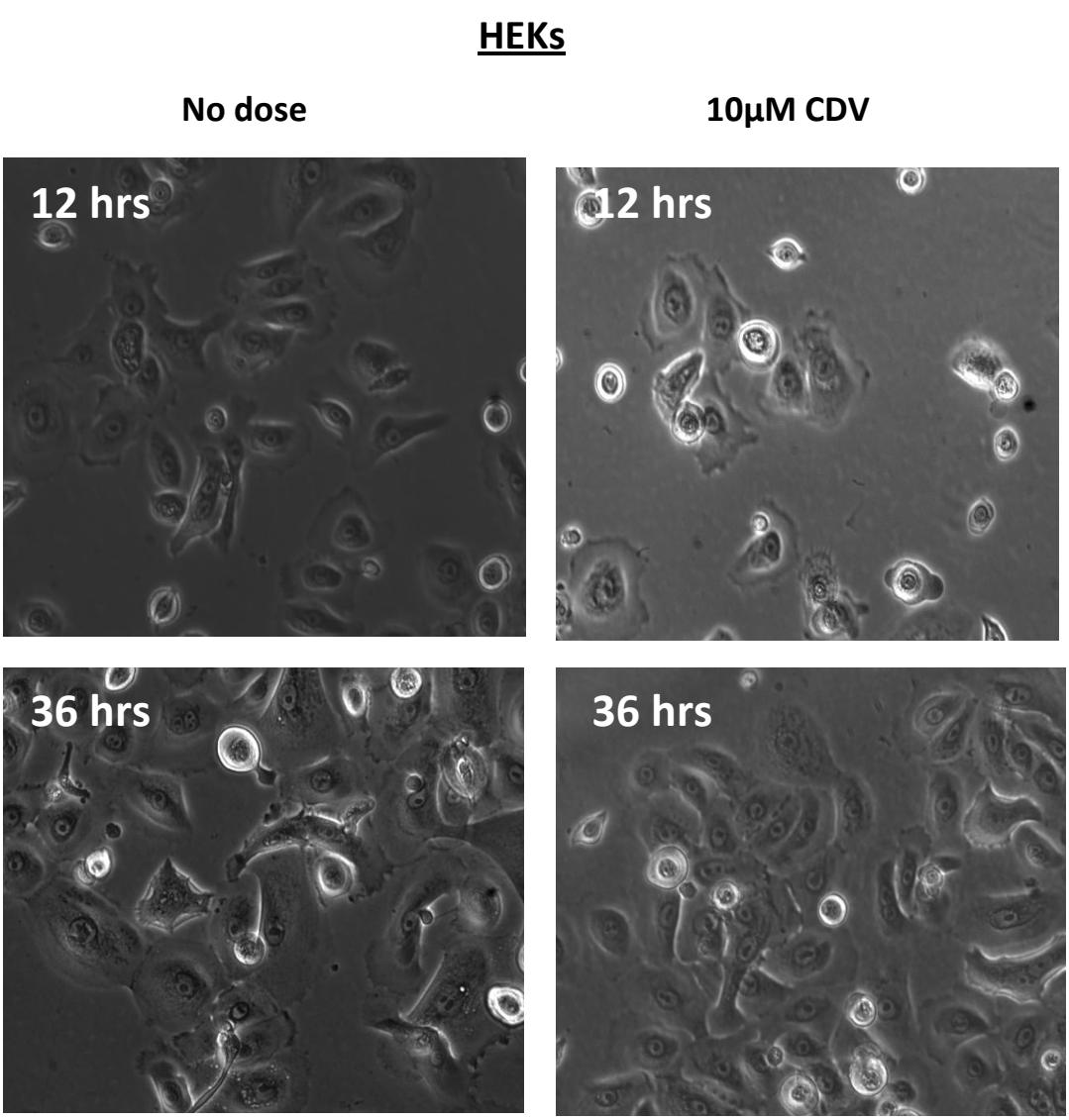

Figure 7.12. Morphology of HEKs during CDV dosing protocol

Cultures of HEKs at P3 were visualised at 320x total magnification under light microscopy and a snapshot taken 12 and 36 hours after being dosed with and without CDV in CDV dosing protocol experiment 2.

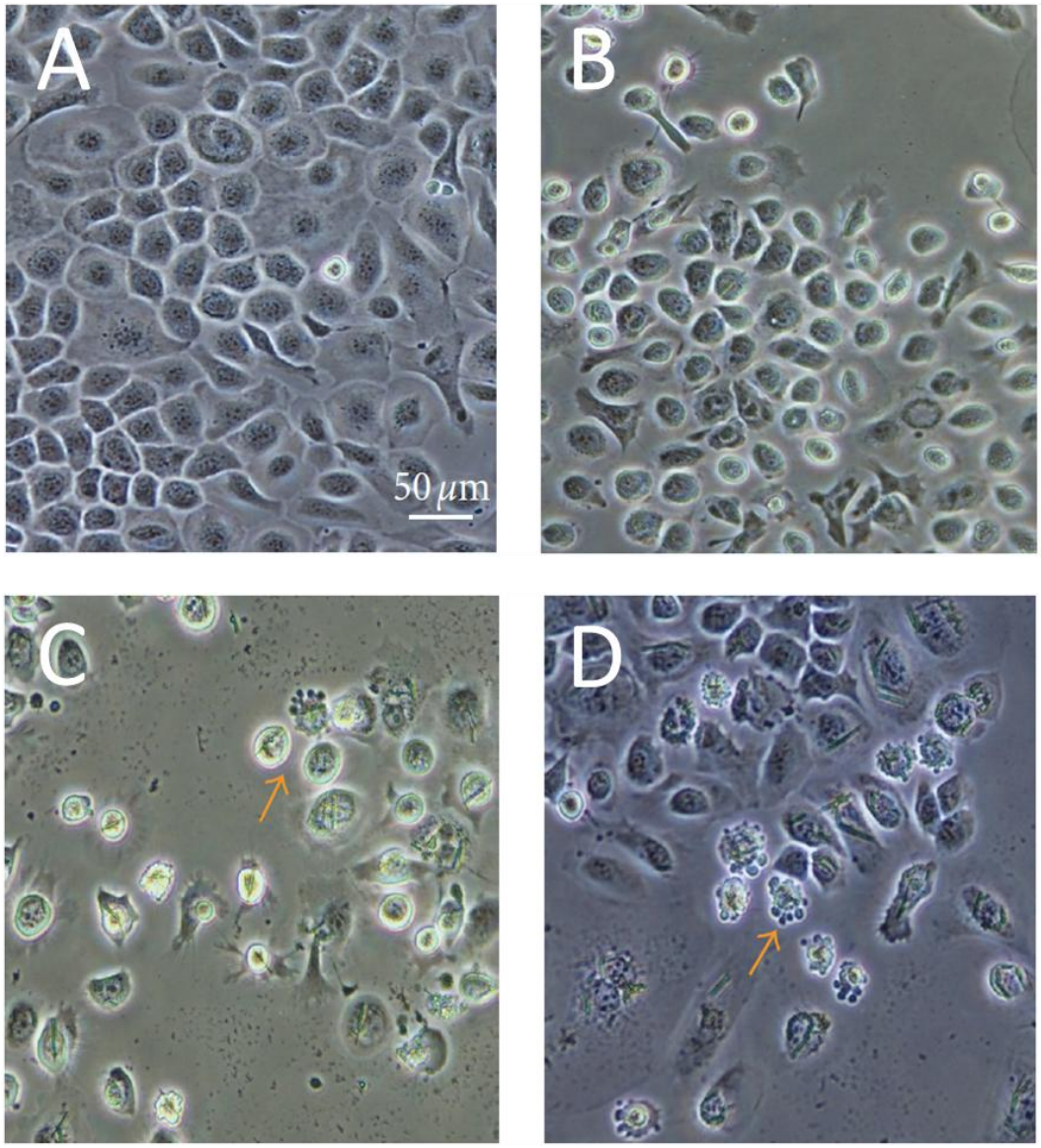

Figure 7.13. Example image showing induction of apoptosis in mouse keratinocytes

This image is included to show the morphological appearance of apoptosing keratinocytes. It shows the effects of treatment with 0, 2.5, 5, and 10 μg/ml tanshinone IIA (A-D respectively) in mouse keratinocytes 48 hours post treatment. Membrane blebbing, chromatin condensation and nuclear fragmentation increase the dose dependent manner. Apoptosing cells are indicated with an orange arrow. Image taken from (Li et al., 2012).

7.3.3 Relative expression of HPV oncogenes, E6 and E7

Relative expression of HPV genes E2, E6 and E7 were assessed and normalised to stable house-keeping genes TBP2 and HRPT, which are constitutively expressed in keratinocytes. Expression was quantified relative to CaSki cDNA as a standard.

Relative expression of HPV genes was investigated using RNA extracted from CDV treated and untreated clonal cell lines at each time point of the CDV dosing protocol as previously described. RNA was reverse transcribed to cDNA prior to performing qPCR and analysis, as previously described.

Relative expression levels of E2, E6 and E7 for CDV treated and untreated vulval cell lines (M08 and P08) and vaginal cell lines (A09 and H09) are illustrated in Figure 7.14 and Figure 7.15, repectively (Appendix IV). In vulval cell lines M08 and P08, E2 was absent which is consistent with the expression profiles presented in Figure 5.6. In M08, relative expression of E6 and E7 was detected at levels comparable with CaSki and appeared relatively stable in CDV treated and untreated cells at all time point. After 12 and 36 hours treatment, there was no significant difference in E6 and E7 expression between treated and untreated samples of M08 (12 hours, E6: $p = 2.3733.$, E7: $p = 2.1443$, at $p < 0.05$ (2-tailed t-test)). In P08, E6 and E7 appear stable 12 hours after treatment with and without CDV at approximately 50% of the levels detectable in CaSki; there was no significant difference in E6 and E7 expression between treated and untreated samples of P08 after 12 hours (E6: $p = 1.9663.$, E7: $p = 1.9534$). However E6 and E7 mRNA increased three fold at 36 hours after CDV treatment to levels 40-50% higher than found in CaSki. Expression of E6 and E7 was found to be significantly different after treatment with CDV compared to no dose control at this time-point (36 hours: E6 $P = 0.0062$, E7 $p = 0.0103$). In vulval cell line A09, relative quantification ratios of E2, E6 and E7 were all lower than observed with CaSki. mRNA levels for HPRT could not be quantified in the 36 hours sample and despite several repeats this problem was not resolved, thus normalisation to both

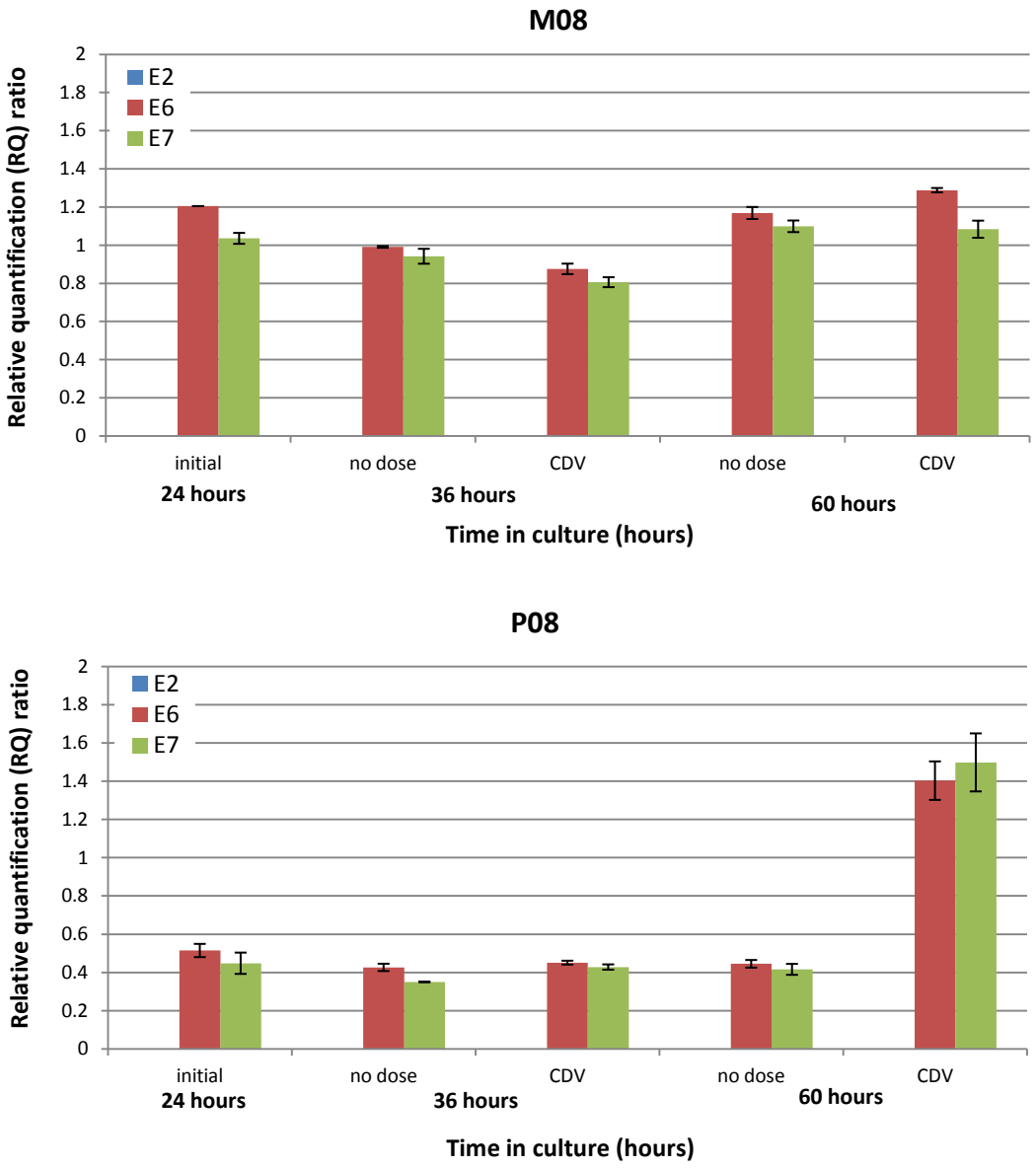

Figure 7.14. Relative expression of HPV E2, E6, and E7 in treated and untreated clonal cell lines M08 and P08

Relative expression of HPV oncogenes E2, E6 and E7 was investigated in 10µM CDV treated and untreated P11 M08 and P08. Relative expression was assessed during the CDV dosing protocol. An initial assessment was performed 24 hours after seeding. Cultures were dosed 24 hours after seeding and relative expression assessed 12 hours and 36 hours after being treated (36 and 60 hours after seeding). Expression is relative to CaSki as a standard; a value of 1 indicates the same level of expression detected in the CaSki cell line. HPV gene expression levels were normalised to house-keeping genes TBP2 and HRPT. Error bars signify standard deviations. There was no statistically significant difference in E6 and E7 expression at 12 and 36 hours between treated and untreated M08 (12 hours, E6: $p = 2.3733$., E7: $p = 2.1443$) ($P < 0.05$, $p < 0.05$ (2-tailed t-test)). There was noo statistically significant difference in E6 and E7 expression at 12 hours in treated and untreated P08 (E6: $p = 1.9663$., E7: $p = 1.9534$), however expression of E6 and E7 was found to be statistically different 36 hours after treatment (E6 $P = 0.0062$, E7 $p = 0.0103$).

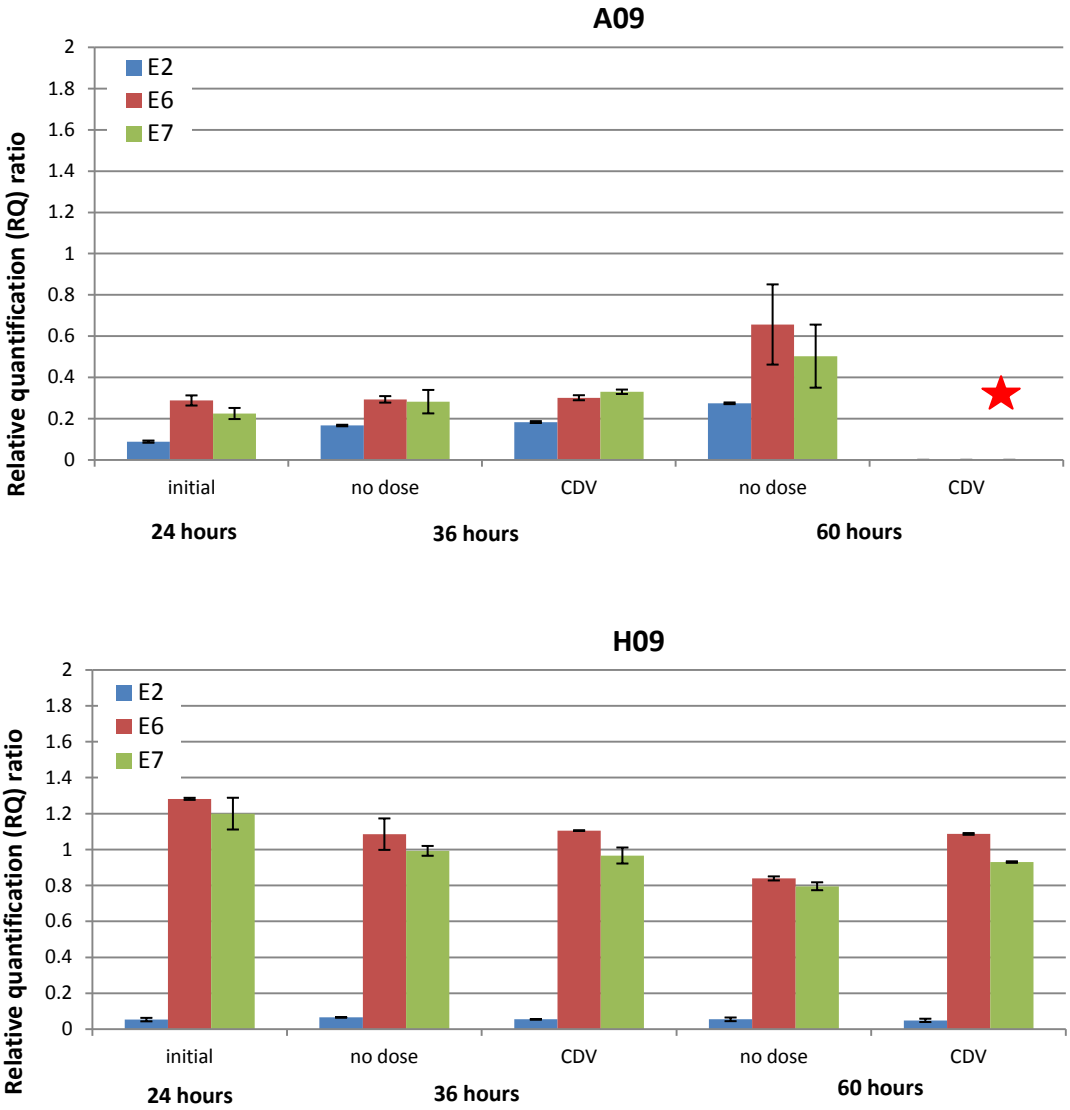

Figure 7.15. Relative expression of HPV E2, E6, and E7 in treated and untreated clonal cell lines A09 and H09

Relative expression of HPV oncogenes E2, E6 and E7 was investigated in 10µM CDV treated and untreated P11 A09 and H09. Relative expression was assessed during the CDV dosing protocol. An initial assessment was performed 24 hours after seeding. Cultures were dosed 24 hours after seeding and relative expression assessed 12 hours and 36 hours after being treated (36 and 60 hours after seeding). Expression is relative to CaSki as a standard; a value of 1 indicates the same level of expression detected in the CaSki cell line. HPV gene expression levels were normalised to house-keeping genes TBP2 and HRPT. The absent data highlighted with a red star, represents anomalous HPRT expression, and as a result relative expression of HPV genes could not be normalised to both TBP2 and HPRT and was therefore not presented. Error bars signify standard deviation. In H09, E2 relative expression was stable in treated and untreated samples at both time points; there was no significant difference between treated and untreated samples (E2, 12 hours: $p = 1.4351$., 36 hours: $p = 1.3841$, at $p < 0.05$ (2-tailed t-test). There was no significant difference in E6 and E7 expression between treated and untreated samples of H09 (12 hours, E6: $p = 2.3144$., E7: $p = 1.8341$., 36 hours, E6: $p = 1.0768$., E7: $p = 1.6055$) at $p < 0.05$ (2-tailed t-test).

HPRT and TBP2 could not be performed and data was therefore not presented. Figure 7.16 illustrates the missing data set by normalising E2, E6 and E7 to TBP2 only. In vaginal cell line H09, relative expression of E2 was stable in treated and untreated samples at both time points; there was no significant difference between treated and untreated samples at 12 and 36 hours (12 hours: $p = 1.4351.$, 36 hours: $p =$, at $p < 0.05$ (2-tailed t-test)). Relative expression of E6 and E7 was detected at levels comparable with CaSki and appeared relatively stable in CDV treated and untreated cells at all time points; there was no significant difference in E6 and E7 expression between treated and untreated samples (12 hours, E6: $p = 2.3144.$, E7: $p = 1.8341.$, 36 hours, E6: $p = 1.0768.$, E7: $p = 1.6055$ at $p < 0.05$ (2-tailed t-test)).

7.4 Discussion

The main conclusions of these experiments were as follows:

1. A more considerable response to CDV was detected in vulval clonal cell lines (M08 and P08) compared to vaginal clonal cell lines (A09 and H09) through viable cell counts (with statistical significance).
2. Reponse to CDV was detected in HEK cell line through viable cell counts and was comparable and a more marked effect was not obvious in clonal cell lines (no significant difference statistically).
3. Cell cytoplasmic enlargement was observed during microscopic analysis of CDV treated clonal cell lines, but not in HEK lines.
4. It could not be concluded that CDV induces apoptosis in treated clonal or HEK cell lines.

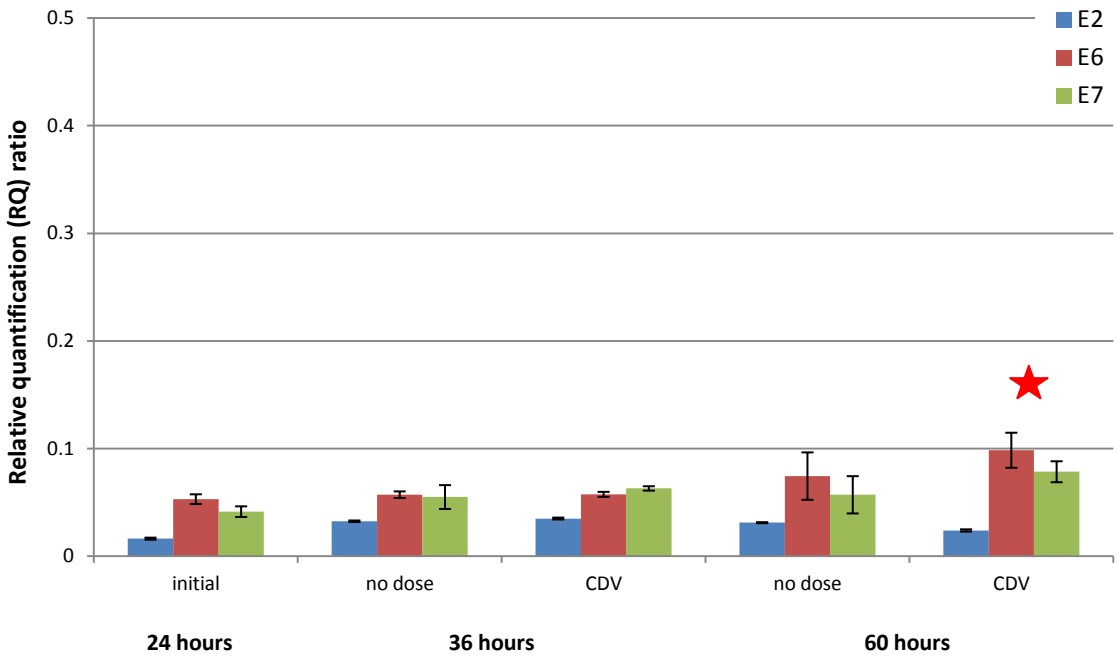

Figure 7.16. Relative expression in A09 normalised to TBP2

Relative expression of HPV oncogenes E2, E6 and E7 was normalised to house-keeping gene TBP2 only, in order to give an example of the expression levels obtained 36 hours after cells were treated with and without 10µM CDV (highlighted with red star). Error bars signify standard deviation.

5. In all clonal cell lines except P08, CDV treatment did not result in decreased E6 and E7 expression levels (with statistical significance).

The data on viable cell counts is consistent with results generated in earlier experiments and confirmed that the cells had been treated with CDV at an approximate IC_{50} dose. However the morphological data showed enlarged cells post treatment with CDV. Enlarged cells are more consistent with CDV preventing DNA replication and cell division, but not interfering with cellular growth pathways, and might be indicative of cell senescence. Confirmation of apoptosis could not be carried out through FACS (annexin V/7- 7-AAD staining) as previously explained; keratinocytes adhered to the lining of the tubes leading to the counting chamber causing repetitive blockage problems; this problem was not resolved and therefore data was not generated. The data on E6 and E7 expression were generally consistent, i.e. that dosing with CDV at approximately IC_{50} levels did not result in reduced levels of mRNA encoding HPV E6 and E7 in any of the cell lines.

7.4.1 Correlating viability, morphology and oncogene expression in P08

A link between cell viability, morphology and oncogene expression in response to CDV treatment was evident in clonal cell line P08, which appeared to respond distinctly differently to the other cell lines. The surviving fraction of cells 12 hours after treatment was 0.59 (59%) and 24 hours later (36 hours after being treated) survival fraction had increased by 9% (0.68 = 68%). P08 keratinocytes appeared extensively enlarged 12 hours after CDV treatment, however 36 hours after treatment keratinocytes appeared to have reduced and recovered tessellation pattern within the monolayer. Similarly, 36 hours after CDV treatment expression levels of E6 and E7 were approximately 10 fold higher than untreated cells at the same time point (and at all time points throughout the study, which were maintained at relatively stable levels). The increase in E6 and E7 36 hours after CDV treatment reached expression levels comparable to CaSki.

One possible explanation for the viability and morphology data would be that a sub-population of cells were unaffected by CDV treatment (i.e. remained viable) and may have rapidly proliferated, accounting for a higher survival fraction 36 hours after CDV treatment, and causing keratinocyte morphology to become gradually restored within the cell culture. The 10 fold increase in E6 and E7 expression after treatment at the same time point may play a part in the revival of the keratinocytes described. Expression of HPV oncogenes E6 and E7 are required for optimal proliferation of cervical carcinoma cells (HeLa) (DeFilippis et al., 2003) and have been shown to generate keratinocyte cell lines with indefinite growth potential through transfection of plasmids with intact E6 and E7 ORFs (Hawley-Nelson et al., 1989). Increased levels of E6 and E7 36 hours after CDV dosing might therefore be associated with the increased survival fraction and reversion to the typical keratinocyte morphology.

7.4.2 CDV sensitivity in HPV positive and negative lines

Response to CDV in HPV positive and negative cell lines (clonal lines and HEK lines, respectively) was investigated through annexin V viable cell counts and microscopic analysis of cell morphology. Cell cytoplasmic enlargement was observed post treatment in clonal lines but this was not observed in the HEK line. However viable cell counts were reduced post treatment in both clonal and HEK lines. In this study reduced viable cell counts were detected in response to CDV regardless of HPV presence or absence. In the confinement of this study, CDV was not found to have increased sensitivity in cells infected with HPV, in contrast to the published literature.

HEK cell lines are human epidermal keratinocytes with foreskin origin, and provided a HPV negative keratinocyte model for anogenital sites. The literature suggests that cells infected with HPV are more sensitive to CDV than HPV negative cells (Johnson and Gangemi, 1999). Specifically in a study by Andrei and colleagues (2001), annexin V staining showed that CDV reduced the percentage of viable cells, while no significant changes in the percentages of

viable cells were noted in HPV negative primary human keratinocytes. Moreover, reduced viable counts detected in HPV positive lines were further found to be correlated with induction of apoptosis.

The results from this study are not consistent with existing literature; a sensitivity of CDV to HPV infected cells was not found. Similarly the reduction of viable counts for HPV negative HEK lines with no observed morphological changes also confounded interpretation of data. For that reason, subjective morphological analyses were not considered in this instance, and viable cell count data only taken in to account (which is a more accurate, and more commonly used method of assessing response to drug treatment). The actual cause of reduced viable counts also remains unclear and requires further investigation.

7.4.3 Strengths and weaknesses

The data presented are based on two separate CDV dosing protocols, and within each protocol cell cultures were prepared in duplicate. Viability counts were robust, as manual trypan blue cell counts were performed in triplicate from duplicate TC dishes, and combined for each dosing protocol. A mixture of quantitative and qualitative measures were assessed, and the data describing morphological appearance in particular are necessarily subjective; it should be stressed that the microscopic images presented represent only a small portion of the cell cultures that were assessed. The E6 and E7 expression data was assessed in the first of the CDV dosing protocols (i.e. at several time points and in four different cell lines), and relative quantification of gene expression was calculated from duplicate repeats.

7.4.4 Mechanism of action of CDV

Most studies that have looked at the effects of CDV *in vitro* are consistent in finding that treatment reduces cell proliferation, and several suggest that this effect is greater in HPV positive cells compared to HPV negative cells (Johnson and Gangemi, 1999, Andrei et al.,

2000). In terms of comparing response to CDV in HPV positive or negative keratinocytes in this study, morphological analysis of keratinocytes suggested that HPV positive lines were most susceptible to CDV treatment, however surviving fractions showed that response to CDV in HEKs and M08 were comparable both 12 and 36 hours after treatment.

There is less consistency in whether authors attribute the effects of CDV on proliferation to apoptosis. In the experiments described in this chapter, no morphological evidence for apoptosis was observed and this is consistent with the results of Abdulkarim et al., 2002. It is difficult to explain why published reports of induction of apoptosis by CDV are so variable. It seems likely that the variety of experimental systems (cell lines), the dose levels and assays employed, may contribute. The genetic background of the cell lines is likely to be particularly important especially with regard to p53 mutational status.

Since evidence of apoptosis was not confirmed in response to CDV treatment in this study, the results observed in a parallel study (undertaken by Miss Aine Flynn - Cardiff Univeristy, HPV Research Group) have been included for speculation. Induction of caspase-3 activity was assessed as a marker of apoptosis following treatment of the M08, A09 and HEK cells with CDV. Caspase-3 activity was assessed using a fluorogenic assay for activated caspase and by western blotting for cleaved caspase-3, and did not increase in response to CDV treatment in either the M08 or A09 cell lines (data shown in Appendix V). Similarly, there was no increase in p53 levels or phosphorylation in response to CDV treatment, or in levels of the p53 transcriptional target p21 (Appendix VI). Taken together, these results strongly suggest that in this model of early neoplasia, at these specific dose levels, treatment with CDV did not induce cellular apoptosis.

8 Whole transcriptome sequencing

8.1 Results

The transcriptome represents all the transcripts present in a cell at a particular time point, and can be assessed through RNA sequencing (RNA-seq). RNA-sequencing is a quantitative, and highly sensitive method of transcript profiling, with several advantages over other techniques, as described previously. RNA-seq was performed using RNA extracts of clonal cell lines 12 hours after CDV treatment (and no dose control) as part of the CDV dosing study. Generated transcript profiles of treated and untreated cells at the same time point, allowed differential gene expression to be analysed. Gene transcripts also underwent gene ontology over-representation analysis (GO ORA) which involved the grouping of significant gene sets into related functional categories for easier interpretation (Ashburner et al., 2000); GO groups are biological process (BP), cellular component (CC), and molecular function (MF), as previously described. RNA-seq followed by differential gene expression and GO analysis, was performed on CDV treated and untreated cell lines to investigate the molecular mechanism(s) of action of CDV; RNA-seq provided a more in depth approach for examining gene transcripts that encompasses the entire genome, and could potentially provide a more thorough insight in to the mechanism of action of CDV.

In HPV positive cell lines, CDV treatment has previously been suggested to induce apoptosis and reduce expression of HPV oncogenes E6 and E7 (Andrei et al., 2001, Abdulkarim et al., 2002, Amine et al., 2009), as previously described. Based on this published research, we had expected to observe apoptosis in response to CDV, however this was not apparent; as described in chapter 7, cell viabililty counts were reduced in response to CDV treatment, and the morphology of keratinocytes appeared to be consistent with cellular senescence. Cellular senescence, like apoptosis, is thought to be a programmed protective response of a cell to

damage. Cellular senescence has been shown to occur as a result of inflicting damage to cultured cells. DNA damage to human fibroblasts have been shown to induce terminal growth arrest resulting in phenotypic changes that resemble cells undergoing senescence (Di Leonardo et al., 1994, Robles and Adami, 1998). Given that CDV may be incorportated into DNA and RNA causing chain termination, and possibly stalling of transcription and of replication forks, it is also possible that treatment with CDV could result in DNA damage and stress responses. Thus, transcript profiles of CDV treated cell lines were investigated for significantly expressed gene transcripts relating to induction of apoptosis, senescence, stress response pathways, and response to DNA damage.

Clonal cell lines previously characterised at a molecular level (chapter 5) were found to possess distinct HPV gene expression profiles (via real-time quantitative reverse-transcription PCR (qRT-PCR)) and HPV integration status (via amplification of papillomavirus oncogene transcripts (APOT)). Therefore HPV gene transcripts were investigated to confirm HPV expression profiles and HPV integrated transcripts in clonal cell lines.

In summary, clonal cell line transcript profiles generated through RNA-seq were used to:

1. validate HPV gene expression profiles previously determined by qRT-PCR
2. validate HPV integration status previously determined by APOT
3. assess differentially expressed genes to define transcript variation between clonal cell lines from the same patient but with different HPV gene expression profiles
4. assess differentially expressed genes to define transcript variation in treated vs. untreated clonal cell lines

This section of research was novel as it was the first time cells of this type have undergone a high sensitivity next generation sequencing technique for transcriptome profiling.

8.1.1 Aims and objectives

The central aim was to assess differential gene expression encompassing the entire transcriptome in clonal cell lines after treatment with CDV, and validate gene expression profiles and HPV integration status characterised previously.

The following objectives structured this section of work:

1. Investigate whether RNA-seq gene transcripts are consistent with qRT-PCR expression profiles obtained previously
2. Investigate whether RNA-seq integrated gene transcripts are consistent with HPV integrated transcripts detected previously via APOT
3. Investigate differentially expressed genes in clonal cell lines after treatment with CDV that are related to:
    a. HPV E6 and E7 genes
    b. Genes involved in apoptosis
    c. Genes involved in senescence
    d. Genes involved in stress response pathways
    e. genes involved in DNA damage response.

8.1.2 Study sample

Clonal cell lines derived from VIN; M08 (HPV16 integrated) and P08 (HPV16 status inconclusive (chapter 5)), were subjected to CDV dosing and subsequent RNA extraction, as previously described. The following RNA extracts underwent SOLiD™ transcriptome sequencing and analysis:

1. clonal cell line M08 12 hour no treatment
2. clonal cell line M08 12 hours post treatment with 10 µM CDV
3. Cell line P08 12 hours no treatment

4. Cell line P08 post 12 hours post treatment with 10 µM CDV

8.2 Quality control

Quality control of RNA extracts was carried out to ensure RNA quality was sufficient for SOLiD™ transcriptome sequencing. The sequence data generated for each sample was also assessed to ensure they met the expected quality standards for inclusion in down-stream data analyses.

8.2.1 RNA quality control

RNA extracts were initially analysed using NanoDrop 2000 spectrophotometer to obtain RNA concentration and assess RNA purity, as previously described. RNA spectrophotometric measurements showed that sample quality was adequate since the ratio of absorbance at 260 nm and 280 nm fell between 1.8 and 2.2 for all samples. The following RNA concentrations were obtained:

Cell line M08 12 hours post no treatment = 136 ng/µl

Cell line M08 12 hours post 10 µM CDV = 149 ng/µl

Cell line P08 12 hours post no treatment = 211 ng/µl

Cell line P08 12 hours post 10 µM CDV = 187 ng/µl

Quantitation and quality control of RNA was also performed using an Agilent 2100 Bioanalyzer through Central Biotechnology Services (CBS) (Cardiff University). The RNA integrity numbers (RIN) generated by Agilent 2100 were greater than 7 (all samples had RIN scores of 10) and were therefore suitable for SOLiD RNA sequencing (Appendix VII).

8.2.1.1 *Main findings*

Total RNA extracts were found to be suitable for SOLID™ transcriptome sequencing.

8.2.2 Quality control of sequence data

Total RNA extracts underwent SOLiD™ transcriptome sequencing and analysis. Resulting sequence data was obtained for 3/4 samples; due to a fault in the library preparation process, no sequence data was generated from untreated P08. The 3 remaining sequence data sets had low data yield and reduced read quality; untreated M08 generated the most sequence reads at 368 million, and CDV treated M08 and P08 generated 134 and 190 million sequence reads, respectively. The percentage of sequence reads that mapped successfully to target was low in all 3 samples, with 16.2% mapped reads in untreated M08, 47% in CDV treated M08, and 48.2% in CDV treated P08.

Although the percentage of mapped reads was low for all samples, for the purposes of this thesis the available sequence data sets for 3 out of 4 samples were recommended of sufficient quality for provisional down-stream sequence analysis.

As SOLiD™ sequencing data was not generated for untreated P08, CDV treated P08 was used to validate HPV gene expression profiles and HPV integration status of P08, in later sections.

8.2.3 Quality control of transcript reads

Sequence data was translated to transcript reads, which were checked to identify any underlying issues with transcript distributions for each sample. Box plots of raw transcript counts, Reads Per Kilobase exon Model per million mapped reads (RPKM values normalised for gene length), and edgeR normalised counts were prepared for each sample as shown in Figure 8.1. The box plots were showed similar distributions to each other illustrating that there were no underlying issues with transcript data distribution in any of the samples.

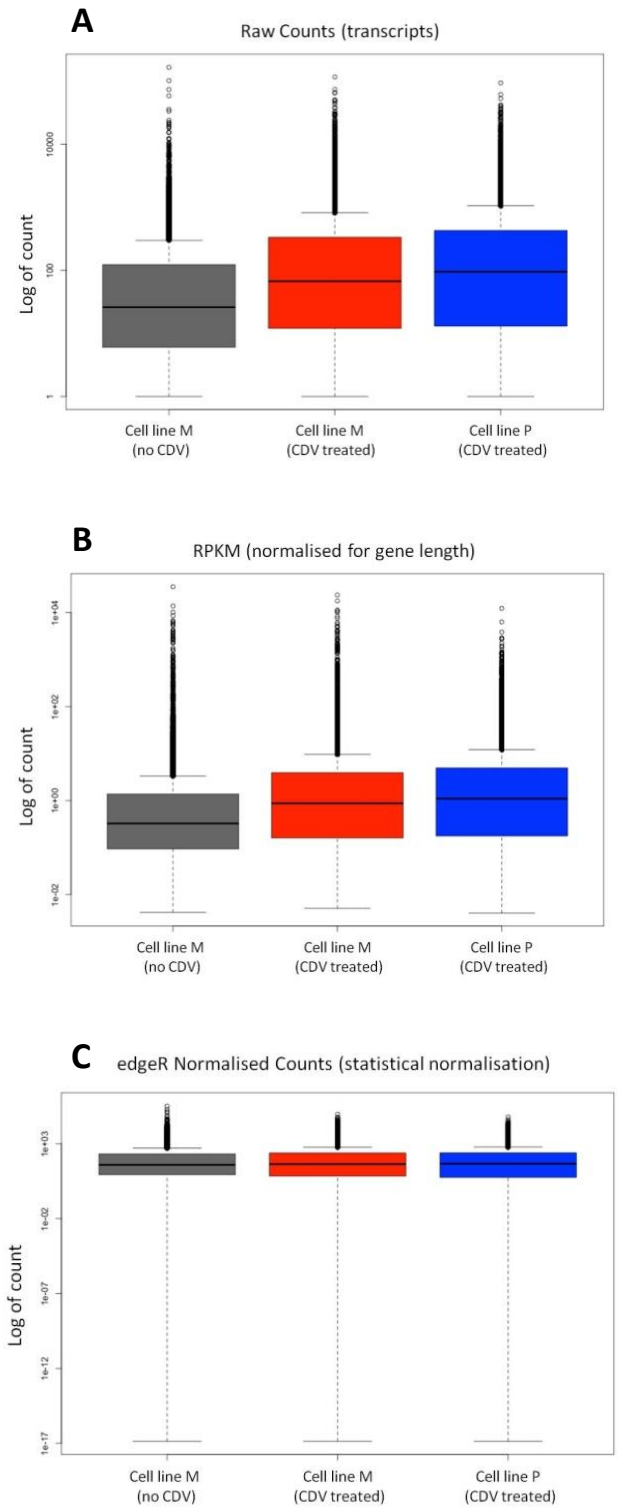

Figure 8.1. Box plots of raw counts (A), RPKM values (B),and edgeR normalised counts (C) for transcript data of untreated M08, CDV treated M08, and CDV treated P08.

Each box plot illustrates the smallest value, lower-median-upper quantile, and largest value, for each sample, which provides an indication of the distribution of each data set. Illustration kindly provided by Dr Peter Giles (Wales Gene Park).

A pair-wise comparison of transcript reads for each sample was also carried out to assess samples for anomalies against each other. MvA plots were produced from pair-wise comparisons as illustrated in Figure 8.2; all comparisons were found to resemble a right pointing arrow centred around a red zero fold-change line, showing there were no irregularities in the edgeR normalised data in these plots. Additionally, the data distribution appeared more tightly focussed around the red zero fold-change line in Figure 8.2(A), compared to Figure 8.2(B) and (C) which were more dispersed. Prior to performing more detailed analysis of this data, pair-wise comparisons of transcript reads indicated that there were more differences in transcripts reads between cell lines M08 and P08, than between CDV treated and untreated cells of the same cell line (M08).

8.2.3.1 *Main findings*

Transcript reads for each sample showed no underlying irregularities and transcript data was accepted as adequate for down-stream analyses. Prior to carrying out more detailed down-stream analyses of transcript data, pairwise comparisons gave an indication of possible differences in transcript profiles between each sample.

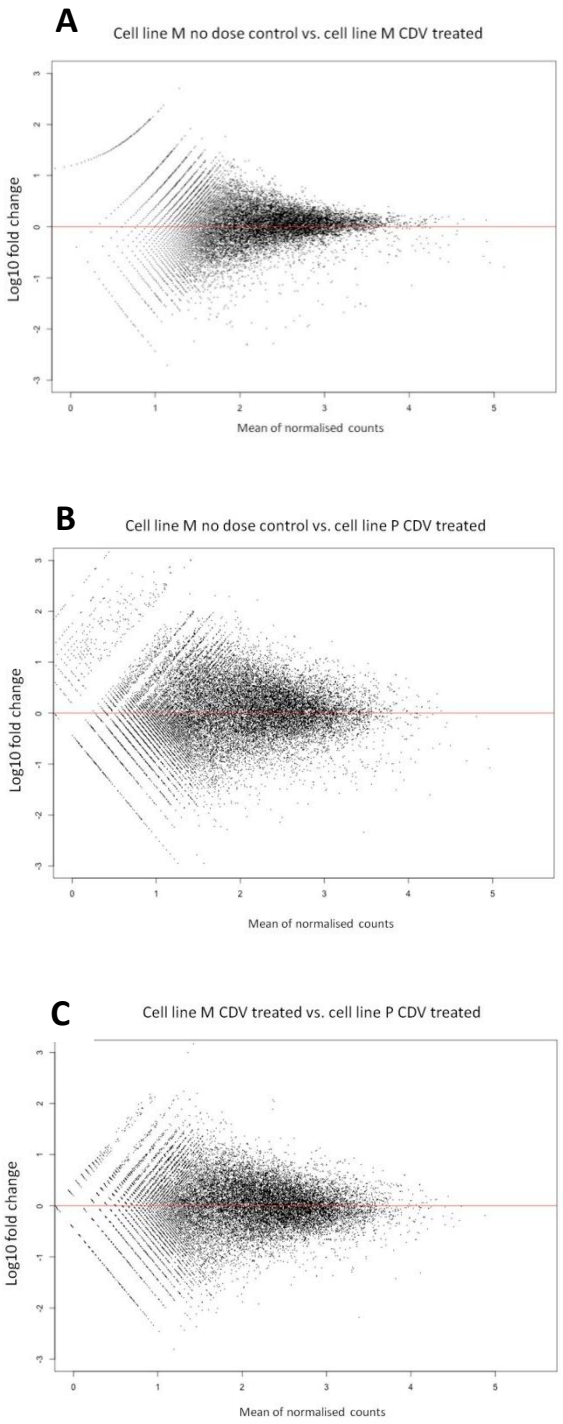

Figure 8.2. MvA plots for all pairwise comparisons of transcript data.

MvA plots compare transcript reads for untreated M08 vs. CDV treated M08 (**A**), untreated M08 vs. CDV treated P08 (**B**), and CDV treated M08 vs. CDV treated P08 (**C**). All pair-wise comparisons are illustrated as scatter plots that are centred around a red zero fold change line. Illustration kindly provided by Dr Peter Giles (Wales Gene Park).

8.3 SOLiD™ transcript data

8.3.1 Validation of HPV gene expression

qRT-PCR was previously performed using RNA extracts of M08 and P08 to quantify HPV16 E2, E4, E5, E6, and E7 gene expression. E2 expression was not detected in M08 and P08. E6 and E7 gene expression was detected in M08 and P08 at all passages, however E4 and E5 was detected at all passages in P08 but not at any passage in M08 (Figure 5.6).

Mapped transcripts of SOLiD™ sequence data for M08 and P08 were visualised using the Integrative Genomic Viewer (IGV) (Figure 8.3) to assess transcript profiles using HPV16 genome model (NC_001526) as reference. In M08, mapped transcript reads of E6 and E7 were present however E2, E4, and E5 transcripts were not. In P08, mapped transcript reads for a small region of E2 were detected, and transcript reads mapped to full length E4, E5, E6, and E7.

8.3.1.1 *Main findings*

SOLiD™ transcription profiles of clonal cell lines M and P visualised through IGV were consistent with transcription profiles previously obtained by qRT-PCR. This validated the use of both qRT-PCR and SOLiD™ transcriptome sequencing coupled with IGV as methods of determining gene expression profiles in these cell lines.

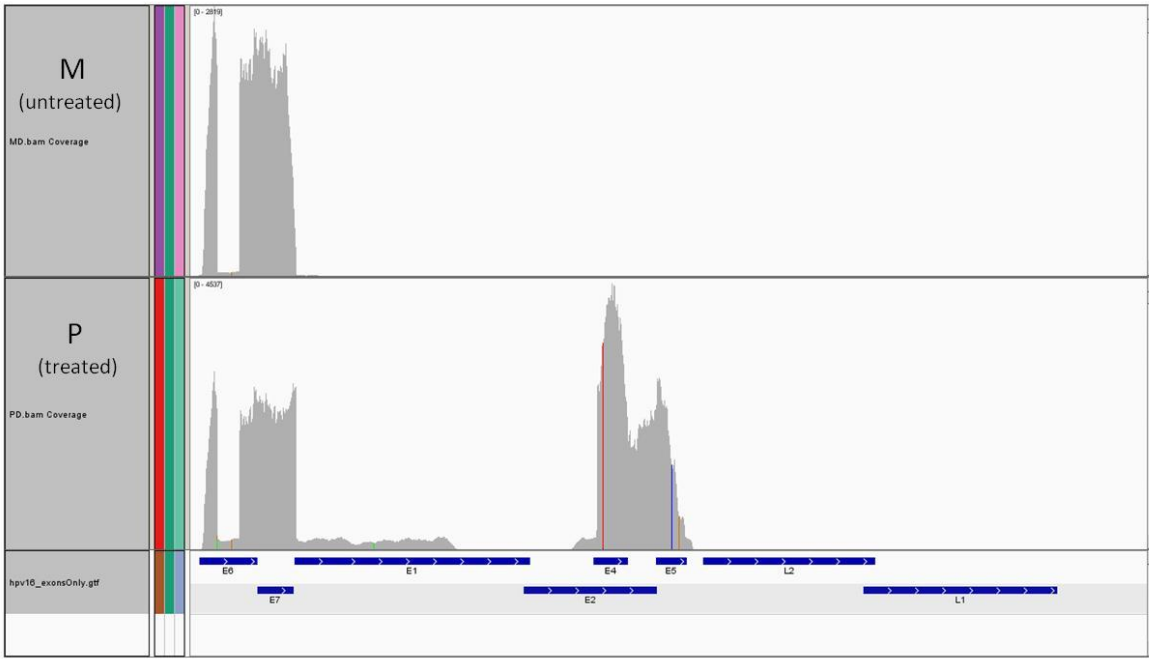

Figure 8.3. IGV screen shot showing a histogram of M08 and P08 mapped transcript reads with reference to HPV genome model (downloaded from NCBI, accession no: NC_001526.2).

8.3.2 Validation of HPV integration status

APOT was performed using RNA extracts of clonal cell line M and P to investigate the presence of HPV integrated transcripts as part of molecular characterisation (Table 5.2). In M08 at early and late passages, APOT detected multiple sized type 1 integrated transcripts at different sites mapping to chromosome 3q28, specifically within *LEPREL1* gene. In early and late passages of P08, episomal HPV transcripts were detected as E7-E1 spliced to E4 constructs; integrated transcripts were not detected.

8.3.2.1 *Clonal cell line M08*

SOLiD™ transcript data for untreated M08 was visualised as Circos plots to identify HPV-human fusion transcripts (integration), as shown in Figure 8.4A; grey lines associating the HPV genome with the human genome represent pair-end reads where one read mapped to HPV16 and the other to human sequence. Multiple grey lines visible as a thick black streak linked the E6/E7 region of the HPV genome with chromosome 3 of the human genome, representing multiple fusion transcripts of E6/E7 and chromosome 3. This was consistent with APOT data previously obtained which detected integration within chromosome 3q28 (*LEPREL1*). Single grey lines also linked E6/E7 with other human genomic loci in the Circos plot, but these were not detected previously by APOT and were difficult to interpret. The fusion transcript in the Circos plot linking E6/E7 and chromosome 3 was also visualised through IGV, shown in Figure 8.4B. This also confirmed that the integrated transcript was constructed of E6/E7 fused to chromosome 3, specifically within the gene *LEPREL1*; again this was consistent APOT data. Single grey lines that linked the HPV genome with various other loci of the human genome were not identified through IGV.

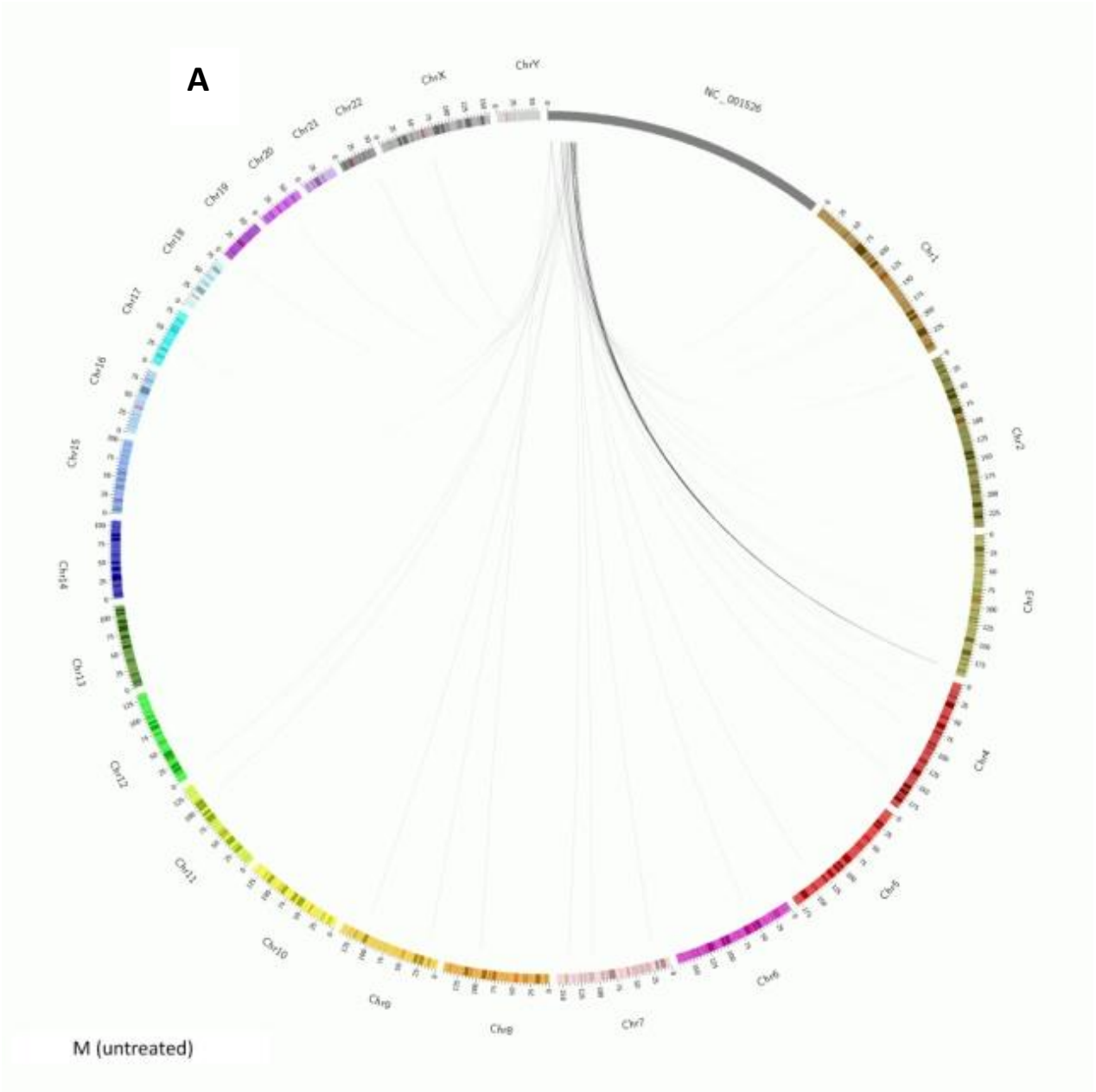
A
ChrX
ChrY
NC_001526
Chr22
Chr21
Chr20
Chr19
Chr18
Chr17
Chr16
Chr15
Chr14
Chr13
Chr12
Chr11
Chr10
Chr9
Chr8
Chr7
Chr6
Chr5
Chr4
Chr3
Chr2
Chr1
M (untreated)

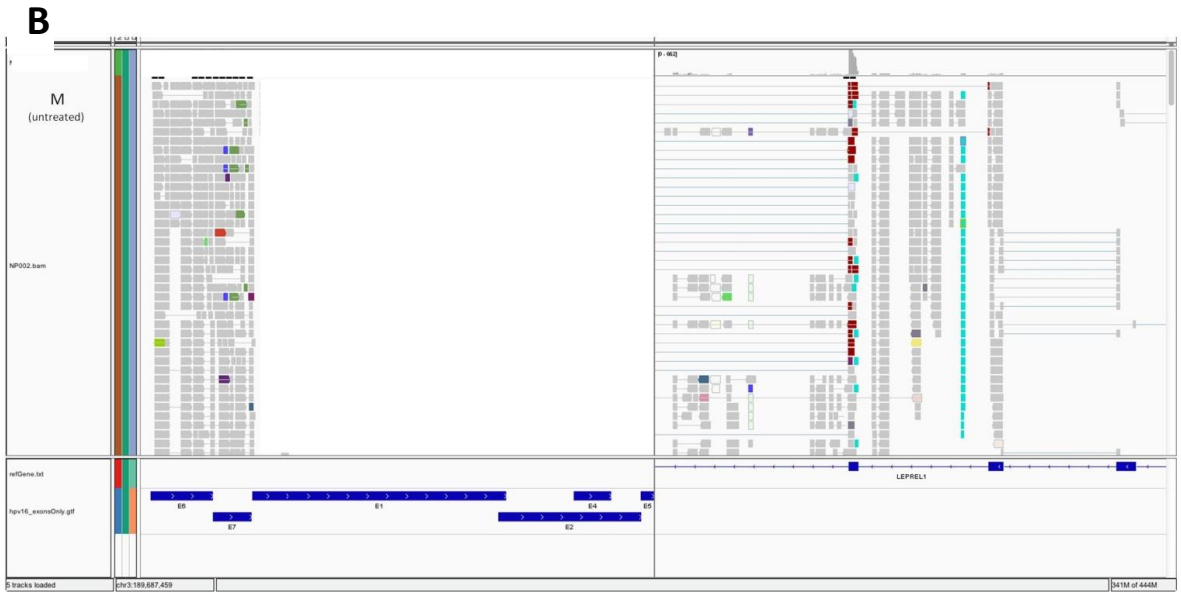

Figure 8.4. SOLiD™ transcript data for M08 visualised as Circos plots and through Integrative Genomic Viewer (IGV).

Linkage between HPV genome and the human genome in untreated M08 illustrated as a Circos plot (**A**), and through Integrative Genomic Viewer (IGV) as a split-screen shot used to visualise mapped locations of HPV-human fused transcripts (**B**). In Circos plots, possible HPV integrated transcripts were represented by grey lines connecting the HPV genome (downloaded from NCBI, accession no: NC_001526.2) with chromosomes (chr) of the human genome (UCSC human reference hg19 site); Multiple grey lines connect the HPV genome with chromosome 3, illustrated by a black streak suggesting an integrated transcript. Single grey lines also link HPV with other regions of the human genome. In IGV, the same reference genomes were used to define transcript locations; transcript reads that map within expectation are represented by gray shaded tags whilst those mapping over extended distances are illustrated as coloured tags, with the colour indicating the chromosome to which the transcript corresponded. Transcript fusion between HPV16 E7 and chromosome 3, specifically within *LEPREL1* (multiple cyan coloured tags) is illustrated in the split-screen.

8.3.2.2 *Clonal cell line P08*

SOLiD™ transcript data for CDV treated P08 was visualised in a Circos plot as illustrated in Figure 8.5A. Multiple grey lines visible as a dark grey streak linked E6 of the HPV genome with chromosome 10 of the human genome. This represented a fusion transcript of E6 and chromosome 10; APOT did not detect any integrated transcripts in P08. Single grey lines also linked E6, E7 and E4 with other human genomic loci; these were also not detected previously by APOT. This fusion transcript of E6 and chromosome 10 could not be identified when the data was visualised through IGV, however, episomal HPV constructs were detected using IGV (Figure 8.5B), which consisted of E7-E1 spliced to E4 transcripts (consistent with previous APOT data).

8.3.2.3 *Main findings*

SOLiD™ HPV integration status in M08 and P08 visualised through IGV was consistent with HPV integration status previously determined by APOT. This validated the use of both APOT and SOLiD™ transcriptome sequencing coupled with IGV as methods of determining HPV integration status in these cell lines.

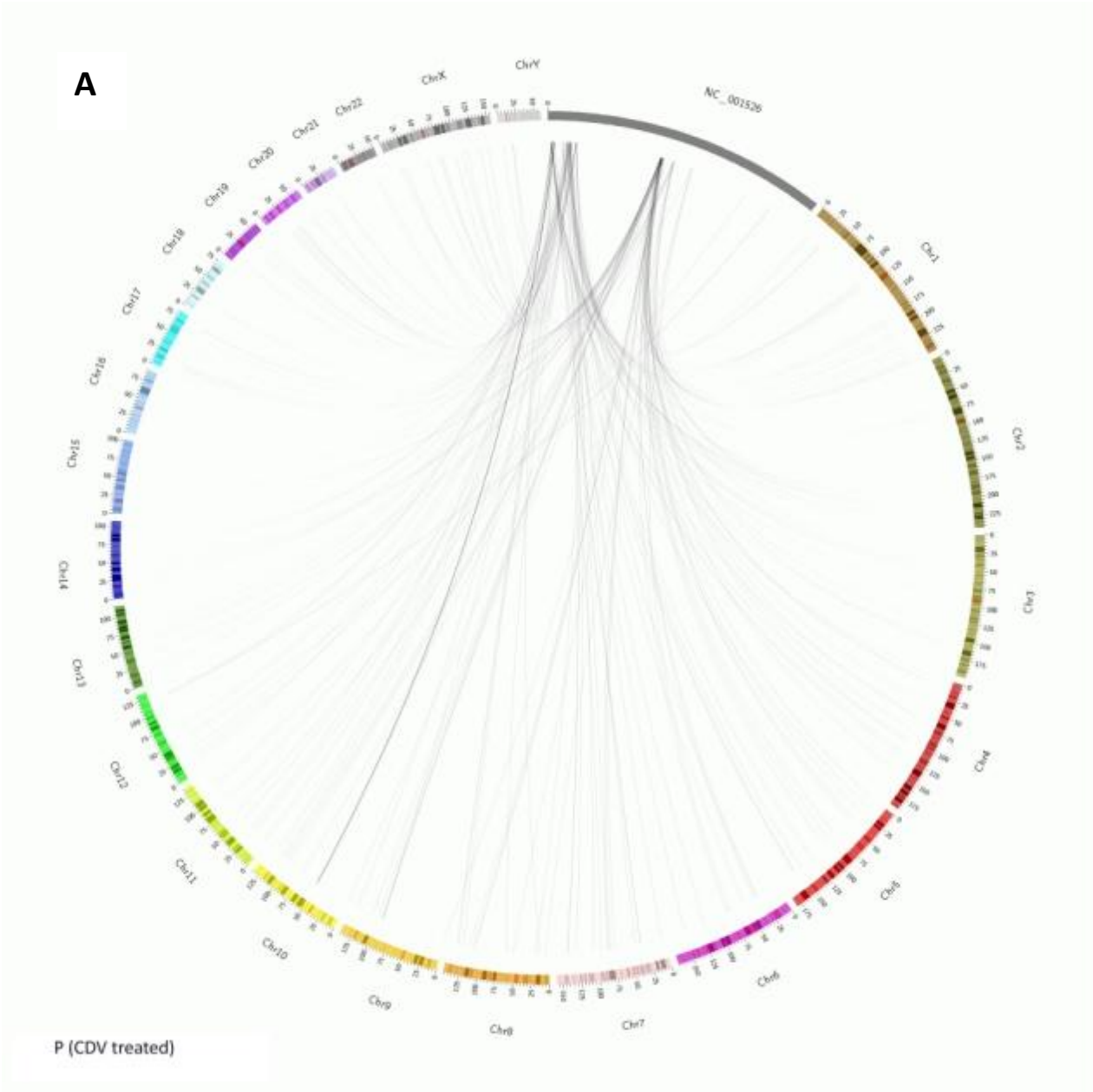
A
ChrX
ChrY
NC_001526
Chr1
Chr2
Chr3
Chr4
Chr5
Chr6
Chr7
Chr8
Chr9
Chr10
Chr11
Chr12
Chr13
Chr14
Chr15
Chr16
Chr17
Chr18
Chr19
Chr20
Chr21
Chr22
P (CDV treated)

B

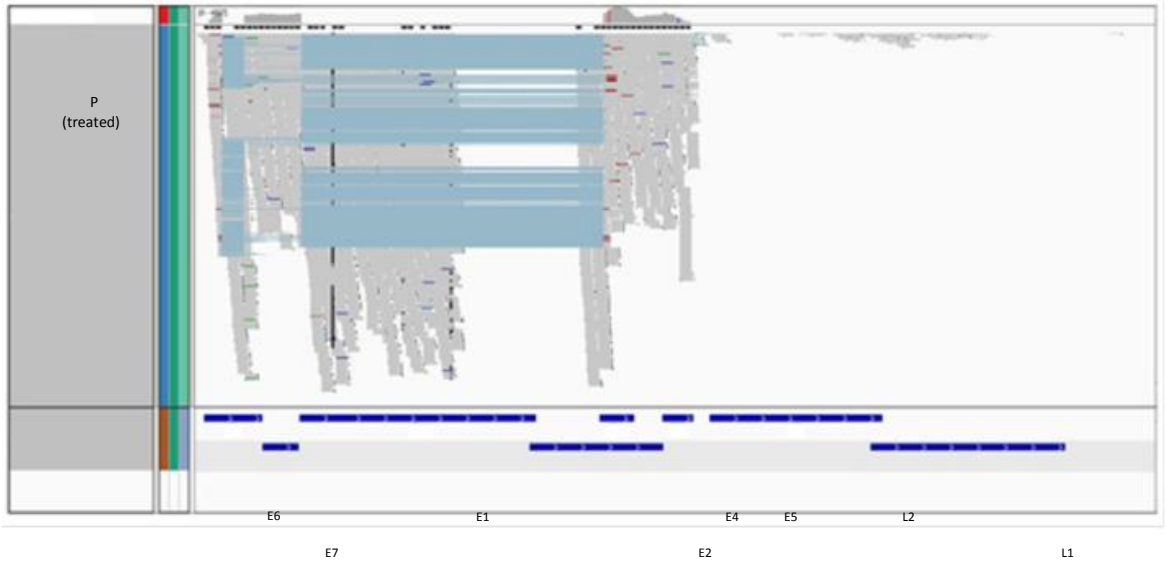

Figure 8.5. SOLiD™ transcript data for P08 visualised as Circos plots and through Integrative Genomic Viewer (IGV).

Linkage between HPV genome and the human genome in untreated P08 illustrated as a Circos plot (**A**), and through Integrative Genomic Viewer (IGV) as a split-screen shot used to visualise mapped locations of HPV-human fused transcripts (**B**). In Circos plots, possible HPV integrated transcripts were represented by grey lines connecting the HPV genome (downloaded from NCBI, accession no: NC_001526.2) with chromosomes (chr) of the human genome (UCSC human reference hg19 site). Multiple grey lines connected HPV genome with chromosome 10, illustrated by a dark grey streak suggesting an integrated transcript. Single grey lines also linked HPV with other regions of the human genome. In IGV, the same reference genomes were used to define transcript locations; transcript reads that mapped within expectation are represented by gray shaded tags whilst those mapping over extended distances are illustrated as multiple coloured tags, and the colour used indicates the chromosome to which the transcript corresponded. Transcript fusion was only detected between HPV E6, E7 and E4 (pale blue horizontal lines linking HPV transcripts), illustrating multiple episomal fused constructs. Multiple coloured tags were not visible, suggesting the absence of integrated fused transcripts.

8.3.3 Differential gene expression

Differentially expressed genes were identified between CDV treated and untreated samples of M08; differentially expressed genes could not be assessed in P08 as sequence data was not generated for the untreated sample. As part of DEG analysis, corrected p-values were used to identify transcripts that showed a significant difference between the mean expression of untreated compared to CDV treated. The data was filtered using a false discovery rate (FDR) multiple testing correction and a cut-off of $p<0.05$, to identify transcripts where there was 95% certainty of there being a real difference in expression and an FDR of 5%. A heatmap showing the results of this analysis is shown in Appendix VIII.

In total 39688 transcripts were tested, 2158 were significant at $p<0.05$, and after FDR correction ($p<0.05$) 66 gene transcripts were identified as being statistically differentially expressed after treatment with CDV in M08. Of these 66, genes with a large range of apparently unrelated functions were found to be significantly under-expressed due to CDV treatment. Among a large number of poorly annotated genes, this list included genes for matrix proteins (*PRELP*), transmembrane proteins and sodium channel subunits (*TMEM174*, *SCN2A*), heparanases (*HPSE*), heme group catabolism (*HMOX1*), gemini bodies (*GEMIN4*), histone components (*H2BFM*), potential tumour suppressors (*CSMD1*) and coagulation factor receptors (*F2RL3*) and nucleotide metabolism (*RGL1*). Only two significantly overexpressed genes were observed, these encoded chemokines (*CCL20*) and deoxyguanosine kinase that is involved in maintaining mitochondrial DNA (*DGUOK*). Cell cycle control genes encoding cyclin dependent kinases, cyclins, DNA polymerases, p53, telomerase and others relating to cellular CDV phosphorylation (i.e. NME1/NME2, guanylate kinases etc) were not found to be significantly differently expressed.

8.3.3.1 *Main findings*

A range of genes were significantly differentially expressed as a result of CDV treatment in M08, however no biological mechanism was apparent. This justified further a more directed means of analysing overexpressed genes through GO analysis.

8.3.4 Gene Ontology – Over Representation Analysis (GO ORA)

The list of genes found to be differentially expressed in CDV dosed M08 was difficult to interpret, therefore GO ORA was applied to the significant gene transcripts to sort them in to GO categories; GO ORA identified groups of functionally or structurally related genes that were differentially expressed. This made assessment more relevant from a biological perspective and easier to interpret by identifying potential relationships between gene transcripts.

In total, 374 categories were identified as differentially expressed in M08 as a result of CDV treatment. The top 500 most significant ($p<0.05$) individual gene transcripts underwent GO ORA. GO categories were identified using the database at the Gene Ontology project that related to various search terms (The Gene Ontology Consortium, 2013).

Initially, only the top 20 most significant GO categories were considered Table 8.1. Of the 20 GO categories, 12 (60%) were found to be related to adenine and guanine nucleotide biosynthesis, nucleobase metabolic process, RNA polymerase activity, and DNA-directed RNA polymerase II. These encompassed all 3 GO groups (BP, CC, and MF). The gene *DGUOK* listed under the GO term 'nucleobase metabolic process', was overexpressed 2577 fold in CDV treated M08 compared to no treatment, and was also present in the top 66 significantly expressed genes.

Among the 374 GO categories identified were four which related to senescence. These categories were (CC) senescence-associated heterochromatin focus, (BP) senescence-

GOID	Ontology	Term	p.value
GO:0003938	MF	IMP,dehydrogenase,activity	0.000227
GO:0003899	MF	DNA-directed,RNA,polymerase,activity	0.000387
GO:0034062	MF	RNA,polymerase,activity	0.000387
GO:0021891	BP	olfactory,bulb,interneuron,development	0.001128
GO:0005665	CC	DNA-directed,RNA,polymerase,II,,core,complex	0.001367
GO:0006177	BP	GMP,biosynthetic,process	0.001446
GO:0033129	BP	positive,regulation,of,histone,phosphorylation	0.001907
GO:0009112	BP	nucleobase,metabolic,process	0.002108
GO:0014805	BP	smooth,muscle,adaptation	0.00215
GO:0000428	CC	DNA-directed,RNA,polymerase,complex	0.002532
GO:0055029	CC	nuclear,DNA-directed,RNA,polymerase,complex	0.002532
GO:0046037	BP	GMP,metabolic,process	0.002576
GO:0021889	BP	olfactory,bulb,interneuron,differentiation	0.002614
GO:0030880	CC	RNA,polymerase,complex	0.002617
GO:0006385	BP	transcription,elongation,from,RNA,polymerase,III, promoter	0.002816
GO:0006386	BP	termination,of,RNA,polymerase,III,transcription	0.002816
GO:0071496	BP	cellular,response,to,external,stimulus	0.003371
GO:0031401	BP	positive,regulation,of,protein,modification,process	0.003675
GO:0061042	BP	vascular,wound,healing	0.003765
GO:0070534	BP	protein,K63-linked,ubiquitination	0.003893

Table 8.1. Top 20 most significant Gene Ontology groupings

Based on 500 most significantly differentially expressed transcripts. BP = biological process, CC = cellular component and MF = molecular function.

associated heterochromatin focus assembly, (BP) cell aging and (BP) aging which are broadly associated withcharacteristics of cellular senescence. No evidence of differential expression of GO groups relating to apoptosis or DNA repair was observed.

8.3.4.1 *Main findings*

In the top 500 most significant gene transcripts of 374 GO categories, 4 categories were associated with cellular senescence. Over half of the 20 most significant GO categories appeared to be associated with nucleotide synthesis and processing, and the remaining associated with RNA polymerase activity.

8.4 Discussion

The main findings of these investigations were:

1. RNA sequence data was not generated for sample corresponding to untreated P08.
2. The quality of sequence data was below threshold value for all samplesn but deemed suitable for anaylsis, here.
3. There was consensus between HPV gene expression visualised through IGV and qRT-PCR, confirming:
    i. expression of E6 and E7 and absence of E2, in M08.
    ii. Expression of E4, E5, E6 and E7 in P08, and presence of partial transcripts of E2.
4. There was consensus between HPV integration status determined by sequencing and APOT for:
    i. integrated transcripts of E7-3q28 (*LEPREL1*) in M08
    ii. episomal HPV transcripts corresponding to E7-E1 spliced to E4 in P08.

5. DEG analysis and GO ORA showed that a large percentage of the top 20 most significant GO categories were involved in nucleotide synthesis and processing and RNA polymerase activity.
6. DEG analysis and GO ORA showed that 4 GO categories relating to cellular senescence were found over 300 GO categories comprising the top 500 most significant gene transcripts.

The aims of performing RNA sequencing on M08 and P08 were to confirm HPV gene expression and integration status, which had previously been characterised using other molecular techniques. RNA sequencing was considered a sensitive method with which to validate data from qRT-PCR and APOT. Also, this study made an attempt to define the molecular mechanism(s) of action of CDV by investigating the transcriptomes of CDV treated and untreated cells using differential gene expression and GO analyses. Exploring the entire transcriptome without restriction to predefined hypotheses could potentially identify unknown mechanism(s) of action of CDV at a molecular level.

8.4.1 Failure to generate sequence data and low data yield

Total RNA extracts underwent SOLiD™ RNA-seq but sequence data was not generated for 1/4 samples. This was due to an error in library preparation. Unfortunately insufficient RNA was available for this procedure to be repeated.

SOLiD™ RNA-seq generated sequence data for 3/4 total RNA extracts, but the sequence data was of low data yield and reduced read quality; this refers to the quantity of sequence data obtained and how well the sequence data mapped to reference. The minimum sequencing yield specified post sequencing varies, and is crudely estimated and dependent on the sensitivity of an experiment. RNA-sequencing data sets tend to map less well to reference due to more frequent occurrence of low quality reads and sequence artefacts which can contribute

to reduced sequence read quality. The quality of the RNA undergoing RNA-seq (i.e. partially degraded RNA) might otherwise affect the quantity of the sequence data generated, and might have occurred after RNA integrity had been investigated, prior to being sequenced.

8.4.2 Strengths and weaknesses

Techniques such as 'first generation' Sanger-sequencing and RNA microarrays have been used to generate transcript profiles of cells but are limited to predefined selections of genes (i.e. the primer sequences present in the amplification, or on the microarray). RNA sequencing provides a sensitive, high throughput technique of transcriptome profiling (Wang et al., 2009)with advantages over other methods, including the generation of transcripts comprising the entire transcriptome, quantifying and mapping transcripts more precisely, the potential to identify transcript splice variants, and assess differential gene expression. Thus far RNA-seq has been used to characterise the transcriptomes of a small selection of eukaryotic organisms (Mortazavi et al., 2008, Nagalakshmi et al., 2008), and this was the first time HPV16 infected vulval and vaginal keratinocyte cells had undergone transcriptome sequencing.

Sequence data for untreated P08 was not generated, therefore a comparison between CDV treated and untreated cells of P08 could not be carried out. Hence assessments of HPV genes expressed and HPV integration status using sequence data for CDV treated P08. This was not thought to influence the data but it is possible that both integration and HPV gene expression could be altered by CDV treatment.

RNA sequencing data validated HPV integration data previously determined by APOT, and qRT-PCR HPV gene expression data, this increased confidence in all of the techniques used. There were some discrepancies identified with APOT data when RNA-seq data was visualised as Circos plots to illustrate HPV and human fused transcripts, i.e. Circos plots suggested the presence of low frequency integration events that were not detected by APOT or visualised

using IGV. These data were interpreted as low-frequncy integrations events (in Circos plots 1 link = 1 mapped transcript) but equally they could potentially be artefacts of the RNA-seq process. This could potentially be determined by examination of RNA-seq data sets from cell lines that were HPV untransformed and genetically stable.

In P08, transcripts were mapped to only a short region of E2. E2 PCR data previously showed that a truncated E2 fragment was present in P08 and integrated transcripts were not detected via APOT (episomal E7-E1 spliced to E4 transcripts were detected). RNA-seq data visualised through IGV also confirmed the episomal transcript described, however when visualised through Circos plots, multiple linkages (= multiple transcripts) were observed between HPV E6/E7 and a region in chromosome 10. Integration at this site was not confirmed due to time restrictions. It was thought that integration disrupting E2 would result in loss of transcription of downstream ORF. However, transcripts of E4 and E5, were detected in P08 through qRT-PCR and confirmed through IGV. This potential integrated transcript was not explored further due to project time restrictions, but interrogation of RNA with primers mapping to this integration loci would provide interesting future work and contribute to fully characterising P08.

The main weakness of these analyses was the small sample size, lack of replicates and the fact that with the exception of HPV gene expression, data were not confirmed by independent qPCRs.

8.4.3 Reponse to CDV in M08

The GO analysis showed that following CDV treatment genes belonging to several ontologies were significantly over-represented. These ontologies included several relating to nucleotide synthesis and processing, and RNA polymerase activity. CDV is an nucleotide analogue and therefore competes with natural nucleotides (adenine, guanine, cytosine and thymidine), during DNA synthesis by incorporating in to the extending DNA strand. Classically, CDV is a

prodrug and required phosphorylation before it is activated, and has a high affinitiy for viral RNA polymerase. It has also been shown to have affinitiy (but relatively less) for human RNA polymerase. It could be proposed that expression of genes involved in nucleotide metabolism might be altered just as a result of adding a nucleotide analogue to the media through dosing cells in culture with CDV. Similarly, RNA polymerase genes were also significantly overexpressed which may be linked with affinity of CDV for RNA polymerase. The specific gene *DGUOK* listed under 'nucleobase metabolic process' was overexpressed significantly. The protein product of *DGUOK* has previously shown to be required for the phosphorylation of several deoxyribonucleosides and certain nucleotide analogues widely employed as antiviral and chemotherapeutic agents (Van Rompay et al., 2003). This could suggest that considerable over expression of *DGUOK* might be linked to phosphorylation of CDV into the active form.

One other study has previously examined the transcriptional response to CDV using genome wide technology. This was a study by De Schutter and colleagues, which examined SiHa (HPV16+), HeLa (HPV18+) and HaCaT (HPV negative) immortalized cell lines and primary human keratinocytes 24, 48 and 72 hours after treatment with 50 µg/mL (159 µM) CDV usng whole genome gene expression microarrays, with validation of the array data by qRT-PCR De Schutter (De Schutter et al., 2013). In SiHa cells twenty genes showed similar changes in expression in both the 48 and 72 hour samples. Expression was also examined in HeLa, HaCaT and normal keratinocytes at 72 hours. Only 2 genes (*AOX1* and *CLIC3*) were differentially expressed in all 4 cell lines. GO analysis of differentially expressed genes showed 'immune response' and 'inflammatory response' to be the only functional groupings up-regulated in all four cell lines. Further functional analysis showed that HPV positive cells showed differential regulation of genes linked to "cell death of tumour cells" following CDV treatment. It is not clear why there was little consistency between the De Schutter study and the current investigation, though it was notable that the published study used both higher doses and

longer treatment periods. The time period of 12 hours was chosen for the current study to ensure that changes in expression related to a response to CDV rather than showing characteristics of cells that had survived CDV treatment.

It was perhaps surprising that genes involved in DNA damage and stress responses did not appear to be effected by CDV treatment, given that cells were treated with an IC_{50} equivalent dose of CDV more noticeable effects were expected. It might be possible that such effects might have been noted if a longer or shorter time frame had been examined or if higher or lower doses of CDV had been examined.

9 General discussion

The aims of this study were to develop novel *in vitro* models of HPV-associated vulval and vaginal neoplasia and to use them to investigate the mechanism of action of the nucleoside analogue Cidofovir.

Working with early passage short term cell lines was technically challenging and time consuming. Nonetheless, clonal cell lines were successfully isolated from heterogeneous vulval and vaginal cell lines and were characterised with respect to HPV integration state and gene expression. These analyses suggested that the clones differed in terms of HPV integration state, integration sites and in patterns of gene expression. These cells lines represent the best available models with which to investigate the molecular biology and treatment of HPV associated early stage neoplasia. Potential advantages of the clonal lines include the small number of passages between their derivation and use, and the fact that they were derived from neoplasia rather than cancers. It is also potentially useful that different patterns of HPV gene expression were present, as this may allow investigation of how potential therapeutics are affected by individual HPV gene products. For instance E5 expression was absent in the M08 line; E5 expression has a dramatic effect on the composition of cell membranes (DiMaio and Petti, 2013) and may affect uptake of drugs across the cell membrane. Whether HPV is integrated or episomal is also likely to influence response to drug treatments, as treatments that induce an interferon mediated response are likely to result in clearance of episomal HPV infection, but may be less effective in the presence of integrated infections (Pett et al., 2006)

It appears likely that clonal lines representing episomal and integrated infection were derived for PC09 and these are likely to be useful in investigating the effects of integration on HPV gene expression (as has been the case for the CIN1-derived W12 cell line (Pett and Coleman,

2007). For the majority of the study it appeared that episomal and integrated lines had also been derived from PC08, however the E2 PCR sequencing and mRNA sequencing data sets, obtained towards the end of the project, suggest that clonal line P08 actually contains integrated HPV. This shows that DIPS and APOT failed to detect integration, possibly because of the particular sequence context within which the integration event occurred. The failure of APOT and DIPS to detect this integration event does not appear to be due to the sensitivity of the assays, as the failure of the E2 PCRs to amplify any product except the truncated one, suggests that this event was present in every cell.

A further strength is that these lines represent true natural infections, with HPV gene expression under the control of native promotor in the natural target cell. This is a significant advantage over artificial systems where HPV genes are placed under the control of non-native promotors in cells that are not the natural target.

The clonal cell lines do have several limitations as models of neoplasia. For instance, they are likely to be less useful in the study of agents that induce cell-mediated immune responses, as immune effector cells are not present in monolayer cultures. Furthermore, when grown in a monolayer cells do not accurately recapitulate a stratified epithelium and this also limits the accuracy of the model. Despite being genetically and temporally close to the original biopsy, a degree of selection will have occurred during the development of these lines as only cells that survived single cell cloning and grew rapidly thereafter were used.

A dose of 10 μM was used to investigate the effects of CDV on cell proliferation, morphology and gene expression. These studies demonstrated that:

1. CDV reduced cell proliferation in all four HPV-positive clonal lines and also in the HPV negative HEK cells. The surviving fractions at 36 hrs ranged from 49% to 76% for the HPV positive lines. The surviving fraction for the HEK cells was 62%. Overall response

to CDV in terms of cell viability was comparable in HPV positive and HPV negative lines; a specific increased sensitivity for CDV to HPV positive cell lines was not found, here.

2. CDV treatment did not cause significant reduction in expression of HPV E6 or E7. In the P08 cell line, treatment appeared to significantly increase E6 and E7 mRNA levels at one timepoint.
3. CDV treatment at this dose did not appear to have major effects on the host cell transcriptome.

There was no evidence that CDV was selective for HPV positive cells. This is in marked contrast to observations made in clinical practice. In the RT3VIN clinical trial (UK, 2013) approximately half of the patients treated with CDV showed a complete histological response, which was preceded by ulceration of the lesion, but not of surrounding normal tissue (Dr Amanda Tristram – RT3VIN Chief Investigator – personal communication). Both HPV positive and negative cells responded to CDV treatment *in vitro*, but *in vivo* normal cells are apparently unaffected; this could mean that the cell line model was inadequate. Specifically this appears to suggest that the model of normal cells, rather than the model of HPV infected cells could be at fault. The likely explanation for this difference is the presence *in vivo* of a fully stratified squamous epithelium with an intact stratum corneum composed of fully differentiated keratinised cells at the epithelial surface.

A study by Cundy and colleagues (Cundy et al., 1997) investigated uptake of radiolabelled CDV following topical application of a 1% CDV gel to the skin of rabbits. Uptake through intact and abraded skin was assessed in two groups each containing four rabbits. The final bioavailability of CDV in the intact skin group was 2.1% of the applied dose, however in the abraded skin group final bioavailability was increased 20 fold to 41%. The half-life of CDV applied in this way was 2.61 hours relative to an intravenous half-life of 5.4 hours. The authors interpreted these

findings as suggesting rapid absorption of the topical drug across the skin was facilitated when the stratum corneum was removed. They explained these observations by noting that CDV is a dianion at physiological pH and in the presence of an intact stratum corneum, the highly polar molecule displays low permeability. A similar study of topical uptake of 1% CDV across mouse skin also observed considerable increases in uptake (400 fold increase) following tape stripping of the stratum (Aspe et al. 1999).

These data may be highly relevant in the context of the current study, and may suggest that where proliferating cells are exposed at the epithelial surface (which they are, by definition, in VIN3) they are likely to be more vulnerable to the effects of CDV than when they are protected by an intact stratum corneum. The presence or absence of an intact cornified layer would hence explain the contrasting results observed in clinical practice and *in vitro*.

The mRNA sequencing data provided useful confirmation that the earlier assays had been conducted properly. However it is puzzling as to why greater differences were not observed in gene expression between the CDV treated and untreated samples. The dose used was sufficient to reduce proliferation of the treated sample by 50% and it seems highly unusual that this could occur without causing more significant changes in gene expression. This may suggest that the time frame for sampling (12 hours) was too short or the dose was too low. Higher doses and longer time frames were used in a similar study that did identify significant changes in the gene expression (De Schutter et al., 2013). This raises the question of, what constitutes the correct dose? In the context of this project, the correct dose is the one that most accurately approximates the dose received *in vivo*. In the RT3VIN clinical trial, patients applied 1% CDV gel, hence the maximum dose possible, assuming a single application represents around 1 gram of gel, would be 1% of 1 g = 10 mg. If CDV was taken into cells at the maximum level seen in animal studies this would equate to a maximum possible dose of 10 mg x 0.021 = 210 µg. It is difficult to relate this to the concentrations used in cell culture, as this

dose would be spread over lesions that may vary considerably in size and uptake through rabbit skin may be different to uptake through human skin, but it suggests that the dose of 10 µM (which equates to 3.15 µg/ml) may be towards the lower end of the physiologically relevant range. It should also be noted that the relevance of *in vitro* data may also be limited by the short time frames used for dosing studies. In the RT3VIN trial, patients applied CDV three times per week for 24 weeks. This could not be replicated *in vitro* because long-term low level dosing with CDV would be likely to produce resistance (as recently described for SiHa cells by De Schutter et al. 2013) while excessive repetitive dosing with CDV would be likely to kill the population. Additionally it would have been impossible to relate such data to undosed controls which would quickly have become confluent.

It therefore seems that while this study has produced data that contradicts several of the proposed mechanisms of action of CDV, i.e. reduced expression of HPV E6 and E7 (Abdulkarim et al., 2002, Amine et al., 2009) and induction of apoptosis (Andrei et al., 2000, Amine et al., 2009) has not produced data to conclusively support an alternative mechanism. Future work would be useful to study uptake of CDV through cornified epithelia and this could be achieved using organotypic raft cultures that have recently been developed in our laboratory.

9.1 Conclusion

A selection of early passage clonal cell lines derived from VIN3 and VaIN3 lesions were successfully isolated and maintained in culture, representing a novel cell culture system of vulval and vaginal neoplasia. They have been shown to comprise a selection of unique naturally occurring HPV16 infected cell lines with differing phenotypic and molecular characteristics. A CDV dosing protocol was optimised in these cell lines and was used to assess cellular response(s) to CDV treatment. Under the conditions described CDV did cause a reduction in cell viability, although the mechanism of action could not be confirmed; based on

viable counts, cells infected with and without HPV were found to be sensitivie to CDV treatment. Under the conditions described, it cannot be confirmed whether CDV induces apoptosis. CDV did not appear to reduce E6 and E7 expression levels. Cell enlargement was observed in response to CDV treatment also. DEG analysis showed that 60% of the top 20 most significant gene transcripts were azssocaited with nucleotide syntheses and RNA polymerase activity. Additionally, 300 GO categories comprising the top 500 most significant gene transcripts were associated with cellular senescence. The actual mechanism by which CDV reduces cell proliferation requires further investigation.

References

ABDULKARIM, B., SABRI, S., DEUTSCH, E., CHAGRAOUI, H., MAGGIORELLA, L., THIERRY, J., ESCHWEGE, F., VAINCHENKER, W., CHOUAIB, S. & BOURHIS, J. 2002. Antiviral agent Cidofovir restores p53 function and enhances the radiosensitivity in HPV-associated cancers. *Oncogene,* 21**,** 2334-46.

ALAZAWI, W., PETT, M., ARCH, B., SCOTT, L., FREEMAN, T., STANLEY, M. A. & COLEMAN, N. 2002. Changes in cervical keratinocyte gene expression associated with integration of human papillomavirus 16. *Cancer Res,* 62**,** 6959-65.

ALITALO, K., KUISMANEN, E., MYLLYLA, R., KIISTALA, U., ASKO-SELJAVAARA, S. & VAHERI, A. 1982. Extracellular matrix proteins of human epidermal keratinocytes and feeder 3T3 cells. *J Cell Biol,* 94**,** 497-505.

ALLEN, D., WINTERS, E., KENNA, P. F., HUMPHRIES, P. & FARRAR, G. J. 2008. Reference gene selection for real-time rtPCR in human epidermal keratinocytes. *J Dermatol Sci,* 49**,** 217-25.

AMERICAN TYPE CULTURE COLLECTION (ATCC). 2012a. *C-33A* [Online]. [Accessed].

AMERICAN TYPE CULTURE COLLECTION (ATCC). 2012b. *CaSki* [Online]. [Accessed].

AMERICAN TYPE CULTURE COLLECTION (ATCC). 2012c. *HeLa* [Online]. [Accessed].

AMERICAN TYPE CULTURE COLLECTION (ATCC). 2012d. *SiHa* [Online]. [Accessed].

AMINE, A., RIVERA, S., OPOLON, P., DEKKAL, M., BIARD, D. S., BOUAMAR, H., LOUACHE, F., MCKAY, M. J., BOURHIS, J., DEUTSCH, E. & VOZENIN-BROTONS, M. C. 2009. Novel anti-metastatic action of cidofovir mediated by inhibition of E6/E7, CXCR4 and Rho/ROCK signaling in HPV tumor cells. *PLoS One,* 4**,** e5018.

ANDREI, G., SNOECK, R., PIETTE, J., DELVENNE, P. & DE CLERCQ, E. 1998. Antiproliferative effects of acyclic nucleoside phosphonates on human papillomavirus (HPV)-harboring cell lines compared with HPV-negative cell lines. *Oncol Res,* 10**,** 523-31.

ANDREI, G., SNOECK, R., SCHOLS, D. & DE CLERCQ, E. 2000. Induction of apoptosis by cidofovir in human papillomavirus (HPV)-positive cells. *Oncol Res,* 12**,** 397-408.

ANDREI, G., SNOECK, R., SCHOLS, D. & DE CLERCQ, E. 2001. Induction of apoptosis by cidofovir in human papillomavirus (HPV)-positive cells. *Oncology Research,* 12**,** 397-408.

ASHBURNER, M., BALL, C. A., BLAKE, J. A., BOTSTEIN, D., BUTLER, H., CHERRY, J. M., DAVIS, A. P., DOLINSKI, K., DWIGHT, S. S., EPPIG, J. T., HARRIS, M. A., HILL, D. P., ISSEL-TARVER, L., KASARSKIS, A., LEWIS, S., MATESE, J. C., RICHARDSON, J. E., RINGWALD, M., RUBIN, G. M. & SHERLOCK, G. 2000. Gene ontology: tool for the unification of biology. The Gene Ontology Consortium. *Nat Genet,* 25**,** 25-9.

ASHIDA, S., FURIHATA, M., KATAGIRI, T., TAMURA, K., ANAZAWA, Y., YOSHIOKA, H., MIKI, T., FUJIOKA, T., SHUIN, T., NAKAMURA, Y. & NAKAGAWA, H. 2006. Expression of novel molecules, MICAL2-PV (MICAL2 prostate cancer variants), increases with high Gleason score and prostate cancer progression. *Clin Cancer Res,* 12**,** 2767-73.

ASHRAFI, G. H., TSIRIMONAKI, E., MARCHETTI, B., O'BRIEN, P. M., SIBBET, G. J., ANDREW, L. & CAMPO, M. S. 2002. Down-regulation of MHC class I by bovine papillomavirus E5 oncoproteins. *Oncogene,* 21**,** 248-59.

BALLATORE, C., MCGUIGAN, C., DE CLERCQ, E. & BALZARINI, J. 2001. Synthesis and evaluation of novel amidate prodrugs of PMEA and PMPA. *Bioorganic & medicinal chemistry letters,* 11**,** 1053-6.

BASTIEN, N. & MCBRIDE, A. A. 2000. Interaction of the papillomavirus E2 protein with mitotic chromosomes. *Virology,* 270**,** 124-34.

BENJAMINI, Y. & HOCHBERG, Y. 1995. Controlling the false discovery rate: a practical and powerful approach to multiple testing. *Journal of the Royal Statistical Society,* 57**,** 289-300.

BORLAK, J., MEIER, T., HALTER, R., SPANEL, R. & SPANEL-BOROWSKI, K. 2005. Epidermal growth factor-induced hepatocellular carcinoma: gene expression profiles in precursor lesions, early stage and solitary tumours. *Oncogene,* 24**,** 1809-19.

BRENTJENS, M. H., YEUNG-YUE, K. A., LEE, P. C. & TYRING, S. K. 2002. Human papillomavirus: a review. *Dermatol Clin,* 20**,** 315-31.

BRONCKAERS, A., BALZARINI, J. & LIEKENS, S. 2008. The cytostatic activity of pyrimidine nucleosides is strongly modulated by Mycoplasma hyorhinis infection: Implications for cancer therapy. *Biochemical Pharmacology,* 76**,** 188-197.

BRUCHIM, I., GOTLIEB, W. H., MAHMUD, S., TUNITSKY, E., GRZYWACZ, K. & FERENCZY, A. 2007. HPV-related vulvar intraepithelial neoplasia: outcome of different management modalities. *Int J Gynaecol Obstet,* 99**,** 23-7.

BRUNI, L., DIAZ, M., CASTELLSAGUE, X., FERRER, E., BOSCH, F. X. & DE SANJOSE, S. 2010. Cervical human papillomavirus prevalence in 5 continents: meta-analysis of 1 million women with normal cytological findings. *J Infect Dis,* 202**,** 1789-99.

BURD, E. M. 2003. Human papillomavirus and cervical cancer. *Clin Microbiol Rev,* 16**,** 1-17.

BURDALL, S. E., HANBY, A. M., LANSDOWN, M. R. & SPEIRS, V. 2003. Breast cancer cell lines: friend or foe? *Breast Cancer Res,* 5**,** 89-95.

CALISTA, D. 2009. Topical 1% cidofovir for the treatment of vulvar intraepidermal neoplasia (VIN1) developed on lichen sclerosus. *Int J Dermatol,* 48**,** 535-6.

CAMPION, M. J. & SINGER, A. 1987. Vulval intraepithelial neoplasia: clinical review. *Genitourin Med,* 63**,** 147-52.

CAMPISI, J. & D'ADDA DI FAGAGNA, F. 2007. Cellular senescence: when bad things happen to good cells. *Nature reviews. Molecular cell biology,* 8**,** 729-40.

CASTELLSAGUE, X. 2008. Natural history and epidemiology of HPV infection and cervical cancer. *Gynecol Oncol,* 110**,** S4-7.

CENTERS FOR DISEASE CONTROL. 2013. *Genital HPV Infection - Fact Sheet* [Online]. Available: http://www.cdc.gov/std/hpv/stdfact-hpv.htm [Accessed 12.12.2013 2013].

CHAN, A. M., MCGOVERN, E. S., CATALANO, G., FLEMING, T. P. & MIKI, T. 1994. Expression cDNA cloning of a novel oncogene with sequence similarity to regulators of small GTP-binding proteins. *Oncogene,* 9**,** 1057-63.

CIHLAR, T. & CHEN, M. S. 1996. Identification of enzymes catalyzing two-step phosphorylation of cidofovir and the effect of cytomegalovirus infection on their activities in host cells. *Mol Pharmacol,* 50**,** 1502-10.

CLOONAN, N., FORREST, A. R., KOLLE, G., GARDINER, B. B., FAULKNER, G. J., BROWN, M. K., TAYLOR, D. F., STEPTOE, A. L., WANI, S., BETHEL, G., ROBERTSON, A. J., PERKINS, A. C., BRUCE, S. J., LEE, C. C., RANADE, S. S., PECKHAM, H. E., MANNING, J. M., MCKERNAN, K. J. & GRIMMOND, S. M. 2008. Stem cell transcriptome profiling via massive-scale mRNA sequencing. *Nat Methods,* 5**,** 613-9.

COLLINS, S. I., CONSTANDINOU-WILLIAMS, C., WEN, K., YOUNG, L. S., ROBERTS, S., MURRAY, P. G. & WOODMAN, C. B. 2009. Disruption of the E2 gene is a common and early event in the natural history of cervical human papillomavirus infection: a longitudinal cohort study. *Cancer Res,* 69**,** 3828-32.

COUTURIER, J., SASTRE-GARAU, X., SCHNEIDER-MAUNOURY, S., LABIB, A. & ORTH, G. 1991. Integration of papillomavirus DNA near myc genes in genital carcinomas and its consequences for proto-oncogene expression. *J Virol,* 65**,** 4534-8.

CUNDY, K. C., LYNCH, G. & LEE, W. A. 1997. Bioavailability and metabolism of cidofovir following topical administration to rabbits. *Antiviral Res,* 35**,** 113-22.

DALL, K. L., SCARPINI, C. G., ROBERTS, I., WINDER, D. M., STANLEY, M. A., MURALIDHAR, B., HERDMAN, M. T., PETT, M. R. & COLEMAN, N. 2008. Characterization of Naturally

Occurring HPV16 Integration Sites Isolated from Cervical Keratinocytes under Noncompetitive Conditions. *Cancer Research,* 68**,** 8249-8259.

DE CLERCQ, E. 2011. The clinical potential of the acyclic (and cyclic) nucleoside phosphonates. The magic of the phosphonate bond. *Biochemical pharmacology,* 82**,** 99-109.

DE CLERCQ, E. & HOLY, A. 2005. Acyclic nucleoside phosphonates: a key class of antiviral drugs. *Nat Rev Drug Discov,* 4**,** 928-40.

DE SANJOSE, S., ALEMANY, L., ORDI, J., TOUS, S., ALEJO, M., BIGBY, S. M., JOURA, E. A., MALDONADO, P., LACO, J., BRAVO, I. G., VIDAL, A., GUIMERA, N., CROSS, P., WAIN, G. V., PETRY, K. U., MARIANI, L., BERGERON, C., MANDYS, V., SICA, A. R., FELIX, A., USUBUTUN, A., SEOUD, M., HERNANDEZ-SUAREZ, G., NOWAKOWSKI, A. M., WILSON, G., DALSTEIN, V., HAMPL, M., KASAMATSU, E. S., LOMBARDI, L. E., TINOCO, L., ALVARADO-CABRERO, I., PERROTTA, M., BHATLA, N., AGORASTOS, T., LYNCH, C. F., GOODMAN, M. T., SHIN, H. R., VIARHEICHYK, H., JACH, R., CRUZ, M. O., VELASCO, J., MOLINA, C., BORNSTEIN, J., FERRERA, A., DOMINGO, E. J., CHOU, C. Y., BANJO, A. F., CASTELLSAGUE, X., PAWLITA, M., LLOVERAS, B., QUINT, W. G., MUNOZ, N. & BOSCH, F. X. 2013. Worldwide human papillomavirus genotype attribution in over 2000 cases of intraepithelial and invasive lesions of the vulva. *Eur J Cancer,* 49**,** 3450-61.

DE SCHUTTER, T., ANDREI, G., TOPALIS, D., NAESENS, L. & SNOECK, R. 2013. Cidofovir selectivity is based on the different response of normal and cancer cells to DNA damage. *Bmc Medical Genomics,* 6.

DE VILLIERS, E. M., FAUQUET, C., BROKER, T. R., BERNARD, H. U. & ZUR HAUSEN, H. 2004. Classification of papillomaviruses. *Virology,* 324**,** 17-27.

DE VUYST, H., CLIFFORD, G. M., NASCIMENTO, M. C., MADELEINE, M. M. & FRANCESCHI, S. 2009. Prevalence and type distribution of human papillomavirus in carcinoma and intraepithelial neoplasia of the vulva, vagina and anus: a meta-analysis. *Int J Cancer,* 124**,** 1626-36.

DEFILIPPIS, R. A., GOODWIN, E. C., WU, L. & DIMAIO, D. 2003. Endogenous human papillomavirus E6 and E7 proteins differentially regulate proliferation, senescence, and apoptosis in HeLa cervical carcinoma cells. *Journal of Virology,* 77**,** 1551-63.

DI LEONARDO, A., LINKE, S. P., CLARKIN, K. & WAHL, G. M. 1994. DNA damage triggers a prolonged p53-dependent G1 arrest and long-term induction of Cip1 in normal human fibroblasts. *Genes Dev,* 8**,** 2540-51.

DIMAIO, D. & PETTI, L. M. 2013. The E5 proteins. *Virology,* 445**,** 99-114.

DIVYA, C. S. & PILLAI, M. R. 2006. Antitumor action of curcumin in human papillomavirus associated cells involves downregulation of viral oncogenes, prevention of NFKB and AP-1 translocation and modulation of apoptosis. *Molecular Carcinogenesis,* 45**,** 320-332.

DOORBAR, J. 2005. The papillomavirus life cycle. *J Clin Virol,* 32 Suppl 1**,** S7-15.

DOORBAR, J. 2006. Molecular biology of human papillomavirus infection and cervical cancer. *Clin. Sci.,* 110**,** 525-541.

DURST, M., CROCE, C. M., GISSMANN, L., SCHWARZ, E. & HUEBNER, K. 1987. Papillomavirus sequences integrate near cellular oncogenes in some cervical carcinomas. *Proc Natl Acad Sci U S A,* 84**,** 1070-4.

EINSTEIN, M. H., CRUZ, Y., EL-AWADY, M. K., POPESCU, N. C., DIPAOLO, J. A., VAN RANST, M., KADISH, A. S., ROMNEY, S., RUNOWICZ, C. D. & BURK, R. D. 2002. Utilization of the human genome sequence localizes human papillomavirus type 16 DNA integrated into the TNFAIP2 gene in a fatal cervical cancer from a 39-year-old woman. *Clin Cancer Res,* 8**,** 549-54.

EISENHAUER, E. A., THERASSE, P., BOGAERTS, J., SCHWARTZ, L. H., SARGENT, D., FORD, R., DANCEY, J., ARBUCK, S., GWYTHER, S., MOONEY, M., RUBINSTEIN, L., SHANKAR, L.,

DODD, L., KAPLAN, R., LACOMBE, D. & VERWEIJ, J. 2009. New response evaluation criteria in solid tumours: revised RECIST guideline (version 1.1). *Eur J Cancer,* 45**,** 228-47.

EMRICH, S. J., BARBAZUK, W. B., LI, L. & SCHNABLE, P. S. 2007. Gene discovery and annotation using LCM-454 transcriptome sequencing. *Genome Res,* 17**,** 69-73.

EUROPEAN MEDICINES AGENCY. 2011. *Summary of product characteristics (Annex I)* [Online]. [Accessed].

EVANDER, M., EDLUND, K., GUSTAFSSON, A., JONSSON, M., KARLSSON, R., RYLANDER, E. & WADELL, G. 1995. Human papillomavirus infection is transient in young women: a population-based cohort study. *J Infect Dis,* 171**,** 1026-30.

FERBER, M. J., MONTOYA, D. P., YU, C., ADERCA, I., MCGEE, A., THORLAND, E. C., NAGORNEY, D. M., GOSTOUT, B. S., BURGART, L. J., BOIX, L., BRUIX, J., MCMAHON, B. J., CHEUNG, T. H., CHUNG, T. K., WONG, Y. F., SMITH, D. I. & ROBERTS, L. R. 2003a. Integrations of the hepatitis B virus (HBV) and human papillomavirus (HPV) into the human telomerase reverse transcriptase (hTERT) gene in liver and cervical cancers. *Oncogene,* 22**,** 3813-20.

FERBER, M. J., THORLAND, E. C., BRINK, A. A., RAPP, A. K., PHILLIPS, L. A., MCGOVERN, R., GOSTOUT, B. S., CHEUNG, T. H., CHUNG, T. K., FU, W. Y. & SMITH, D. I. 2003b. Preferential integration of human papillomavirus type 18 near the c-myc locus in cervical carcinoma. *Oncogene,* 22**,** 7233-42.

FERENCZY, A. & FRANCO, E. 2002. Persistent human papillomavirus infection and cervical neoplasia. *Lancet Oncol,* 3**,** 11-6.

FLORIN, L., SAPP, C., STREECK, R. E. & SAPP, M. 2002. Assembly and translocation of papillomavirus capsid proteins. *J Virol,* 76**,** 10009-14.

FRESHEY, I. R. & FRESHNEY, M. 2002. Culture of epithelial cells. *In:* FRESHNEY, R. I. F. A. M. (ed.) *Culture of specialised cells.* Wiley-liss Incorporated.

FRESHNEY, I. R. 2005a. Quantitation. *Culture of Animal Cells: A Manual of Basic Technique* John Wiley & Sons.

FRESHNEY, I. R. 2010. Cloning and Selection. *Culture of Animal Cells: A Manual of Basic Technique and Specialized Applications.* John Wiley & Sons.

FRESHNEY, R. I. (ed.) 2005b. *Culture of Animal Cells,* Hobocan: Wiley.

FRIEDL, F., KIMURA, I., OSATO, T. & ITO, Y. 1970. Studies on a new human cell line (SiHa) derived from carcinoma of uterus. I. Its establishment and morphology. *Proceedings of the Society for Experimental Biology and Medicine. Society for Experimental Biology and Medicine,* 135**,** 543-5.

FUNK, J. O., WAGA, S., HARRY, J. B., ESPLING, E., STILLMAN, B. & GALLOWAY, D. A. 1997. Inhibition of CDK activity and PCNA-dependent DNA replication by p21 is blocked by interaction with the HPV-16 E7 oncoprotein. *Genes Dev,* 11**,** 2090-100.

GECZ, J., BIELBY, S., SUTHERLAND, G. R. & MULLEY, J. C. 1997. Gene structure and subcellular localization of FMR2, a member of a new family of putative transcription activators. *Genomics,* 44**,** 201-13.

GEWIN, L. & GALLOWAY, D. A. 2001. E box-dependent activation of telomerase by human papillomavirus type 16 E6 does not require induction of c-myc. *J Virol,* 75**,** 7198-201.

GEY, G. O., COFFMAN, W. D. & KUBICEK, M. T. 1952. Tissue Culture Studies of the Proliferative Capacity of Cervical Carcinoma and Normal Epithelium. *Cancer Research,* 12**,** 264-265.

GIULIANO, A. R., TORTOLERO-LUNA, G., FERRER, E., BURCHELL, A. N., DE SANJOSE, S., KJAER, S. K., MUNOZ, N., SCHIFFMAN, M. & BOSCH, F. X. 2008. Epidemiology of human papillomavirus infection in men, cancers other than cervical and benign conditions. *Vaccine,* 26 Suppl 10**,** K17-28.

GLAXOSMITHKLINE. 2013. *Our medicines and products* [Online]. [Accessed 15.12.2013].

GRASSMANN, K., RAPP, B., MASCHEK, H., PETRY, K. U. & IFTNER, T. 1996. Identification of a differentiation-inducible promoter in the E7 open reading frame of human papillomavirus type 16 (HPV-16) in raft cultures of a new cell line containing high copy numbers of episomal HPV-16 DNA. *Journal of Virology,* 70**,** 2339-49.

GRAY, E., PETT, M. R., WARD, D., WINDER, D. M., STANLEY, M. A., ROBERTS, I., SCARPINI, C. G. & COLEMAN, N. 2010. In vitro progression of human papillomavirus 16 episome-associated cervical neoplasia displays fundamental similarities to integrant-associated carcinogenesis. *Cancer Research,* 70**,** 4081-91.

HACKAM, D. G. & REDELMEIER, D. A. 2006. Translation of research evidence from animals to humans. *JAMA,* 296**,** 1731-2.

HAFNER, N., DRIESCH, C., GAJDA, M., JANSEN, L., KIRCHMAYR, R., RUNNEBAUM, I. B. & DURST, M. 2008. Integration of the HPV16 genome does not invariably result in high levels of viral oncogene transcripts. *Oncogene,* 27**,** 1610-7.

HAMID, N. A., BROWN, C. & GASTON, K. 2009. The regulation of cell proliferation by the papillomavirus early proteins. *Cell Mol Life Sci,* 66**,** 1700-17.

HAMID, R., PATTERSON, J. & BRANDT, S. J. 2008. Genomic structure, alternative splicing and expression of TG-interacting factor, in human myeloid leukemia blasts and cell lines. *Biochim Biophys Acta,* 1779**,** 347-55.

HANSEN, R. S., CANFIELD, T. K., FJELD, A. D., MUMM, S., LAIRD, C. D. & GARTLER, S. M. 1997. A variable domain of delayed replication in FRAXA fragile X chromosomes: X inactivation-like spread of late replication. *Proc Natl Acad Sci U S A,* 94**,** 4587-92.

HAWLEY-NELSON, P., VOUSDEN, K. H., HUBBERT, N. L., LOWY, D. R. & SCHILLER, J. T. 1989. HPV16 E6 and E7 proteins cooperate to immortalize human foreskin keratinocytes. *The EMBO journal,* 8**,** 3905-10.

HAYFLICK, L. 1965. The Limited in Vitro Lifetime of Human Diploid Cell Strains. *Experimental cell research,* 37**,** 614-36.

HELLEMANS, J., MORTIER, G., DE PAEPE, A., SPELEMAN, F. & VANDESOMPELE, J. 2007. qBase relative quantification framework and software for management and automated analysis of real-time quantitative PCR data. *Genome Biol,* 8**,** R19.

HIETANEN, S., AUVINEN, E., GRENMAN, S., LAKKALA, T., SAJANTILA, A., KLEMI, P. & MAENPAA, J. 1992. Isolation of two keratinocyte cell lines derived from HPV-positive dysplastic vaginal lesions. *Int J Cancer,* 52**,** 391-8.

HILLEMANNS, P. & WANG, X. 2006. Integration of HPV-16 and HPV-18 DNA in vulvar intraepithelial neoplasia. *Gynecol Oncol,* 100**,** 276-82.

HINES, C. S., MEGHOO, C., SHETTY, S., BIBURGER, M., BRENOWITZ, M. & HEGDE, R. S. 1998. DNA structure and flexibility in the sequence-specific binding of papillomavirus E2 proteins. *J Mol Biol,* 276**,** 809-18.

HO, G. Y., BURK, R. D., KLEIN, S., KADISH, A. S., CHANG, C. J., PALAN, P., BASU, J., TACHEZY, R., LEWIS, R. & ROMNEY, S. 1995. Persistent genital human papillomavirus infection as a risk factor for persistent cervical dysplasia. *J Natl Cancer Inst,* 87**,** 1365-71.

HOLOWATY, P., MILLER, A. B., ROHAN, T. & TO, T. 1999. Natural history of dysplasia of the uterine cervix. *J Natl Cancer Inst,* 91**,** 252-8.

HOWLEY, P. M. & LOWY, D. R. 2007. *Papillomaviruses. In Field's Virology*, Lippincott Williams and Wilkins.

HUANG, L. W., CHAO, S. L. & LEE, B. H. 2008. Integration of human papillomavirus type-16 and type-18 is a very early event in cervical carcinogenesis. *J Clin Pathol,* 61**,** 627-31.

IKEDA, J., ODA, T., INOUE, M., UEKITA, T., SAKAI, R., OKUMURA, M., AOZASA, K. & MORII, E. 2009. Expression of CUB domain containing protein (CDCP1) is correlated with prognosis and survival of patients with adenocarcinoma of lung. *Cancer Sci,* 100**,** 429-33.

IKEDA, K., IYAMA, K., ISHIKAWA, N., EGAMI, H., NAKAO, M., SADO, Y., NINOMIYA, Y. & BABA, H. 2006. Loss of expression of type IV collagen alpha5 and alpha6 chains in colorectal cancer associated with the hypermethylation of their promoter region. *Am J Pathol,* 168**,** 856-65.

ILVES, I., KIVI, S. & USTAV, M. 1999. Long-term episomal maintenance of bovine papillomavirus type 1 plasmids is determined by attachment to host chromosomes, which Is mediated by the viral E2 protein and its binding sites. *J Virol,* 73**,** 4404-12.

INTERNATIONAL AGENCY FOR RESEARCH ON CANCER (IARC). 2013. *Agents Classified by the IARC Monographs* [Online]. [Accessed 28.12.2013].

INTERNATIONAL STANDARD RANDOMISED CONTROLLED TRIAL NUMBER (ISRCTN) REGISTER. 2013. *A Randomised phase II multi-centre Trial of topical treatment in women with Vulval Intraepithelial Neoplasia* [Online]. [Accessed].

IRELAND, J. A., REID, M., POWELL, R. & PETRIE, K. J. 2005. The role of illness perceptions: psychological distress and treatment-seeking delay in patients with genital warts. *Int J STD AIDS,* 16**,** 667-70.

JOHNSON, J. A. & GANGEMI, J. D. 1999. Selective inhibition of human papillomavirus-induced cell proliferation by (S)-1-[3-hydroxy-2-(phosphonylmethoxy)propyl]cytosine. *Antimicrob Agents Chemother,* 43**,** 1198-205.

JOHNSON, J. A. & GANGEMI, J. D. 2003. Alpha interferon augments cidofovir's antiviral and antiproliferative activities. *Antimicrob Agents Chemother,* 47**,** 2022-6.

JONES, H. W., JR., MCKUSICK, V. A., HARPER, P. S. & WUU, K. D. 1971. George Otto Gey. (1899-1970). The HeLa cell and a reappraisal of its origin. *Obstetrics and gynecology,* 38**,** 945-9.

JORDAN, J. & SINGER, A. 1976. *The Cervix*, The Whitefriars Press Limited London.

JOURA, E. A. 2002. Epidemiology, diagnosis and treatment of vulvar intraepithelial neoplasia. *Curr Opin Obstet Gynecol,* 14**,** 39-43.

KAJITANI, N., SATSUKA, A., KAWATE, A. & SAKAI, H. 2012. Productive Lifecycle of Human Papillomaviruses that Depends Upon Squamous Epithelial Differentiation. *Front Microbiol,* 3**,** 152.

KAMMER, C., WARTHORST, U., TORREZ-MARTINEZ, N., WHEELER, C. M. & PFISTER, H. 2000. Sequence analysis of the long control region of human papillomavirus type 16 variants and functional consequences for P97 promoter activity. *J Gen Virol,* 81**,** 1975-81.

KANG, M. K., BIBB, C., BALUDA, M. A., REY, O. & PARK, N. H. 2000. In vitro replication and differentiation of normal human oral keratinocytes. *Experimental cell research,* 258**,** 288-97.

KAUFMAN, R. H. 1995. Intraepithelial neoplasia of the vulva. *Gynecol Oncol,* 56**,** 8-21.

KERN, E. R., HARTLINE, C., HARDEN, E., KEITH, K., RODRIGUEZ, N., BEADLE, J. R. & HOSTETLER, K. Y. 2002. Enhanced inhibition of orthopoxvirus replication in vitro by alkoxyalkyl esters of cidofovir and cyclic cidofovir. *Antimicrob Agents Chemother,* 46**,** 991-5.

KINES, R. C., THOMPSON, C. D., LOWY, D. R., SCHILLER, J. T. & DAY, P. M. 2009. The initial steps leading to papillomavirus infection occur on the basement membrane prior to cell surface binding. *Proc Natl Acad Sci U S A,* 106**,** 20458-63.

KLAES, R., WOERNER, S. M., RIDDER, R., WENTZENSEN, N., DUERST, M., SCHNEIDER, A., LOTZ, B., MELSHEIMER, P. & VON KNEBEL DOEBERITZ, M. 1999. Detection of high-risk cervical intraepithelial neoplasia and cervical cancer by amplification of transcripts derived from integrated papillomavirus oncogenes. *Cancer Res,* 59**,** 6132-6.

KNIPE, D. M. & HOWLEY, P. M. 2007. *Papillomaviridae*. *Fields Virology.* 5th ed.: Lippincott Williams & Wilkins, a Wolters Kluwers Business.

KOGAN, S. C. 2007. Mouse models of acute promyelocytic leukemia. *Curr Top Microbiol Immunol,* 313**,** 3-29.

KOONSAENG, S., VERSCHRAEGEN, C., FREEDMAN, R., BOSSENS, M., KUDELKA, A., KAVANAGH, J., SITTISOMWONG, T., DECLERCQ, E. & SNOECK, R. 2001. Successful treatment of recurrent vulvar intraepithelial neoplasia resistant to interferon and isotretinoin with cidofovir. *J Med Virol,* 64**,** 195-8.

KUBBUTAT, M. H., JONES, S. N. & VOUSDEN, K. H. 1997. Regulation of p53 stability by Mdm2. *Nature,* 387**,** 299-303.

KULMALA, S. M., SYRJANEN, S. M., GYLLENSTEN, U. B., SHABALOVA, I. P., PETROVICHEV, N., TOSI, P., SYRJANEN, K. J. & JOHANSSON, B. C. 2006. Early integration of high copy HPV16 detectable in women with normal and low grade cervical cytology and histology. *J Clin Pathol,* 59**,** 513-7.

LEHMAN, C. W. & BOTCHAN, M. R. 1998. Segregation of viral plasmids depends on tethering to chromosomes and is regulated by phosphorylation. *Proc Natl Acad Sci U S A,* 95**,** 4338-43.

LI, F. L., XU, R., ZENG, Q. C., LI, X., CHEN, J., WANG, Y. F., FAN, B., GENG, L. & LI, B. 2012. Tanshinone IIA Inhibits Growth of Keratinocytes through Cell Cycle Arrest and Apoptosis: Underlying Treatment Mechanism of Psoriasis. *Evidence-based complementary and alternative medicine : eCAM,* 2012**,** 927658.

LONGWORTH, M. S. & LAIMINS, L. A. 2004. Pathogenesis of human papillomaviruses in differentiating epithelia. *Microbiol Mol Biol Rev,* 68**,** 362-72.

LOUGHRAN, O., MALLIRI, A., OWENS, D., GALLIMORE, P. H., STANLEY, M. A., OZANNE, B., FRAME, M. C. & PARKINSON, E. K. 1996. Association of CDKN2A/p16INK4A with human head and neck keratinocyte replicative senescence: relationship of dysfunction to immortality and neoplasia. *Oncogene,* 13**,** 561-8.

LUFT, F., KLAES, R., NEES, M., DURST, M., HEILMANN, V., MELSHEIMER, P. & VON KNEBEL DOEBERITZ, M. 2001. Detection of integrated papillomavirus sequences by ligation-mediated PCR (DIPS-PCR) and molecular characterization in cervical cancer cells. *Int J Cancer,* 92**,** 9-17.

MARUR, S. & FORASTIERE, A. A. 2008. Head and neck cancer: changing epidemiology, diagnosis, and treatment. *Mayo Clin Proc,* 83**,** 489-501.

MATIZONKAS-ANTONIO, L. F., LIBORIO, T. N., AQUINO XAVIER, F. C., SILVA-VALENZUELA, M., MICHALUARTE-JUNIOR, P. & NUNES, F. D. 2011. Detection of TGIF1 homeobox gene in oral squamous cell carcinoma according to histologic grading. *Oral Surg Oral Med Oral Pathol Oral Radiol Endod,* 111**,** 218-24.

MATSUKURA, T., KANDA, T., FURUNO, A., YOSHIKAWA, H., KAWANA, T. & YOSHIIKE, K. 1986. Cloning of monomeric human papillomavirus type 16 DNA integrated within cell DNA from a cervical carcinoma. *J Virol,* 58**,** 979-82.

MCBRIDE, A. A. 2013. The papillomavirus E2 proteins. *Virology,* 445**,** 57-79.

MCCLUGGAGE, W. G. 2009. Recent developments in vulvovaginal pathology. *Histopathology,* 54**,** 156-73.

MEISSNER, J. D. 1999. Nucleotide sequences and further characterization of human papillomavirus DNA present in the CaSki, SiHa and HeLa cervical carcinoma cell lines. *J Gen Virol,* 80 (Pt 7)**,** 1725-33.

MERCK SHARP & DOHME. 2013. *Gardasil [Human Papillomavirus Quadrivalent Vaccine, Recombinant]* [Online]. [Accessed 15.12.2013].

METZKER, M. L. 2010. Sequencing technologies - the next generation. *Nat Rev Genet,* 11**,** 31-46.

MEUWISSEN, R. & BERNS, A. 2005. Mouse models for human lung cancer. *Genes Dev,* 19**,** 643-64.

MINCHEVA, A., GISSMANN, L. & ZUR HAUSEN, H. 1987. Chromosomal integration sites of human papillomavirus DNA in three cervical cancer cell lines mapped by in situ hybridization. *Med Microbiol Immunol,* 176**,** 245-56.

MINNER, F. & POUMAY, Y. 2009. Candidate housekeeping genes require evaluation before their selection for studies of human epidermal keratinocytes. *J Invest Dermatol,* 129**,** 770-3.

MOHR, I. J., CLARK, R., SUN, S., ANDROPHY, E. J., MACPHERSON, P. & BOTCHAN, M. R. 1990. Targeting the E1 replication protein to the papillomavirus origin of replication by complex formation with the E2 transactivator. *Science,* 250**,** 1694-9.

MOLE, S., MCFARLANE, M., CHUEN-IM, T., MILLIGAN, S. G., MILLAN, D. & GRAHAM, S. V. 2009. RNA splicing factors regulated by HPV16 during cervical tumour progression. *J Pathol,* 219**,** 383-91.

MONSONEGO, J., CORTES, J., GREPPE, C., HAMPL, M., JOURA, E. & SINGER, A. 2010. Benefits of vaccinating young adult women with a prophylactic quadrivalent human papillomavirus (types 6, 11, 16 and 18) vaccine. *Vaccine,* 28**,** 8065-72.

MORTAZAVI, A., WILLIAMS, B. A., MCCUE, K., SCHAEFFER, L. & WOLD, B. 2008. Mapping and quantifying mammalian transcriptomes by RNA-Seq. *Nat Methods,* 5**,** 621-8.

MUNGER, K., BASILE, J. R., DUENSING, S., EICHTEN, A., GONZALEZ, S. L., GRACE, M. & ZACNY, V. L. 2001. Biological activities and molecular targets of the human papillomavirus E7 oncoprotein. *Oncogene,* 20**,** 7888-98.

MUÑOZ, N., BOSCH, F. X., CASTELLSAGUÉ, X., DÍAZ, M., DE SANJOSE, S., HAMMOUDA, D., SHAH, K. V. & MEIJER, C. J. L. M. 2004. Against which human papillomavirus types shall we vaccinate and screen? the international perspective. *International Journal of Cancer,* 111**,** 278-285.

MUNOZ, N., CASTELLSAGUE, X., DE GONZALEZ, A. B. & GISSMANN, L. 2006. Chapter 1: HPV in the etiology of human cancer. *Vaccine,* 24 Suppl 3**,** S3/1-10.

NAGALAKSHMI, U., WANG, Z., WAERN, K., SHOU, C., RAHA, D., GERSTEIN, M. & SNYDER, M. 2008. The transcriptional landscape of the yeast genome defined by RNA sequencing. *Science,* 320**,** 1344-9.

NAKAHARA, T., PEH, W. L., DOORBAR, J., LEE, D. & LAMBERT, P. F. 2005. Human Papillomavirus Type 16 E1{wedge}E4 Contributes to Multiple Facets of the Papillomavirus Life Cycle. *Journal of Virology,* 79**,** 13150-13165.

NAKAKUKI, K., IMOTO, I., PIMKHAOKHAM, A., FUKUDA, Y., SHIMADA, Y., IMAMURA, M., AMAGASA, T. & INAZAWA, J. 2002. Novel targets for the 18p11.3 amplification frequently observed in esophageal squamous cell carcinomas. *Carcinogenesis,* 23**,** 19-24.

NOUTOMI, Y., OGA, A., UCHIDA, K., OKAFUJI, M., ITA, M., KAWAUCHI, S., FURUYA, T., UEYAMA, Y. & SASAKI, K. 2006. Comparative genomic hybridization reveals genetic progression of oral squamous cell carcinoma from dysplasia via two different tumourigenic pathways. *J Pathol,* 210**,** 67-74.

OH, S. T., KYO, S. & LAIMINS, L. A. 2001. Telomerase activation by human papillomavirus type 16 E6 protein: induction of human telomerase reverse transcriptase expression through Myc and GC-rich Sp1 binding sites. *J Virol,* 75**,** 5559-66.

OSTOR, A. G. 1993. Natural history of cervical intraepithelial neoplasia: a critical review. *Int J Gynecol Pathol,* 12**,** 186-92.

PAAVONEN, J. 2007. Human papillomavirus infection and the development of cervical cancer and related genital neoplasias. *Int J Infect Dis,* 11 Suppl 2**,** S3-9.

PARKINSON, K. E. & YEUDALL, A. W. 2002. The Epidermis. *In:* FRESHNEY, I. R. & FRESHNEY, M. (eds.) *Culture of Epithelial Cells.* Wiley-liss Incorporated.

PATER, M. M., DUNNE, J., HOGAN, G., GHATAGE, P. & PATER, A. 1986. Human papillomavirus types 16 and 18 sequences in early cervical neoplasia. *Virology,* 155**,** 13-8.

PATTILLO, R. A., HUSSA, R. O., STORY, M. T., RUCKERT, A. C., SHALABY, M. R. & MATTINGLY, R. F. 1977. Tumor antigen and human chorionic gonadotropin in CaSki cells: a new epidermoid cervical cancer cell line. *Science,* 196**,** 1456-8.

PECORINIO, L. 2008. *Molecular Biology of Cancer – Mechanisms, Targets and Therapeutics*, Oxford University Press.

PEEHL, D. M. & HAM, R. G. 1980. Growth and differentiation of human keratinocytes without a feeder layer or conditioned medium. *In Vitro,* 16**,** 516-25.

PEITSARO, P., JOHANSSON, B. & SYRJANEN, S. 2002. Integrated human papillomavirus type 16 is frequently found in cervical cancer precursors as demonstrated by a novel quantitative real-time PCR technique. *J Clin Microbiol,* 40**,** 886-91.

PETT, M. & COLEMAN, N. 2007. Integration of high-risk human papillomavirus: a key event in cervical carcinogenesis? *The Journal of pathology,* 212**,** 356-67.

PETT, M. R., HERDMAN, M. T., PALMER, R. D., YEO, G. S., SHIVJI, M. K., STANLEY, M. A. & COLEMAN, N. 2006. Selection of cervical keratinocytes containing integrated HPV16 associates with episome loss and an endogenous antiviral response. *Proc Natl Acad Sci U S A,* 103**,** 3822-7.

PHELPS, W. C. & HOWLEY, P. M. 1987. Transcriptional trans-activation by the human papillomavirus type 16 E2 gene product. *J Virol,* 61**,** 1630-8.

POUND, P., EBRAHIM, S., SANDERCOCK, P., BRACKEN, M. B. & ROBERTS, I. 2004. Where is the evidence that animal research benefits humans? *BMJ,* 328**,** 514-7.

REIS, E. M., OJOPI, E. P., ALBERTO, F. L., RAHAL, P., TSUKUMO, F., MANCINI, U. M., GUIMARAES, G. S., THOMPSON, G. M., CAMACHO, C., MIRACCA, E., CARVALHO, A. L., MACHADO, A. A., PAQUOLA, A. C., CERUTTI, J. M., DA SILVA, A. M., PEREIRA, G. G., VALENTINI, S. R., NAGAI, M. A., KOWALSKI, L. P., VERJOVSKI-ALMEIDA, S., TAJARA, E. H., DIAS-NETO, E., BENGTSON, M. H., CANEVARI, R. A., CARAZZOLLE, M. F., COLIN, C., COSTA, F. F., COSTA, M. C., ESTECIO, M. R., ESTEVES, L. I., FEDERICO, M. H., GUIMARAES, P. E., HACKEL, C., KIMURA, E. T., LEONI, S. G., MACIEL, R. M., MAISTRO, S., MANGONE, F. R., MASSIRER, K. B., MATSUO, S. E., NOBREGA, F. G., NOBREGA, M. P., NUNES, D. N., NUNES, F., PANDOLFI, J. R., PARDINI, M. I., PASINI, F. S., PERES, T., RAINHO, C. A., DOS REIS, P. P., RODRIGUS-LISONI, F. C., ROGATTO, S. R., DOS SANTOS, A., DOS SANTOS, P. C., SOGAYAR, M. C., ZANELLI, C. F., HEAD & NECK ANNOTATION, C. 2005. Large-scale transcriptome analyses reveal new genetic marker candidates of head, neck, and thyroid cancer. *Cancer Res,* 65**,** 1693-9.

RHEINWALD, J. G. & GREEN, H. 1975. Serial cultivation of strains of human epidermal keratinocytes: the formation of keratinizing colonies from single cells. *Cell,* 6**,** 331-43.

RHEINWALD, J. G. & GREEN, H. 1977. Epidermal growth factor and the multiplication of cultured human epidermal keratinocytes. *Nature,* 265**,** 421-4.

RHEINWALD, J. G., HAHN, W. C., RAMSEY, M. R., WU, J. Y., GUO, Z., TSAO, H., DE LUCA, M., CATRICALA, C. & O'TOOLE, K. M. 2002. A two-stage, p16(INK4A)- and p53-dependent keratinocyte senescence mechanism that limits replicative potential independent of telomere status. *Molecular and cellular biology,* 22**,** 5157-72.

RICE, J. 2012. Animal models: Not close enough. *Nature,* 484**,** S9.

ROBERTS, I., NG, G., FOSTER, N., STANLEY, M., HERDMAN, M. T., PETT, M. R., TESCHENDORFF, A. & COLEMAN, N. 2008. Critical evaluation of HPV16 gene copy number quantification by SYBR green PCR. *BMC Biotechnol,* 8**,** 57.

ROBINSON, M. D., MCCARTHY, D. J. & SMYTH, G. K. 2010. edgeR: a Bioconductor package for differential expression analysis of digital gene expression data. *Bioinformatics,* 26**,** 139-40.

ROBLES, S. J. & ADAMI, G. R. 1998. Agents that cause DNA double strand breaks lead to p16INK4a enrichment and the premature senescence of normal fibroblasts. *Oncogene,* 16**,** 1113-23.

ROMANCZUK, H. & HOWLEY, P. M. 1992. Disruption of either the E1 or the E2 regulatory gene of human papillomavirus type 16 increases viral immortalization capacity. *Proc Natl Acad Sci U S A,* 89**,** 3159-63.

SANDERS, C. M. & STENLUND, A. 2000. Transcription factor-dependent loading of the E1 initiator reveals modular assembly of the papillomavirus origin melting complex. *J Biol Chem,* 275**,** 3522-34.

SCHAEFFER, W. I. 1990. Terminology associated with cell, tissue, and organ culture, molecular biology, and molecular genetics. Tissue Culture Association Terminology Committee. *In Vitro Cell Dev Biol,* 26**,** 97-101.

SCHEFFNER, M. 1998. Ubiquitin, E6-AP, and their role in p53 inactivation. *Pharmacol Ther,* 78**,** 129-39.

SCHEFFNER, M., HUIBREGTSE, J. M., VIERSTRA, R. D. & HOWLEY, P. M. 1993. The HPV-16 E6 and E6-AP complex functions as a ubiquitin-protein ligase in the ubiquitination of p53. *Cell,* 75**,** 495-505.

SCHEFFNER, M., WERNESS, B. A., HUIBREGTSE, J. M., LEVINE, A. J. & HOWLEY, P. M. 1990. The E6 oncoprotein encoded by human papillomavirus types 16 and 18 promotes the degradation of p53. *Cell,* 63**,** 1129-36.

SCHERL-MOSTAGEER, M., SOMMERGRUBER, W., ABSEHER, R., HAUPTMANN, R., AMBROS, P. & SCHWEIFER, N. 2001. Identification of a novel gene, CDCP1, overexpressed in human colorectal cancer. *Oncogene,* 20**,** 4402-8.

SCHILLER, J. T., DAY, P. M. & KINES, R. C. 2010. Current understanding of the mechanism of HPV infection. *Gynecol Oncol,* 118**,** S12-7.

SCHLECHT, N. F., KULAGA, S., ROBITAILLE, J., FERREIRA, S., SANTOS, M., MIYAMURA, R. A., DUARTE-FRANCO, E., ROHAN, T. E., FERENCZY, A., VILLA, L. L. & FRANCO, E. L. 2001. Persistent human papillomavirus infection as a predictor of cervical intraepithelial neoplasia. *JAMA,* 286**,** 3106-14.

SCHMITZ, M., DRIESCH, C., JANSEN, L., RUNNEBAUM, I. B. & DURST, M. 2012. Non-random integration of the HPV genome in cervical cancer. *PLoS One,* 7**,** e39632.

SCHNEIDER-MAUNOURY, S., CROISSANT, O. & ORTH, G. 1987. Integration of human papillomavirus type 16 DNA sequences: a possible early event in the progression of genital tumors. *J Virol,* 61**,** 3295-8.

SCHWARTZ, S. 2000. Regulation of human papillomavirus late gene expression. *Ups J Med Sci,* 105**,** 171-92.

SHAH, R., SMITH, P., PURDIE, C., QUINLAN, P., BAKER, L., AMAN, P., THOMPSON, A. M. & CROOK, T. 2009. The prolyl 3-hydroxylases P3H2 and P3H3 are novel targets for epigenetic silencing in breast cancer. *Br J Cancer,* 100**,** 1687-96.

SHRIVASTAV, M., DE HARO, L. P. & NICKOLOFF, J. A. 2008. Regulation of DNA double-strand break repair pathway choice. *Cell Res,* 18**,** 134-47.

SHYLASREE, T. S., KARANJGAOKAR, V., TRISTRAM, A., WILKES, A. R., MACLEAN, A. B. & FIANDER, A. N. 2008. Contribution of demographic, psychological and disease-related factors to quality of life in women with high-grade vulval intraepithelial neoplasia. *Gynecol Oncol,* 110**,** 185-9.

SKIADOPOULOS, M. H. & MCBRIDE, A. A. 1998. Bovine papillomavirus type 1 genomes and the E2 transactivator protein are closely associated with mitotic chromatin. *J Virol,* 72**,** 2079-88.

SMITH, J. S., BACKES, D. M., HOOTS, B. E., KURMAN, R. J. & PIMENTA, J. M. 2009. Human papillomavirus type-distribution in vulvar and vaginal cancers and their associated precursors. *Obstet Gynecol,* 113**,** 917-24.

SMOTKIN, D. & WETTSTEIN, F. O. 1986. Transcription of human papillomavirus type 16 early genes in a cervical cancer and a cancer-derived cell line and identification of the E7 protein. *Proc Natl Acad Sci U S A,* 83**,** 4680-4.

SNOECK, R., BOSSENS, M., PARENT, D., DELAERE, B., DEGREEF, H., VAN RANST, M., NOEL, J. C., WULFSOHN, M. S., ROONEY, J. F., JAFFE, H. S. & DE CLERCQ, E. 2001. Phase II double-blind, placebo-controlled study of the safety and efficacy of cidofovir topical gel for the treatment of patients with human papillomavirus infection. *Clin Infect Dis,* 33**,** 597-602.

SNOECK, R., NOEL, J. C., MULLER, C., DE CLERCQ, E. & BOSSENS, M. 2000. Cidofovir, a new approach for the treatment of cervix intraepithelial neoplasia grade III (CIN III). *J Med Virol,* 60**,** 205-9.

STANLEY, M. 2007. Prophylactic HPV vaccines. *J Clin Pathol,* 60**,** 961-5.

STANLEY, M. A. 2002. Culture of Human Cervical Epithelial Cells. *In:* FRESHNEY, I. R. & FRESHNEY, M. (eds.) *Culture of Epithelial Cells.* Wiley-liss Incorporated.

STANLEY, M. A., BROWNE, H. M., APPLEBY, M. & MINSON, A. C. 1989. Properties of a non-tumorigenic human cervical keratinocyte cell line. *Int J Cancer,* 43**,** 672-6.

STANLEY, M. A., PETT, M. R. & COLEMAN, N. 2007. HPV: from infection to cancer. *Biochemical Society transactions,* 35**,** 1456-60.

STEGER, G. & CORBACH, S. 1997. Dose-dependent regulation of the early promoter of human papillomavirus type 18 by the viral E2 protein. *J Virol,* 71**,** 50-8.

STRAGIER, I., SNOECK, R., DE CLERCQ, E., VAN DEN OORD, J. J., VAN RANST, M. & DE GREEF, H. 2002. Local treatment of HPV-induced skin lesions by Cidofovir. *J Med Virol,* 67**,** 241-5.

SUTHERLAND, G. R., BAKER, E. & RICHARDS, R. I. 1998. Fragile sites still breaking. *Trends Genet,* 14**,** 501-6.

TAYLOR-ROBINSON, D. & BEBEAR, C. 1997. Antibiotic susceptibilities of mycoplasmas and treatment of mycoplasmal infections. *Journal of Antimicrobial Chemotherapy,* 40**,** 622-630.

THE GENE ONTOLOGY CONSORTIUM. 2013. *The Gene Ontology* [Online]. [Accessed].

THORLAND, E. C., MYERS, S. L., GOSTOUT, B. S. & SMITH, D. I. 2003. Common fragile sites are preferential targets for HPV16 integrations in cervical tumors. *Oncogene,* 22**,** 1225-37.

TODARO, G. J. & GREEN, H. 1963. Quantitative studies of the growth of mouse embryo cells in culture and their development into established lines. *J Cell Biol,* 17**,** 299-313.

TRISTRAM, A. & FIANDER, A. 2005. Clinical responses to Cidofovir applied topically to women with high grade vulval intraepithelial neoplasia. *Gynecol Oncol,* 99**,** 652-5.

UK, C. R. 2013. *A trial of two new treatments for vulval intraepithelial neoplasia (RT3 VIN)* [Online]. [Accessed].

VALKENBURG, K. C. & WILLIAMS, B. O. 2011. Mouse models of prostate cancer. *Prostate Cancer,* 2011**,** 895238.

VAN BEURDEN, M., TEN KATE, F. J., SMITS, H. L., BERKHOUT, R. J., DE CRAEN, A. J., VAN DER VANGE, N., LAMMES, F. B. & TER SCHEGGET, J. 1995. Multifocal vulvar intraepithelial neoplasia grade III and multicentric lower genital tract neoplasia is associated with transcriptionally active human papillomavirus. *Cancer,* 75**,** 2879-84.

VAN BEURDEN, M., TEN KATE, F. W., TJONG, A. H. S. P., DE CRAEN, A. J., VAN DER VANGE, N., LAMMES, F. B. & TER SCHEGGET, J. 1998. Human papillomavirus DNA in multicentric vulvar intraepithelial neoplasia. *Int J Gynecol Pathol,* 17**,** 12-6.

VAN DE NIEUWENHOF, H. P., BULTEN, J., HOLLEMA, H., DOMMERHOLT, R. G., MASSUGER, L. F., VAN DER ZEE, A. G., DE HULLU, J. A. & VAN KEMPEN, L. C. 2011. Differentiated vulvar

intraepithelial neoplasia is often found in lesions, previously diagnosed as lichen sclerosus, which have progressed to vulvar squamous cell carcinoma. *Mod Pathol,* 24**,** 297-305.

VAN DE NIEUWENHOF, H. P., VAN DER AVOORT, I. A. & DE HULLU, J. A. 2008. Review of squamous premalignant vulvar lesions. *Crit Rev Oncol Hematol,* 68**,** 131-56.

VAN DEN BROEK, G. B., WREESMANN, V. B., VAN DEN BREKEL, M. W., RASCH, C. R., BALM, A. J. & RAO, P. H. 2007. Genetic abnormalities associated with chemoradiation resistance of head and neck squamous cell carcinoma. *Clin Cancer Res,* 13**,** 4386-91.

VAN DER WORP, H. B., HOWELLS, D. W., SENA, E. S., PORRITT, M. J., REWELL, S., O'COLLINS, V. & MACLEOD, M. R. 2010. Can animal models of disease reliably inform human studies? *PLoS Med,* 7**,** e1000245.

VAN PACHTERBEKE, C., BUCELLA, D., ROZENBERG, S., MANIGART, Y., GILLES, C., LARSIMONT, D., VANDEN HOUTE, K., REYNDERS, M., SNOECK, R. & BOSSENS, M. 2009. Topical treatment of CIN 2+ by cidofovir: results of a phase II, double-blind, prospective, placebo-controlled study. *Gynecol Oncol,* 115**,** 69-74.

VAN ROMPAY, A. R., JOHANSSON, M. & KARLSSON, A. 2003. Substrate specificity and phosphorylation of antiviral and anticancer nucleoside analogues by human deoxyribonucleoside kinases and ribonucleoside kinases. *Pharmacol Ther,* 100**,** 119-39.

VAN SETERS, M., VAN BEURDEN, M., TEN KATE, F. J., BECKMANN, I., EWING, P. C., EIJKEMANS, M. J., KAGIE, M. J., MEIJER, C. J., AARONSON, N. K., KLEINJAN, A., HEIJMANS-ANTONISSEN, C., ZIJLSTRA, F. J., BURGER, M. P. & HELMERHORST, T. J. 2008. Treatment of vulvar intraepithelial neoplasia with topical imiquimod. *N Engl J Med,* 358**,** 1465-73.

VELDMAN, T., HORIKAWA, I., BARRETT, J. C. & SCHLEGEL, R. 2001. Transcriptional activation of the telomerase hTERT gene by human papillomavirus type 16 E6 oncoprotein. *J Virol,* 75**,** 4467-72.

VINOKUROVA, S., WENTZENSEN, N., KRAUS, I., KLAES, R., DRIESCH, C., MELSHEIMER, P., KISSELJOV, F., DURST, M., SCHNEIDER, A. & VON KNEBEL DOEBERITZ, M. 2008. Type-dependent integration frequency of human papillomavirus genomes in cervical lesions. *Cancer Res,* 68**,** 307-13.

WALBOOMERS, J. M., JACOBS, M. V., MANOS, M. M., BOSCH, F. X., KUMMER, J. A., SHAH, K. V., SNIJDERS, P. J., PETO, J., MEIJER, C. J. & MUNOZ, N. 1999. Human papillomavirus is a necessary cause of invasive cervical cancer worldwide. *J Pathol,* 189**,** 12-9.

WANG-JOHANNING, F., LU, D. W., WANG, Y., JOHNSON, M. R. & JOHANNING, G. L. 2002. Quantitation of human papillomavirus 16 E6 and E7 DNA and RNA in residual material from ThinPrep Papanicolaou tests using real-time polymerase chain reaction analysis. *Cancer,* 94**,** 2199-210.

WANG, Q., GRIFFIN, H., SOUTHERN, S., JACKSON, D., MARTIN, A., MCINTOSH, P., DAVY, C., MASTERSON, P. J., WALKER, P. A., LASKEY, P., OMARY, M. B. & DOORBAR, J. 2004. Functional analysis of the human papillomavirus type 16 E1=E4 protein provides a mechanism for in vivo and in vitro keratin filament reorganization. *J Virol,* 78**,** 821-33.

WANG, Z., GERSTEIN, M. & SNYDER, M. 2009. RNA-Seq: a revolutionary tool for transcriptomics. *Nat Rev Genet,* 10**,** 57-63.

WECHSLER, E. I., WANG, Q., ROBERTS, I., PAGLIARULO, E., JACKSON, D., UNTERSPERGER, C., COLEMAN, N., GRIFFIN, H. & DOORBAR, J. 2012. Reconstruction of Human Papillomavirus Type 16-Mediated Early-Stage Neoplasia Implicates E6/E7 Deregulation and the Loss of Contact Inhibition in Neoplastic Progression. *Journal of Virology,* 86**,** 6358-6364.

WEINBERG, R. A. 2013. *The Biology of Cancer*, Garland Science.

WENTZENSEN, N., VINOKUROVA, S. & VON KNEBEL DOEBERITZ, M. 2004. Systematic review of genomic integration sites of human papillomavirus genomes in epithelial dysplasia and invasive cancer of the female lower genital tract. *Cancer Res,* 64**,** 3878-84.

WHEELER, C. M. 2007. Advances in primary and secondary interventions for cervical cancer: human papillomavirus prophylactic vaccines and testing. *Nature Clinical Practice Oncology,* 4**,** 224-235.

WORLD HEALTH ORGANISATION (WHO). 2013. *Human papillomavirus (HPV) and cervical cancer* [Online]. [Accessed].

WORLD HEALTH ORGANIZATION 2010. Recommendations for the evaluation of animal cell cultures as substrates for the manufacture of biological medicinal products and for the characterization of cell banks. WHO technical report series.

XIE, W., RIMM, D. L., LIN, Y., SHIH, W. J. & REISS, M. 2003. Loss of Smad signaling in human colorectal cancer is associated with advanced disease and poor prognosis. *Cancer J,* 9**,** 302-12.

XIONG, X., SMITH, J. L. & CHEN, M. S. 1997. Effect of incorporation of cidofovir into DNA by human cytomegalovirus DNA polymerase on DNA elongation. *Antimicrob Agents Chemother,* 41**,** 594-9.

YEE, C., KRISHNAN-HEWLETT, I., BAKER, C. C., SCHLEGEL, R. & HOWLEY, P. M. 1985. Presence and expression of human papillomavirus sequences in human cervical carcinoma cell lines. *Am J Pathol,* 119**,** 361-6.

YOUNG, L., SUNG, J., STACEY, G. & MASTERS, J. R. 2010a. Detection of Mycoplasma in cell cultures. *Nature Protocols,* 5**,** 929-934.

YOUNG, L., SUNG, J., STACEY, G. & MASTERS, J. R. 2010b. Detection of Mycoplasma in cell cultures. *Nat Protoc,* 5**,** 929-34.

YOUNG, M. D., WAKEFIELD, M. J., SMYTH, G. K. & OSHLACK, A. 2010c. Gene ontology analysis for RNA-seq: accounting for selection bias. *Genome Biol,* 11**,** R14.

ZHENG, Z. M. & BAKER, C. C. 2006. Papillomavirus genome structure, expression, and post-transcriptional regulation. *Front Biosci,* 11**,** 2286-302.

ZIEGERT, C., WENTZENSEN, N., VINOKUROVA, S., KISSELJOV, F., EINENKEL, J., HOECKEL, M. & VON KNEBEL DOEBERITZ, M. 2003. A comprehensive analysis of HPV integration loci in anogenital lesions combining transcript and genome-based amplification techniques. *Oncogene,* 22**,** 3977-84.

ZUR HAUSEN, H. 2002. Papillomaviruses and cancer: from basic studies to clinical application. *Nat Rev Cancer,* 2**,** 342-50.

Appendix 1 – PC08, PC09, and clonal cell culture data

Cell line	Cumulative days in culture	Initial cell count (seeding cell no.) ($X10^5$)	Initial count adjusted for PE* ($X10^5$)	Final cell count (total cell no.) ($X10^6$)	DT	PD
A09	12	8	1.6	4.3	2.53	4.75
	27	8	1.6	8	2.66	5.64
	40	8	1.6	14	2.02	6.45
	62	8	1.6	14		
	76	8	1.6	20		
	84	8	1.6	10		
Mean DT					1.76	
Total PD						36.21
D09	9	8	1.6	14	1.40	
	21	8	1.6	7.5	2.16	
	36	8	1.6	10	2.52	
	49	8	1.6	20	1.87	
	70	8	1.6	16	3.16	
	86	8	1.6	20	2.30	
Mean DT					2.23	
Total PD						38.52
H09	9	8	1.6	3.3	2.75	
	21	8	1.6	7.5	2.70	
	36	8	1.6	8	2.30	
	49	8	1.6	8	3.90	
	70	8	1.6	13	2.21	
	86	8	1.6	10	1.34	
Mean DT					1.88	
Total PD						33.50
M08	13	8	1.6	8	2.30	
	21	8	1.6	2	2.20	
	41	8	1.6	3.6	4.46	
	51	8	1.6	7.6	1.80	
	63	8	1.6	8	2.13	
Mean DT					1.69	
Total PD						24.98
P08	13	8	1.6	6	2.49	
	21	8	1.6	1.5	2.48	
	41	8	1.6	3	4.73	
	51	8	1.6	8	1.77	
	63	8	1.6	8	2.13	
Mean DT					1.77	
Total PD						23.96
Y08	13	8	1.6	5.4	2.56	5.07
	21	8	1.6	1.7	2.35	3.41
	30	8	1.6	5	1.81	4.96
	41	8	1.6	4.5	2.29	4.81
	51	8	1.6	7	1.84	5.45

Mean DT Total PD					1.81	38.52
PC08	7	8	1.6	1.7	1.3	5.27
	14	8	1.6	5	1.0	6.70
	23	8	1.6	7.8	1.2	7.59
	29	8	1.6	5.3	0.9	6.71
	35	8	1.6	5.5	0.9	6.78
	42	8	1.6	8.4	1.1	6.49
	51	8	1.6	8.5	1.3	6.73
	58	8	1.6	4.3	1.3	5.41
	66	8	1.6	6.3	1.1	6.96
	73	8	1.6	14.3	0.9	8.16
	80	8	1.6	7.3	1.0	7.18
	87	8	1.6	10	0.9	7.68
	94	8	1.6	8.3	1.0	7.36
	101	8	1.6	1.1	0.9	7.78
Mean DT Total PD					1.1	98.68
PC09	7	8	1.6	12.3	0.9	7.94
	15	8	1.6	3.03	1.4	5.65
	28	8	1.6	3	2.4	5.49
	35	8	1.6	2.2	1.4	5.06
	42	8	1.6	3.9	1.1	6.47
	51	8	1.6	4.2	1.5	6.14
	57	8	1.6	2.8	1.0	5.78
	63	8	1.6	5.3	0.9	6.72
	70	8	1.6	3.3	1.2	5.78
	79	8	1.6	8.5	1.3	7.14
	86	8	1.6	4.3	1.3	5.41
	94	8	1.6	6.3	1.1	6.96
	101	8	1.6	7.3	1.0	7.18
	108	8	1.6	7.3	1.0	7.28
	115	8	1.6	10.3	0.9	7.68
	122	8	1.6	8.3	1.0	7.36
	129	8	1.6	10	0.9	7.65
Mean DT Total PD					1.2	111.58

Figure I.a. Raw data from short-term culture of clonal cell lines and heterogeneous PC08 and PC09

Clonal cell lines A09, D09, H09, M08, P08 and Y08 underwent short term culture for 84, 86, 86, 63, 63, and 51 days, respectively . Heterogeneous PC08 and PC09 cell lines underwent a more lengthy cell culture period for 101 and 129 days, respectively. The raw data underlying these cell culture periods are illustrated and the calculated doubling time (DT) and population doublings (DT). * represents initial cell count corrected for plating efficiency (PE); every seeded cell would not give rise to colonies (even in highly proliferating lines like SiHa and HeLa, which show PE values of 0.2-0.5. To correct for PE in the calculations a PE of 0.2 has been assumed (i.e. approximately one fifth of cells would establish and give rise to colonies).

Appendix II – Example of qRT-PCR fluorescence curves in M08 (cell culture confluency study)

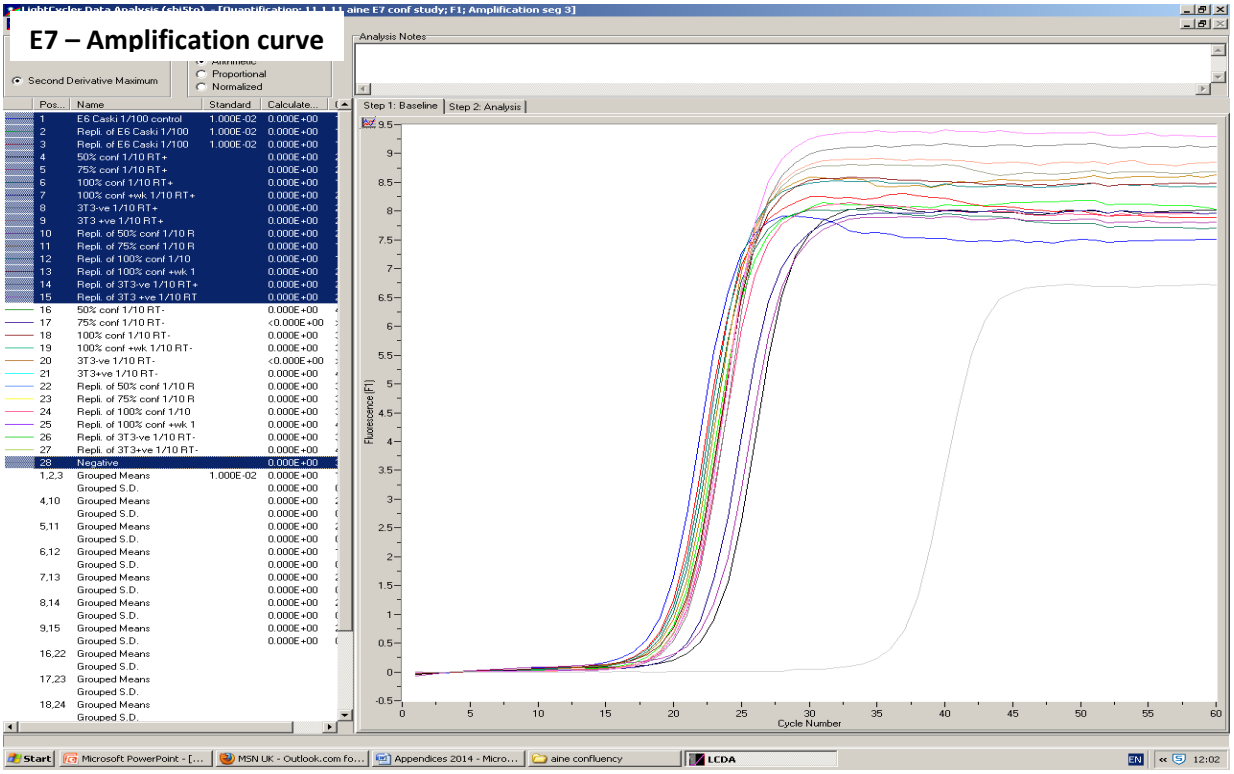

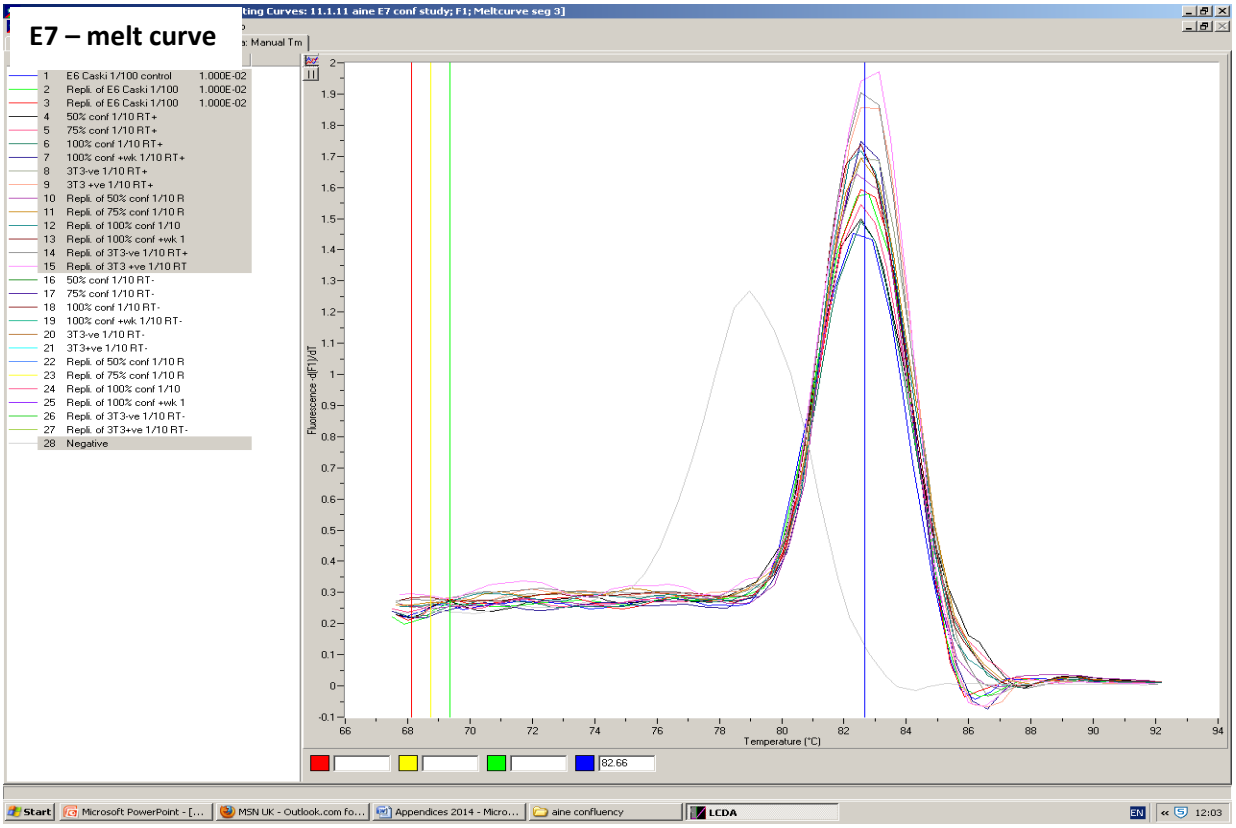

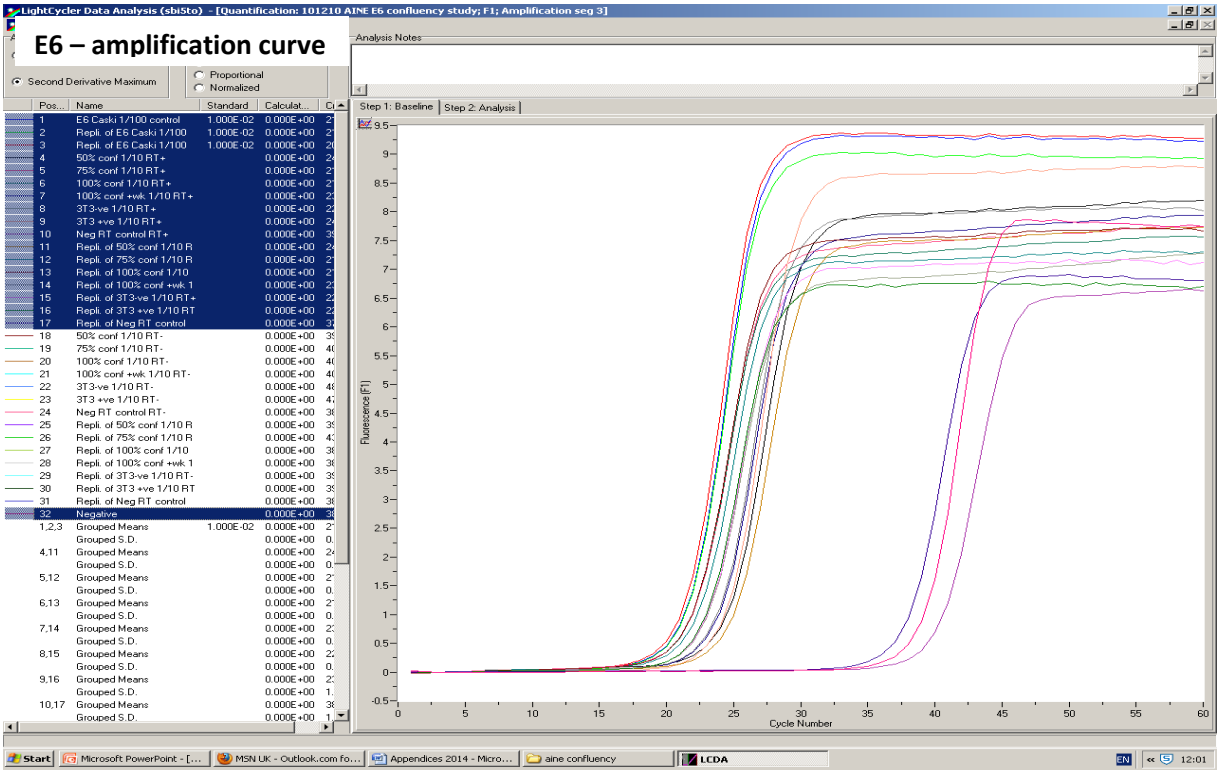
E6 – amplification curve
LightCycler Data Analysis (sbiSto) - [Quantification: 101210 AINE E6 confluency study; F1; Amplification seg 3]
Analysis Notes
Second Derivative Maximum
Proportional
Normalized
Step 1: Baseline
Step 2: Analysis
Fluorescence [F1]
Cycle Number

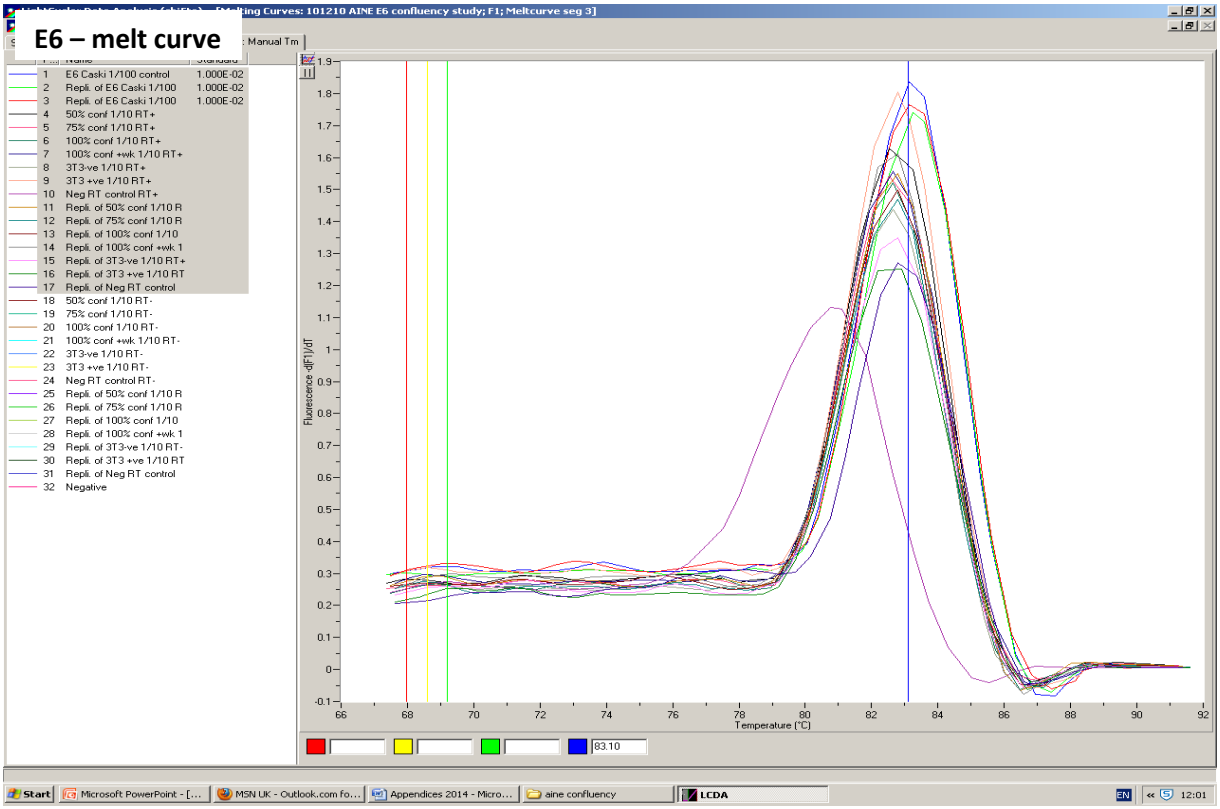
E6 – melt curve
Manual Tm
Fluorescence -d(F1)/dT
Temperature (°C)

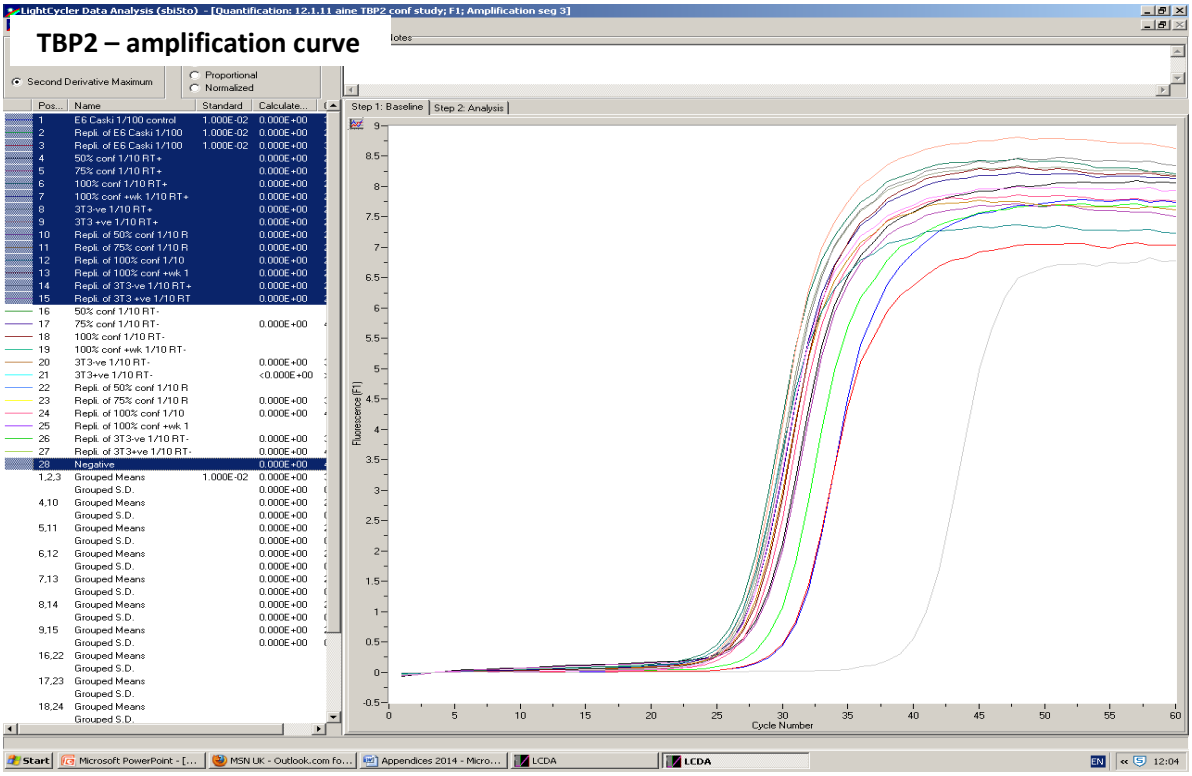

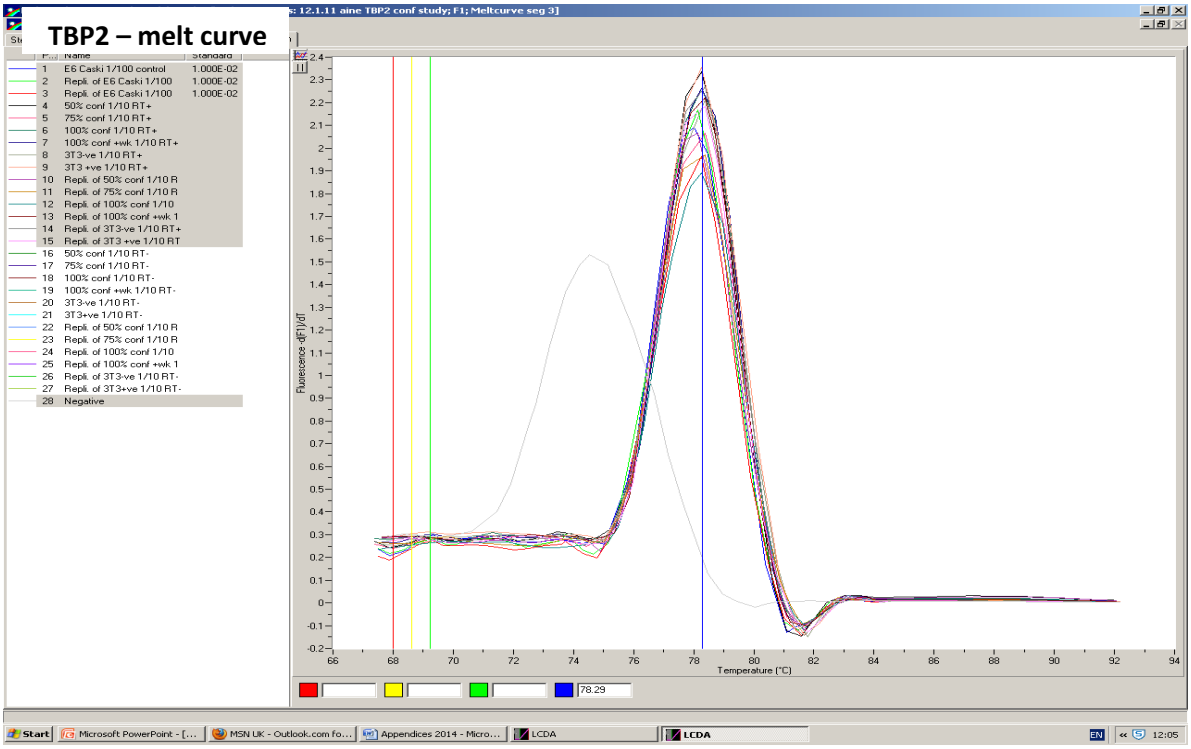

Figure II.a. An example of real-time fluorescent traces of HPV genes and housekeeping genes in cell line M08

qPCR amplification and melt curves are illustrated for HPV 16 E6, E7 and housekeeping genes TBP2 performed to investigate the effect of confluency on HPV expression levels (relative to CaSki).

Appendix III - Example of qRT-PCR fluorescence curves in H09 (molecular characterisation study)

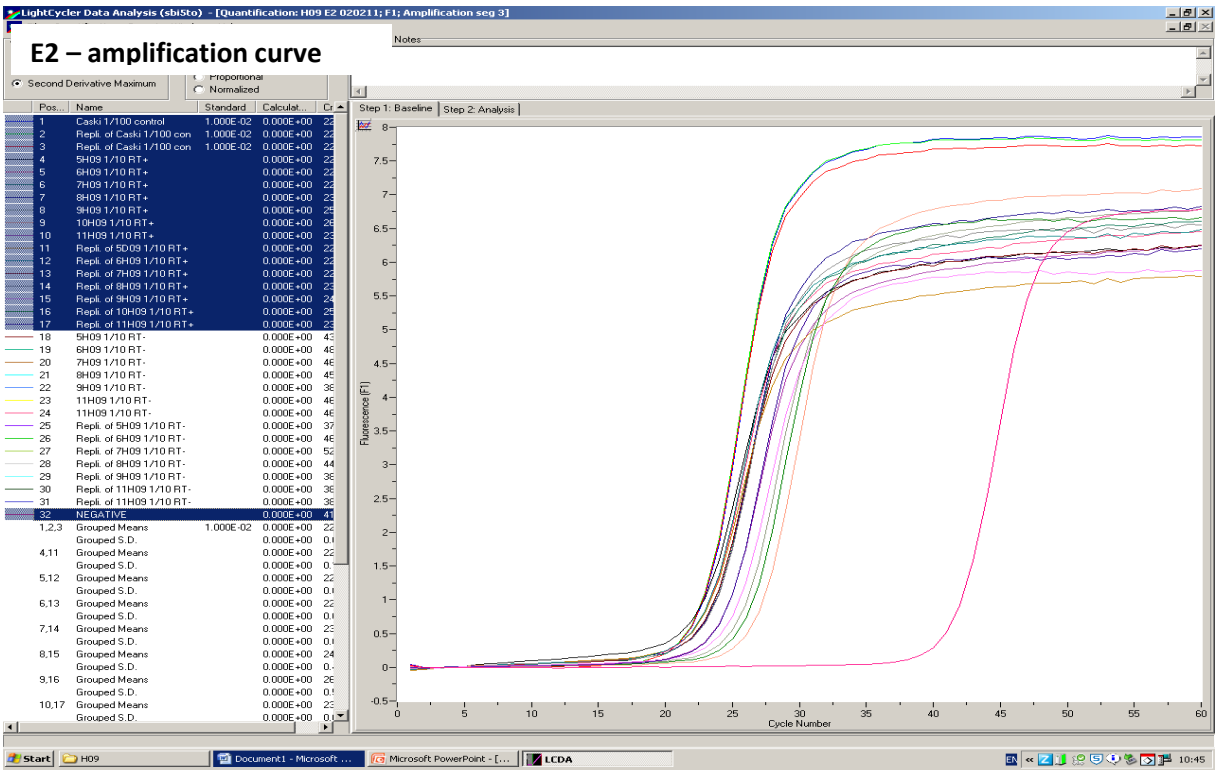

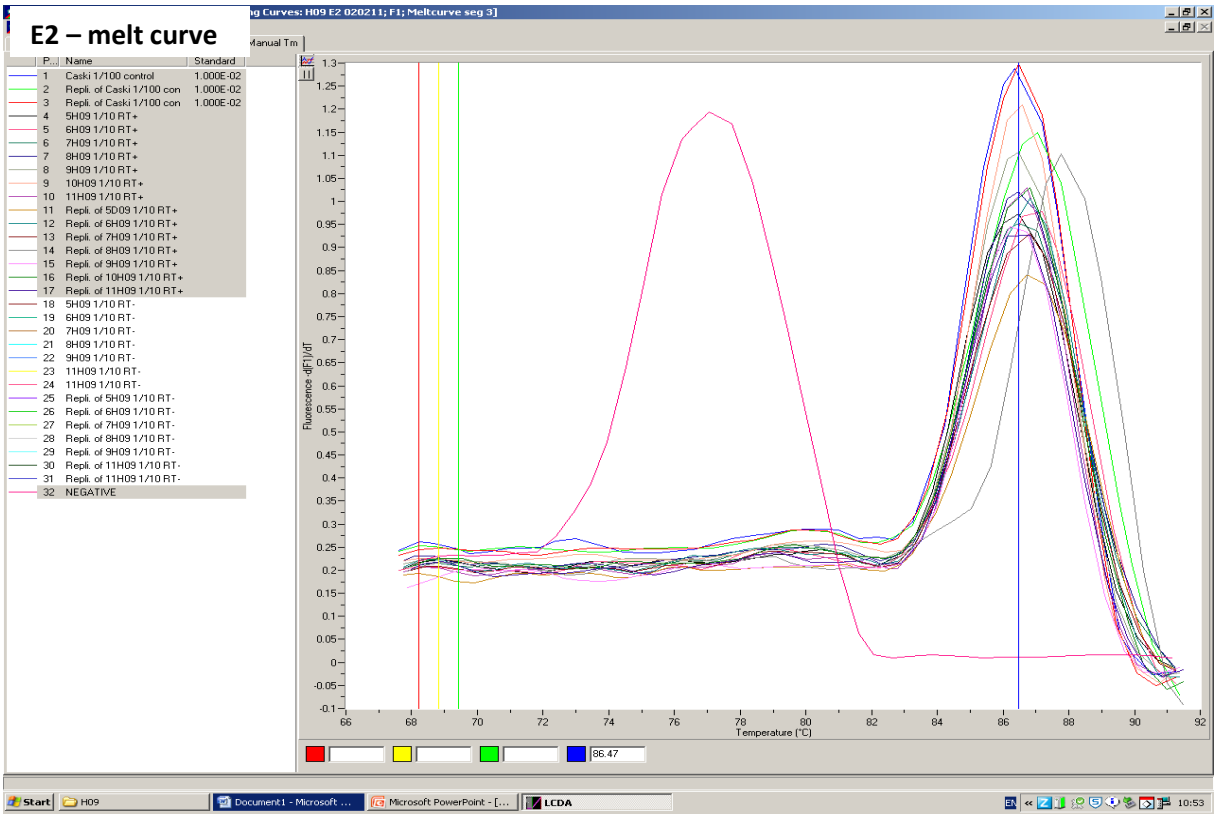

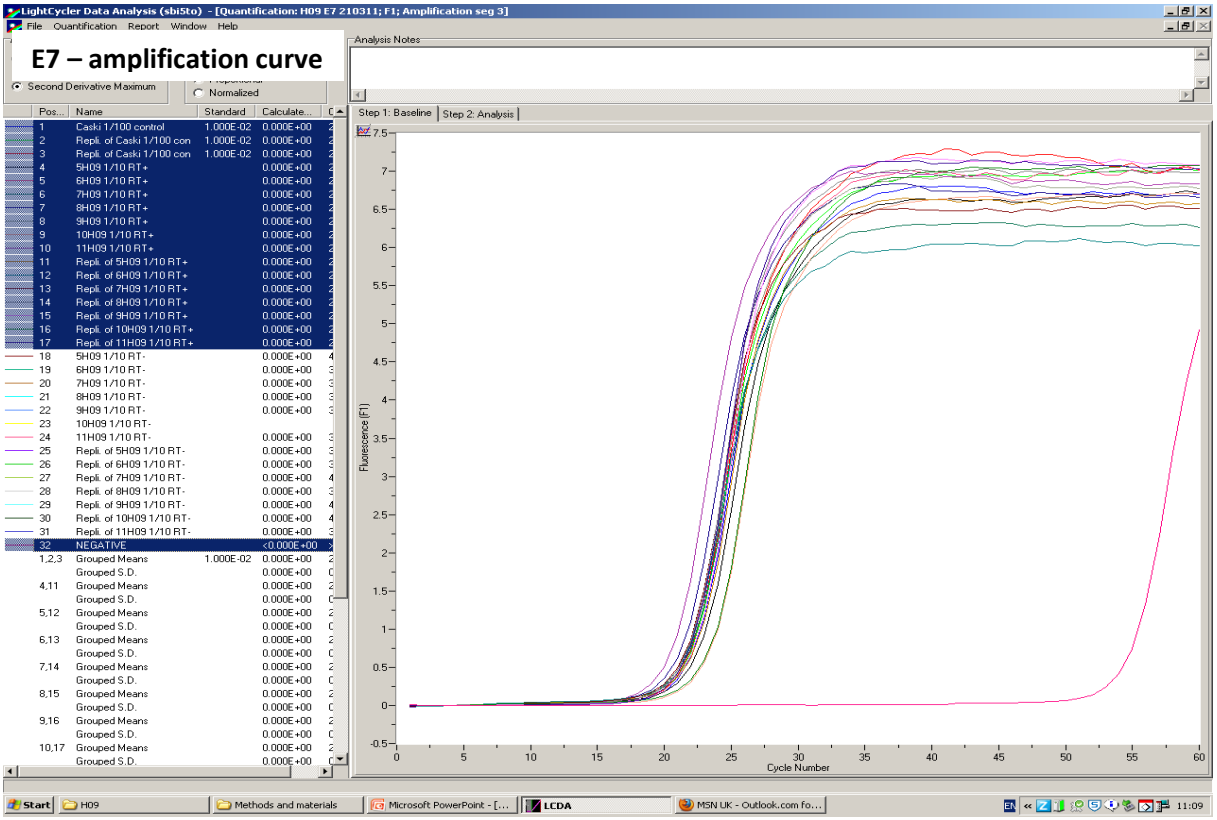
E7 – amplification curve
LightCycler Data Analysis (sbi5to) - [Quantification: H09 E7 210311; F1; Amplification seg 3]
Fluorescence (F1)
Cycle Number

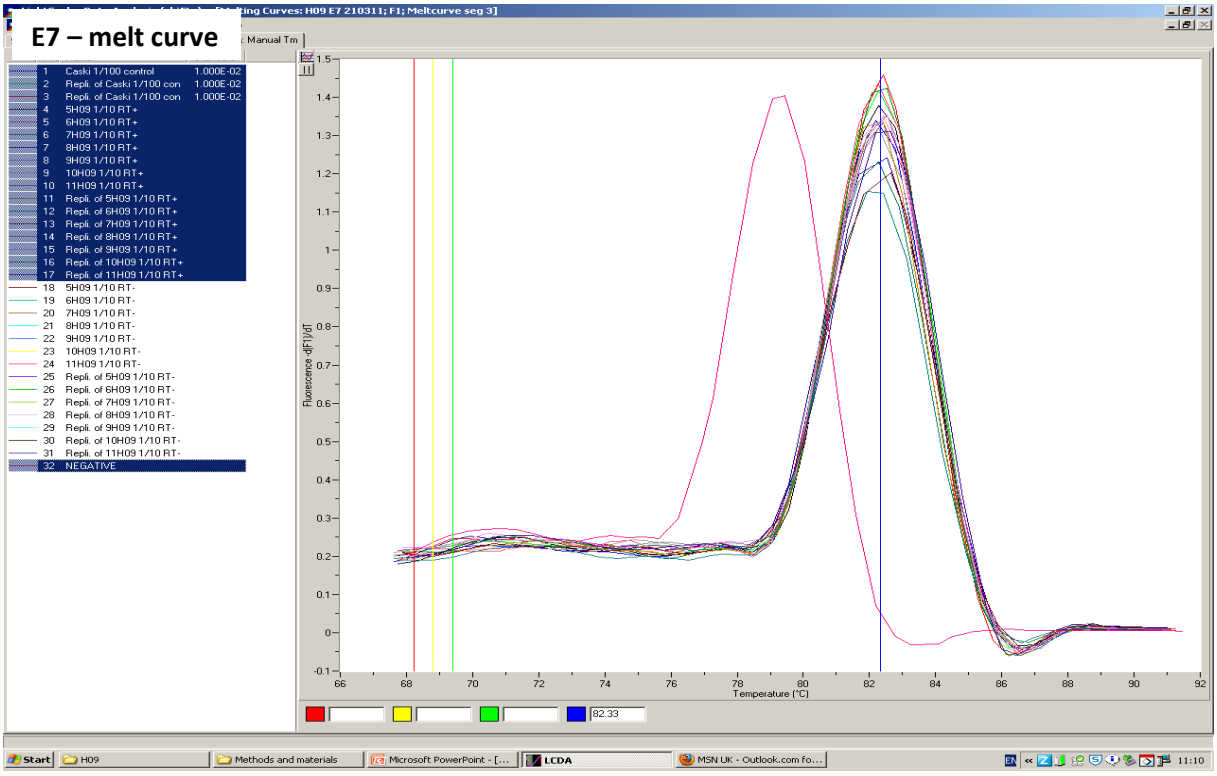
E7 – melt curve
Fluorescence -d(F1)/dT
Temperature (°C)

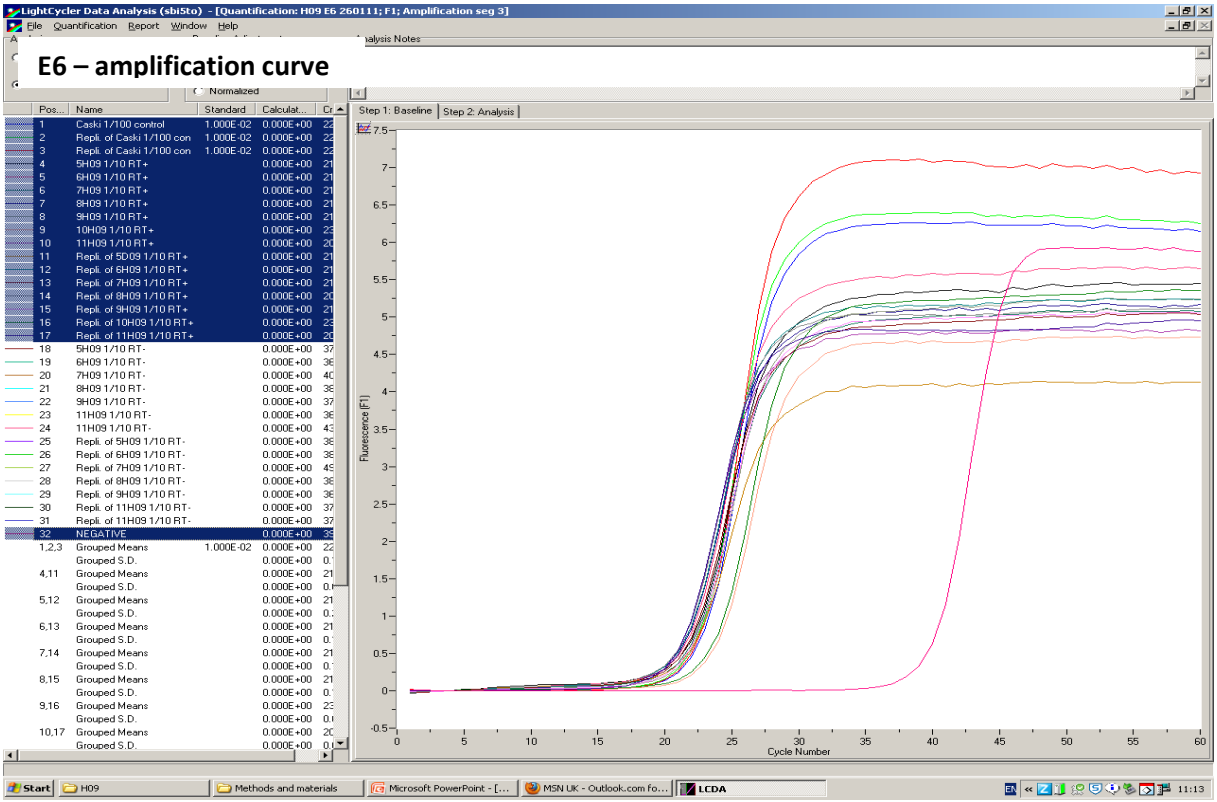
E6 – amplification curve
LightCycler Data Analysis (sbi5to) - [Quantification: H09 E6 260111; F1; Amplification seg 3]
File Quantification Report Window Help
Normalized
Pos... Name Standard Calculat...
Step 1: Baseline Step 2: Analysis
Fluorescence [F1]
Cycle Number

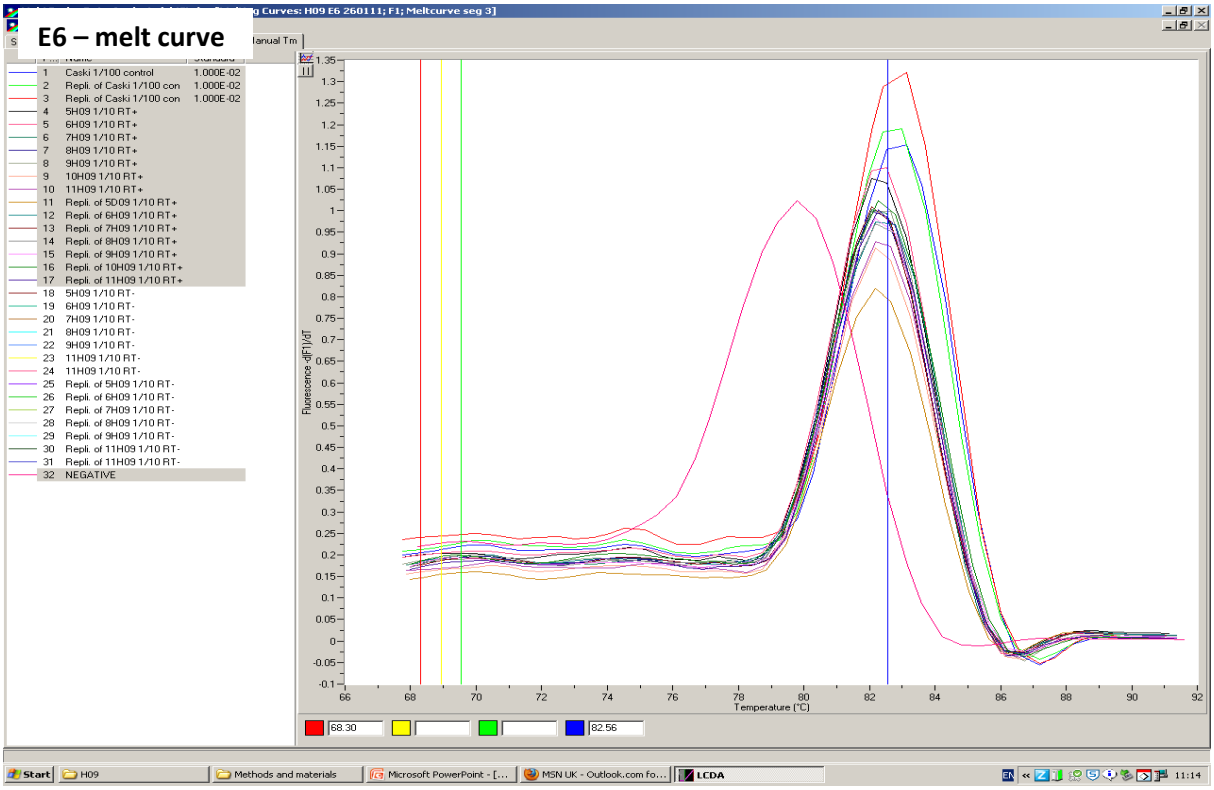
E6 – melt curve
Curves: H09 E6 260111; F1; Meltcurve seg 3]
Manual Tm
Fluorescence -dF1/dT
Temperature (°C)
68.30
82.56

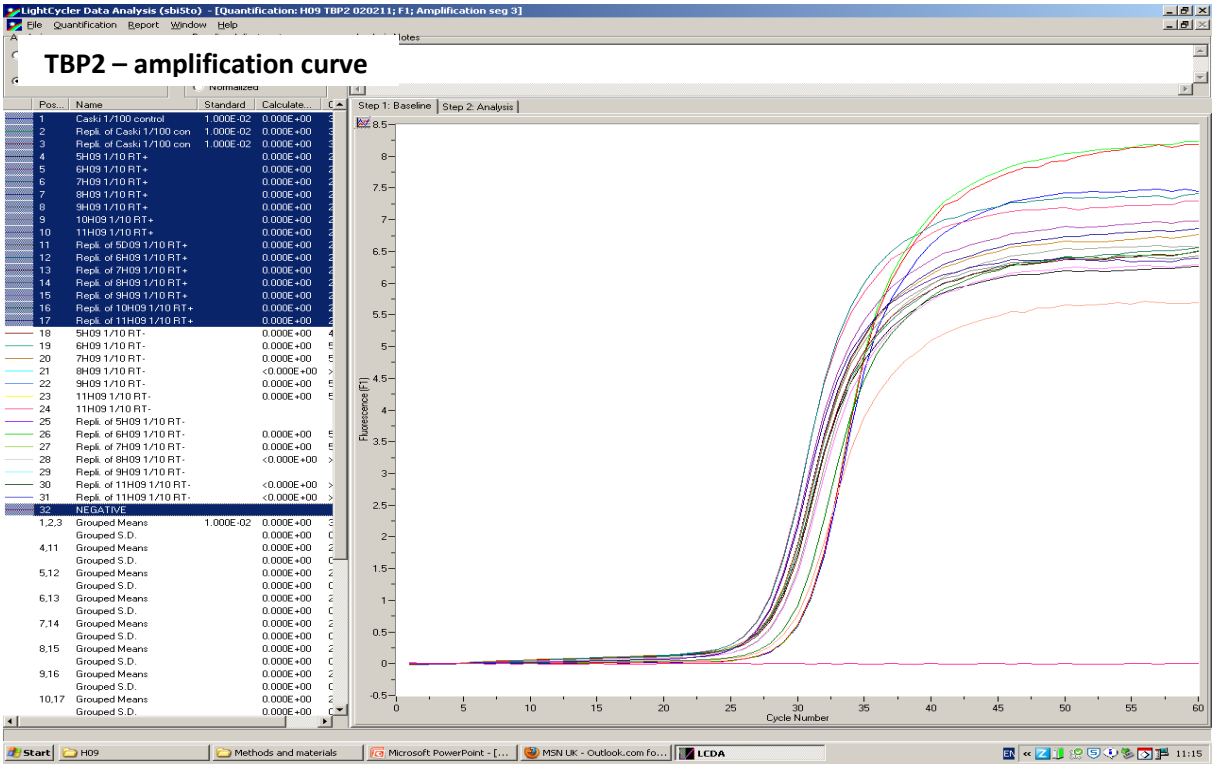
TBP2 – amplification curve
LightCycler Data Analysis (sbiSto) - [Quantification: H09 TBP2 020211; F1; Amplification seg 3]
File Quantification Report Window Help
Step 1: Baseline
Step 2: Analysis
Fluorescence [F1]
Cycle Number

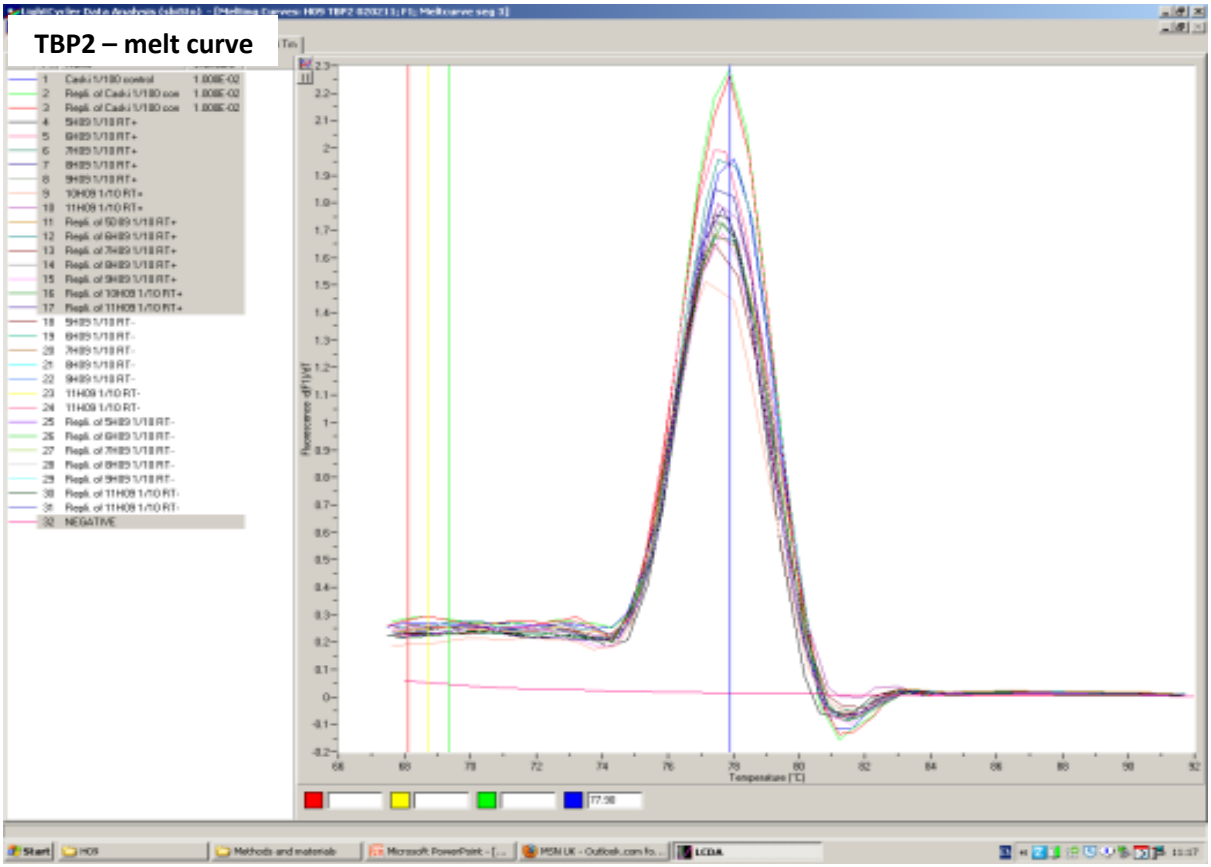
TBP2 – melt curve
Temperature [°C]

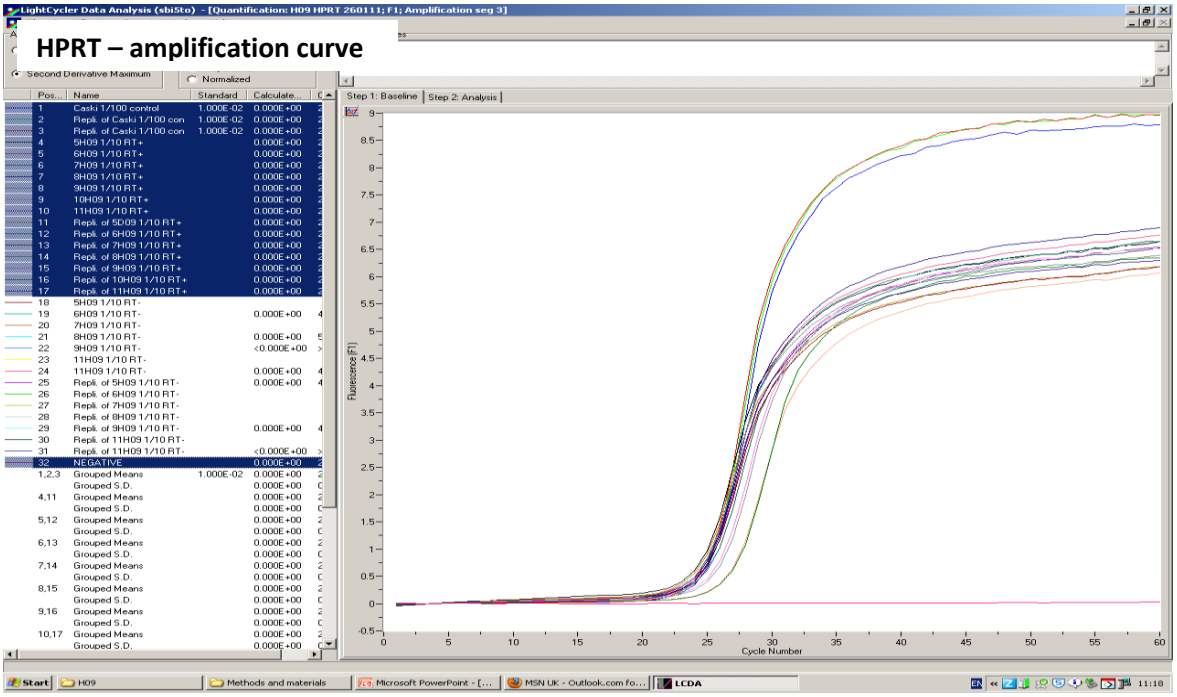

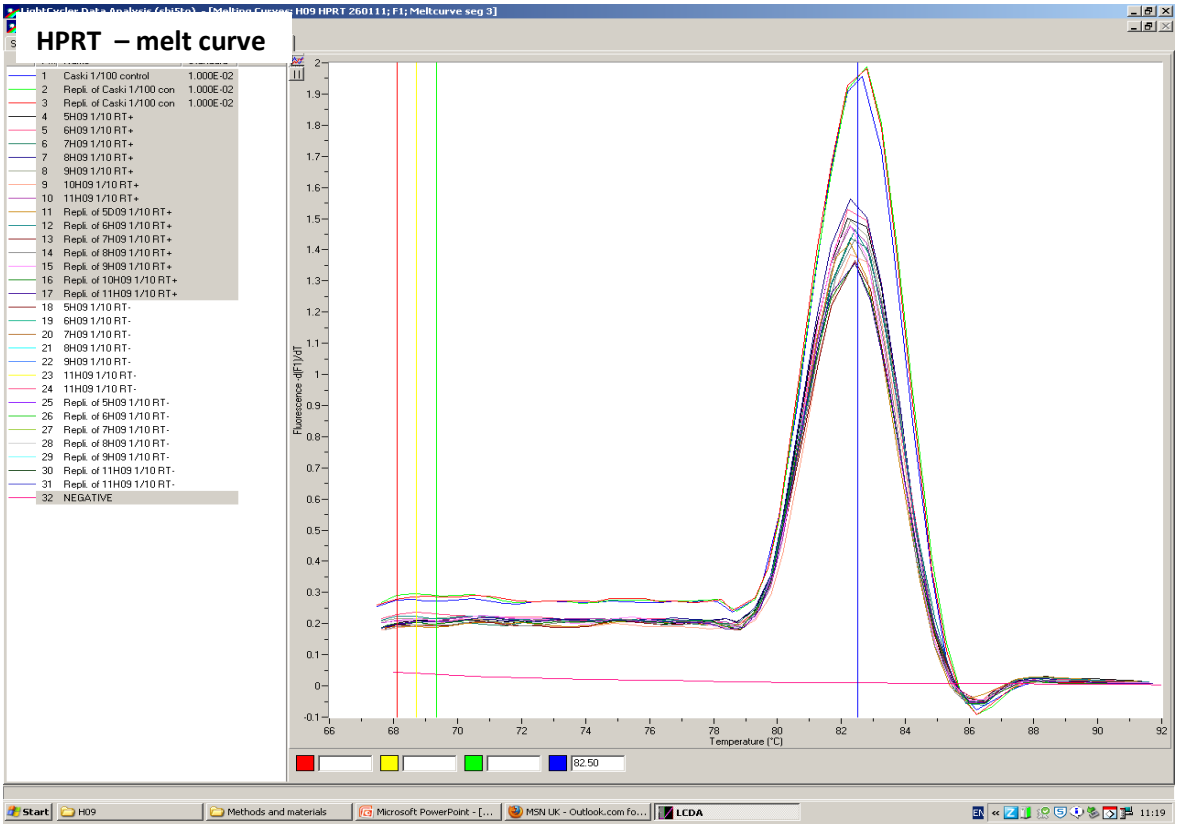

Figure III.a. An example of real-time fluorescent traces of HPV genes and housekeeping genes in cell line H09

qPCR amplification and melt curves are illustrated for HPV 16 E2, E6, E7 and housekeeping genes TBP2 and HPRT. Gene expression (relative to CaSki) was performed during short-term culture.

Appendix IV - Example of qRT-PCR fluorescence curves in H09 (CDV dosing study)

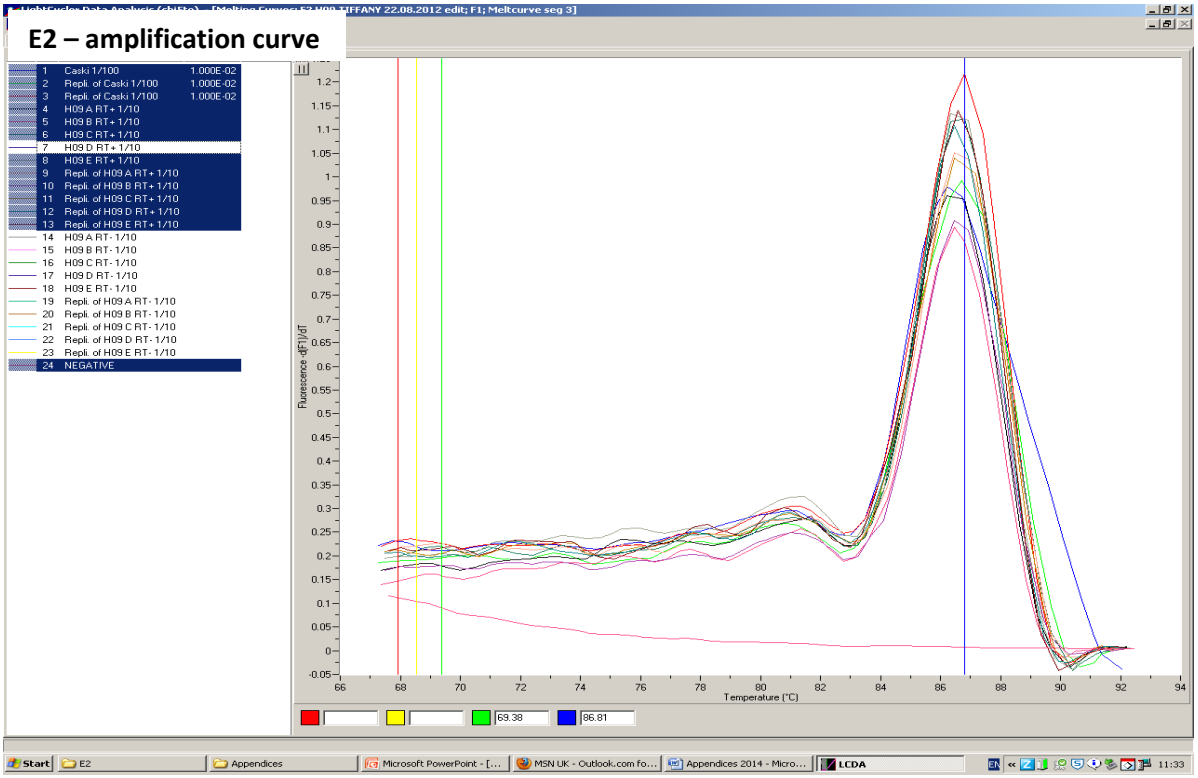

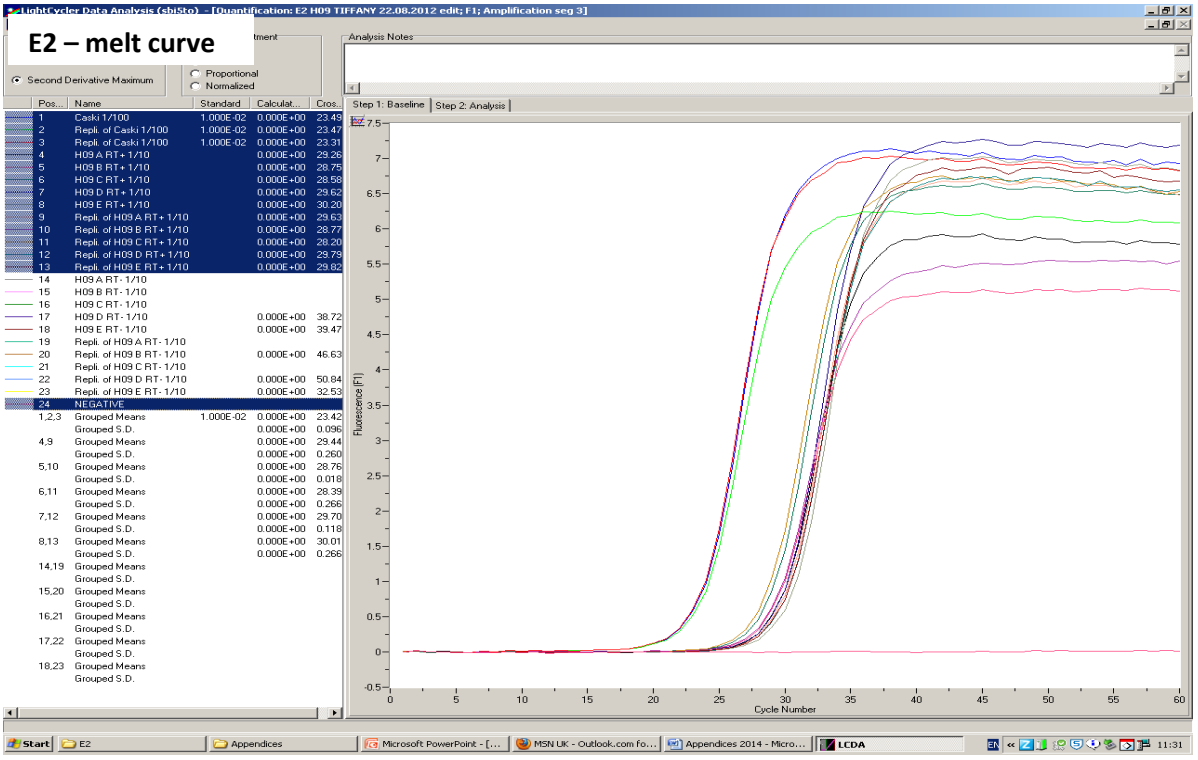

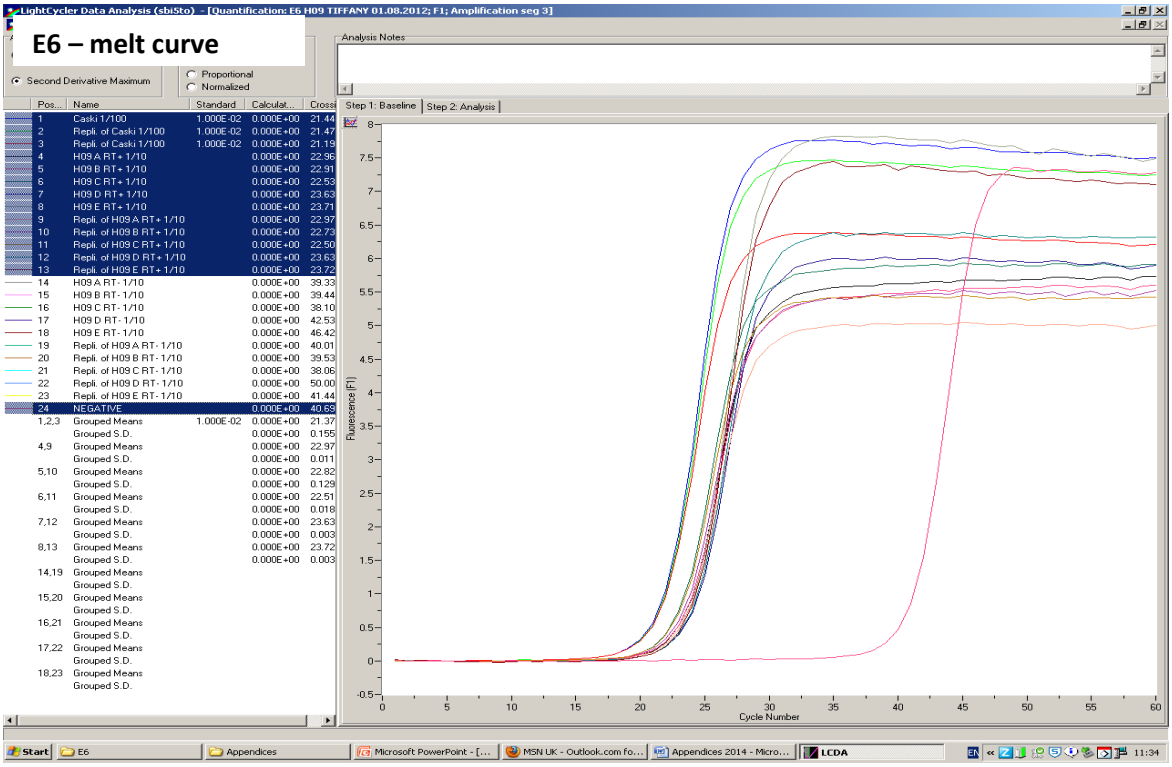
E6 – melt curve
LightCycler Data Analysis (sbiSto) - [Quantification: E6 H09 TIFFANY 01.08.2012; F1; Amplification seg 3]
Analysis Notes
Second Derivative Maximum
Proportional
Normalized
Step 1: Baseline
Step 2: Analysis
Fluorescence [F1]
Cycle Number

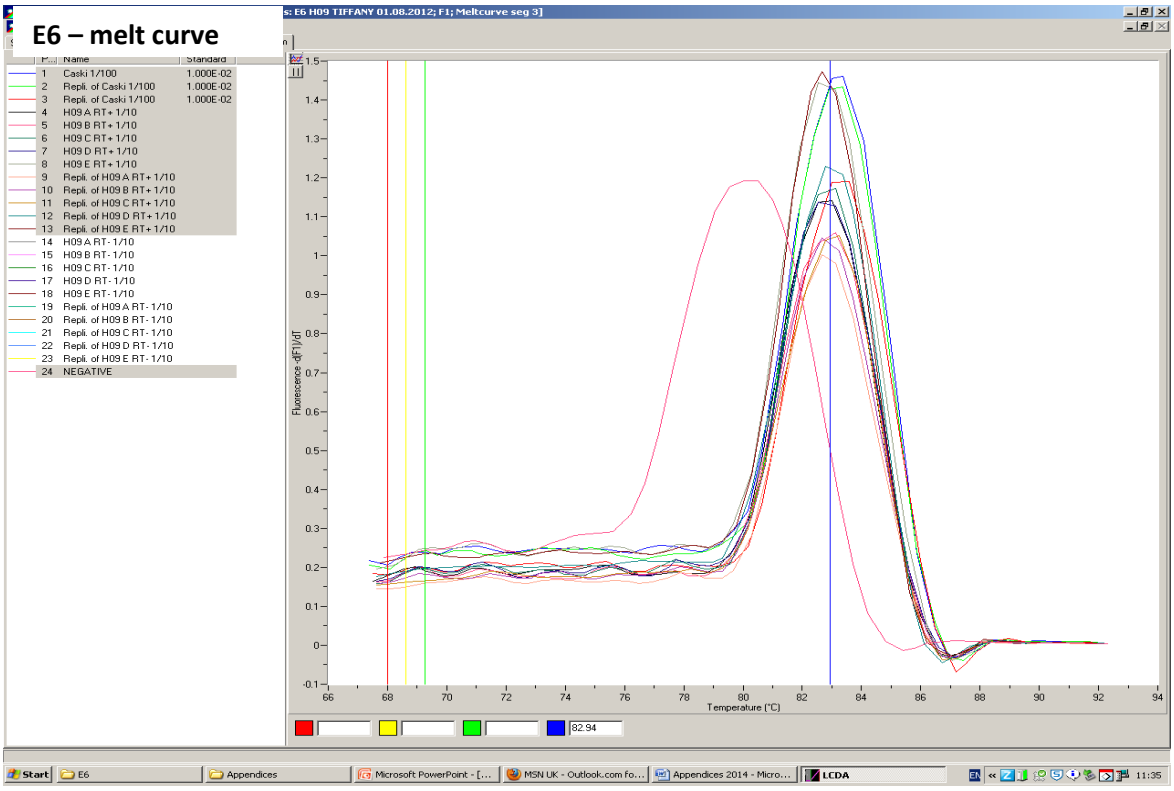
E6 – melt curve
Fluorescence -d(F1)/dT
Temperature (°C)

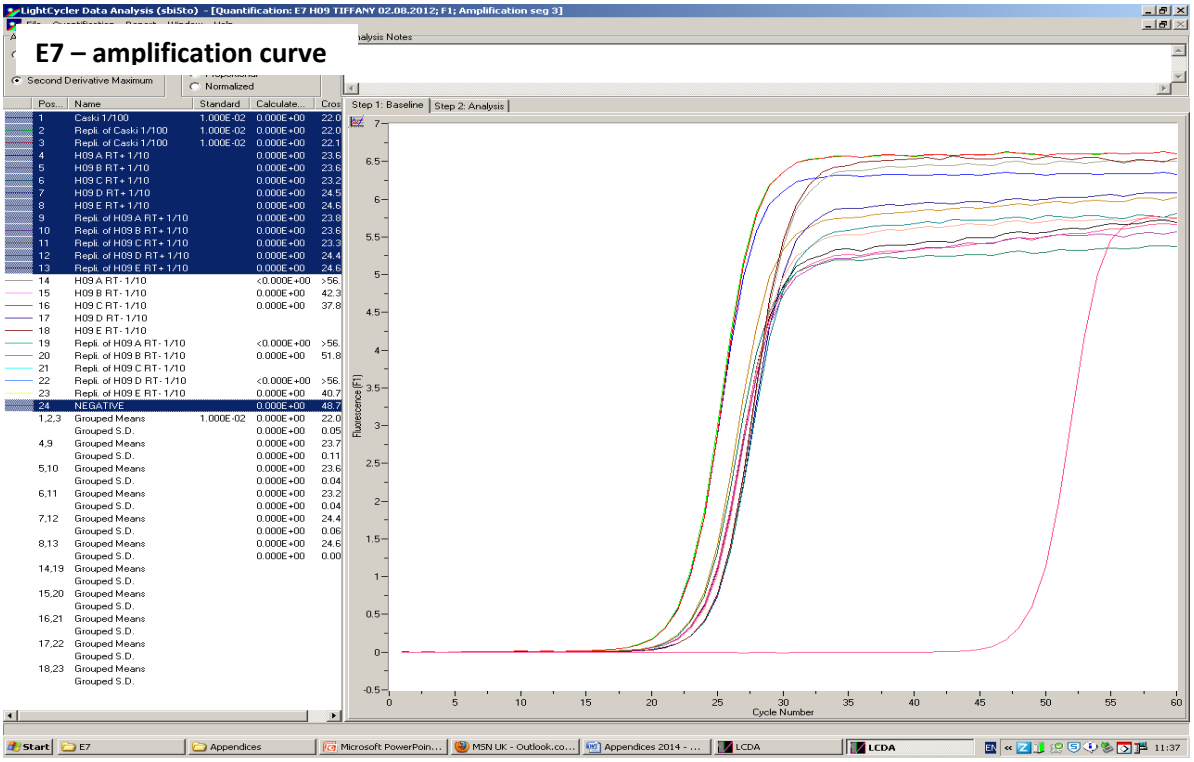
E7 – amplification curve
LightCycler Data Analysis (sbiSto) - [Quantification: E7 H09 TIFFANY 02.08.2012; F1; Amplification seg 3]
Second Derivative Maximum
Normalized
Step 1: Baseline
Step 2: Analysis
Fluorescence (F1)
Cycle Number

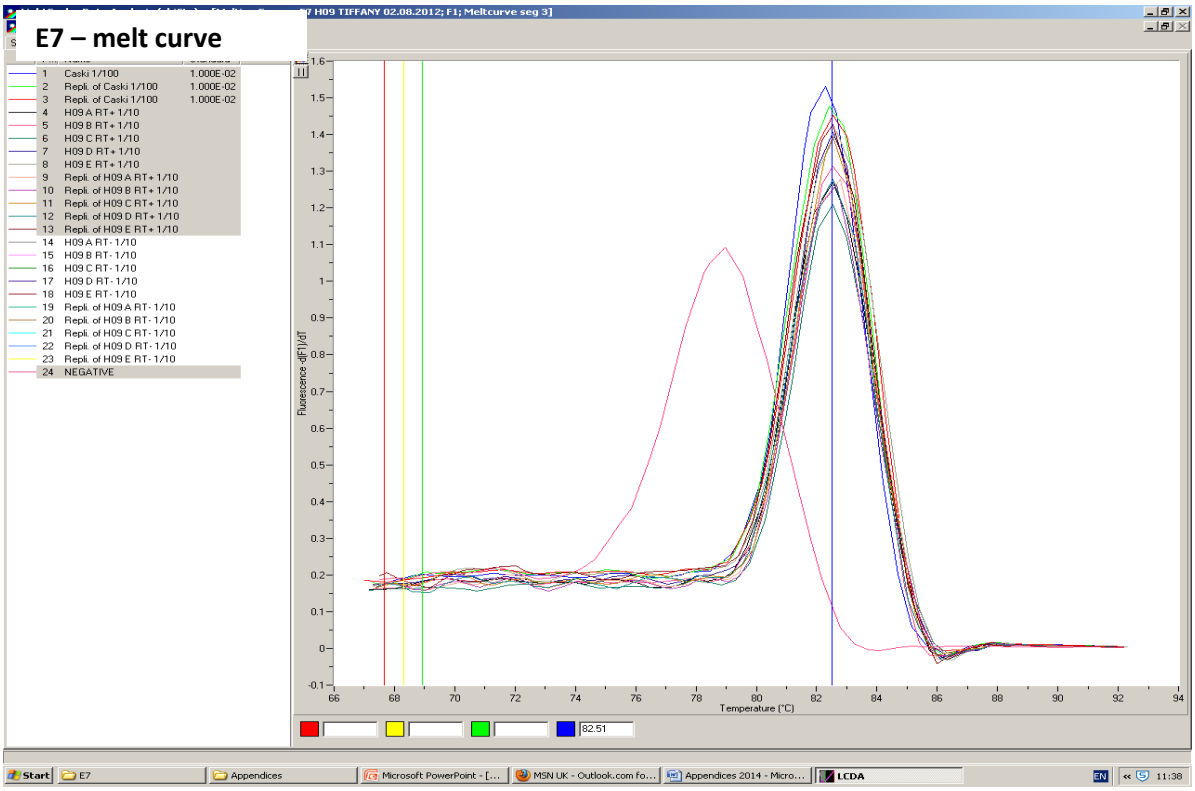
E7 – melt curve
Fluorescence -d(F1)/dT
Temperature (°C)
82.51

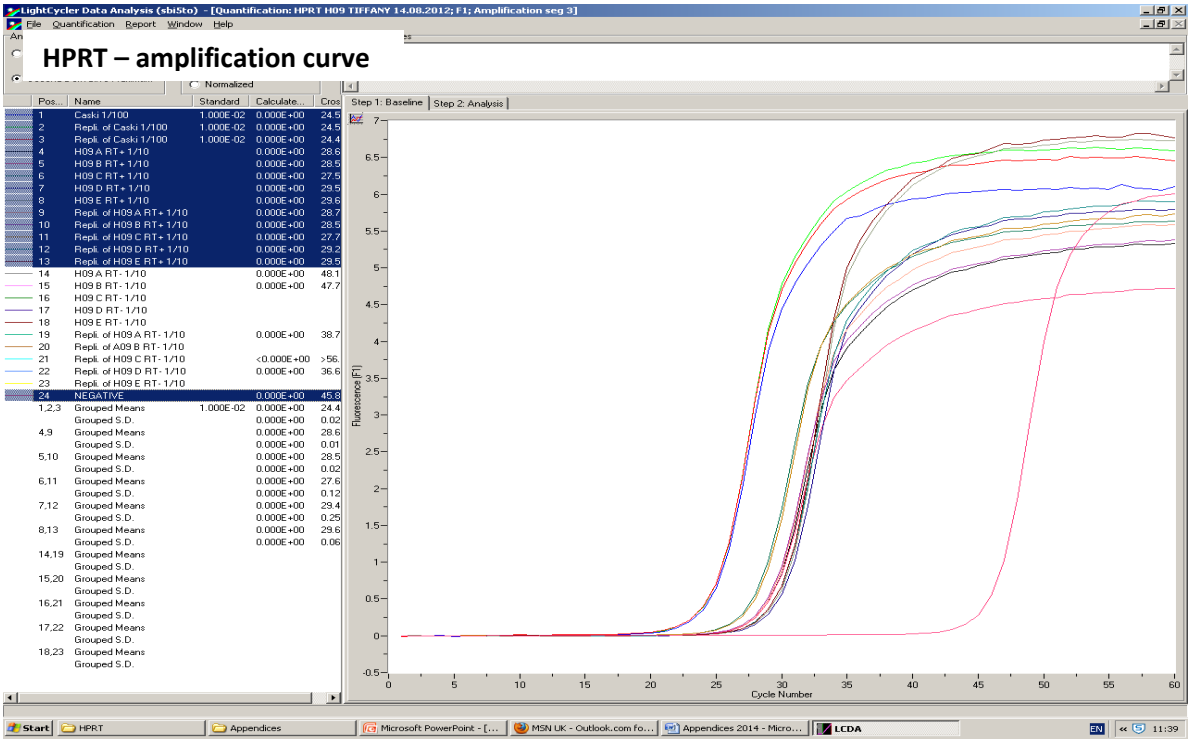
HPRT – amplification curve
LightCycler Data Analysis (sbi5to) - [Quantification: HPRT H09 TIFFANY 14.08.2012; F1; Amplification seg 3]
File Quantification Report Window Help
Normalized
Pos. Name Standard Calculate... Cros
Step 1: Baseline
Step 2: Analysis
Fluorescence (F1)
Cycle Number
Start
HPRT
Appendices
Microsoft PowerPoint - [...
MSN UK - Outlook.com fo...
Appendices 2014 - Micro...
LCDA
11:39

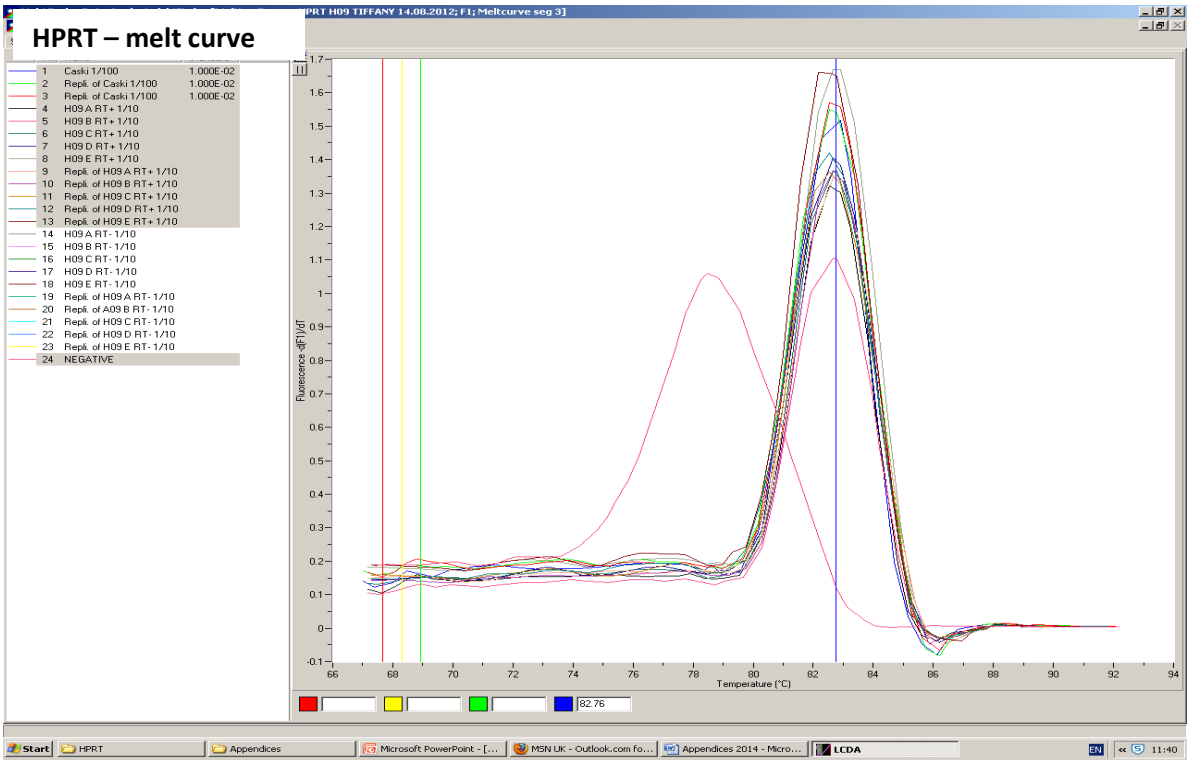
HPRT – melt curve
PRT H09 TIFFANY 14.08.2012; F1; Meltcurve seg 3]
Fluorescence -d(F1)/dT
Temperature (°C)
82.76
Start
HPRT
Appendices
Microsoft PowerPoint - [...
MSN UK - Outlook.com fo...
Appendices 2014 - Micro...
LCDA
11:40

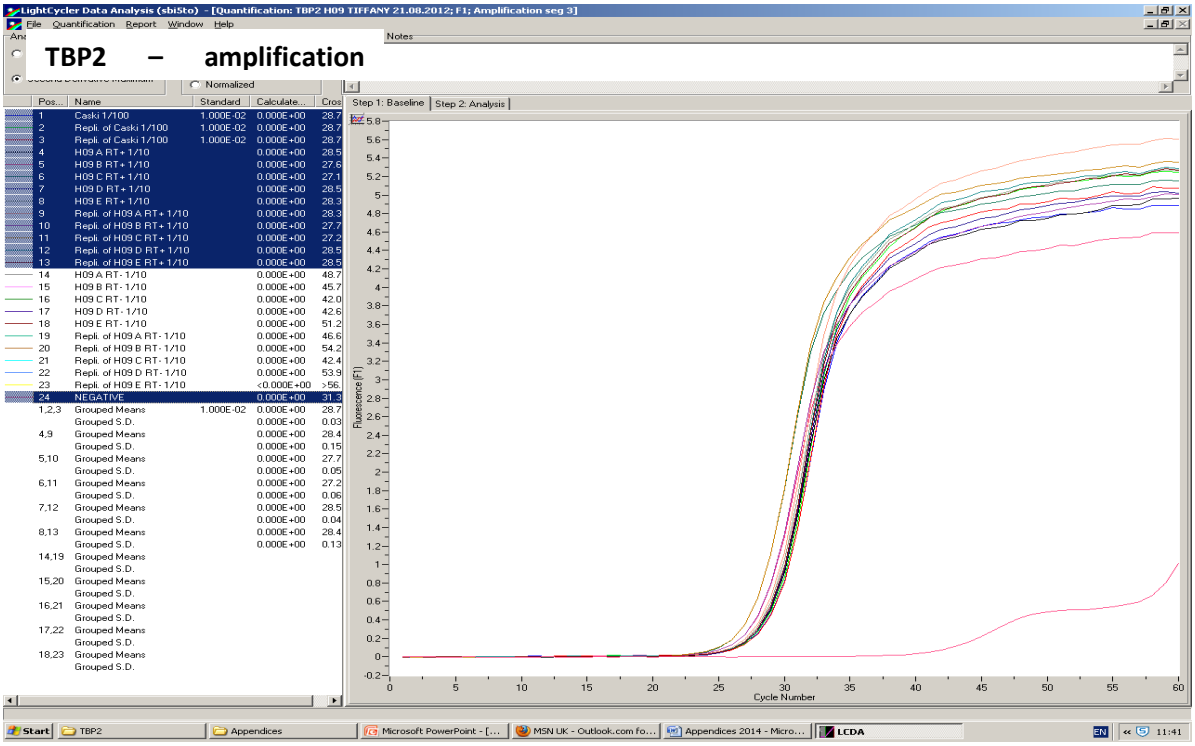

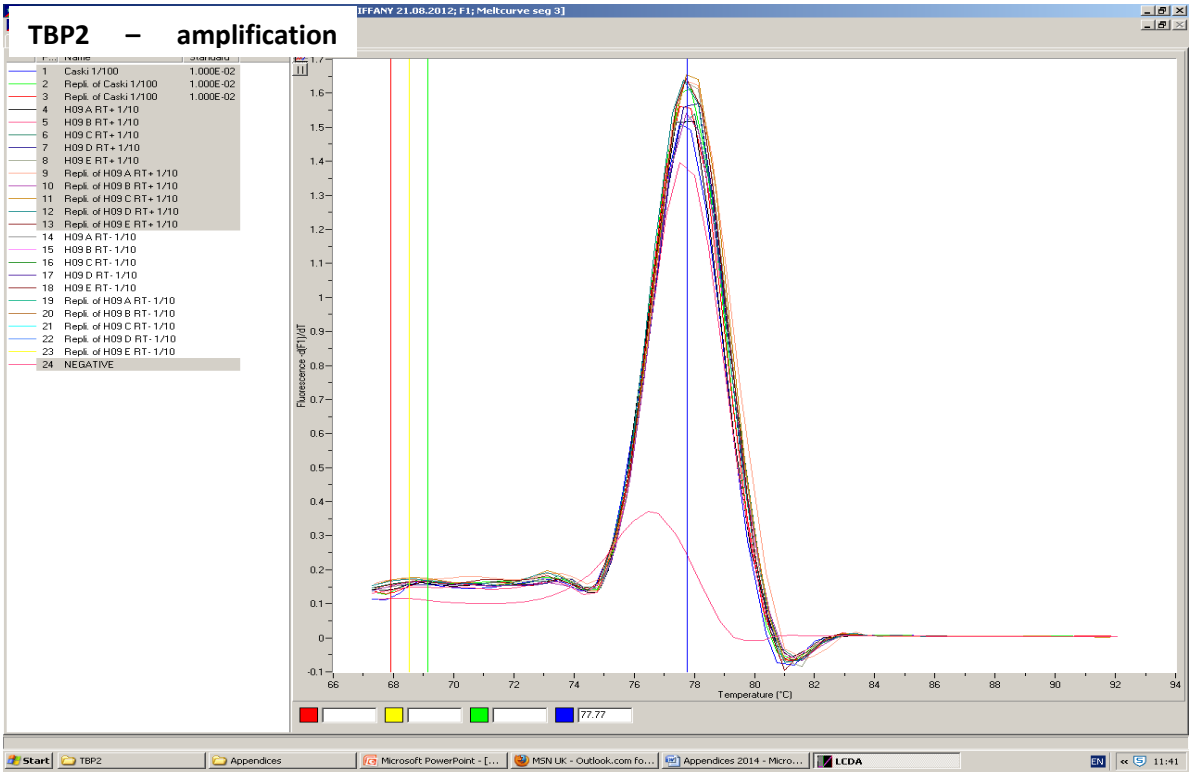

Figure IV.a. An example of real-time fluorescent traces of HPV genes and housekeeping genes in CDV treated and untreated cell line H09

qPCR amplification and melt curves are illustrated for HPV 16 E2, E6, E7 and housekeeping genes TBP2 and HPRT. Gene expression (relative to CaSki) was performed during CDV dosing protocol.

Appendix V – Caspase-3 activity via analysis of apoptotic cells in A09 and M08

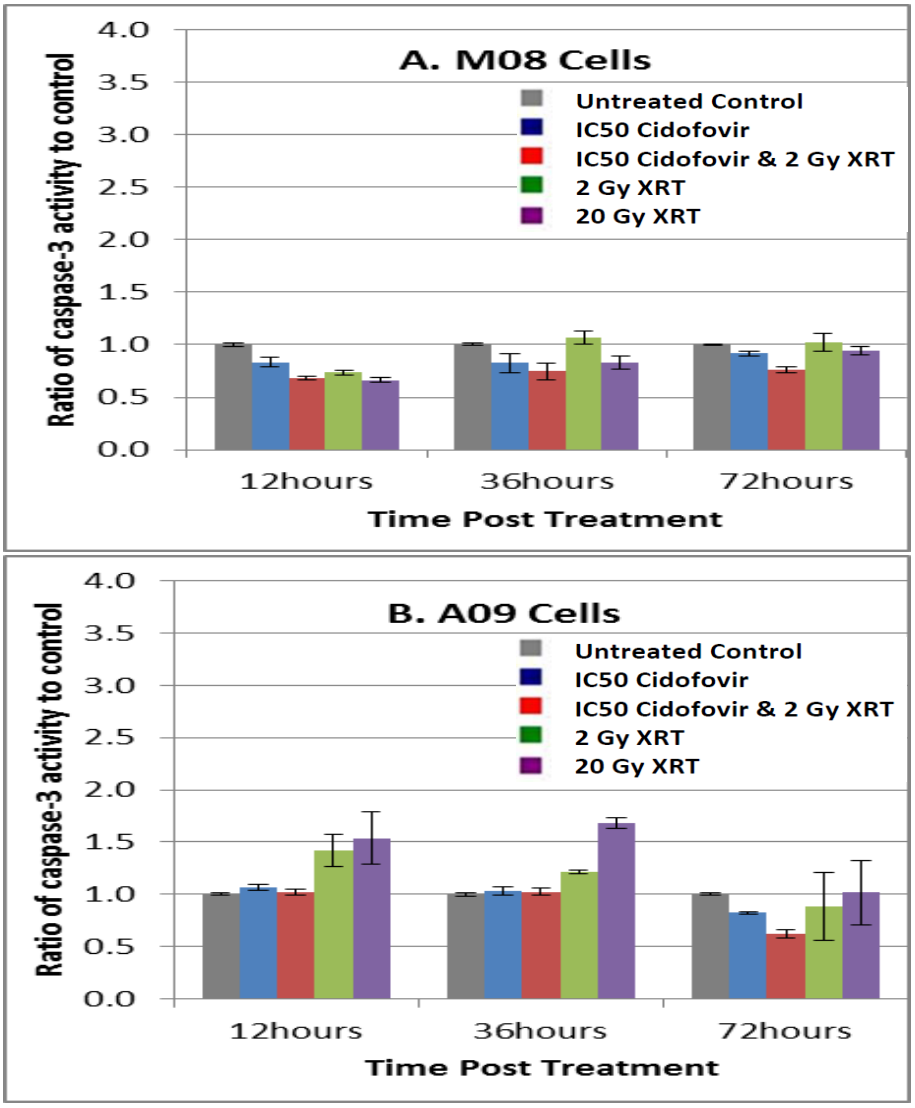

Figure V.a. Caspase-3 activity in M08 and A09 cells in response to Cidofovir and ionising radiation

Caspase-3 activity was assessed using the Caspase-3 activity kit from Cell Signalling (Massachusetts USA) which used a fluorogenic substrate (Ac-DEVD-AMC) for activated caspase-3 to quantify apoptotic cells. Positive and negative assay controls were included (AMC and water). Cells were treated for 12, 36 and 72 hrs with IC50 doses of CDV plus or minus ionising radiation. Illustration kindly provided by Miss A. Flynn (Cardiff University, HPV Research Group).

Appendix VI – Capsase-3 activity via analysis of western blots in A09 and M08

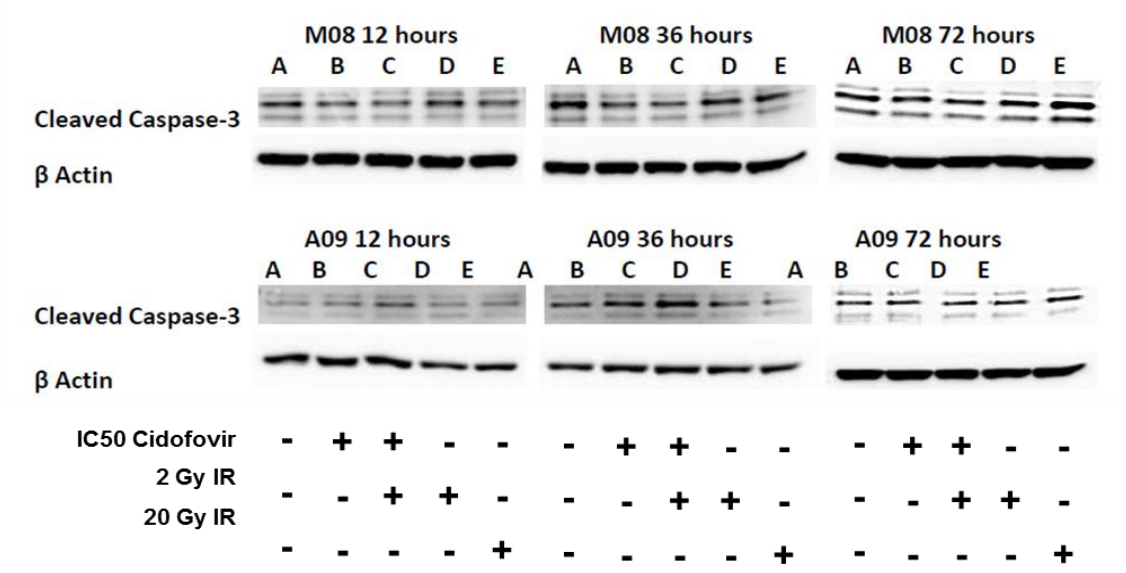

Figure VI.a. Western blots for cleaved Caspase-3 in M08 and A09 cells in response to Cidofovir and ionising radiation

Levels of cleaved Caspase-3 activity were assessed by western blotting using the cleaved caspase 3 antibody (Asp 175 #9664) from Cell Signalling (Massachusetts USA). Illustration kindly provided by Miss A. Flynn (Cardiff University, HPV Research Group).

Appendix VII – Assessment of RNA integrity using Agilent

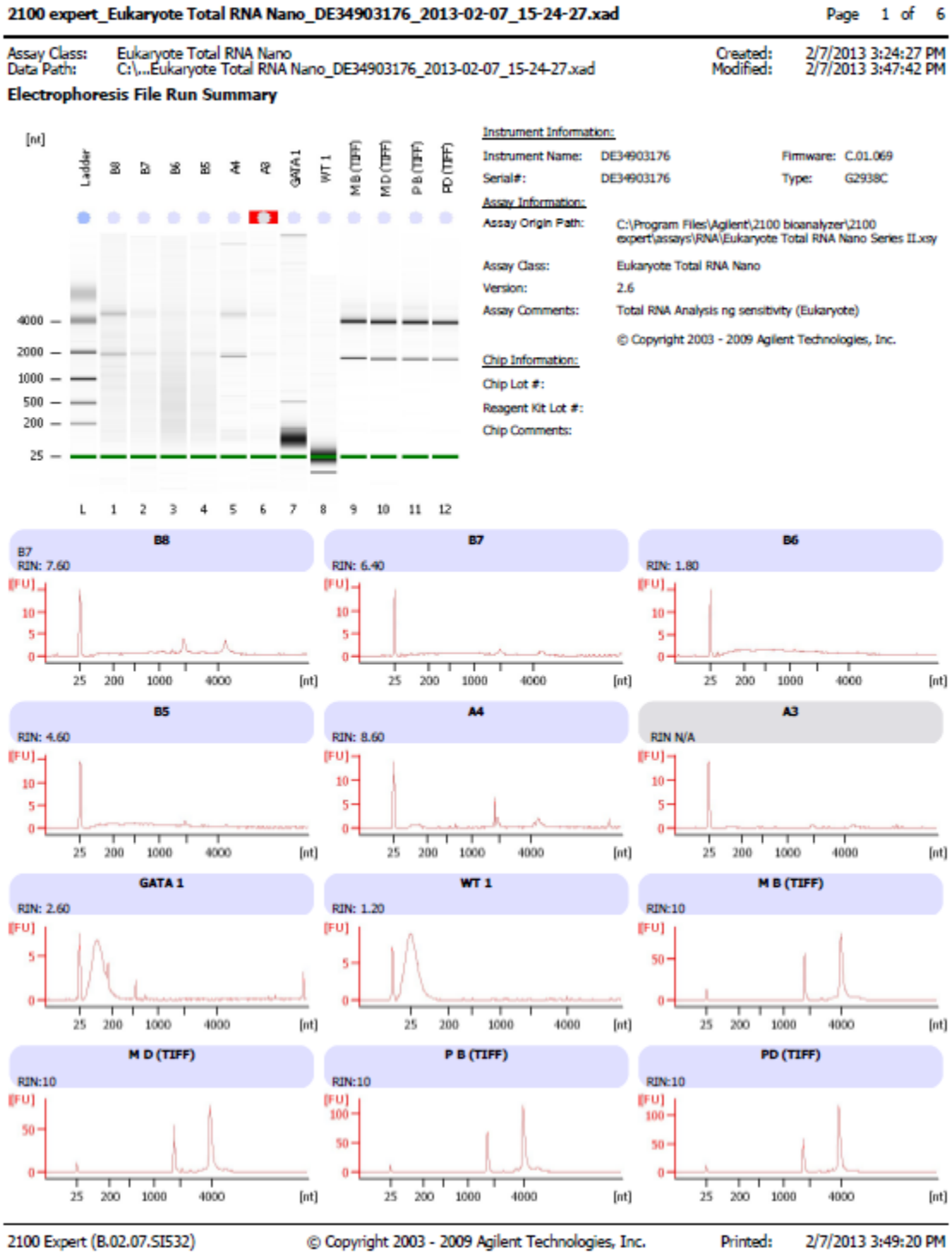

Assay Class: Eukaryote Total RNA Nano
Data Path: C:\...Eukaryote Total RNA Nano_DE34903176_2013-02-07_15-24-27.xad

Created: 2/7/2013 3:24:27 PM
Modified: 2/7/2013 3:47:42 PM

Electrophoresis File Run Summary (Chip Summary)

Sample Name	Sample Comment	Status	Result Label	Result Color
B8	B7	✔	RIN: 7.60	
B7		✔	RIN: 6.40	
B6		✔	RIN: 1.80	
B5		✔	RIN: 4.60	
A4		✔	RIN: 8.60	
A3		✔	RIN N/A	
GATA 1		✔	RIN: 2.60	
WT 1		✔	RIN: 1.20	
M B (TIFF)		✔	RIN:10	
M D (TIFF)		✔	RIN:10	
P B (TIFF)		✔	RIN:10	
PD (TIFF)		✔	RIN:10	

Chip Lot # **Reagent Kit Lot #**

Chip Comments :

Assay Class: Eukaryote Total RNA Nano
Data Path: C:\...Eukaryote Total RNA Nano_DE34903176_2013-02-07_15-24-27.xad
Created: 2/7/2013 3:24:27 PM
Modified: 2/7/2013 3:47:42 PM

Electrophoresis Assay Details

General Analysis Settings

Number of Available Sample and Ladder Wells (Max.) : 13
Minimum Visible Range [s] : 17
Maximum Visible Range [s] : 70
Start Analysis Time Range [s] : 19
End Analysis Time Range [s] : 69
Ladder Concentration [ng/µl] : 150
Lower Marker Concentration [ng/µl] : 0
Upper Marker Concentration [ng/µl] : 0
Used Lower Marker for Quantitation
Standard Curve Fit is Logarithmic
Show Data Aligned to Lower Marker

Integrator Settings

Integration Start Time [s] : 19
Integration End Time [s] : 69
Slope Threshold : 0.6
Height Threshold [FU] : 0.5
Area Threshold : 0.2
Width Threshold [s] : 0.5
Baseline Plateau [s] : 6

Filter Settings

Filter Width [s] : 0.5
Polynomial Order : 4

Ladder

Ladder Peak	Size
1	25
2	200
3	500
4	1000
5	2000
6	4000

Assay Class: Eukaryote Total RNA Nano
Data Path: C:\...Eukaryote Total RNA Nano_DE34903176_2013-02-07_15-24-27.xad

Created: 2/7/2013 3:24:27 PM
Modified: 2/7/2013 3:47:42 PM

Electropherogram Summary

Ladder

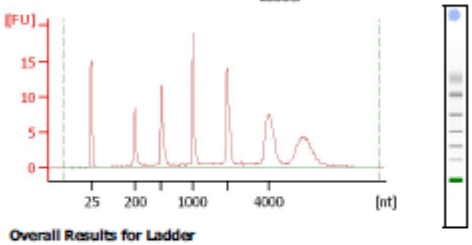

Overall Results for Ladder

RNA Area:	134.4
RNA Concentration:	150 ng/µl
Result Flagging Color:	
Result Flagging Label:	All Other Samples

M B (TIFF)

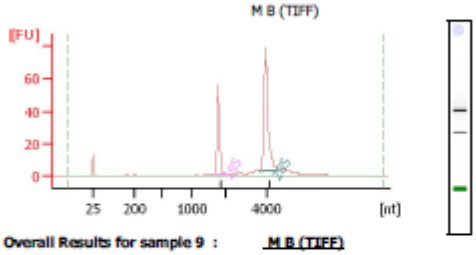

Overall Results for sample 9 : M B (TIFF)

RNA Area:	221.5
RNA Concentration:	247 ng/µl
rRNA Ratio [28s / 18s]:	2.3
RNA Integrity Number (RIN):	10 (B.02.07)
Result Flagging Color:	
Result Flagging Label:	RIN:10

Fragment table for sample 9 : M B (TIFF)

Name	Start Size [nt]	End Size [nt]	Area	% of total Area
18S	1,728	2,094	48.1	21.7
28S	3,674	4,717	109.0	49.2

M D (TIFF)

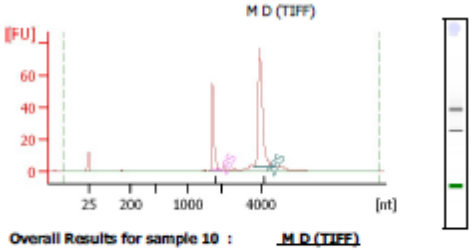

Overall Results for sample 10 : M D (TIFF)

RNA Area:	220.6
RNA Concentration:	246 ng/µl
rRNA Ratio [28s / 18s]:	2.3
RNA Integrity Number (RIN):	10 (B.02.07)
Result Flagging Color:	
Result Flagging Label:	RIN:10

Fragment table for sample 10 : M D (TIFF)

Name	Start Size [nt]	End Size [nt]	Area	% of total Area
18S	1,705	2,045	46.8	21.2
28S	3,628	4,674	106.9	48.5

P B (TIFF)

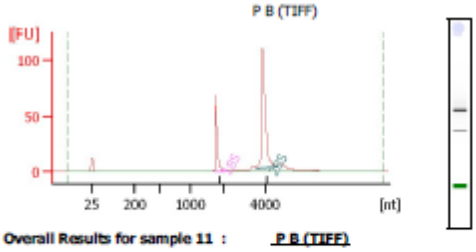

Overall Results for sample 11 : P B (TIFF)

RNA Area:	306.5
RNA Concentration:	342 ng/µl
rRNA Ratio [28s / 18s]:	2.5
RNA Integrity Number (RIN):	10 (B.02.07)
Result Flagging Color:	
Result Flagging Label:	RIN:10

Fragment table for sample 11 : P B (TIFF)

Name	Start Size [nt]	End Size [nt]	Area	% of total Area
18S	1,694	2,027	60.2	19.6
28S	3,598	4,598	148.4	48.4

Assay Class: Eukaryote Total RNA Nano
Data Path: C:\...Eukaryote Total RNA Nano_DE34903176_2013-02-07_15-24-27.xad

Created: 2/7/2013 3:24:27 PM
Modified: 2/7/2013 3:47:42 PM

Electropherogram Summary Continued ...

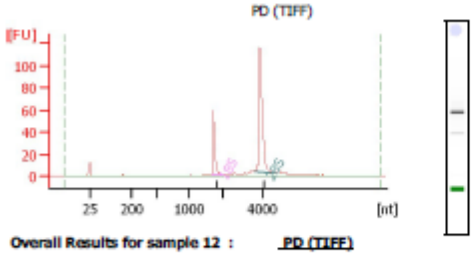

Overall Results for sample 12 : PD (TIFF)

RNA Area:	263.2
RNA Concentration:	294 ng/µl
rRNA Ratio [28s / 18s]:	2.7
RNA Integrity Number (RIN):	10 (B.02.07)
Result Flagging Color:	
Result Flagging Label:	RIN:10

Fragment table for sample 12 : PD (TIFF)

Name	Start Size [nt]	End Size [nt]	Area	% of total Area
18S	1,886	2,029	50.6	19.2
28S	3,581	4,594	136.1	51.7

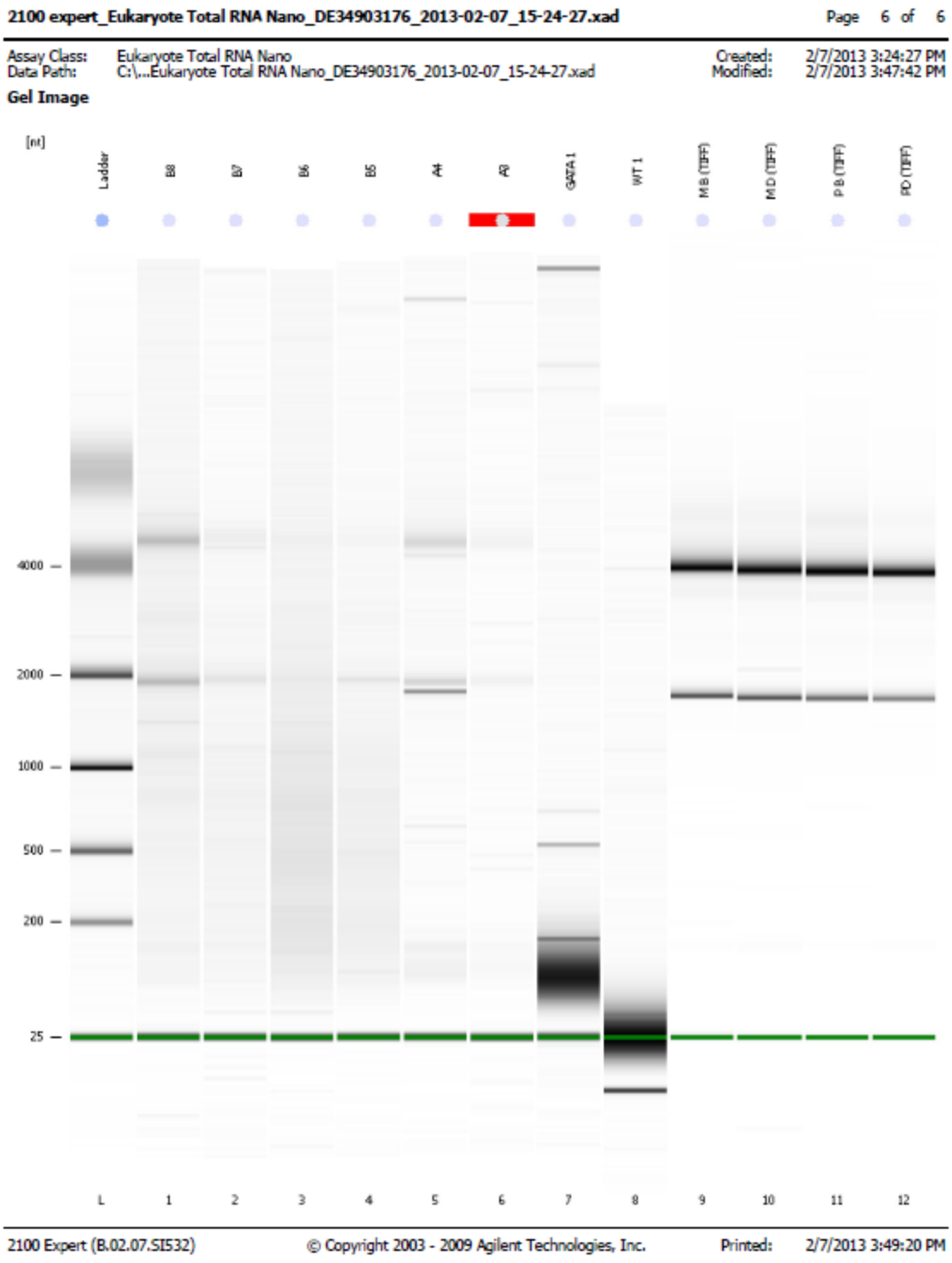

Figure VII.a. RNA integrity data obtained using Agilent

RNA Integrity Number (RIN) values were >10 and therefore suitable for SOLiD™ RNA-sequencing .
In the illustration, clonal cell lines M08 untreated, M08 CDV treated, P08 untreated and P08 CDV treated are referred to as: MB (TIFF), MD (TIFF), PB (TIFF) and PD (TIFF), respectively.

Appendix VIII – Heat map showing differential gene expression in M08 and P08

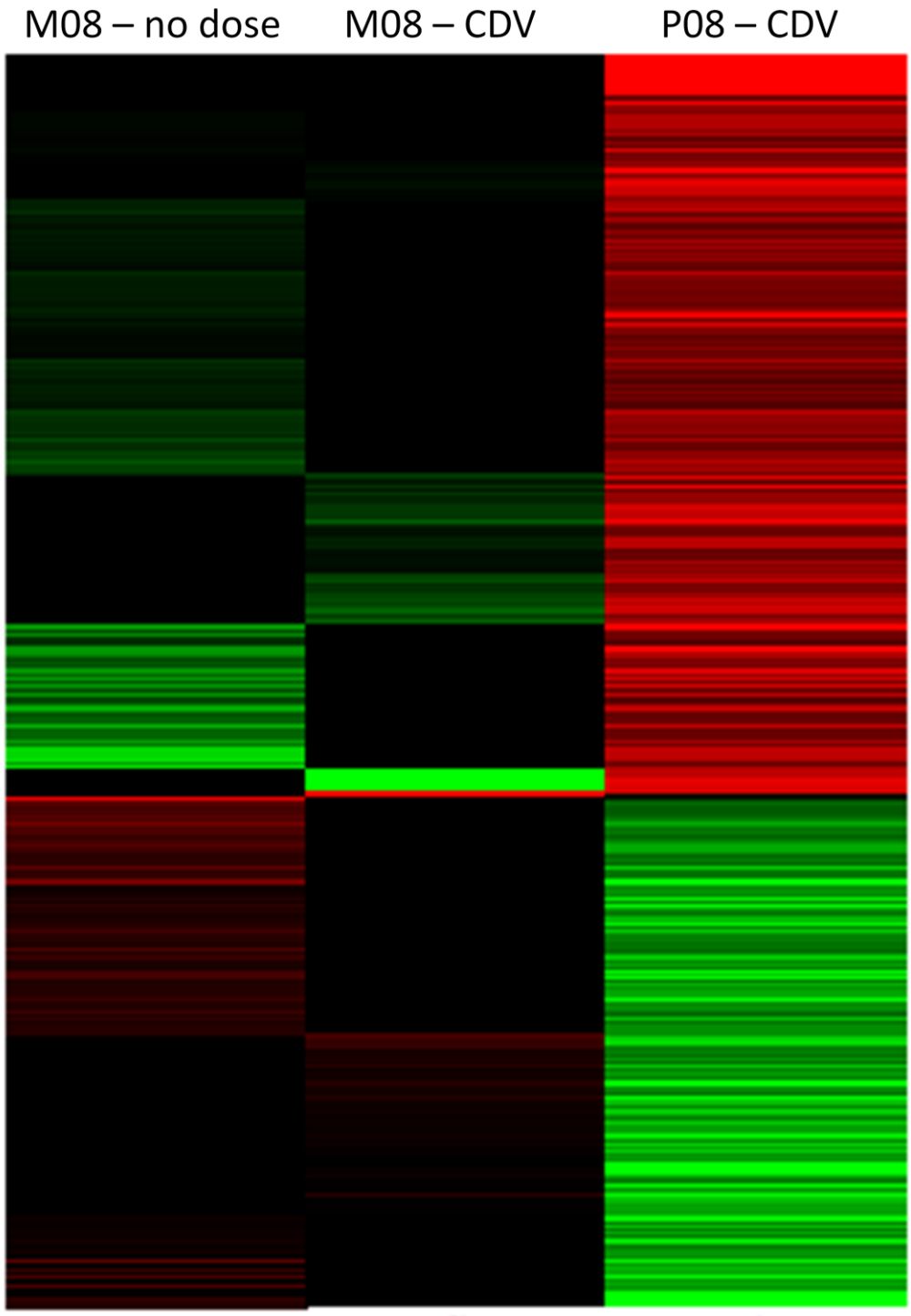

Figure VIII.a. Heat map showing differentially expressed genes in M08 and P08

Green indicates reduced gene expression and red indicates increased gene expression.